Excitotoxicity, Oxidative Stress and Neuroprotection in Cerebellar Granule Neurones

Dr. Andrew John Smith

MBChB (Aberdeen)

Submitted in fulfilment of the requirements for the Degree of PhD

University of Glasgow

Institute of Biomedical and Life Sciences

Division of Neuroscience and Biomedical Systems

March 2008

Abstract

Neuronal death due to excitotoxicity and oxidative stress is a critical part of several major disease processes, including ischaemic brain damage and Alzheimer's disease. This study used cultures of cerebellar granule neurones as a model for investigation of these processes, considering both their pharmacological and molecular aspects. Another important part of the study was the development and investigation of a mode of neuroprotection which was effective in protecting against these factors. Additionally, the optimal culturing conditions for neurone survival were determined and the efficacy of two cell viability assays established.

Examination of excitotoxicity and oxidative stress considered the effects of glutamate, *N*-methyl-D-aspartate, 3-nitropropionic acid and oxygen-glucose deprivation. Additionally, extensive study was carried out of the actions of increased glucose concentration and a range of metabolites of the essential amino acid tryptophan. It was demonstrated that several tryptophan metabolites induced neurotoxic effects, including 5-hydroxyanthranilic acid, which caused neuronal death via oxidative damage mediated by generation of reactive oxygen species and prevented by catalase but not superoxide dismutase. 5-Hydroxyanthranilic acid treatment also led to activation of the p38 signalling pathway, although the cell death caused was independent of caspase-3 activation.

Investigation of neuroprotection was concerned with establishing an effective method of protection, with a range of stimuli used to precondition neurones, such as *N*-methyl-D-aspartate, 3-nitropropionic acid, hydrogen peroxide, bicuculline and 4-aminopyridine. Preconditioning with 100μM *N*-methyl-D-aspartate at 8 DIV was effective in protecting against the neurotoxic effects of glutamate or 3-nitropropionic acid applied 24 hours after the commencement of preconditioning, but was not effective against oxygen-glucose deprivation of 4 hours duration. Preconditioning with 2.5mM 4-aminopyridine was effective in providing protection against a range of insults (glutamate, *N*-methyl-D-aspartate, 3-nitropropionic acid). This protection was independent of *N*-methyl-D-aspartate receptor activation, reduced by blockade of depolarisation and was effective in protecting against caspase-3-independent cell death.

Table of Contents

List of Tables

List of Figures

Acknowledgements

I would like to first thank my supervisors, Professor Trevor Stone and Professor Rob Smith for their extensive advice and guidance on many aspects of the work in this project. I was also given advice and assistance by others working in this laboratory: Dr. Sarah Mackay, Dr. Caroline Forrest and Dr. Gillian Mackay (for carrying out the HPLC running and result quantification); also Dr. Amos Fatokun, Mr. Majed Al-Gonaiah, Ms. Alex Ferguson and Dr. Duncan MacGregor.

During this project, I was fortunate enough to be able to visit the National Research Council's Institute of Biological Sciences in Ottawa, Canada, courtesy of Dr. Sheng Hou, who kindly allowed me to carry out some work in his lab, using TUNEL and Western blotting techniques, for which I was advised by Dr. Susan Jiang. Also, Dr. Joe Tauskela generously provided valuable advice and suggestions concerning my work on preconditioning and so I would like to sincerely thank all three for their contributions. Dr. Christopher Connolly and Dr. Sam Greenwood of the University of Dundee kindly provided the protocol used for cerebellar granule neurone culture preparation.

Professor Brian Morris, in addition to fulfilling the role of my Assessor during this project, generously gave both advice and free use of his laboratory for my early trials of Western blotting, with guidance also provided by Dr. Claire Guilding and Dr. Kara McNair. The laboratory of Professor Mandy MacLean freely provided the necessary gases for my OGD experiments and also gave advice on certain aspects of the Western blotting procedure, this provided particularly by Dr. Yvonne Dempsie and Dr. Ian Morecroft.

Professor Billy Martin and Mr. John Craig kindly provided tetrodotoxin for my preconditioning experiments. Dr. Yannis Pitsiladis and Dr. Niall MacFarlane were kind enough to provide free access to their lab to enable the use of the Fluoroskan equipment. Mr. Paul Paterson and Mr. Ian Watt provided free use of Douglas bags and gas analysis equipment for my OGD work. Dr. Ben Torsney was kind enough to provide me with time to discuss and advise me on some queries regarding the application of ANOVA and post-hoc tests. Professor Alan Taylor kindly allowed me the use of his oxygen probe equipment and gave advice on the best way to achieve an accurate assay with this.

Author's Declaration

I hereby declare that all work contained within this study was performed by myself, except where otherwise credited. I have read and understood the University's guidelines regarding plagiarism.

Andrew Smith

Abbreviations

ADP	Adenosine diphosphate
AIDS	Acquired Immunodeficiency Syndrome
AMP	Adenosine monophosphate
AMPA	α-Amino-3-hydroxy-5-methylisoxazole-4-propionate
ANOVA	Analysis of variance
AP	Action potential
4-AP	4-Aminopyridine
APV	D-(-)-2-amino-5-phosphonovalerate
ATP	Adenosine triphosphate
Bcl-2	Beta cell lymphoma 2
BDNF	Brain-derived neurotrophic factor
Bic	Bicuculline methobromide
BSA	Bovine serum albumin
CGN	Cerebellar granule neurone
CPP	3-(2-carboxypiperazin-4-yl)propyl-1-phosphonate
CRE	Cyclic-AMP response element
CREB	Cyclic-AMP response element binding protein
CRMP-3	Collapsin response mediator protein 3
Cu	Copper
Cu^{+}	Cuprous
Cu^{2+}	Cupric
DCD	Delayed calcium deregulation
DEPC	Diethyl pyrocarbonate
DIDS	4,4'-Diisothiocyanostilbene-2,2'-disulfonic acid
DIV	Days *in vitro*

DNase	Deoxyribonuclease
DPQ	3,4-Dihydro-5-[4-1(piperidinyl) buthoxy]-1(2H)-isoquinolone
DRG	Dorsal root ganglion
EAA	Excitatory amino acid
ECL	Enzymatic chemiluminescence
EDTA	Ethylene diamine tetra-acetic acid
EGTA	Ethylene glycol tetra-acetic acid
ERK	Extracellular regulated kinase
FAD	Flavin adenine dinucleotide
FDA	Fluorescein diacetate
Fe	Iron
Fe^{2+}	Ferrous ion
Fe^{3+}	Ferric ion
FMN	Flavin mononucleotide
GABA	Gamma-aminobutyric acid
GAPDH	Glyceraldehyde phosphate dehydrogenase
GFAP	Glial fibrillary acid protein
GSK-3β	Glycogen synthase kinase 3β
3-HAA	3-Hydroxyanthranilic acid
5-HAA	5-Hydroxyanthranilic acid
HBSS	Hank's balanced salt solution
5-HD	5-Hydroxydecanoate
HIF	Hypoxia-inducible factor
HIV	Human immunodeficiency virus
3-HK	3-Hydroxykynurenine
HNE	4-Hydroxy-2-nonenal
H_2O_2	Hydrogen peroxide

HPLC	High-performance liquid chromatography
ICC	Immunocytochemistry
ICER	Inducible cAMP early repressor
JNK	c-Jun *N*-terminal kinase
K^+	Potassium
K_{ATP}	ATP-sensitive potassium channel
KCl	Potassium chloride
LDH	Lactate dehydrogenase
LTP	Long-term potentiation
MAPK	Mitogen-activated protein kinase
MCA	Middle cerebral artery
MEM	Minimum essential medium
mGluR	Metabotropic glutamate receptor
MK-801	(+)-5-Methyl-10,11-dihydro-5*H*-dibenzo(*a*,*d*)cyclohepten-5,10-imine hydrogen maleate
Mn	Manganese
MPP^+	1-Methyl-4-phenyl-2,3-dihydropyridinium
MPT	Mitochondrial permeability transition
MPTP	1-Methyl-4-phenyl-1,2,3,6-tetrahydropyridine
MTT	3-(4,5-Dimethylthiazol-2-yl)-2,5-diphenyltetrazolium bromide
NAD	Nicotinamide adenine dinucleotide
NADH	Nicotinamide adenine dinucleotide (reduced)
NADP	Nicotinamide adenine dinucleotide phosphate
NAME	*N*-nitro-L-arginine methyl ester
NGF	Nerve growth factor
NMDA	*N*-methyl-D-aspartate
NO	Nitric oxide
NOS	Nitric oxide synthase

3-NPA	3-Nitropropionic acid
OGD	Oxygen-glucose deprivation
PBS	Phosphate-buffered saline
PDL	Poly-D-lysine
PI	Propidium iodide
PKC	Protein kinase C
pp38	Phosphorylated p38
PVDF	Polyvinylidene difluoride
QA	Quinolinic acid
RIPA	Radio-immuno precipitation assay
ROS	Reactive oxygen species
SBTI	Soy bean trypsin inhibitor
SDS	Sodium dodecyl sulphate
SEM	Standard error of mean
SOD	Superoxide dismutase
TBS	Tris-buffered saline
TdT	Terminal deoxynucleotidyl transferase
TMPO	2,3,5,5-Tetramethyl-pyridine-*N*-oxide
TNFα	Tumour necrosis factor alpha
TTX	Tetrodotoxin
TUNEL	Terminal dUTP nick-end labelling
Z-VAD-fmk	Carbonbenzoxy-valyl-alanyl-aspartyl-[O-methyl]-fuoromethylketone
Zn	Zinc

1 Introduction

1.1 Background pathology

1.1.1 Ischaemia and stroke

Ischaemia is a major cause of morbidity and mortality in the Western world, primarily due to damage and destruction of cardiac and brain tissue, in the form of myocardial infarctions and strokes respectively. Stroke has an annual incidence throughout Europe of 200-500 per 100,000 in the general population, and thus, even in areas with relatively low prevalence, it causes a significant impact on public health, with an additional notable economic cost associated with this (Taylor *et al.*, 1996, Bejot *et al.*, 2007).

In the context of cerebral ischaemia, an interruption of the blood supply sufficient to cause permanent damage is termed a cerebro-vascular accident (CVA), with the majority of cases (~80%) being due to blockage of the arterial lumen, and the remainder caused by a bleed from a supplying artery or arteriole (Bejot *et al.*, 2007, Ribo and Grotta, 2006). The most common cause of vessel occlusion is thrombus (blood clot) forming over a ruptured arteriosclerotic plaque in the vessel wall (the cause of ~75% of occlusive strokes), or due to thrombo-embolism (lumen blockade with thrombus formed in a distant location, commonly in the heart due to irregular flow) (Bejot *et al.*, 2007). This sudden interruption of blood supply causes tissue death due to a variety of mechanisms, with the area of cell death due to ischaemia referred to as an infarct.

Due to the high demand of brain tissue for glucose for oxidative phosphorylation, the loss of oxygen and glucose is felt very rapidly, with cell death proceeding more rapidly than in the case of other tissues subjected to ischaemia (Dirnagl *et al.*, 1999). The cause of neuronal death is not only due to loss of substrates for neuronal energy requirements, but the effects of ischaemia on excitatory neurotransmitter release and the resultant depolarisation of neurones.

Due to loss of energy, maintenance of the ionic gradients that sustain the membrane potential is lost, causing depolarisation and influx of sodium and chloride initially. These effects of depolarisation lead to influx of water due to the osmotic pressure from increased intracellular sodium and chloride, and of

calcium due to activation of voltage-sensitive calcium channels. The effect of this influx of water is to cause neuronal swelling at a cellular level and oedema at a tissue level, which can further restrict perfusion and worsen ischaemia due to direct pressure of patent vessels.

The influx of calcium leads in turn to pre-synaptic release of excitatory amino acids (EAAs), causing a rise in extracellular glutamate concentrations within minutes of the onset of ischaemia. This release of glutamate causes activation of *N*-methyl-D-aspartate (NMDA) and metabotropic glutamate receptors, which causes further calcium influx in post-synaptic neurones. Furthermore, activation of α-amino-3-hydroxy-5-methylisoxazole-4-propionate (AMPA) and kainate receptors causes additional sodium influx and depolarisation in post-synaptic neurones. Another cause of increased glutamate release is the stimulation of volume-regulated anion channels, an effect predominantly found in the outer areas of an infarct (Feustel *et al.*, 2004). This is consistent with the dependency on adenosine triphosphate (ATP) of these channels, as the ATP levels available during an ischaemic event depend on the cell's location within the infarct, Cells at the centre of the infarction (the infarct 'core') have little or no ATP available to them, whereas cells on the periphery (the infarct 'penumbra') have more ATP available (Hou and MacManus, 2002).

The process of cell death due to over-stimulation by excitatory neurotransmitters is known as excitotoxicity (Olney and de Gubareff, 1978) and is a major component of the damage caused by ischaemia in neurones, acting early in the sequence of damaging events (Dirnagl *et al.*, 1999).

The loss of ATP production causes failure of the sodium-potassium pump on the plasma membrane, triggering depolarisation (due both to loss of sodium and failure to preserve a polarised state by potassium gradient maintenance). Also, potassium released from lysed cells following an ischaemic insult will cause further depolarisation, with attendant excitotoxicity in glutamatergic neurones due to this causing release of intracellular glutamate. An association between this process of additional depolarisation and increased infarct size has been demonstrated in animal models, with blockade of NMDA receptors causing a reduction in current shift and infarct size (Iijima *et al.*, 1992, Mies *et al.*, 1993).

Ischaemia causes increased production of reactive oxygen species (ROS), highly reactive molecules that are capable of damaging cellular structures extensively. Cellular damage due to these molecules is termed oxidative stress, a major component of ischaemia-induced damage.

Inflammation is another significant aspect of damage following an ischaemic event, occurring due to nuclear factor kappa B (NF-κB) and hypoxia inducible factor 1 (HIF1), in response to hypoxia and generation of ROS (O'Neill and Kaltschmidt, 1997, Ruscher *et al.*, 1998). This leads to increased expression of inflammatory mediators (tumour necrosis factor α (TNFα) and interleukin 1ß), which due to increased adhesion molecule expression cause neutrophils, monocytes and macrophages to infiltrate the infarct (Iadecola, 1997), in addition to the activation of microglia in the affected area. These processes lead to increased activity of nitric oxide synthase (NOS) and cyclo-oxygenase 2, causing increases in nitric oxide (NO) and superoxide respectively. Nitric oxide is capable of reacting with superoxide to produce peroxynitrite, a highly reactive molecule that causes extensive damage. Peroxynitrite is particularly damaging in neurones, which are highly sensitive to damage from ROS (see section 1.3.4).

Ischaemia-induced neuronal cell death cannot be described as either completely necrotic or completely apoptotic in character, as neurones that suffer an ischaemic insult display biochemical signs of apoptotic cell death, although cytological examination reveals the appearance of necrotic cell death (Martin, 2001, Hou and MacManus, 2002).

The pathway of cell death followed depends partly on the level of energy, in the form of ATP available to the cell. When higher levels of ATP are available, then the cell activates the pathway of ordered DNA fragmentation and cell death via apoptosis. If available ATP levels are lower or non-existent then the cell, unable to activate the apoptotic pathway, dies due to necrosis. As cells at the infarct core have little or no ATP available, they die due to necrosis. Conversely, cells in the penumbra (where more ATP is available) follow the apoptotic pathway of ordered cell destruction (Hou and MacManus, 2002).

In the intermediate area of the infarct the means of cell death may involve stages of both the necrotic and apoptotic pathways. This can be explained by a fall in the ATP level causing cells that had initially activated an apoptotic

pathway to change to a necrotic type of cell death, as the fall in ATP prevents completion of the apoptotic process (Roy and Sapolsky, 1999, Hou and MacManus, 2002).

Apoptosis is a process of energy-dependent controlled cell death, which occurs both during disease and as a physiological control of cell numbers during development (in the latter case the process is referred to as 'programmed cell death'). The process involves breakdown of cells into components that are then packaged into and contained in vesicles, genetically controlled by the bcl-2 (beta-cell lymphoma 2) family of genes and the gene p53 (Kam and Ferch, 2000). The pathways followed by apoptosis depend on the activation of cell death signalling proteins such as the members of the extracellular-regulated kinase (ERK) family, c-Jun-*N*-terminal kinase (JNK) and p38. Activation of caspases such as caspases 8, 9 and 12, then occurs due to: release of cytochrome c from the mitochondria, which forms a pro-apoptotic complex (termed an apoptosome) with pro-caspase 9; Fas receptor activation leads to caspase-8 activation; release of calcium from the endoplasmic reticulum causes activation of caspase-12 (Sima, 2003). This subsequently leads to activation of caspases 1 and 3, caspases which act directly to cleave cellular structures.

The process of apoptosis in the penumbra take some time to be completed, with the possibility that interruption of its activation by blockade of one or more of the executioner caspases will prevent cell death several hours after an ischaemic episode (Cheng *et al.*, 1998, Fink *et al.*, 1998). This indicates that the window of opportunity for effective damage-limiting treatment may be notably longer in CVA patients than was previously believed. However, the need to develop an effective preventative therapy which allows improved neuronal survival in the infarct core during an ischaemic event remains.

1.1.2 Neurodegeneration

In addition to brain damage due to ischaemia, there are several progressive neurodegenerative disorders which have a substantial impact in terms of both long-term morbidity and associated mortality from complications. These disorders can occur in any part of the brain: cerebral cortex and hippocampus (Alzheimer's disease), the striatum (Huntingdon's disease), deep nuclei

(Parkinson's disease) or with a more generalised distribution (AIDS dementia complex).

Alzheimer's disease is a neurodegenerative disorder characterised clinically by progressive loss of higher mental functions, particularly cognitive and emotional tasks, and pathologically by 'neurofibrillary tangles' and amyloid plaques, with generalised cerebral atrophy seen in long-standing, extensive disease. Neurofibrillary tangles are in fact composed of collections of the microtubule-associated protein tau, associated with oxidative stress; the plaques are accumulations of amyloid-ß peptide (Cummings *et al.*, 1998), which is capable of inducing apoptosis directly in cultured cortical neurones (Loo *et al.*, 1993).

Amyloid-ß can induce lipid peroxidation in neuronal plasma membranes, which leads to reduced trans-membrane transport of ions and glucose, with resultant depolarisation and ATP depletion and associated calcium influx and impaired mitochondrial function (Mattson, 1998). There is evidence that Alzheimer's disease involves DNA fragmentation (Su *et al.*, 1994) and activation of caspases 3, 8 and 9 (Stadelmann *et al.*, 1999, Rohn *et al.*, 2001, Rohn *et al.*, 2002), with protection against amyloid-ß-induced damage provided by antioxidants or by anti-apoptotic neurotrophins (Mattson, 1998). The specific actions of amyloid-ß include stimulation of nicotinic acetylcholine receptors (particularly the alpha-7 subunit), leading to increased calcium influx; amyloid-ß also causes reduction of glutamate re-uptake (Liu and Wu, 2006). Furthermore, JNK signalling-dependent down-regulation of the anti-apoptotic protein bcl-w due to amyloid-ß has also been identified (Yao *et al.*, 2005), and amyloid- ß can induce mitochondrial permeability transition (MPT) pore formation in isolated mitochondria (Rodrigues *et al.*, 2000).

Huntington's disease is inherited in an autosomal dominant fashion and is characterised clinically by a progressive increase in choreaform movements and dementia, due to loss of neurones in the striatum and cerebral cortex. Clinical appearances of the disease typically manifest from the fourth or fifth decade of life, by which time the disease has usually been passed to the next generation. The pathological cause is due to a gene mutation which due to an expanded trinucleotide sequence (CAG) codes for the production of an abnormal protein

named huntingtin, containing an excessive series of repeats of glutamine (Brandt *et al.*, 1996).

The expression of the mutated huntingtin protein causes caspase-8-dependent apoptosis, and Huntington's disease has been associated with abnormalities of mitochondrial function (Sanchez *et al.*, 1999, Sawa *et al.*, 1999) and activation of caspases 1 and 3 (Ona *et al.*, 1999). A further finding related to the pathogenesis of Huntington's disease is that remarkably similar lesions can be induced by direct injection of the specific NMDA receptor agonist quinolinic acid (QA). Quinolinic acid is a product of tryptophan catabolism, which is capable of inducing neuronal death due to excitotoxicity and has been found to be present in higher concentration in cerebral cortical and striatal tissue in Huntington's disease patients (Guidetti and Schwarcz, 1999, Guidetti *et al.*, 2004).

The clinical manifestations of Parkinson's disease are termed Parkinsonism, as the condition can be reproduced by causes other than Parkinson's disease, such as exposure to 1-methyl-4-phenyl-1,2,3,6-tetrahydropyridine (MPTP). This compound is metabolised to 1-methyl-4-phenyl-2,3-dihydropyridinium (MPP^+), which inhibits mitochondrial electron transport, an effect prevented by glutathione (Annepu and Ravindranath, 2000). The clinical syndrome is comprised of bradykinesia (slowness and difficulty in initiating movements), fine resting tremor and rigidity of muscle tone. The pathological basis for these symptoms is degeneration of dopaminergic neurones in the substantia nigra, either idiopathically in the case of Parkinson's disease or due to an identified neurotoxic action in the case of MPTP, with oxidative stress and associated apoptosis integral to progression of the disease (Jenner and Olanow, 1998).

The AIDS dementia complex is a process of cognitive decline which can supervene in long-standing HIV infection complicated by AIDS, with the pathology as yet unclear although with several indications that the involvement of oxidative damage is a key component in pathogenesis. The severity of clinical neurological decline has been correlated with higher concentrations of QA in both early and late-stage infection (Heyes *et al.*, 1991). Additionally, QA applied at nanomolar concentrations for 24 hours has been demonstrated to induce apoptosis in human astrocytes (Guillemin *et al.*, 2005).

There are indications that the increased concentration of QA may be due to production by microglia and macrophages, as astrocytes produce no QA and in fact produce the neuroprotective metabolite kynurenic acid (Guillemin *et al.*, 2001). This suggests that increased QA production is a manifestation of extensive inflammation and associated macrophage and microglial activation (Espey *et al.*, 1997), consistent with the association between extent of infection and increased QA levels.

This brief review of the pathology of these conditions emphasises the importance of excitotoxicity and oxidative stress as causes of neuronal damage, with a variety of routes of inducing this damage, such as: direct induction of oxidative stress by toxic agents, enhanced vulnerability to excitotoxicity and oxidative damage and damage from excitotoxic by-products of inflammation. Therefore, the scope of use for treatments aimed at alleviating the damage done by excitotoxic and oxidative stressors is broad, with study of these processes offering the potential for important interventions in disease progression.

1.2 Excitotoxicity

1.2.1 Neurotransmission

1.2.1.1 Excitatory amino acids

Excitatory amino acids are a group of neurotransmitters including glutamate and aspartate, which transmit excitatory signals in the CNS. The most important neurotransmitter of this group is glutamate, which is synthesised primarily from intermediate metabolites in the Krebs cycle and also from glutamine. Storage of glutamate in neurones is in synaptic vesicles, with the compound released during neurotransmission by exocytosis, a calcium-dependent process (Rang *et al.*, 1995). Cerebellar granule neurones are capable of generating glutamate through carboxylation of pyruvate, indicating no dependence on glutamate synthesised from glutamine by glial cells (Hassel and Bråthe, 2000).

Glutamate mediates its actions via four classes of receptor: the ionotropic NMDA, AMPA and kainate receptors, and the metabotropic glutamate receptors. The AMPA and kainate receptors are involved in fast excitatory post-synaptic responses, the NMDA receptors in slow post-synaptic potential generation and

the metabotropic rectors (reflecting their less rapidly-acting mode of action) in delayed neuromodulatory responses (Rang *et al.*, 1995).

1.2.1.2 Gamma-amino-butyric acid

Gamma-amino-butyric acid (GABA) is found extensively in the brain and acts as an inhibitory neurotransmitter on the receptor subtypes $GABA_A$, $GABA_B$ and $GABA_C$. Synthesis of GABA is via the action of glutamic acid decarboxylase, which uses glutamate as its substrate (Rang *et al.*, 1995). Inhibition of excitatory neurotransmission by $GABA_A$ receptors is mostly post synaptic, due to increased influx of chloride ions causing hyperpolarisation of the membrane. In contrast, $GABA_B$ receptors act mainly presynaptically to reduce calcium influx and increase potassium efflux, these actions respectively reducing excitatory transmitter release and inducing hyperpolarisation (Rang *et al.*, 1995). $GABA_C$ receptors are ligand-gated ion channels that are predominantly located in the retina, but have been speculated to elsewhere be involved in memory formation (Chebib, 2004). It has already been established that $GABA_A$ receptors are involved with memory formation, and that transgenic mice deficient in the α5 subunit of the $GABA_A$ receptor show enhanced learning and memory in water maze testing (Collinson *et al.*, 2002). Earlier in neuronal development, GABA receptors can have an excitatory function: this is because intracellular concentrations of chloride are higher, so opening chloride channels can cause efflux of chloride, sodium influx and activation of voltage-gated calcium channels (Ben-Ari *et al.*, 2007). As GABA excitatory transmission is established earlier than glutamatergic neurotransmission, it can have a significant impact on synaptic plasticity, and thus on neuronal survival and development (Ben-Ari *et al.*, 2007).

1.2.2 Glutamate (NMDA, AMPA, kainate, metabotropic receptors)

1.2.2.1 *N*-methyl-D-aspartate receptors

Stimulation of NMDA receptors causes activation of cation channels, inducing influx of calcium and sodium ions. There are a variety of NMDA receptor subunits, grouped into three subtype categories: NR1, NR2 and NR3 (each category encompassing several varieties of subunit), with a set of four subunits (two NR1 and two NR2 or occasionally NR3 subunits) believed to be grouped together to construct a complete receptor (Paoletti and Neyton, 2007).

Activation of NMDA receptors requires the stimulation of two sites on the receptor, namely the glutamate recognition site (on the NR2 subunit) and the glycine binding site (on the NR1 subunit) and also the removal of a voltage-dependent magnesium block of the associated ion channel: once the receptor is activated, the ion channel allows entry of calcium and sodium (Lynch and Guttmann, 2002).

Receptor subunit composition changes with neuronal development: NMDA receptors in immature rat hippocampal cultures are predominantly NR1/2B receptors at developing synapses (Waxman and Lynch, 2005). By 14 days *in vitro* (DIV), NR2A expression increases and the dominant synaptic receptor configuration is NR1/2A/2B, with NR1/2B levels higher at extra-synaptic locations: p38 phosphorylation requires NR1/2A/2B activation, which indicates that synaptic NMDA receptor activity induces p38 activation and extra-synaptic activity induces p38 de-phosphorylation (Waxman and Lynch, 2005).

Neuronal NMDA receptors are situated in both synaptic and extra-synaptic locations, with different outcomes resulting from receptor stimulation in these different locations. It has been reported that calcium influx induced by extra-synaptic NMDA receptor stimulation induces neuronal death, whereas calcium influx from synaptic NMDA receptors does not (Hardingham *et al.*, 2002b). This may be due to differences in the responses of mitochondria at these locations to influxes of calcium (Young *et al.*, 2008). It appears that both the intensity and duration of the calcium influx mediated by NMDA receptor stimulation (irrespective of location) are critical to the response that is induced, with pro-survival signalling more likely to be induced by a moderate calcium signal and pro-death signalling more likely in response to an intense or prolonged calcium influx (Soriano and Hardingham, 2007, Hou *et al.*, 2008).

The pro-survival signals activated by NMDA receptor-mediated calcium influx include: Akt, ERK 1/2 and phosphorylation of cyclic-AMP response element binding protein (CREB), whereas the pro-death signals include activation of p38, JNK and calpains (Papadia and Hardingham, 2007).

Receptor activation can be blocked by co-application of D-(-)-2-amino-5-phosphonovalerate (APV, a competitive NMDA antagonist), (+)-5-Methyl-10,11-dihydro-5*H*-dibenzo(*a*,*d*)cyclohepten-5,10-imine hydrogen maleate (MK-801 or

dizocilpine, non-competitive NMDA antagonist, which directly blocks the receptor-associated pore) or by the endogenously-generated glycine co-site antagonist kynurenic acid (Foster *et al.*, 1984, Paoletti and Neyton, 2007).

1.2.2.2 AMPA receptors

Activation of α-amino-3-hydroxy-5-methylisoxazole-4-propionate receptors causes influx of sodium, which can lead to depolarisation and depending on subunit composition, may allow influx of calcium when stimulated, a process integral to development of long-term potentiation (Stone and Addae, 2002, Liu and Zukin, 2007). A major component of AMPA-mediated excitotoxicity is AMPA-induced depolarisation, which removes the voltage-dependent magnesium gate on the NMDA receptor and thus allows influx of calcium through this receptor (review: Hou and Macmanus, 2002).

α-Amino-3-hydroxy-5-methylisoxazole-4-propionate induced neurotoxicity but was not toxic to glia in cultured neonatal rat cerebral cortical tissue (Rzeski *et al.*, 2005). Activation of AMPA receptors was prolonged and associated with enhanced current flow following exposure to a modelled traumatic injury in rat neonatal cortical neurones, a process which was induced by repression of AMPA receptor desensitisation and represents a potential mechanism for post-traumatic neuronal injury (Goforth *et al.*, 1999).

The development of long-term potentiation (LTP), although mediated initially by NMDA receptor stimulation, involves alterations to AMPA receptors. Long-term potentiation is long-lasting enhanced signalling between two neurones resulting from simultaneous stimulation, which is believed to be a major component of learning and memory. Early LTP involves NMDA receptor activation and calcium influx leading to AMPA receptor insertion and increased AMPA receptor conductance (although it should be noted that while NMDA receptor activation is required for LTP in the hippocampus, it is not required for LTP in mossy fibres). Late LTP involves excitation of NMDA, AMPA and metabotropic glutamate receptors (mGluRs), which causes ERK activation: this leads to gene transcription, protein synthesis and morphology changes and ultimately to LTP expression (Izquierdo, 1994). Long-term potentiation is a process believed to be of importance during neuronal development.

The AMPA receptors develop relatively late, with glutamatergic transmission therefore 'silent' initially, as NMDA receptors cannot be stimulated due to the voltage-gated magnesium block. The role of AMPA receptors in providing a rapid excitatory response (which allows removal of the magnesium block) is taken by GABA receptors initially, as mentioned previously (Ben-Ari *et al.*, 1997).

1.2.2.3 Kainate receptors

Activation of kainate receptors is also capable of inducing neuronal death: in parallel with AMPA receptor stimulation, a significant component of kainate receptor-mediated neurotoxicity *in vivo* is depolarisation-induced NMDA receptor activity (Behan and Stone, 2000). This finding was not reproduced in either rat or mouse cerebellar granule neurones (CGNs) *in vitro* however, as blockade with the kainate receptor antagonist 6-cyano-7-nitroquinoxaline-2,3-dione disodium protected against kainate toxicity, but NMDA blockade with MK-801 did not (Simonian *et al.*, 1996, Smith *et al.*, 2003). An additional effect of kainate receptor stimulation is the stimulation of GABA release, acting to induce a negative feedback loop and prevent over-excitation (review: Pinheiro and Mulle, 2006).

Kainate toxicity induces DNA fragmentation and apoptotic appearances but does not involve caspase-3 activation and is not dependent on new protein or RNA synthesis (Simonian *et al.*, 1996, Smith *et al.*, 2003). In neonatal rat CGNs, the neurotoxic effect of kainate, which appeared to involve a necrotic death mechanism, was potentiated by nifedipine or exhaustion of intracellular calcium stores (Leski *et al.*, 1999).

1.2.2.4 Metabotropic glutamate receptors

Metabotropic glutamate receptors mediate their effects via second messenger systems, particularly phospholipase C and adenylate cyclase: due to this mechanism of action, mGluRs act less rapidly than the ionophoric channels. There are eight subtypes of these receptors (mGluR1-8), which are divided into three groups. Group I receptors (mGluRs 1 and 5) are located postsynaptically and act via phospholipase C, increasing the activity of NMDA receptors, with mGluR1 receptors increasing glutamate release via increased calcium influx (Stone and Addae, 2002). However, Group I receptors can also induce inhibitory

post-synaptic potentials and modulate the action of voltage-gated calcium channels. Nontheless, blockade of mGluR1 receptors protects against both oxygen-glucose deprivation (OGD) *in vitro* and ischaemia *in vivo* (Pellegrini-Giampietro *et al.*, 1999).

Group II (mGluRs 2 and 3) and Group II receptors (mGluRs 4, 6, 7 and 8) both act to reduce adenylate cyclase activity, which reduces cyclic AMP levels and NMDA receptor activity. Group II and III mGluRs are mainly presynaptic, although they have been identified at both pre- and postsynaptic locations. Stimulation of mGluR2 and mGluR3 subtypes has been demonstrated as being neuroprotective against the neurotoxic effects of NMDA and traumatic brain damage, with protection also seen with stimulation of mGLuR4 and mGluR7 subtypes (Stone and Addae, 2002).

1.2.3 Mechanisms of damage post-receptor

Excess glutamate damages neurones via the process of excitotoxicity, which involves over-stimulation of neurones with excitatory amino acids (Olney and de Gubareff, 1978). In the case of glutamate, this is primarily mediated via an influx of calcium due to NMDA receptor activation (Manev *et al.*, 1989), which causes calcium, sodium, chloride and zinc influx, and efflux of potassium. This results in depolarisation and increased calcium and water content, which in turn disturbs metabolic function and produces neuronal swelling, damaging the cell membrane (Sapolsky, 2001, Hou and MacManus, 2002). A further effect of glutamate excitotoxicity is the development of dendritic beading, an effect induced by a collapse in mitochondrial ATP production associated with ion (sodium or calcium) influx, which leads to influx of extracellular water and resultant formation of beading on dendrites (Greenwood *et al.*, 2007).

Glutamate-induced excitotoxicity depends on the presence of extracellular calcium (Choi and Rothman, 1990), with cell death due to excitotoxicity proportional to neuronal calcium uptake and attenuated by removal of extracellular calcium up to 30 minutes after glutamate application in CGNs (Manev *et al.*, 1989). Activation of NMDA receptors causes calcium influx, which initially accumulates in mitochondria prior to a subsequent efflux of calcium into the cytoplasm (Budd and Nicholls, 1996). It does not appear however, that this calcium is emitted from the mitochondria (Ward *et al.*, 2005).

Glutamate-induced excitotoxicity leads to MPT pore opening, leading to leakage of calcium, ROS and cytochrome c from the mitochondria (Chalmers and Nicholls, 2003). Further damage to the cell membrane results from glutamate-induced ROS production, which damages cell membrane lipids (Sapolsky, 2001, Hou and MacManus, 2002).

Destruction of the plasma membrane calcium pump by calcium-activated calpains is another feature of excitotoxicity (Bano *et al.*, 2005). This may explain the link between excitotoxicity and necrosis, as plasma membrane calcium pump cleavage leads to excessive intracellular calcium, despite initial activation of apoptosis mechanisms (Schwab *et al.*, 2002). Exposure to glutamate for a short period (30 minutes) has been shown to induce breakdown of the structural proteins laminin and ß-tubulin in neonatal rat CGNs (Ankarcrona *et al.*, 1996).

The possibilities remain that glutamate toxicity induces cell death via both necrotic and apoptotic mechanisms or that cells follow the necrotic pathway of cell death as a 'second choice' when the apoptotic pathway becomes unavailable, analogous to the switch from apoptosis to necrosis due to falling levels of ATP in the penumbra of an infarct (Dessi *et al.*, 1993).

There are several mechanisms by which cells act to reduce or avert glutamate-induced damage, most triggered by glutamate's immediate effects on the neuronal intracellular environment. The potential for depolarisation is affected by small-conductance potassium channels and ATP-dependant potassium channels as follows. The small-conductance channels are calcium-dependant; hence rising intracellular calcium levels due to glutamate stimulation open the channels and produce neuronal hyper-polarisation. Falling levels of ATP, a consequence of ATP consumption due to over-excitation, cause ATP-dependant potassium channel to open. Calcium influx due to NMDA receptor stimulation also increases Na^+/K^+/ATPase activity, which also maintains membrane polarisation, although this effect will be reduced due to falling levels of ATP (Sapolsky, 2001). Glutamate also triggers release of GABA, adenosine and taurine, inhibiting subsequent glutamate release, with adenosine having the additional beneficial effect of being an ATP precursor (Sapolsky, 2001).

The results of glutamate excitotoxicity can themselves limit the damage produced, specifically the increases in calcium and ROS: NMDA receptors can be damaged by the action of calpain, and calcium currents inhibited by the calcium-dependant activation of calcineurin and calmodulin, which are all activated by increasing levels of intracellular calcium (Sapolsky, 2001).

Activation of protein kinase C (PKC) attenuates NMDA-mediated calcium increases, perhaps by feedback inhibition of the NMDA receptor itself by PKC (Snell *et al.*, 1994). Furthermore, damage to intracellular proteins initiates production of 'heat shock proteins', which protect against calcium and ROS-induced protein damage, and also antioxidant enzymes production rises to compensate for increased ROS levels (Sapolsky, 2001).

1.3 Oxidative stress

1.3.1 Energy metabolism

Glycolysis occurs in the cytoplasm, converting glucose initially to glucose-6-phosphate, then through a series of other intermediates to pyruvate. When there is sufficient oxygen to reoxidise the NAD^+ (nicotinamide adenine dinucleotide) reduced during this process, aerobic glycolysis occurs, with the pyruvate becoming the substrate for the first stage of the citric acid cycle and the reduced nicotinamide adenine dinucleotide (NADH) being utilised in oxidative phosphorylation. Alternatively, in the presence of an inadequate oxygen supply, the pyruvate is converted into lactate by anaerobic glycolysis, with the reduced form NADH oxidised back to NAD^+ during lactate production (Champe and Harvey, 1994).

The citric acid cycle occurs in the mitochondrial matrix and is a major source of the reduced cofactors which power oxidative phosphorylation. Pyruvate is converted to acetyl CoA, which then enters the cycle by combining with oxaloacetate to form citrate. Citrate is metabolised over several stages to oxaloacetate, which then re-enters the cycle on combination with a new molecule of acetyl CoA.

Oxidative phosphorylation occurs on the inner mitochondrial membrane, using a series of four inter-linked complexes collectively known as the electron

transport chain. This leads on to a fifth complex which utilises free protons generated by the previous four complexes to synthesise ATP and water from ADP (adenosine diphosphate), free phosphate and oxygen. Cytochromes $a+a_3$, b and c are integral components of the electron transport chain, each containing an iron atom which alternates between the ferrous and ferric states during different stages of electron transport (Champe and Harvey, 1994).

1.3.2 Causes of oxidative stress

The main sources of ROS in the cell are the mitochondria, so abnormalities of mitochondrial function due to inherent defects or abnormal stresses are likely to lead to production of excessive quantities of ROS. When these levels overwhelm the cell's normal antioxidant defences, such as the free radical scavengers found in the inner mitochondrial membrane and antioxidant enzymes such as catalase and superoxide dismutase (SOD), DNA and cellular structures are damaged, a process referred to as oxidative stress. Another route by which oxidative stress can occur is due to antioxidant defences being abnormally impaired, as occurs in amyotrophic lateral sclerosis, an inherited neurodegenerative disorder commonly due to an inherited mutation in Cu,Zn-SOD (Ryu *et al.*, 2005).

Formation of superoxide in the mitochondria can lead to production of hydrogen peroxide (H_2O_2) by the action of Mn-SOD in the mitochondria, or can react with nitric oxide to produce peroxynitrite, a highly reactive ROS with significant potential for oxidative damage. Should superoxide be converted to H_2O_2, it may then either be removed by the action of catalase or glutathione peroxidase, however any remaining H_2O_2 is free to be converted to the highly toxic hydroxyl radical following reaction with free ferrous (Fe^{2+}) ions (Trushina and McMurray, 2007).

1.3.3 Mechanisms of damage

The route by which oxidative stress induces damage in neurones is by direct molecular reactions of the ROS with DNA molecules (both mitochondrial and nuclear) and with structural molecules in the cell, particularly lipids. The main sites of reaction in lipid molecules are the double bonds found in unsaturated fats, with polyunsaturated molecules thus being especially vulnerable (see section 1.3.4, Weisbrot-Lefkowitz *et al.*, 1998).

Damage to cell membranes by lipid peroxidation is due both to direct action on membrane lipids, affecting the viscosity and function of the membrane itself and by damage to membrane proteins (acting as ion channels and transporters) by aldehydes that are produced by this lipid peroxidation (Mattson, 1998, Mattson, 2004). These effects on membrane functions reduce ion transport, hence increasing vulnerability to calcium influx and providing a secondary mechanism by which damage can be multiplied (Mattson, 1998). Furthermore reduced glucose transport secondary to glucose transporter damage causes a rapid decrease in ATP formation which further enhances vulnerability to excitotoxic damage by glutamate (Novelli *et al.*, 1987, Mark *et al.*, 1997).

The damage to mitochondrial function, particularly to the mitochondrial membrane, is a critical step in the cascade leading to apoptosis, as the cycles of further loss of ion balance and ATP production which are established by oxidative damage lead to worsening mitochondrial disruption. This could lead to loss of mitochondrial membrane potential, MPT pore opening and consequent release of calcium and cytochrome c from the mitochondrial matrix, causing activation of caspase-9 and resultant apoptosis. However, triggering of this sequence of events is not dependent on apoptotic mechanisms, as it can also lead to neuronal death by necrosis (Chinopolous and Adam-Vizi, 2006).

1.3.4 Vulnerability of neurones

Cerebral metabolism is notably out of proportion to the volume of tissue concerned: although comprising only 2% of body weight, the brain is responsible for 20% of the body's oxygen use. The substrate used for cerebral energy metabolism is exclusively glucose, although ketone bodies are used in prolonged (three weeks or more) starvation (Champe and Harvey, 1994).

Cell damage due to ischaemia is extensively mediated via ROS, to which the brain is especially vulnerable for several reasons. These include the fact that the brain's high rate of respiration causes the production of a higher quantity of ROS than in other tissues.

Additionally, the brain is especially vulnerable to the oxidative action of ROS due to the extensive amount of polyunsaturated fatty acids present within its

tissues and the lower levels of antioxidant enzymes compared with those available in other tissues (Weisbrot-Lefkowitz *et al.*, 1998).

There is a higher concentration of lipids containing polyunsaturated acyl molecules, which are especially vulnerable to the actions of ROS (Bolanos *et al.*, 1997). This is a potential explanation for the heightened vulnerability; as such damage could rapidly translate into reduced ATP formation and ability to cope with calcium influx due to ongoing neurotransmission, hence the damage to neurones could be rapidly compounded.

1.3.5 Involvement of tryptophan metabolites

The metabolism of tryptophan in the body is unavoidable, as its status as an essential amino acid necessitates its inclusion in the diet (Champe and Harvey, 1994). The kynurenine pathway constitutes the primary route for the catabolism of tryptophan and hence exposure to the compounds found on this pathway will be similarly unavoidable. Therefore it is unfortunate that several of these compounds have neurotoxic properties, with effects noted in neuronal cultures, brain slices and from *in vivo* studies. The reasons that the metabolism of tryptophan, rather than that of other essential amino acids such as phenylalanine, is of interest are that one of its metabolites (QA) is the only known endogenous agonist of the NMDA receptor and another (kynurenic acid) is an endogenous glutamate receptor antagonist (Foster *et al.*, 1984). The pathway therefore provides a unique opportunity to examine endogenous sources of excitotoxic damage.

Tryptophan can be metabolised into melatonin, although the main route for the catabolism of tryptophan in the body is via the kynurenine pathway, which ultimately leads to the production of nicotinamide (Figure 1.1). The first step is the conversion of tryptophan into formylkynurenine by indolamine dioxygenase, which is then converted (by kynurenine formylase) to kynurenine (Stone, 2000).

Kynurenine can then be metabolised in a number of different ways, one of which leads to the production of kynurenic acid, although the main pathway of kynurenine catabolism leads to the production of a number of neurotoxic compounds, capable of effecting damage through both excitotoxic and oxidative mechanisms. There are two sub-pathways through which kynurenine catabolism

may take place, although the common end-point of both, immediately prior to the formation of nicotinamide, is the formation of QA. It is not possible to completely avert metabolism away from this route, as it leads to the synthesis of nicotinamide, which is essential for normal metabolic function in the cell.

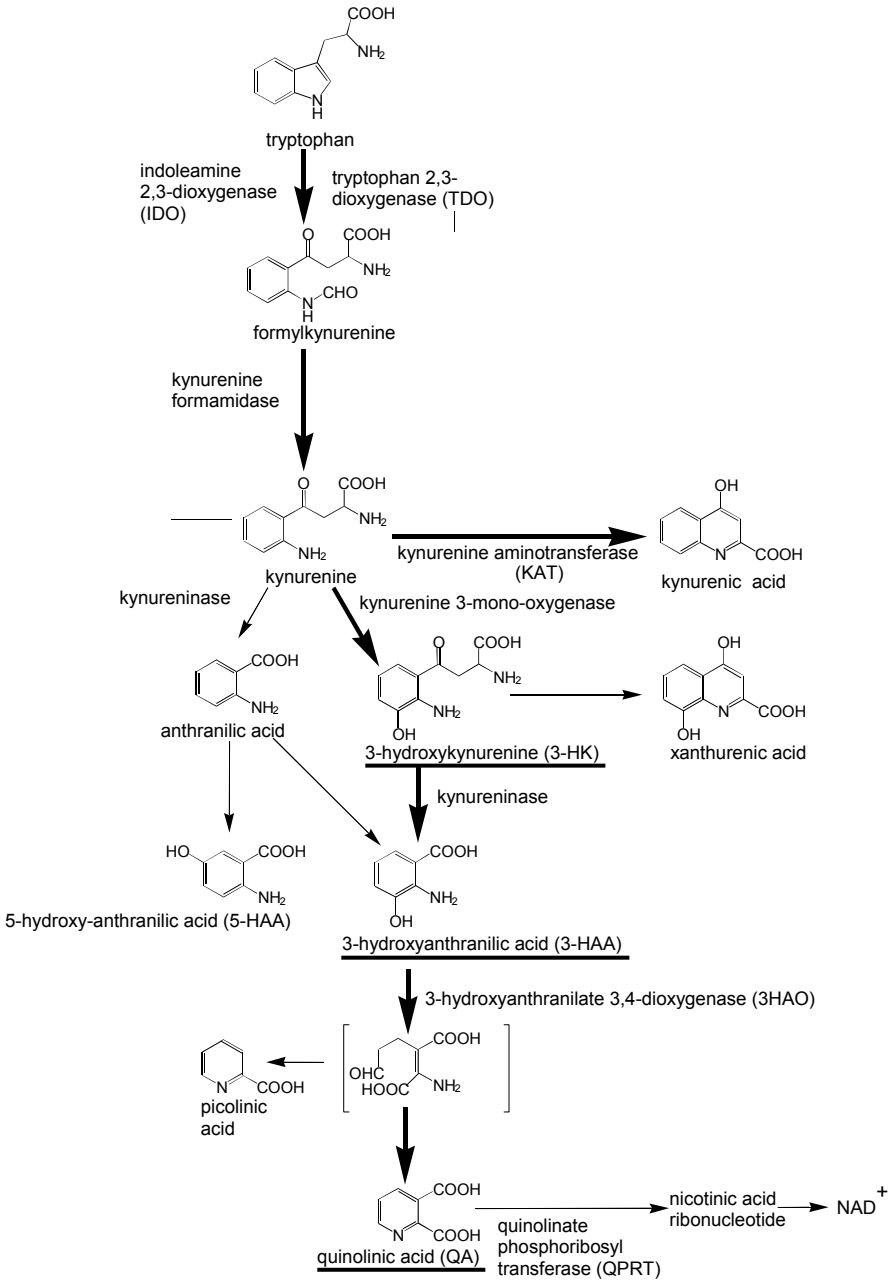

Figure 1.1 – Simplified diagram of kynurenine pathway (adapted from Stone, 2000), showing route of metabolism from tryptophan to nicotinamide and main pathway branches; compounds with previously identified neurotoxic properties marked by underlining.

Quinolinic acid has both excitatory (via NMDA receptors) and neurotoxic properties, with injection of QA in rat striatum *in vivo* producing an axon-sparing neurodegenerative lesion, proportional in volume to the QA dose applied (Perkins and Stone, 1983, Schwarcz *et al.*, 1983, Guidetti and Schwarcz, 1999).

Further study of QA toxicity *in vivo* found that injection of a nanomolar concentration of QA increased expression of JNK and p38 in the lesion core, which although no longer evident at 24 hours correlated with areas of subsequent cell death (Ferrer *et al.*, 2001).

Quinolinic acid neurotoxicity is closely related to its ability to act as an NMDA receptor agonist, as it can be attenuated by co-application of kynurenic acid or MK-801 (Rios and Santamaria, 1991, Chiarugi *et al.*, 2001). It is also clear that QA neurotoxicity involves generation of oxidative stress, as application of QA to rat brain homogenates caused a significant increase in lipid peroxidation and QA-induced damage was reduced in a dose-dependant manner by co-administration of the antioxidant melatonin (Rios and Santamaria, 1991, Behan *et al.*, 1999). Furthermore, the co-application of the free radical generator xanthine oxidase significantly potentiated QA neurotoxicity in rat hippocampus *in vivo*, whereas each compound applied alone caused only minor neuronal loss (Behan and Stone, 2002).

Co-application of the NOS inhibitor, nitroindazole, or the poly (ADP-ribose) polymerase (PARP) inhibitor, 3,4-dihydro-5-[4-1(piperidinyl) buthoxy]-1(2H)-isoquinolone (DPQ), significantly reduced damage due to QA application, although toxicity was not reduced by cyclosporine or the pan-caspase inhibitor, carbonbenzoxy-valyl-alanyl-aspartyl-[O-methyl]-fuoromethylketone (Z-VAD-fmk), indicating that QA neurotoxicity is more likely to induce neuronal death via necrosis rather than apoptosis (Chiarugi *et al.*, 2001). Injection of QA into the somatosensory cortex caused cell death with necrotic features in the core of the injection-induced lesion, with no activation of caspase-3 seen in any neurones, although there was transient positive staining of p38 and JNK in the core, which was absent by 24 hours (Ferrer *et al.*, 2001).

As previously described, there is strong evidence linking QA to the AIDS dementia complex, particularly with regard to increased QA levels, produced by microglia due to neuroinflammatory processes and leading to increased QA levels both in CSF and brain parenchyma. There is also evidence suggesting a link between QA and cerebral malaria, possibly due to the utilisation of the kynurenine pathway in the inflammatory responses mediated by microglia. In a retrospective study, the CSF of children diagnosed with malaria was compared with a control group

of samples taken from healthy adults, with a significant association found between higher QA concentrations in the CSF and an increased risk of mortality in patients with cerebral malaria (Medana *et al.*, 2003).

Although QA is long-established as a neurotoxic product of tryptophan metabolism, two other compounds on the main pathway leading to the formation of QA have also been identified as potent neurotoxins, namely 3-hydroxykynurenine (3-HK) and 3-hydroxyanthranilic acid (3-HAA). As these compounds show similar (although not identical) characteristics, the evidence for the neurotoxic effects of each will be considered together.

Application of 3-HAA for 48 hours induced a significant degree of apoptosis in monocyte-derived cell lines (U937 and THP-1), an effect enhanced by ferrous or manganese ions (Morita *et al.*, 2001). Although the use of the antioxidant enzymes catalase or SOD did not significantly attenuate toxicity, a significant reduction in apoptosis was induced by Trolox, α-tocopherol or allopurinol (Morita *et al.*, 2001). Although these experiments involved exogenous application of the compounds, which if generated in neurones will be cytoplasmic, the generation by cells throughout the body ensure that they will be distributed throughout the body via the bloodstream, and in the case of 3-HK at least, will be taken up by neurones both *in situ* and in the experimental setting.

These effects were reproduced in striatal neurones, with 3-HK causing significant neuronal death, an effect prevented by the co-application of catalase or allopurinol, which indicated that the neurotoxic effect was due to oxidative damage (Okuda *et al.*, 1996). Further evidence reinforcing this was that *N*-acetylcysteine, an antioxidant particularly effective at scavenging the hydroxyl radical, provided protection against 3-HK-induced neurotoxicity (Okuda *et al.*, 1998).

Treatment of striatal neurones with 3-HAA produced a comparable level of neuronal death to that seen with 3-HK (Okuda *et al.*, 1998). Both 3-HK and 3-HAA are capable of generating ROS, specifically H_2O_2 and superoxide, when added to phosphate buffer solution, with both compounds causing reduction of cupric (Cu^{2+}) to cuprous (Cu^{+}), and of ferric (Fe^{3+}) to Fe^{2+}, at physiological pH (Goldstein *et al.*, 2000). Although superoxide was produced by both 3-HK and 3-HAA in phosphate-buffered saline (PBS) alone, the compounds were unable to

generate H_2O_2 in PBS alone, although both produced significant amounts of H_2O_2 in the presence of Cu^{2+}, with copper ions cycling between oxidised and reduced status during cycles of H_2O_2 generation (Goldstein *et al.*, 2000). The increased H_2O_2 production was completely abolished by catalase and notably inhibited by a reduction in molecular oxygen concentration (Goldstein *et al.*, 2000).

The importance of oxygen in the oxidation of 3-HAA was emphasised by a study which reported 3-HAA auto-oxidation in aerobic reaction solution but not anaerobic, with oxidation of 3-HAA increased dramatically by addition of Cu,Zn-SOD (but not Mn-SOD) to anaerobic solution or by re-admittance of air in anaerobic conditions (Liochev and Fridovich, 2001). It seems likely that the enhancement of oxidation by Cu,Zn-SOD was due to copper ions acting as redox reagents, rather than enzymatic activity (Liochev and Fridovich, 2001).

Although 3-HK and 3-HAA are capable of oxidising, they are in fact redox reagents and the antioxidant activity of 3-HK and 3-HAA has been successfully demonstrated in rat cerebral cortex homogenate, with incubation of homogenates with either 3-HK or 3-HAA for 1 hour reducing levels of ROS present (Leipnitz *et al.*, 2006). This effect was achieved with higher (100μM) concentrations of 3-HK and 3-HAA (although not 1 or 10μM), and reproduced in homogenate solutions containing either Fe^{2+} or Fe^{3+} ions (Leipnitz *et al.*, 2006). It should be noted however, that this experiment used predominantly glial cell types (these being the most numerous cell type in adult cerebral cortex homogenate), with similar results achieved using cells of glial tumour origin (Leipnitz *et al.*, 2006).

To further investigate the actions of 3-HAA on Fe^{2+} and Fe^{3+} ions, the effect of 3-HAA on methaemoglobin production (a form of haemoglobin in which the Fe^{2+} ions have become Fe^{3+} ions, and hence cannot function as oxygen transporters) from haemoglobin was studied: 3-HAA caused a concentration-related increase in the percentage of methaemoglobin and also the percentage of damaged 'non-intact' haemoglobin (Dykens *et al.*, 1989). Methaemoglobin formation was exacerbated by the presence of SOD, although not by catalase, with application of both SOD and catalase together giving very similar results to SOD alone (Dykens *et al.*, 1989).

The evidence linking 3-HK or 3-HAA with pathological conditions is less extensive than that implicating QA, although a study of pneumococcal meningitis in infant Wistar rats showed significant increases in 3-HK levels in cortex and hippocampus between 16 and 44 hours post-infection, with no rises found in plasma samples (Bellac *et al.*, 2006). Although 3-HAA levels increased at 44 hours in the hippocampus, the levels in either hippocampus or cortex were lower than those in plasma. There was correlation between 3-HK concentrations and increased apoptosis in the hippocampus; with 3-HK levels of 190nM or higher corresponding to higher levels of apoptosis (Bellac *et al.*, 2006).

Additionally, alterations in the activity levels of the enzymes which catalyze the reaction of the kynurenine pathway were seen, with significant rises in the activities of kynurenine-3-hydroxylase (which converts kynurenine to 3-HK) and kynureninase (converting 3-HK to 3-HAA) in both cortex and hippocampus (Bellac *et al.*, 2006).

1.3.6 Effects of hyperglycaemia

Given that oxidative phosphorylation, fuelled by glucose uptake, leads to ROS production and that an increase in the ratio of ROS: antioxidant defences leads to oxidative stress, it would be expected that hyperglycaemia or raised exogenous glucose would cause such damage. It has been shown that hyperglycaemia *in vivo* and raised glucose concentrations *in vitro* both cause a variety of effects, with increased neurotoxic effects seen due to hyperglycaemia/raised glucose directly and also manifested as heightened vulnerability to oxidative damage from other sources.

Streptozotocin-induced diabetes caused a significant increase in the lipid peroxidation product 4-hydroxy-2-nonenal (HNE) in hippocampal CA1 and CA3 regions and in Cu,Zn-SOD levels in rats subjected to restraint-induced stress, both indicating an increase in oxidative stress (Grillo *et al.*, 2003).

Hyperglycaemia *in vivo* enhances vulnerability to ischaemia, with ischaemia inducing significant increases in release of mitochondrial cytochrome c into the cytosol between 0.5 and 3 hours reperfusion, positive caspase-3 staining after 1 and 3 hours and positive terminal dUTP nick-end labelling (TUNEL) staining after 3 hours (Li *et al.*, 2001, Muranyi *et al.*, 2003). Cytochrome c release was

correlated with increased TUNEL staining compared to normoglycaemic animals subjected to ischaemia (Li *et al.*, 2001, Muranyi *et al.*, 2003).

Transient (30 minutes) middle cerebral artery (MCA) occlusion in diabetic rats caused more extensive ischaemia-related damage 3 and 6 hours post-occlusion in diabetic than non-diabetic rats (Muranyi *et al.*, 2003). Examination 7 days post-occlusion showed continued development of damage beyond 6 hours' reperfusion in non-diabetic but not in diabetic animals, although infarct volume in diabetic animals was significantly larger, demonstrating that ischaemic damage in diabetic animals was both more extensive and of more rapid onset (Muranyi *et al.*, 2003).

Comparable effects exist *in vitro*: exposing embryonic rat dorsal root ganglion (DRG) neurones cultured in medium with 25mM glucose to 'hyperglycaemia' (induced by raising the concentration to 45mM), demonstrated that this increase in glucose caused a range of effects. These included: increased NADH oxidase activity, increased ROS generation, mitochondrial swelling and disruption of inner cristae, caspase-3 cleavage and TUNEL staining, and greater responses from antioxidant defences, with expression of SOD and catalase increased (Vincent *et al.*, 2005).

Although hyperglycaemia can increase apoptosis due to osmotic effects, glucose has an effect beyond hyperosmolarity and DRG neurones of diabetic rats suffered from a progressive increase in intracellular calcium (Sima, 2003). Additionally, increased glucose levels induce alterations in redox status, dysregulation of glutathione synthesis and glucose autoxidation, generating ROS (Sima, 2003).

N-methyl-D-aspartate receptor activation in neonatal rat CGNs caused a concentration-dependent increase in glucose uptake which was seen from 2 DIV, reaching its maximum by 8 DIV, with increases also seen following kainate and AMPA receptor stimulation (Minervini *et al.*, 1997).

It appears however, that the concentration-dependent effect of increasing exogenous glucose concentrations can be limited: the rate of glucose oxidation in cultured mouse cortical neurones became saturated when the extracellular concentration of glucose reached 1.4mM, with no further rise when this concentration was increased up to 16.7mM (Gorus *et al.*, 1984). Use of radio-

labelled 2-deoxyglucose in neonatal rat CGNs showed that saturation occurred at 4mM (Minervini *et al.*, 1997). 2-Deoxyglucose is an effective tool for studying this effect, as it is phosphorylated (phosphorylation being the rate-limiting step of glucose utilisation), although it should be noted that phosphorylation uses ATP rather than generates it (Whitesell *et al.*, 1995).

However, as with the *in vivo* studies, the possibility remains of a more subtle increase in underlying vulnerability to subsequent damage from a neurotoxic stimulus, despite the absence of any obvious increase in cell death. It should be noted that such strikingly raised glucose levels as decribed above will be rare in diabetic patients, with diagnosis and subsequent treatment acting to avert such increases. However, notable increases will still occur, which although less extensive in size will be for much more prolonged periods than in the studies described above.

1.4 Preconditioning

1.4.1 Background overview

Extensive study has been carried out concerning the protective mechanism termed 'preconditioning' following work by Murry *et al.* (1986). This term referred to the protection conferred on tissue by brief periods of ischaemia against a subsequent, more severe ischaemic episode. This protective effect was initially demonstrated in canine myocardium, using a protocol of four 5-minute circumflex artery occlusions, after which an infarction was caused by a sustained 40-minute occlusion of the circumflex. The resultant average infarct in preconditioned animals was reduced in size by 75% relative to the average infarct seen in control animals.

It has been recognised that preconditioning can occur in two ways: early and delayed preconditioning, which take place over approximate periods of up to 2 hours and from 24 hours to 3 days respectively (review: Halestrap *et al.*, 2007). Early preconditioning has received the greatest attention in studies concerned with cardiac preconditioning.

There is evidence that the generation of ROS during cardiac preconditioning causes activation of protein kinase C, specifically the epsilon subtype. This

protein appears to play an integral part in mediating protection, as ischaemic preconditioning cannot be induced in mice with the protein kinase C gene knocked out (Saurin *et al.*, 2002). Activation of protein kinase C by ROS is a critical step, with scavengers of free radicals preventing protein kinase C activation and preconditioning (Baines *et al.*, 1997).

Inhibition of the opening of the MPT pore is a major component of the mechanism of cardiac preconditioning: this opening is triggered by calcium influx combined with oxidative stress, hence reduction of these by preconditioning acts to inhibit MPT pore opening (Halestrap *et al.*, 2007). A possible mechanism for this is that preconditioning causes opening of mitochondrial ATP-sensitive potassium (K_{ATP}) channels, resulting in a reduction in mitochondrial polarisation which reduced ROS formation due to decreased calcium uptake, but not sufficient to impair ATP formation.

Another phenomenon identified following the discovery of preconditioning was postconditioning, which refers to intermittent interruptions in blood flow which occur *after* an ischaemic insult. This method is effective in inducing a degree of protection similar to early preconditioning, although there does not appear to be an additive effect on protection from the use of both in rat (Zhao and Vinten-Johanson, 2006), however combined treatments did give synergistic protection in rabbit (Yang *et al.*, 2004).

It is not clear whether protection due to postconditioning is induced by the recurrence of brief episodes of ischaemia or of reperfusion, but to be effective postconditioning must occur immediately after the commencement of reperfusion (Zhao and Vinten-Johanson, 2006). There are several mechanisms common to both pre- and postconditioning, including increased mitochondrial ROS generation, protein kinase C signalling, activation of K_{ATP} channels and inhibition of MPT pore opening (Zhao and Vinten-Johanson, 2006).

However, a notable finding regarding the clinical potential of preconditioning is that ischaemia severe enough to cause pain (pre-infarction angina) was not associated with a reduction in infarct size or improvement in clinical outcome following acute myocardial infarction (Psychari *et al.*, 2004). This suggests that the degree of stress to which cells are subjected must be of considerable severity for cardiac early preconditioning to effectively occur. A possible

candidate for a ‘common link’ of convergence of pathways triggered by preconditioning is inhibition of glycogen synthase kinase 3β (GSK-3β), preventing MPT pore formation (Juhaszora *et al.*, 2004).

A link between the mechanisms of preconditioning thus far identified and protection against oxidative damage in the brain is that a hippocampal neuronal cell line (HT22) which expresses elevated levels of GSK-3β shows increased resistance to neurotoxicity induced by glutamate or H_2O_2 (Schäfer *et al.*, 2004).

Both early and delayed preconditioning have been studied in brain tissue, with the first finding concerning ischaemic preconditioning *in vivo* by Kitagawa *et al.* (1990). A wide range of studies of this phenomenon have been performed, in a large number of laboratories using different neuronal types (Damschroder-Williams *et al.*, 1995, Blondeau *et al.*, 2001, Tauskela *et al.*, 2001, Meller *et al.*, 2005). Studies concerning the investigation of early preconditioning involved mechanisms similar to those described in cardiac preconditioning, whereas delayed preconditioning in neurones involves different mechanisms, with particular focus on NMDA receptor activation.

The preconditioning protocol used in the first demonstration was of two 2-minute ischaemic episodes, followed after a two-day interval by a 5-minute ischaemic event (caused by occlusion of both common carotids), which yielded a significant protective effect (Kitagawa *et al.*, 1990). Similar benefits were achieved using ischaemia to precondition the cerebral cortex of adult male Sprague-Dawley rats (Zhang *et al.*, 2003). This work used a preconditioning protocol of two 20-minute carotid artery occlusions 20 minutes prior to occlusion of the ipsilateral middle cerebral artery for six hours, which reduced the average infarct volume by 60% in preconditioned animals relative to non-preconditioned subjects.

The discovery of ischaemic preconditioning in the brain *in vivo* was complemented by findings of Schurr *et al.* (1986) that exposure of adult rat hippocampal slices to a brief period of anoxia allowed them to regain electrical activity after exposure to a subsequent longer episode of hypoxia.

The protective effect of ischaemia *in vivo* can be reproduced with OGD *in vitro*: preconditioning by OGD for 5-30 minutes protected cultured murine cortical

neurones against a subsequent 45-55 minute insult, with the protective effect present between 7 and 72 hours (Grabb and Choi, 1999). Preconditioning with OGD in rat cortical neurones gave protection against a subsequent severe OGD insult, which was effective against both necrotic and apoptotic cell death (Arthur *et al.*, 2004).

There are interactions between NMDA and adenosine receptors, with stimulation of presynaptic adenosine A_1 receptors reducing calcium influx and glutamate release, and stimulation of postsynaptic A_1 receptors increasing potassium efflux, with resultant hyper-polarisation of cell membranes (review: de Mendonça *et al.*, 2000). Both of these effects reduce NMDA receptor stimulation and therefore decrease calcium influx. However, A_{2a} receptors act to stimulate glutamate release (Popoli *et al.*, 1995). In the context of ischaemia, application of an A_1 receptor agonist reduced ischaemia-related increase in extracellular glutamate and other excitatory amino acids (Goda *et al.*, 1998).

The role of adenosine receptors in preconditioning is complex, with some receptor subtypes mediating a protective effect and other subtypes harmful effects. Antagonism of adenosine A_{2a} receptors reduces damage in cerebral infarction, whereas antagonism of A_1 receptors enhances ischaemic damage (Phillis *et al.*, 1995, Melani *et al.*, 2003). However, it should be noted that not all models required A_1 receptor activation (Tauskela *et al.*, 2003).

Early preconditioning-induced protection in rat hippocampal slices with sublethal OGD against subsequent otherwise lethal OGD completely prevented by A_1 receptor antagonists, whereas A_3 receptor antagonists enhanced the protection of preconditioning (Pugliese *et al.*, 2003). The use of A_{2a} antagonists in this study was not found to have any identifiable effect on preconditioning (Pugliese *et al.*, 2003).

Although A_1 receptor stimulation is generally accepted to be beneficial and A_3 receptor stimulation harmful, the role of the A_{2a} receptor is rather less clear-cut, with a study of the effect of A_{2a} agonists and antagonists on kainate-induced excitotoxicity finding protective effects from both groups (Jones *et al.*, 1998).

Another interesting aspect of the role of adenosine receptors is the difference in effect seen when comparing acute and chronic use of A_1 receptor agonists and

antagonists. Agonists were protective when applied acutely, but detrimental when applied chronically, with the detrimental effect of A_1 antagonists' acute application reversed when applied chronically (review: de Mendonça *et al.*, 2000).

An important question is whether the preconditioning phenomenon actually exists in humans; otherwise the clinical benefit of understanding the mechanisms of preconditioning may be minor or even non-existent. There is however evidence which suggests that a protective preconditioning effect may indeed be inducible in humans suffering sub-lethal ischaemia.

A study of patients presenting with their first CVA (cerebro-vascular accident, i.e. a stroke) involved MRI imaging of the patients' brains within twelve hours of the onset of their CVA symptoms (Wegener *et al.*, 2004). It was found that patients who had experienced a transient ischaemic attack (TIA, in which symptoms and signs consistent with a CVA resolve fully within 24 hours) within the four week period prior to the CVA had smaller final infarct sizes than those patients with no history of a previous TIA (Wegener *et al.*, 2004).

A larger study concerning clinical evaluation of the severity of patients' presenting symptoms, and the extent of final recovery, identified that a previous TIA was associated with both reduced severity in presenting symptoms of a first-presentation CVA, and with a more favourable outcome, with a prolonged interval between TIA and CVA reducing protection (Moncayo *et al.*, 2000, Sitzer *et al.*, 2004). The protective effect was such that despite compensating for the reduced severity of presenting symptoms, previous TIA was still associated with a greater likelihood of a more complete recovery (Sitzer *et al.*, 2004).

1.4.2 NMDA receptor involvement and associated mechanisms

Preconditioning neurones with a subtoxic concentration of NMDA prior to a toxic application of glutamate or OGD will greatly improve rates of neuronal survival against the toxic insult (Marini and Paul, 1993, Tauskela *et al.*, 2001). However, this protection was significantly reduced by inhibition of protein or RNA synthesis at the time of NMDA preconditioning (Marini and Paul, 1993, Damschroder-Williams *et al.*, 1995). The period over which the application of

sub-toxic NMDA provided protection against a toxic application of glutamate was over a range of 12-48 hours (Damschroder-Williams *et al.*, 1995).

Stimulation of NMDA receptors in CGNs caused release of brain-derived neurotrophic factor (BDNF), with subsequent increase in neurotrophin receptor TrkB tyrosine phosphorylation, due to BDNF binding with and activating TrkB. Blockade of either the NMDA receptor site or of TrkB receptor prevented preconditioning (Marini *et al.*, 1998).

The transcription factor nuclear factor kappa B (NF-κB) was also involved in the mediation of NMDA receptor-induced protection, with preconditioning completely lost if cells were pre-treated with NF-κB target DNA acting as a 'decoy' for the transcription factor and blocking any protein synthesis that would have been mediated by it (Marini *et al.*, 1998, Ravati *et al.*, 2001). Nuclear factor kappa B is a family of transcription factors that regulate genes involved in several processes, including growth factor regulation, cell proliferation and apoptosis. Normally found in the cytosol, in an inactive complex with the inhibitory protein IκBα, NF-κB is phosphorylated and degraded upon complex activation, with active NF-κB subsequently released (Ravati *et al.*, 2001).

Preconditioning rat cortical cell cultures with either sub-lethal OGD or NMDA provides protection against subsequent otherwise lethal exposure to either glutamate or OGD, i.e. cross-tolerance between the two toxic insults was demonstrated (Tauskela *et al.*, 2001).

There are complicated interactions between delayed preconditioning and adenosine, with findings from different studies frequently at variance. The use of adenosine or a range of adenosine A_1 receptor antagonists before, during and after OGD preconditioning did not affect protection against lethal OGD (Tauskela *et al.*, 2003). In contrast, Boeck *et al.* (2005) found that co-application of the A_1 receptor antagonist 8-cyclopentyl-1,3-dimethylxanthine (8-CPT) prevented NMDA preconditioning.

A study of the involvement of adenosine receptors investigated the effect on NMDA preconditioning against a subsequent glutamate insult of the co-application of A_1 and A_{2a} receptor antagonists, showing that the adenosine A_1

antagonist 8-CPT prevented NMDA preconditioning, whereas the A_{2a} receptor antagonist 4-(2-[7-amino-2-(2-furyl{1,2,4}-triazolo{2,3-a{1,3,5}triazian-5-yl-aminoethyl)phenol (ZM 241385) did not affect the protection (Boeck *et al.*, 2005). It was suggested that NMDA preconditioning reduces the amount of adenosine formed by AMP hydrolysis, this adenosine having preferentially activated A_{2a} receptors (Boeck *et al.*, 2005).

Pre-treatment of neonatal rat CGNs with kainate or glutamate and glycine, followed by exposure to an otherwise lethal glutamate and glycine insult, significantly reduced the neurotoxic calcium influx induced by glutamate and glycine (Ward *et al.*, 2005). However, this contrasted with the findings of Chuang *et al.* (1992), who successfully preconditioned CGNs with NMDA, but not kainate, and with another study which found no protection by kainate preconditioning in murine neuronal cultures (Grabb and Choi 1999).

Pre-treatment of rat CGNs with the QA for 6 hours prior to application of a neurotoxic glutamate treatment caused a 68% reduction in apoptosis in QA-treated cultures compared with controls (Sei *et al.*, 1998). Protection was lost in the absence of glucose and magnesium, or in the presence of an NMDA receptor antagonist. However QA was incapable of protecting against necrosis induced by glutamate and this protective effect was not evident against apoptosis induced by exposing neurones to 5mM potassium chloride (KCl) (Sei *et al.*, 1998).

1.4.3 Alternative methods

An alternative approach to inducing protection by preconditioning has recently been examined, using lower-intensity stimulation of NMDA receptors for a more prolonged period, prior to subjecting the neurones thus treated to a neurotoxic stimulus. This has been investigated in cultures of hippocampal and also of cerebral cortical neurones, with a significant degree of protection provided in each case to a variety of neurotoxic insults (Papadia *et al.*, 2005, Soriano *et al.*, 2006, Tauskela *et al.*, 2008).

The stimulation of rat hippocampal neurones in culture with the $GABA_A$ receptor inhibitor bicuculline is effective in causing an increase in neuronal firing, due to stimulation with glutamate released because of the loss of GABA-mediated inhibition. This caused NMDA receptor stimulation and a resultant increase in

action potential (AP) firing, with receptor stimulation restricted to synaptic NMDA receptors only. This treatment was effective in conferring resistance to apoptosis induced by trophin deprivation or a variety of toxic agents: staurosporine, C-2 ceramide, retinoic acid or okadaic acid (Papadia *et al.*, 2005).

These actions were potentiated by co-application of the potassium channel inhibitor 4-aminopyridine (4-AP), which was effective in amplifying both the AP-generating and neuroprotective effects of bicuculline treatment. The importance of AP generation in inducing protection was confirmed by use of the sodium channel blocker tetrodotoxin (TTX), co-application of which abolished protection (Papadia *et al.*, 2005).

This method of stimulation significantly increased CREB (cyclic-AMP response element binding protein) phosphorylation, an NMDA receptor-dependent effect. Although blockade of CREB gene expression with inducible cAMP early repressor (ICER), an inhibitor of CREB, significantly reduced CREB gene expression in bicuculline-stimulated cultures, it did not prevent the bicuculline-mediated protective effect when stimulation was continued until the toxic stimulus.

Although the CREB pathway is not involved in protection in the short term, when bicuculline treatment was followed by a pause preceding a toxic insult, CREB pathway activation was important, as protection induced by the bicuculline and 4-AP increased neuronal survival was blocked by ICER. Nuclear calcium and calmodulin signalling were necessary for the delayed form of neuroprotection, but not for short-term protection (Papadia *et al.*, 2005).

Another method for providing stimulation of NMDA receptors in rat hippocampal neurones was the use of very low concentrations of NMDA itself, applied for 12-24 hours to stimulate both synaptic and extra-synaptic receptors prior to a neurotoxic insult (although the majority of the resultant calcium influx occurs via synaptic NMDA receptors). Neuroprotection was demonstrated against both excitotoxic and apoptotic stimuli (glutamate, staurosporine or neurotrophin deprivation), with effective protection generated in both acute and long-lasting forms (Soriano *et al.*, 2006). Protection was again dependent on AP production, and was still evident 48 hours after termination of the NMDA stimulus (Soriano *et al.*, 2006).

This method of preconditioning did not affect mitochondrial membrane potential (although higher concentrations of NMDA caused a progressive decrease in mitochondrial membrane potential and an associated increase in toxicity). Intracellular Rhodamine red dye showed that levels of NMDA that induced effective preconditioning caused transient increases in mitochondrial calcium, whereas toxic levels of NMDA caused sustained rises in mitochondrial calcium (Soriano *et al.*, 2006). There were further differences in calcium influx patterns, with preconditioning stimuli causing cytoplasmic calcium levels to 'spike' briefly and then oscillate at a lower level, whereas cytoplasmic calcium rises in response to higher concentrations of NMDA were sustained and non-oscillatory (Soriano *et al.*, 2006).

As with bicuculline-induced neuroprotection, NMDA treatment induced AP generation-dependent CREB activation and was also associated with an increase in BDNF mRNA expression (which could be blocked by TTX). A similar AP-dependent effect was seen with phosphorylation of TrkB, the BDNF receptor (Soriano *et al.*, 2006).

A further demonstration of the effectiveness of lower-intensity NMDA receptor stimulation as a neuroprotective stimulus was identified by the use of bicuculline and 4-AP to effectively protect rat cerebral cortical neurones against OGD (Tauskela *et al.*, 2008). This protection was induced by treatment for 48 hours prior to OGD exposure for 65-80 minutes and was effective over an interval of 24 to 72 hours between preconditioning and OGD, although if the intervening period was extended to 96 hours then protection was lost.

Calcium influx, as with the studies using hippocampal neurones, was seen in response to bicuculline and 4-AP treatment, and was abolished by TTX or by NMDA receptor blockade, with the associated protection prevented by TTX treatment and reduced by NMDA antagonism (Tauskela *et al.*, 2008).

Activation of CREB was also identified in this work, with phosphorylation abolished by TTX. Blockade of NMDA receptors reduced CREB phosphorylation due to stimulation with lower doses of 4-AP, but CREB phosphorylation induced by higher concentrations of 4-AP was not prevented by NMDA antagonism (Tauskela *et al.*, 2008).

Taken together, these results demonstrate that an effective, AP-driven mechanism of preconditioning exists, which utilises the activation of CREB to provide protection against neurotoxic damage from a wide range of agents. This represents a potential method for the development of preconditioning-based protection, but without the necessity for a moderate-to-severe stimulus which puts neurones in jeopardy of suffering excitotoxic or oxidative damage.

1.5 Cerebellar granule neurones

1.5.1 CGN anatomy and physiology

The cerebellum is part of the hindbrain, with connections to each part of the brainstem: the inferior peduncle connects with the medulla oblongata, the middle peduncle with the pons, and the superior peduncle with the junction of the pons and midbrain. The prime function of the cerebellum is to coordinate motor activity through connections with brainstem motor centres.

Like the cerebral hemispheres, each of the cerebellar hemispheres has a layer of grey matter on its surface, comprised of three cell layers. The most superficial layer is the molecular layer; the middle layer consists of a single layer of Purkinje cells, with dendrites extending to reach the molecular layer and axons projecting in the opposite direction (i.e. away from the cerebellar cortical surface). The innermost layer of the cortex consists primarily of CGNs, the dendrites of which receive afferent input from the cortex, whereas axons of these cells extend to the superficial layer, where they branch at an angle parallel to the cerebellar hemisphere's surface, forming interconnections between neurones (Bowsher, 1988, Trenkner, 1998).

Cerebellar granular neurones are small, with a large nucleus, and are by far the commonest neuronal subtype in mammals, with more than 70 billion found in the adult human cerebellum (Lange, 1975). After birth, the CGNs migrate from the external to the internal granule cell layers, where they receive excitatory input from mossy fibre neurones. If they do not migrate to the correct location, the granule neurones die from apoptosis, probably due to loss of depolarising input from mossy fibres (Wood *et al.*, 1993). A similar process has been recognised in cultured CGNs, specifically that calcium flux due to depolarisation is essential for survival in neonatal rat CGNs (Gallo *et al.*, 1987).

When CGNs are depolarised, calcium influx via voltage-dependent calcium channels increases, activating calcium-calmodulin dependent kinases and calcineurin phosphatase (Nakanishi and Okazawa, 2006). Calcineurin phosphatase activation is associated with genes involved in CGN differentiation and neurite growth in the external granule layer, whereas inactivation of calcinueurin is associated with genes coding for $GABA_A$ receptor and NR2C subunits, both integral to synaptic transmission involved in CGN maturation in the internal granule layer (Nakanishi and Okazawa, 2006).

The developing cerebellar cortex of Sprague-Dawley rats is affected by the mothers (prior to the birth of the test subjects) being fed a diet deficient in tryptophan, when compared to both rats fed a generally protein deficient diet, and those fed a normal diet. This tryptophan-deficient diet was associated with retarded maturation of Bergmann glial cells (manifested by the persistence of basal filopedia, which normally disappear at 15-19 days) and abnormal migration of CGNs, with granule cells staying in the upper molecular layer of the cerebellar cortex for longer than in control animals before migrating to the granular layer (Del Angel-Meza *et al.*, 2001).

Cerebellar granule neurones in rat neonates actively transport glucose via the GLUT3 transporter, a neurone-specific and high-affinity glucose transporter identified in pre- and post-synaptic areas of neurones and with mitochondria (Maher *et al.*, 1996, Leino *et al.*, 1997).

1.5.2 Reason for use of CGNs in present study

As the cerebellum contains only a small number of neuronal subtypes, with CGNs massively outnumbering Purkinje cells by a ratio of 897 to 1 in rat (or by 2991 to 1 in humans), cerebellar material provides a model with a highly purified and homogenous population of neurones (Lange, 1975). Cerebellar granule neurones are known to release glutamate as their principal neurotransmitter and can produce glutamate independently of glial cells (Hassel and Bråthe, 2000). Cultures of this type of neurone have been used in studies concerning cell viability, excitotoxicity, oxidative stress and preconditioning (White *et al.*, 1996, Atlante *et al.*, 1997, Marini *et al.*, 1998, Ward *et al.*, 2005); with CGN cultures well-recognised as an effective tool for investigation in these areas.

Another reason that use of CGN cultures was suitable was that this cell type is known to produce BDNF, rather than the alternative neurotrophins nerve growth factor, neurotrophin-3 or neurotrophins-4/5, as BDNF has been demonstrated to be involved in the establishment of preconditioning (Marini *et al.*, 1998).

An additional benefit of using this neuronal type was that the cells were prepared from neonatal rather than embryonic animals, as CGNs continue to develop post-natally, and can therefore be harvested later than cerebral cortical neurones for example (Trenkner, 1998). Therefore the actual number of cerebella available was known in advance, allowing experimental design to be tailored to best utilise the available material.

1.5.3 Advantages of cell culture technique

The use of cell culture allows the effects of neurotoxic insults on neurones themselves to be identified and studied in isolation, as glial cells can be eliminated, thereby preventing any protective or potentiating actions of that cell population occurring. When using cell cultures, there is the option of using cell lines, with immortalised cells which reproduce and form monolayer cultures consisting entirely of clones of one cell. This allows complete homogeneity of cultures, but the very nature of these cells means that they are substantially altered; raising questions over how relevant any findings made would be to normal tissue (Smith and Jiang, 1994). For this reason, primary cultured neuronal cells are preferable for use in studies *in vitro*.

The effect of alteration in cell environment, such as the concentration of glucose and ions in the culture medium, can be studied with great accuracy, as it is possible to control medium conditions precisely.

Similarly, an experimental protocol involving exposure of cultured neurones to (for example) OGD for a set period can be achieved with a high degree of consistency across all repetitions of the experiment. Furthermore, the use of one isolated cell type reduces a number of potential sources of variation, allowing results with a higher degree of consistency to be produced.

It should be noted that although this reductive approach has these advantages, there are also limitations: for instance, the absence of glial cells causes

alterations to the formation of synapses, as there are no glial cells to sheath these connections as would normally be the case. Additionally, the cell preparation process itself must unavoidably involve a short period of stress for the neurones, although as cultures were maintained for at least 8 days prior to treatments, the effect of this on the CGNs during experiments was minimised.

1.6 Rationale of study

1.6.1 Reasons for study

As the processes of excitotoxicity and oxidative stress are integral to the generation of neuronal death during ischaemia and neurodegenerative disease, the current study set out to investigate these processes and means of protecting against them. Elevated glucose and tryptophan metabolites are two sources of potential oxidative damage which are both widespread and unavoidable, and therefore were selected for detailed study.

The use of preconditioning to protect against neuronal death provides a potential endogenously-generated source of effective neuroprotection, with great potential benefit.

1.6.2 Aims of study

The initial aims of the study were to establish reliable neuronal cell culture methods, optimise the conditions for neuronal growth and development and ascertain the effectiveness of available viability assays, in order to select the most appropriate.

A major part of this study was to determine the optimal methods of inducing excitotoxic and oxidative damage in neuronal cultures, and to establish the most suitable method for subjecting CGN cultures to OGD. Particular focus was given to the study of selected tryptophan metabolites, including investigation of the mechanisms of damage in both a pharmacological and molecular context.

The investigation of preconditioning protection was another key area of this study and development of two different methods of generating this protection was carried out. The mechanisms involved in the most effective method were explored, again with regard to both pharmacological and molecular aspects.

2 Materials and Methods

2.1 CGN culture procedures

The following reagents and consumables were used routinely in preparing primary cultures of cerebellar granule neurones.

2.1.1 Culture preparation materials

Minimum Essential Medium (Gibco, 32360-026)

Fetal Calf Serum –heat inactivated (Sigma, F9665)

L-Glutamine 200mM solution (Gibco, 25030-024)

Potassium chloride (BDH Laboratory Supplies, 101984L)

Gentamicin 50mg/ml (Gibco, 17570-037)

Phosphate Buffered Saline 1x, (Gibco, 14200-067)

Magnesium sulphate powder (FSA Laboratory Supplies, M/1050)

Bovine Serum Albumin (Sigma, A2153)

D (+)-Glucose powder (Fisher Scientific, G/0500/53)

Trypsin [porcine pancreas] powder (Sigma, T4799)

Soy Bean Trypsin Inhibitor liquid (Sigma, T6414)

Deoxyribonuclease I powder (Sigma, D5025)

96-well plate (Corning Costar 3596)

24-well plate (Corning Costar 3524)

13mm Borosilicate Glass coverslips (BDH, 406/0189/12)

100-mm Petri dish (Nunc Delta 150350)

Poly-D-lysine (Sigma, P7280)

DEPC-Treated water (Invitrogen, 750024)

Trypan Blue dye (Sigma, T8154)

Cytosine arabinoside (Sigma, C1768)

Millipore filter (Minisart, 0.2μm pore size)

2.1.2 CGN medium, buffer and enzyme solutions

Eagle's minimum essential medium, supplemented with 10% fetal calf serum, 2mM glutamine, 50µg/ml gentamicin and KCl to a final concentration of 25mM was used. In some studies potassium supplementation was omitted, in which case a potassium concentration of approximately 5.4mM present from the serum and buffer alone was used for routine culture. Medium was prepared the day before plating and used within 5 days or discarded, to minimise the risk of L-glutamine degradation. In experiments requiring high-glucose medium, glucose powder was added to a concentration of 25mM in total (the medium's basal glucose concentration without supplement was 5.5mM). Medium was filter-sterilised before use and stored at 4°C.

The buffer solution was made of single-strength PBS, supplemented with 1ml of magnesium sulphate from 3.82% stock solution, 250mg of D-glucose and 300mg of BSA (bovine serum albumin) dissolved in a total volume of 100ml. If required, pH was adjusted to 7.4 with titrated 1M sodium hydroxide. Buffer was filter-sterilised before use and stored at 4°C.

This buffer was used as the diluent for the trypsin solution and both the 'weak' and 'concentrated' solutions of soy bean trypsin inhibitor (SBTI) and deoxyribonuclease (DNase). A stock solution of trypsin (5mg/ml) was prepared by dissolving trypsin powder in sterile water. 1ml of this stock was added to 19ml of buffer (i.e. a final concentration of 0.25mg/ml trypsin solution or 0.25%). SBTI stock was aliquotted directly from the supplier's stock solution, and DNase stock was produced from DNase I powder dissolved in sterile water at a concentration of 10,000 U/ml. The SBTI and DNase were added to the buffer to give respective concentrations of 5% and 500U/ml in the 'concentrated' solution and 0.75% and 80U/ml in the 'weak' solution.

2.1.3 Culture plate and dish preparation

96-well plates were used routinely for viability studies, with 24-well plates used in some preliminary work. For immunocytochemical (ICC) studies, cultures were plated in both 24-well (containing glass coverslips) and 96-well plates. Cultures for producing protein samples for Western blots were maintained in 100mm diameter Petri dishes to yield the required quantity of cell material.

In all cases, plates or coverslips were coated with poly-D-lysine (PDL) prior to the application of cells to enhance adhesion to the substratum. This involved dissolving PDL in DEPC (diethyl pyrocarbonate)-treated water to a final concentration of 15µg/ml for viability or Western blot studies and 50µg/ml for ICC work, the solution being applied to the growth surface for at least 24 hours. Plates were rinsed in sterile water for one hour, drained, and allowed to dry for a further 24 hours before plating neurones.

For 96-well plates, 50µl of PDL solution was applied to each well; for 24-well plates, 100µl was applied per well; for 100mm dishes, 5ml was applied per dish. An increased concentration of PDL was applied to ICC experiment plates to minimise cell detachment due to repeated aspirations and rinses during the ICC procedure.

Poly-D-lysine is widely used in cell culture work as a plating substrate. However, it is recommended that sterile water be used to wash away any free poly-D-lysine before cell plating, since otherwise the free poly-D-lysine may have a cytotoxic effect (Banker and Goslin, 1998).

2.1.4 Glass pipette preparation

Three nine inch disposable glass Pasteur pipettes were sterilised by autoclaving and prepared for trituration of cell suspension during culture preparation. Each Pasteur pipette had a different size of opening, the largest being of normal diameter, the smallest similar to the diameter of a P200 pipette tip and the third approximately half-way between the two. This was achieved by flaming the tips with a small Bunsen burner for varying periods, the pipettes rotated in the flame: this narrowed the tip apertures to the required degree. Following flaming, pipette tips were cooled in sterile water before use with cell material.

2.1.5 Animals for neuronal culture preparation

Sprague-Dawley rats aged 7-8 days are most commonly used by others using CGNs in studies of oxidative stress, excitotoxicity and preconditioning (Castilho *et al.*, 1998, Chuang *et al.*, 1992, Damschroder-Williams *et al.*, 1995, Marini *et al.*, 1998, Valencia and Morán, 2001). They were therefore used in our method in the present study for comparative purposes.

In 7-8 day old rat neonates, CGNs are still developing, but have begun to express NMDA receptors (Trenkner, 1998), whilst adenosine receptors of all four subtypes have also been identified as being present (Vacas *et al.*, 2003).

Litter sizes ranged from 6 to 16, with an average litter size of 11 (n=70). Neonates of either sex were kept in groups with the mother in cages at 21+/-2 °C, under a 12-hour light/12-hour dark cycle, the mother having access to food and water *ad libitum*.

2.1.6 Euthanasia

In order to minimise suffering, rats were given a lethal intraperitoneal dose of **mg of pentobarbital sodium, also known as 'Euthanal', (which does not interfere with experiments via unwanted effects on either NMDA or adenosine receptors) prior to brain tissue harvesting, thereby following the Home Office regulations for use of animals in scientific research, permitted under schedule 1 of the Animals (Scientific Procedures) Act of 1986.

Given that the harvesting procedure by necessity involves an ischaemic insult to the brain tissue, additional interference from the anaesthetic must be avoided, as this could increase uncertainty in the final results achieved. Of the anaesthetic agents that were easily available for use, pentobarbitone was found to have an acceptably low potential for side effects. Also, pentobarbitone has been demonstrated to have no neuroprotective effect against ischaemia-induced neuronal injury *in vivo* in gerbil hippocampal CA1 region, parietal cortex, caudate putamen and lateral thalamus (Ito *et al.*, 1999).

Pentobarbitone acts mainly on GABA receptors and sodium channels (Wartenberg *et al.*, 1999), and although NMDA receptor activity has been proposed, when tolerance to sedative actions of the NMDA antagonists CGP39551 and CGP37849 was achieved, no cross-tolerance to pentobarbitone was seen, suggesting that tolerance is not due to action at NMDA receptors (Rabbani *et al.*, 1995).

2.1.7 Dissection

The actual harvesting process itself involved the following stages:

- Decapitation (as already indicated, this was done *post-mortem*)
- Recovery of cerebella from cranium
- Separation of cerebella from remaining brain tissue and meninges

All equipment used was sterile, and procedures were carried out using aseptic technique. Decapitation was performed using large scissors, the cut being made through the mid-cervical region of the spine. The undamaged cerebellum was recovered from the cranium using fine dissection scissors to make two incisions from the foramen magnum, advancing anteriorly and laterally to a point approximately halfway between the foramen magnum and the orbit. It was then possible to retract the dorsal section of the skull, now a flap, without risking trauma to the cerebellum from either the incisions or skull retraction.

As the skull at this stage is still relatively soft and cartilaginous, reflecting the flap anteriorly causes the skull at the point of flexure to bend. This puts gentle pressure onto the area of the posterior cerebral hemispheres and midbrain, resulting in the cerebellum being pushed posteriorly and hence was considerably easier to dissect from the remainder of the brain.

The immediate removal of the cerebellum from the cranial cavity was achieved using fine forceps. The forceps blades were advanced anteriorly through the brainstem, held apart to allow the blades to pass immediately above and below the cerebellum. Once in a position anterior to the cerebellum, the blades were closed. This allowed removal of the cerebellum (usually with some adjoined brainstem tissue) from the cranium, after which it was placed in ice-chilled PBS and transferred to a 50mm Petri dish for fine dissection.

To remove unwanted brain tissue and meninges, the cerebellum was held in place using a 23-gauge needle, and fine-tipped forceps used to strip meninges from the surface of the cerebellum. A scalpel blade was used to sever the cerebellary peduncles attaching the cerebellum to any remaining pons and the isolated cerebellum was placed in a fresh container of chilled buffer solution. Isolated cerebella were transferred to a 35mm Petri dish and chopped to a fine

paste using the free scalpel blade to cut two series of twenty vertical strokes through the tissue, the second series oriented perpendicular to the first, and the resulting cell material used to prepare cell cultures.

2.1.8 Culture preparation

The culture plating protocol used for our culture work was based on one used successfully by Sam Greenwood in Dr. C. N. Connolly's group at Dundee University (Ward *et al.*, 2005) with some adaptations added to increase culture uniformity. This was selected as the most effective culture preparation method following attempts with three alternative protocols of culture preparation.

First, cerebellar cell material was transferred into 20ml of 0.25% trypsin solution at room temperature. The tube containing cell material and trypsin was incubated at 37°C for 20 minutes, with gentle swirling of the tube at 5-minute intervals, to allow trypsin to permeate the cell material as fully as possible. After incubation was complete, 20ml of 'weak' SBTI and DNase solution (concentrations of 0.75% and 80U/ml respectively) was added to the tube at room temperature, prior to 2 minutes' centrifugation at 1200 rpm in a Sanyo Harrier 18/80 centrifuge. The supernatant was aspirated and discarded.

Following this, 2ml of ice-chilled 'concentrated' SBTI and DNase solution (concentrations of 5% and 500U/ml respectively) was added to the cell material pellet, which was resuspended with a P1000 pipette tip, then further triturated through the three flame-polished Pasteur pipettes (ten strokes up and down through each pipette). Phosphate buffer solution was added to a final volume of 20ml and the suspension centrifuged at 1200 rpm for 2 minutes, and supernatant aspirated and discarded.

Two ml of culture medium, warmed to 37°C, was added to the cell pellet, and the trituration stage repeated. A 10μl sample of cell suspension was added to each side of an Improved Neubauer haemocytometer counting chamber, in order to calculate the cell suspension density, and consequently the volume of additional medium necessary to adjust the final cell density to the level required for plating.

A viability count was carried out to ensure that a sufficient percentage of cells were viable at the time of plating. This was achieved by adding 100μl of cell suspension to 100μl of Trypan Blue dye: after vortexing and 2 minutes' incubation, another 10μl sample of the resultant suspension was added to each side of a second haemocytometer counting chamber, and a viability count taken, using an inverted binocular microscope and hand-held counter.

Cell viability at plating was consistently found to be at least 95%, with an average viability of 99.4% (n=68). Trypan blue stain was used for a viability count at plating as it provided a rapid cell viability assessment, but was not used for final viability assays as it can be inaccurate when used with older cultures, causing over-estimation of cell viability (Altman *et al.*, 1993).

Cells were plated out on 24- or 96-well culture plates, at a concentration of $1x10^6$ cells per ml. When using 96-well plates, the outer rows of wells were excluded to avoid the risk of interference with results due to excessive evaporation (hence, only the inner 6x10 group of wells of the total plate's 8x12 wells was used). When using 100mm dishes in Western blot studies, a plating density of $1.5x10^6$ cells per ml was used, with additional medium added 24 hours post-plating. Cultures were then transferred to a Flow Laboratories 220 CO_2 incubator, which maintained an interior environmental temperature of 37°C and an atmosphere of 95% air and 5% CO_2.

2.1.9 Elimination of non-neuronal cells from cultures

The cytotoxic agent cytosine arabinoside has been used in many studies to rid cultures of non-neuronal cells (glial cells, residual meningeal cells, etc.) (Castilho *et al.*, 1998, Chuang *et al.*, 1992, Damschroder-Williams *et al.*, 1995, Marini *et al.*, 1998, Orr and Smith, 1988). This was applied 24 hours post-plating at a final concentration of 10μM.

Cytosine arabinoside is a nucleotide analogue, which interferes with DNA replication and repair, and is therefore toxic to dividing cells. As 7-8 day old cerebellar neurones are no longer replicating, the cytotoxic effect selectively destroys replicating non-neuronal cells. This was used in all experiments (except negative controls in ICC studies studying the efficacy of cytosine arabinoside).

2.2 Alamar blue and fluorescein diacetate viability assays

2.2.1 Alamar blue assay

This viability assay involves use of the dye Alamar Blue (Biosource International, DAL1100), an indicator of reduction and oxidation which changes colour (from blue to pink) in response to the chemical reduction of cell culture medium due to metabolic products of cell growth (Fatokun *et al.*, 2007, White *et al.*, 1996). Twenty-four hours after treatments were applied, culture medium was aspirated and fresh medium added at a volume of 100µl per well, containing the dye at a concentration of 10% (v/v) (Abe *et al.*, 2002).

Alamar Blue can be altered in colour by reduction reactions involving nicotinamide adenine dinucleotide phosphate (NADP), NAD, flavin adenine dinucleotide (FAD), flavin mononucleotide (FMN) and cytochromes and it is believed that it only successfully reacts when taken up into the intracellular space. The assay dye was applied to each well, with two control wells, one containing medium only and the other containing medium with 10% Alamar blue dye only. The cultures were incubated at 37°C, with readings of the level of dye oxidation taken at 4 and 6 hours, using an Opsys MR plate-reader (Dynex industries), at wavelengths of 540 and 595nm. The two readings were then combined to determine the fraction of dye that had been reduced in a negative control well (containing no cells) and in each of the wells of treated and control neurones. These values were used to quantify cell viability levels for each treatment group as a percentage, calculated relative to the negative control.

The dual time points were used with the Alamar blue assay as 4 hours is the standard time for this assay, but it had been suggested that a more accurate assessment can be made in CGN cultures using the 6 hour time point (White *et al.*, 1996). Readings were therefore taken at both time points on all occasions that this assay was used, in order to be certain that optimal assay results had been achieved.

2.2.2 Fluorescein diacetate assay

This assay involves application of an esterified form of fluorescein (fluorescein diacetate, Sigma F7378) to cell cultures, which is taken up by living cells and the

acetate groups cleaved from the molecule by intracellular esterases, producing fluorescein. The level of fluorescein in each culture well is quantified by a fluorometer, and cell viability is thus determined, as uptake of fluorescein diacetate (FDA) and subsequent conversion to fluorescein only take place in living cells (Favaron *et al.*, 1988, Rotman and Papermaster, 1966).

Fluorescein diacetate powder was first dissolved in absolute alcohol (5mg in 10ml) and added to 90ml of PBS, producing a solution of 10% ethanol and 50µg/ml FDA. This solution was added to minimum essential medium (MEM), producing another ten-fold dilution, to reach a final FDA concentration of 5µg/ml, and 1% ethanol. This FDA concentration was consistent with that used in previous studies (Novelli *et al.*, 1988, Valencia and Morán, 2001).

The medium in the wells was aspirated and replaced with the solution of MEM containing FDA, after which the plate was incubated at 37°C for ten minutes, to allow the intracellular de-esterification reaction to take place. Then the plate was transferred to the fluorometer for analysis, with the excitation at a wavelength of 485nm and the emission read at a wavelength of 538nm (Valencia and Morán, 2001). The resultant data (including that of the 'calibration' well containing MEM only and the 'blank' well containing 5µg/ml FDA in MEM solution, without either well having any cells present) was collected and analysed.

The incubation time chosen was based on several studies using the assay for neuronal cultures (Dargent *et al.*, 1996, Didier *et al.*, 1990, Favaron *et al.*, 1988, Novelli *et al.*, 1988, Valencia and Morán, 2001). The application times used ranged from one to twenty minutes, so ten minutes was chosen as an approximate median average. It was also sufficiently long to allow some time for incubation at 37°C (as the application process in a 96-well plate takes some time in itself), but brief enough to minimise the risk of the produced fluorescein leaking from the cells.

Co-staining with propidium iodide (PI, Sigma P4170) was achieved by adding to FDA-containing MEM solution to a final concentration of 4.5µM PI (Tauskela *et al.*, 2003), before applying to cultured CGNs for 10 minutes in the normal fashion, with images recorded using an Olympus IX50 phase-contrast microscope and Olympus DP50 digital camera.

2.3 Immunocytochemistry procedure

2.3.1 ICC materials

4% or 8% paraformaldehyde solution (in 0.1M phosphate buffer)

0.1M phosphate buffer solution

0.3% triton solution (in 0.1M PBS)

0.2M PBS

1.5% blocking serum solution in PBS and 0.3% triton

Heidolph Polymax 1040 plate-shaking platform

Six inch glass Pasteur pipette

Olympus IX50 Phase-contrast microscope

Olympus DP50 Digital camera

Olympus TH3 Light source

Olympus U-RFL-T Fluorescent light source

Mouse anti-beta$_{III}$ tubulin antibody (Chemicon MAB1637)

Rabbit anti-glial fibrillary acid protein antibody (Sigma G9269)

FITC-conjugated donkey anti-rabbit antibody (Jackson 711-095-152)

Rhodamine red X-conjugated goat anti-mouse antibody (Jackson 115-295-146)

2.3.2 Immunocytochemistry procedure

A 4% paraformaldehyde solution was applied to cultures immediately following treatment and aspiration of all culture medium. In later experiments, a more consistent result with less subsequent loss of cells was achieved by adding 8% paraformaldehyde solution (at 4°C) at an equivalent volume to the medium in the wells (final concentration of 4%). This solution was left in place for thirty minutes prior to aspiration and rinse in three washes in 0.1M phosphate buffer solution for five minutes to remove fixative. Fixed cultures were flooded with 0.1M phosphate buffer and stored at 4°C prior to ICC staining.

The first stage of ICC staining involves applying 1.5% blocking serum (raised in the same species as the secondary antibody to be used: usually either goat or

donkey serum) for 1 hour at 50μl per well, to prevent interference from non-specific protein binding sites in the subsequent labelling with secondary antibody. Incubations were at room temperature for one hour on a plate-shaking platform to ensure complete coverage of the fixed cultures.

Following this, the blocking serum was aspirated and 50μl per well or 30μl per coverslip of primary antibody added (diluted in PBS and 0.3% triton), following which the plate was placed on the plate-shaker for 5 minutes, before an overnight incubation at 4°C. A set of wells were incubated as negative controls with 50μl of PBS and triton solution added without primary antibody to demonstrate staining specificity.

Following overnight incubation, the fixed cultures were rinsed three times in 50μl of 0.2M PBS for 5 minutes. Once completed, 50μl of secondary antibody (diluted in PBS with 3% triton) was added to each well. As fluorescent conjugated secondary antibodies were routinely used, aliquots were wrapped in tinfoil, as was the plate, to prevent bleaching. To minimise the risk of light-related interference, room lights were switched off during these stages.

The cultures were rinsed twice in phosphate buffer solution, viewed under the microscope with fluorescent light at a wavelength relevant to the fluorochrome of the secondary antibody used and the images were recorded using a digital camera.

2.3.3 Microscopic photography

The software used to obtain the images and to adjust or overlay images if necessary was Cell^D, produced by Soft Imaging System GmbH. This software provides the necessary tools for image capture, labelling (e.g. scale-bars) and subsequent adjustment for consistency of image intensity or contrast. An additional capability is that the software can allow separately captured images to be overlaid and amalgamated into one image; an example of this being the collection of images of the same field using fluorescence at different wavelengths (such as when collecting images of immunocytochemically-stained cultures labelled with more than one fluorochrome).

2.4 Protein sample preparation and protein assay

2.4.1 Protein sample preparation and assay materials

Tris powder (Boehringer Mannheim, 708976)

Sodium chloride powder (BDH, 102415K)

Sodium dodecyl sulphate powder (BDH, 442444H)

Triton X-100 (Sigma, T8787)

IGEPAL (Sigma, I7771)

Protease Inhibitor cocktail tablets (Roche, 11 836 170 001)

PBS (Gibco, 14200-067)

BSA (Sigma, A2153)

BIORAD protein assay dye (BIORAD, 500-0006)

Costar disposable cell scraper (Corning, 3010)

2.4.2 Protein sample preparation procedure

The radio-immuno precipitation assay (RIPA) buffer was prepared as follows: 60mg Tris, 87.6mg NaCl, 10mg sodium dodecyl sulphate (SDS), 50μl Triton X-100, 100μl IGEPAL and 9.85ml sterile distilled water (this came to 50mM Tris, 150mM NaCl, 0.5% Triton, 0.1% SDS, 1% IGEPAL). One protease inhibitor cocktail mini-tablet was added to each 10ml of RIPA buffer.

The culture medium was drained, with residual medium aspirated by pipette. Cultures were washed once with ice-cold PBS, which was drained and aspirated as before.

Next, ice-cold RIPA buffer was added (1ml if 9cm dish; 0.5ml if 5cm dish) if nuclear or cytosolic lysate was sought. After 1 minute, cells were scraped off the plating surface with a Corning Costar cell scraper, and the buffer/cell suspension was transferred to a 1.5ml Eppendorf tube. Finally, cell suspension was centrifuged at 13,000 rpm for 5 minutes at 4°C in an Eppendorf 5417R centrifuge.

2.4.3 Protein assay

The BSA stock solution (20mg/100ml) was diluted 1 in 10 with distilled water and BSA standard solutions (0, 0.25, 0.5, 1.0, 1.5, and 2.0mg/ml) prepared to produce a protein concentration curve. Experimental samples were made into dilutions of 1/100 (thus expressing results in mg/ml) by addition of 4μl sample to 396μl distilled water. The Biorad reagent was diluted by half –sufficient to add 200μl to each standard and sample (a total of 2ml was usually ample). The Biorad reagent was effective with samples containing SDS at or below 0.1%.

200μl of diluted Biorad reagent was added to each standard and sample, then vortexed to ensure thorough mixing of the protein standard or sample and reagent. Each standard and sample was pipetted out in duplicate onto a 96-well plate. Results were read at 595nm on the Opsys MR plate-reader and the total protein concentration in each sample was determined. Samples could then be diluted if necessary to allow a consistent concentration across all protein samples.

2.5 Western blotting procedure

2.5.1 Western blotting materials

12% SDS-Page gel (Invitrogen, NP0341)

Sample buffer (Invitrogen, NP0007)

Sample reducing agent (Invitrogen, NP0004)

SeeBlue protein marker (Invitrogen, LC5925)

MOPS running buffer (Invitrogen, NP0001)

Antioxidant (Invitrogen, NP0005)

Gel running tank: Novex Mini-cell (Invitrogen)

Gel running chamber (Invitrogen)

Protein transfer chamber (Invitrogen, E19051)

Gel knife (Invitrogen)

Nitrocellulose membrane (Invitrogen, LC2001)

PVDF membrane (Invitrogen, LC2005)

‘PowerEase 500’ powerpack (Invitrogen)

Transfer buffer (Invitrogen, NP0006)

Methanol (Fisher, M/4056/17)

Ponceau stain (Sigma, P7170)

Milk powder (Upstate, 20-200)

IgG-free BSA (Sigma, A2058)

Tween-20 (Sigma, 27,434-8)

ECL kit (Amersham, RPN2132)

Photosensitive films (Amersham, RPN3103K)

‘Hypercassette’ film cassette (Amersham RPN12642)

‘Restore’ stripping buffer (Pierce, 21059)

Eppendorf 5417R centrifuge

Anti-GAPDH antibody (Santa Cruz sc-25778, rabbit)

Anti-actin antibody (Santa Cruz sc-1615, goat)

Anti-GAPDH antibody (Santa Cruz sc-20356, goat)

Anti-bcl-2 antibody (Santa Cruz sc-492, rabbit)

Anti-CREB antibody (Santa Cruz sc-186, rabbit)

Anti-phosphorylated CREB antibody (Cell Signaling 9198, rabbit)

Anti-caspase-3 antibody (Santa Cruz sc-7148, rabbit)

Anti-cleaved caspase-3 antibody (Cell Signaling 9664, rabbit)

Anti-p38 antibody (Cell Signaling 9212, rabbit)

Anti-phosphorylated p38 antibody (Cell Signaling 9211, rabbit)

Goat anti-rabbit horseradish peroxidase antibody (Upstate 12-348)

Donkey anti-goat horseradish peroxidase antibody (Santa Cruz sc-2020)

2.5.2 Gel running procedure

Protein samples were added to loading buffer and reducing agent, at the following proportions: 65% sample, 25% sample buffer, 10% reducing agent. They were mixed thoroughly prior to being heated at 70°C for 10 minutes and centrifuged at 2000rpm (425 rcf) at 4°C for 1 minute using an Eppendorf 5417R centrifuge.

The gel tank was filled with MOPS running buffer (from 50ml MOPS buffer concentrate and 950ml distilled water), with 200ml of buffer supplemented with 0.5ml antioxidant set aside for the inner section of the tank containing the gel itself. The gel cassette was rinsed with distilled water and the white paper stripe and gel comb were removed prior to the gel lanes being rinsed with running buffer.

10μl of rainbow protein marker was added to a marker lane at the side of the gel and 20-25μl of each protein sample to the required number of lanes, volume chosen according to concentration to ensure 20-30μg of protein loaded per lane. The tank was closed and run at 150V for 90 minutes, this voltage and time chosen to provide the best placing of the proteins studied in these experiments. The level of current used was 120mAmp for one gel or 240mAmp for two gels.

2.5.3 Protein transfer procedure

The transfer buffer was prepared as the running procedure was taking place, using 50ml of NuPage transfer buffer, 1ml sample antioxidant, 100ml methanol and 850ml distilled water (in experiments using two gels, 200ml methanol and 750ml distilled water were used). 200ml of the resultant solution was set aside in a conical flask for the central compartment. For transfers using a polyvinylidene difluoride (PVDF) membrane, the membrane was soaked in methanol for one minute, prior to soaking in transfer buffer alongside the other equipment for gel transfer. Also one corner of the membrane was cut obliquely, to allow easy identification of the lanes' orientation on the membrane.

The running buffer was emptied from the gel tank and the tank rinsed thoroughly. The gel knife was used to crack open the gel cassette, remove half of the cassette and cut off the gel strands forming the lanes and the thickened

portion at the base of the gel, which prepared the gel for the transfer procedure.

Next the gel was applied to the PVDF membrane: the membrane was applied to the gel surface and suspended over filter paper. The gel knife was then used to gently release a corner of gel, allowing the gel to slowly peel off the cassette onto the filter paper beneath. Finally the second filter paper was placed on the other surface of the gel.

The membrane 'sandwich' was placed on top of two soaked sponges in the tray (cathode core) of the transfer assembly, with the gel beneath the membrane. Two further soaked sponges were placed on top of the 'sandwich', the lid (anode core) of the transfer assembly was placed on top and the entire assembly placed in the tank.

The 200ml of fresh transfer buffer in the conical flask was added to the central compartment to a level 1cm above the 'sandwich', and the remainder of the transfer buffer was added to the outer compartment of the tank until approximately 3/4 full. The power pack was attached, and run at 30V for 1 hour, at a current of 400mAmp.

2.5.4 Ponceau staining

Ponceau stain was used in order to confirm constant protein concentrations across the sample lanes. This simple and rapid procedure allowed confirmation of sample concentration uniformity without an excessive delay in the blotting procedure. The membrane was rinsed twice with distilled water, and immersed in Ponceau solution for 5 minutes. The protein bands were viewed to ensure an equal density in all sample lanes and an image of the bands recorded. Following this, the membrane was rinsed with distilled water and immersed in an aqueous solution of 0.1M sodium hydroxide for approximately 30 seconds, until the stained bands had disappeared. Finally, the membrane was rinsed with running distilled water for 2-3 minutes to ensure all of the Ponceau stain and sodium hydroxide had been thoroughly rinsed out.

2.5.5 Antibody incubation

The membrane was blocked from non-specific binding by immersion with agitation in TBS solution containing 5% milk and 0.05% Tween-20 for 60 minutes. If blotting for phosphorylated proteins, the membrane was washed for 15 minutes in 200ml TBS/0.05% Tween-20 three times to remove any unbound milk proteins. An appropriate dilution of primary antibody solution (in 5% milk and 0.05% Tween-20 TBS solution) was prepared and applied to the membrane for an overnight incubation at 4°C (with agitation). When blotting for phosphorylated proteins, 5% IgG-free BSA solution was used in place of milk solution.

The next day, the membrane was washed in TBS for 15 minutes (with agitation) three times to remove all remaining unbound primary antibody. An appropriate dilution of secondary antibody solution was made in TBS solution with 5% milk and 0.05% Tween-20 and applied to the membrane for incubation at room temperature for 60 minutes (with agitation). Following this, the membrane was again rinsed in TBS for 15 minutes (with agitation) five times to remove all unbound secondary antibody from the membrane.

2.5.6 Enzymatic Chemiluminescence

The final stage of the Western blotting process was to apply the enzymatic chemiluminescence (ECL) solution to the membrane for 5 minutes, apply photosensitive film to the membrane in a darkroom for the required period, and develop the film.

The ECL kit was removed from refrigeration prior to use; for each membrane, 6ml of the large ECL solution bottle was added to 150μl of small ECL bottle solution immediately prior to use (this was done within a container shielded against light, e.g. a centrifuge tube wrapped in foil). The ECL reagent mixture was applied to the membrane for 5 minutes and agitated while shielded from light.

When incubation was complete, excess developing solution was blotted off onto filter paper and the membrane placed in a developing cassette, with a saran wrap cover smoothed over the membrane to eliminate air bubbles. The cassette was transferred to a red-light room, where films were cut to the correct size and

placed over the membrane for the required time to achieve a reproduction of the blotting. The length of time for which the film was applied was adjusted according to how strong a reaction to the ECL solution was occurring. When exposure was complete, the films were fed into the developing machine and the results viewed.

Quantification of the blotting intensity was achieved using the program ImageJ (freeware from NIH, Bethesda), with corrections made according to the densities of the 'housekeeping' proteins (actin or glyceraldehyde phosphate dehydrogenase [GAPDH]).

2.6 Compounds used in experiments

L-Glutamic acid powder (Sigma, G1626)

N-methyl-D-aspartate powder (Sigma, M3262)

3-Nitropropionic acid powder (Sigma, N5636)

Hydrogen peroxide 30% solution (Sigma, H1009)

D (+)-Glucose powder (Fisher Scientific, G/0500/53)

3-*O*-methyl-D-glucopyranose powder (Sigma, M4879)

L-Tryptophan powder (Sigma, T0254)

L-Kynurenine powder (Sigma, K8625)

Kynurenic acid powder (Sigma, K3375)

3-Hydroxykynurenine powder (Sigma, H1771)

3-Hydroxyanthranilic acid powder (Sigma, H9391)

Anthranilic acid powder (Aldrich, A8985-5)

5-Hydroxyanthranilic acid powder (Fluorochem, 011772)

2-Picolinic acid powder (P5503)

Quinolinic acid powder (Aldrich, P6320-4)

Superoxide dismutase powder, bovine erythrocyte (Sigma, S5395)

Catalase powder, bovine liver (Sigma, C1345)

Desferrioxamine mesylate (Sigma, D9533)

Cycloheximide (Sigma, C7698)

Sodium chloride powder (BDH, 102415K)

Potassium chloride (BDH, 101984L)

Calcium chloride (BDH, 190464K)

HEPES (BDH, 442854V)

Glycine (Fisher, G/0800/60)

Magnesium chloride (BDH, 10149)

4-Aminopyridine (Sigma, A0152)

Bicuculline methobromide (550-040-M050, Alexis biochemicals)

Tetrodotoxin (Sigma, T5651)

Nifedipine (Bayer Leverkusen, BAY-a-1040)

MK-801 maleate (Tocris, 0924)

Staurosporine (Tocris, 1285)

2.7 Treatments

The majority of compounds used in these experiments were dissolved into stock solutions using sterile distilled water. The exceptions to this were 3-hydroxyanthranilic acid, which was only soluble when first dissolved in hydrochloric acid, with this solution diluted using distilled water, and kynurenic acid, which required sodium hydroxide solution to dissolve, this solution diluted using distilled water. Denaturing of the enzymes catalase and SOD was achieved by boiling an aliquot of each enzyme for 10 minutes at 100°C.

Preconditioning stimuli (such as *N*-methyl-D-aspartate or 4-aminopyridine) were added to *in situ* culture medium as concentrated solutions to reach the desired final concentration (this minimised the number of evacuations of medium needed and hence reduced unnecessary stresses and sources of variability to the cultures). At the end of the treatment periods the medium was aspirated and replaced with fresh medium.

Toxic treatments (glutamate or QA for example) were applied in culture medium for the indicated durations, then removed and replaced with fresh medium. In the case of 24 or 48-hour insults, the viability assay was performed immediately following treatment, so the medium was replaced by the FDA-containing MEM solution.

Treatments applied to 10cm dishes (to provide protein sample for subsequent Western blotting) were achieved using the same protocols (preconditioning stimuli were added without subjecting the cultures to additional aspiration; toxic treatments were added in medium). In these cases, the cell material was collected at the end of the treatment period (as described under 'protein sample preparation'), so no additional medium change was required.

All treatments were heated to 37°C using a water bath (Grant Instruments, Cambridge) prior to being applied to cultures and culture plates or dishes were placed in an incubator during all treatments.

2.8 Neuronal morphology

Cerebellar granule neurones from neonatal rats appear after dissociation as small neurones with spherical cell bodies, which establish extensive neurite interconnections after approximately 24-48 hours in culture, the extent of the interconnections increasing with the time *in vitro*. Additionally, the neuron cell bodies form small clusters, the size of which increase with increasing plating density (Trenkner, 1998).

When CGNs are subjected to neurotoxic stimuli, the impact can be observed in the appearances of both the neuronal somata and the neurite networks. The somata shrink, and the neurite interconnections initially become beaded, then disintegrate completely, leaving only traces of cellular debris between neurones (Ciotti *et al.*, 1996).

2.9 Hypoxia and OGD procedure

The culture plates were transferred to a previously warmed (37^{o}C) portable anaerobic cylinder (Rodwell) with two valves (allowing simultaneous removal and input of gas) and the cylinder lid sealed. A water pump was attached to the cylinder, and the air inside withdrawn for 5 minutes, then for 5 minutes the cylinder gas was drained while a 95% nitrogen and 5% carbon dioxide mixture was pumped into the chamber, and finally the gas mixture was pumped into the chamber for a further 5 minutes in the absence of gas removal.

In the case of OGD, the cultures had medium aspirated and replaced with a buffer solution (140mM NaCl, 5mM KCl, 2mM $CaCl_2$, 20mM HEPES, 30μM glycine, 800μM $MgCl_2$) without glucose. This buffer was bubbled with the nitrogen-carbon dioxide gas mixture for 10 minutes to lower the level of dissolved oxygen, before being filter-sterilised and warmed to 37°C prior to application.

The relative levels of oxygen and carbon dioxide in the gas mixture were determined using a Servomex 570A oxygen analyser for oxygen and Servomex analyser series 1400 for carbon dioxide, and found to be accurately composed, with carbon dioxide present at an average of 5.04%, with 0.025% oxygen present in the mixture (n=4).

Assay of oxygen saturation levels in the buffer following the culture gassing procedure was performed, using a Strathkelvin Instruments Oxygen Meter model 781. The oxygen probe electrode was placed in a solution of sodium sulphite (which absorbs any dissolved oxygen in the water) and calibrated to 0%, then placed in water fully saturated with oxygen to calibrate for 100% saturation. The electrode was then fitted into a sample chamber and rinsed with distilled water, a buffer sample that had been gassed was run into the chamber and the degree of oxygen saturation recorded. This procedure was carried out for a number of independent repetitions of the gassing procedure, and demonstrated an average pO_2 of 94.45mmHg (60.19% saturation) (n=3).

2.10 High performance liquid chromatography

The experiments using high performance liquid chromatography (HPLC) in this study were carried out by Dr. Gillian Mackay, using samples of medium from experiments performed on neuronal cultures in 24-well plates treated with 100µM tryptophan, 100µM kynurenine, 100µM anthranilic acid, 100µM 3-HK or 100µM 3-HAA. Two methods of HPLC analysis were used, one assaying tryptophan, kynurenine, anthranilic acid and kynurenic acid (based on the method of Hervé *et al.*, 1996); the other assaying 3-HK, 3-HAA and 5-hydroxyanthranilic acid (5-HAA) (adapted from Cannazza *et al.*, 2003).

HPLC involves the injection of 100µl of an extracted sample containing a compound of interest into a stream of liquid solvent (the 'mobile phase'), which is then pumped (at a flow rate of 1ml/min in these experiments) through a steel column packed with solid spherical particles of the 'stationary phase'. The solvent leaving the column is stimulated using fluorescent or ultraviolet light and the responses to this stimulation recorded.

The peak height of the detected response on the resultant chromatogram can then be identified, and this is then quantified against a linear calibration curve calculated from a series of standard solutions of the compound of interest assayed during the same HPLC analysis series. This allows the concentration in the sample to be determined. The standard solutions and samples also contain an internal standard (24µM 3-nitrotyrosine) used to identify any variations during the extraction of the standards and samples, and thus to allow compensatory corrections to be made during the final data analysis.

In 'reversed-phase' HPLC (approximately 80% of HPLC work), the mobile and stationary phases are polar and non-polar respectively (Krstulovic and Brown, 1982). The identification of individual chemical compounds is achieved as compounds have different retention times (passage time of the compound through the column), and hence peak responses to fluorescent or ultraviolet stimulation will occur at predictable times. Retention times may be prolonged due to interactions with the stationary phase: this delay increases in proportion to the extent of non-polar surface area on the compound's molecular structure, as interactions between the non-polar stationary phase particles and the compound hinder passage of the dissolved compound.

Medium samples were treated with perchloric acid and filtered by centrifugation to precipitate and remove any protein prior to HPLC analysis (to prevent protein particles blocking HPLC equipment). Analysis of tryptophan, kynurenine, anthranilic acid and kynurenic acid was carried out at 37°C, using a mobile phase solution of 50mM acetic acid, 100mM zinc acetate and 1.5% acetonitrile (pH 7.4); the stationary phase was Synergi Hydro C18 column (containing packed 4μm silica particles coated with straight hydrocarbon chains). For analysis of 3-HK, 3-HAA and 5-HAA (performed at 30°C) the mobile phase used was 25mM sodium acetate (pH 5) solution and the stationary phase was also a Synergi Hydro C18 column.

Detection of tryptophan was achieved by quantifying absorbance of ultraviolet light at a wavelength of 250nm; kynurenine, 3-HK and 3-nitroyrosine were detected by absorbance at 365nm; kynurenic acid was detected by fluorescence (using an excitation wavelength of 344nm and emission wavelength of 390nm); anthranilic acid, 3-HAA and 5-HAA were detected by fluorescence (using an excitation wavelength of 320nm and emission wavelength of 420nm).

3 Optimising Culture Conditions and Confirming Accuracy of Viability Studies

3.1 Introduction

In order to ascertain that culture conditions were optimal for neuronal survival and development, and that both viability assays used were reliable, confirmatory studies were undertaken. Experiments were carried out in 96-well plates at a plating density of $1x10^6$ cells/ml, in medium containing 5.5mM glucose and 25mM KCl (except where indicated).

A number of variables have been shown to affect the ability of CGNs to survive and form functioning networks in culture; with cell plating density and the concentration of potassium in the culturing medium being of particular importance (Balázs *et al.*, 1988, Young *et al.*, 2000). Therefore, initial studies were carried out to establish the optimum level of each of these.

Elimination of non-neuronal cell types is also a key step in most methodology for establishing primary neuronal cultures; the antimetabolite cytosine arabinoside is frequently used in the preparation of CGN cultures (Castilho *et al.*, 1998, Chuang *et al.*, 1992, Damschroder-Williams *et al.*, 1995, Marini *et al.*, 1998). This compound was applied 24 hours post-plating at a final concentration of 10μM. Cytosine arabinoside is a nucleotide analogue, which is toxic to dividing cells due to its interference with DNA replication and repair. As CGNs are no longer replicating by 7-8 days into the neonatal period, the antimetabolic effects of cytosine arabinoside selectively kill only replicating non-neuronal cells. This treatment was selected for use in our culture system; therefore immunocytochemical studies were carried out to ensure that this treatment was effective and did not cause a discernable decrease in neurite network formation.

During establishment of the protocols, two different cell viability assays, fluorescein diacetate and Alamar blue, were used to quantify the degree of cell death resulting from the various treatments. In order to have complete confidence in the accuracy of each, the assays were trialled against CGN cultures plated at varying densities, to identify a linear increase in assay reading corresponding to increasing cell density. Secondly, the results obtained with

each assay were compared when assessing cultures given identical treatments, to ascertain whether readings from each were directly comparable. Finally, the accuracy of the assay used for the majority of the project's viability studies was compared with the morphological appearances of cells seen microscopically and with PI staining to identify dead cells (Tauskela *et al.*, 2003).

3.2 Aims and Objectives

- Identify the optimum plating density for neonatal rat CGN cultures
- Determine the culture medium potassium concentration for optimal neuronal survival and neurite network formation in neonatal rat CGNs
- Confirm the elimination of non-neuronal cell types by addition of cytosine arabinoside to culture medium
- Determine the ability of CGNs to form comparable neurite networks in either the presence or absence of cytosine arabinoside
- Establish comparative model using neonatal cerebral cortical neurones
- Ascertain the linear increase in assay reading relative to cell density with both FDA and Alamar blue viability assays
- Compare the FDA and Alamar blue viability assays to ensure concordant results
- Confirm the accuracy of FDA assay by comparing fluorescein staining of neurones with morphological appearances
- Utilize PI to stain dead neurones, and correlate this with corresponding morphological appearances
- Confirm reliability of FDA assay by application of both FDA and PI simultaneously

3.3 Cell density

In order to ensure that an optimum cell density was used in our system, a range of plating densities were tested and the appearances of the resultant neuronal cultures recorded. The cell plating densities tested were selected based on review of previous studies using cultured neonatal Sprague-Dawley rat CGNs (Chuang *et al.*, 1992, Wick *et al.*, 2002).

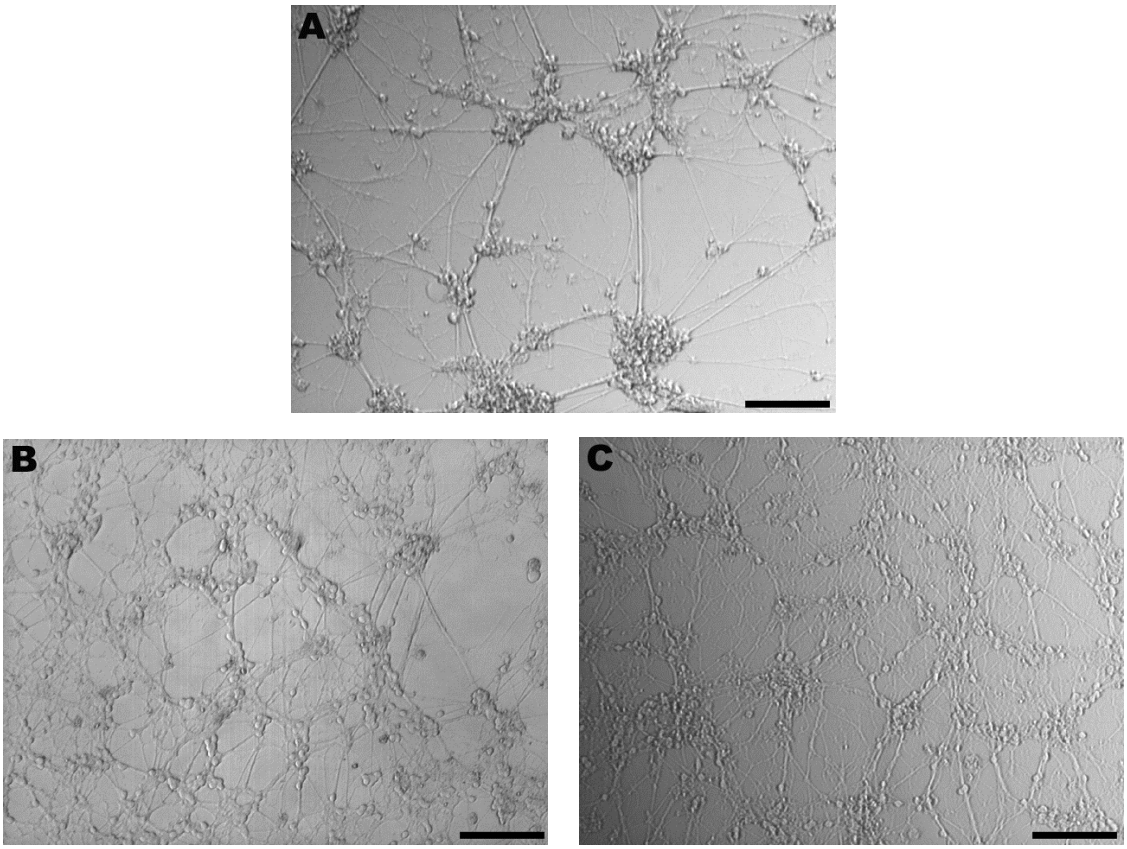

Figure 3.1 CGNs at 9 DIV, plated at a density of: A) 0.75 x10^6 cells/ml B) 1.00 x10^6 cells/ml C) 1.20 x10^6 cells/ml. Bars = 100µm. There was limited variation between densities, although slightly less extensive networks were seen using a plating density of 0.75 x10^6 cells/ml.

As can be seen from the representative images, more extensive networks were formed using cells at a density of 1.0 or 1.2x10^6 cells/ml, compared to cells at a density of 0.75x10^6 cells/ml (Fig 3.1). There was no apparent qualitative difference between cultures plated at 1.0 or 1.2x10^6 cells/ml. A plating density of 1.0x10^6 cells/ml was chosen in order to minimise the risk of increased sensitivity to medium changes associated with higher plating densities (Schramm *et al.*, 1990, Ciotti *et al.*, 1996, Young *et al.*, 2000) and to maximise the material available for experiments each week.

3.4 Effects on culture morphology of potassium concentration in culture medium

As alteration in potassium concentration has been shown to affect survival of cultured CGNs, neurones were plated in a range of potassium concentrations, and the appearance of the resultant cultures observed. A clear correlation was seen between CGNs cultured in higher potassium concentrations and with neuronal survival and neurite network formation. The most commonly used concentration was 25mM KCl, which produced cultures with neurones of consistent, normal morphology and with extensive neurite outgrowth (Fig 3.2D).

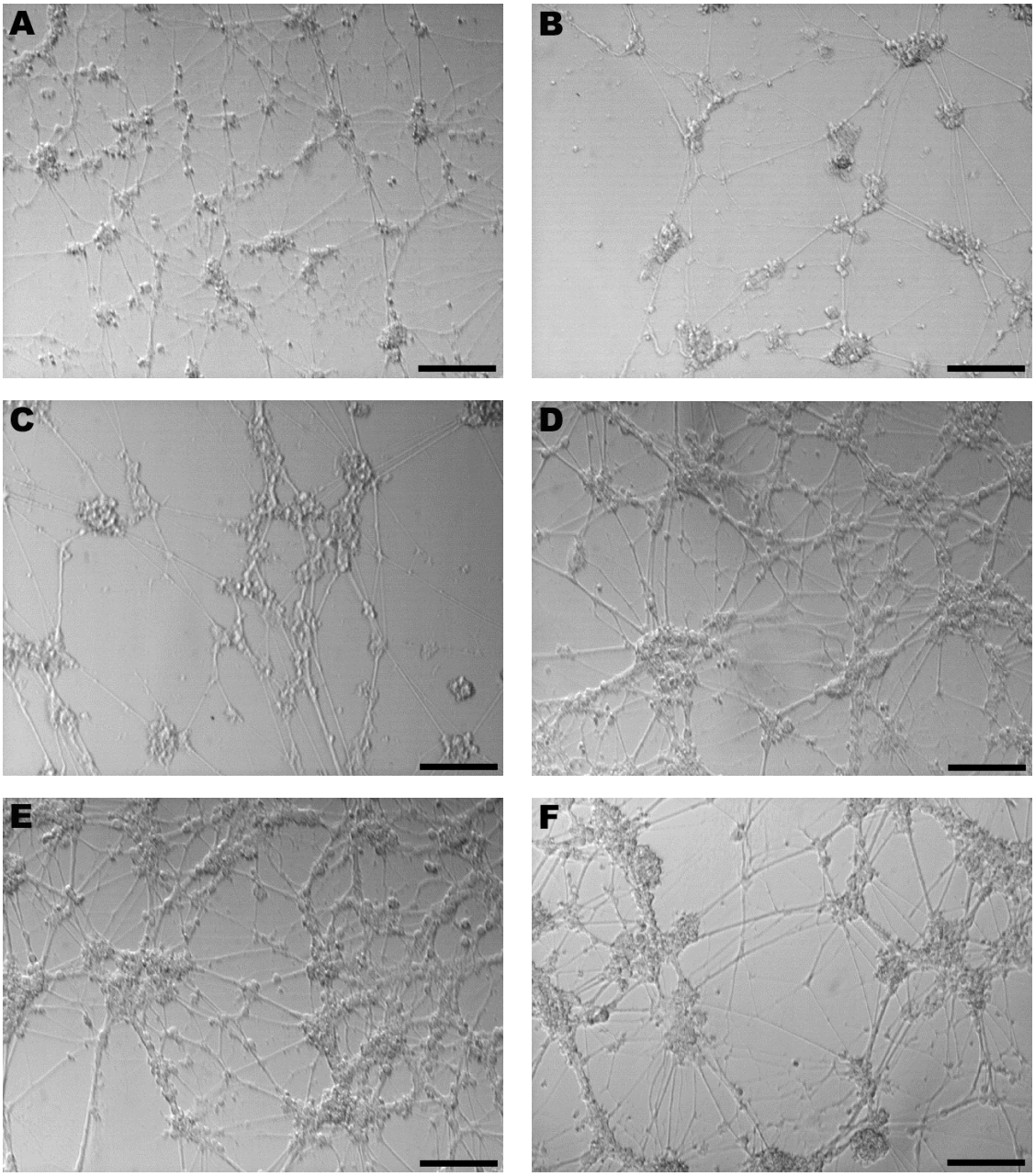

Figure 3.2 Morphological appearances at 9 DIV of CGNs cultured in medium containing: A) 5mM KCl, B) 10mM KCl, C) 15mM KCl, D) 20mM KCl, E) 25mM KCl, F) 30mM KCl. Bars = 100µm. The greater survival of CGNs using higher concentrations of KCl can be seen, with optimal appearances reached at 25mM.

3.5 Immunocytochemical studies of culture purity and neurite network morphology

In order to confirm that cytosine arabinoside treatment was effective but did not inhibit the formation of neurite interconnections between individual neurones, immunocytochemistry was performed to identify both neuronal and non-neuronal populations in the presence or absence of cytosine arabinoside 24 hours after culture plating.

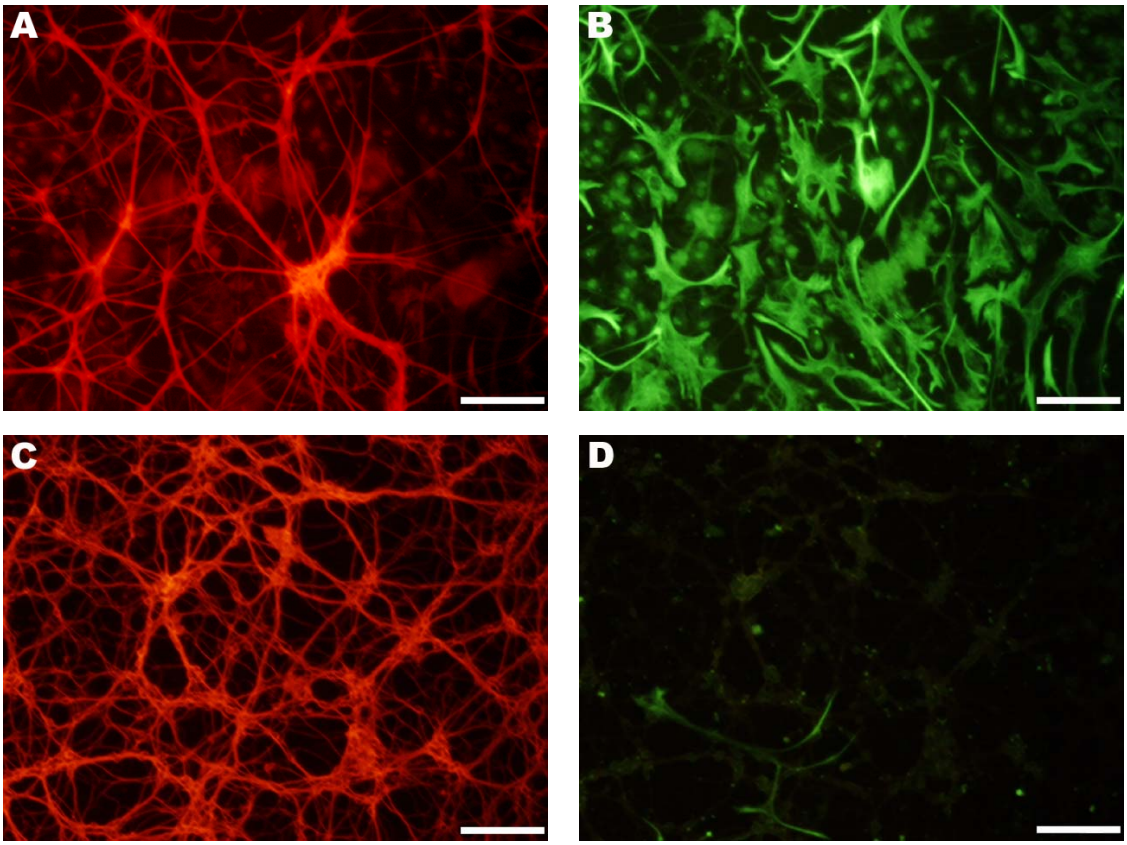

Figure 3.3 Immunocytochemical staining of CGN cultures (fixed at 9 DIV) with and without 10μM cytosine arabinoside added to medium at 1 DIV: A) and B) Cultures without cytosine arabinoside, immunostained against β–tubulin$_{III}$ and glial fibrillary acid protein (GFAP) respectively, C) and D) Cultures with cytosine arabinoside, immunostained against β–tubulin$_{III}$ and GFAP respectively (A and B, C and D are paired images of the same areas). Bars = 100μm. The addition of cytosine arabinoside extensively reduced the presence of glial cells, with no evident effect on neuronal morphology.

Cytosine arabinoside caused an obvious reduction in the number of glial cells present in the cultures (Figs 3.3B and 3.3D) but without any substantial loss of neurones (Figs 3.3A and 3.3C). Furthermore, cytosine arabinoside did not reduce the establishment of networks of neurite interconnections or cause any changes in morphology. Figs 3.4 and 3.5 show the clear differences in morphology between cells with ß-tubulin$_{III}$ stained and those with GFAP stained.

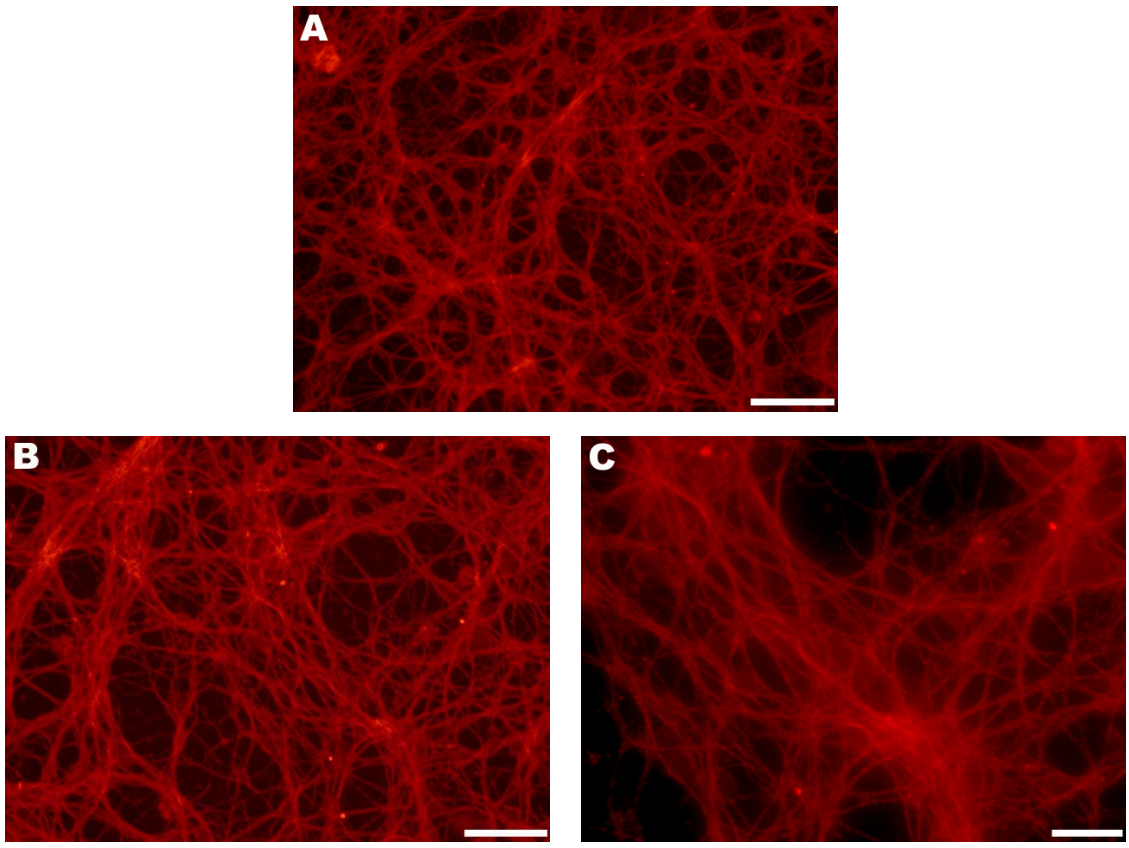

Figure 3.4 Immunocytochemical staining of CGN cultures (fixed at 9 DIV) immunostained against β–tubulin$_{III}$ (cultures with 10μM cytosine arabinoside added to medium at 1 DIV) at different magnifications. Bars = 100μm (A), 50μm (B), 20μm (C). The extensive neurite connections between neurones can be seen clearly.

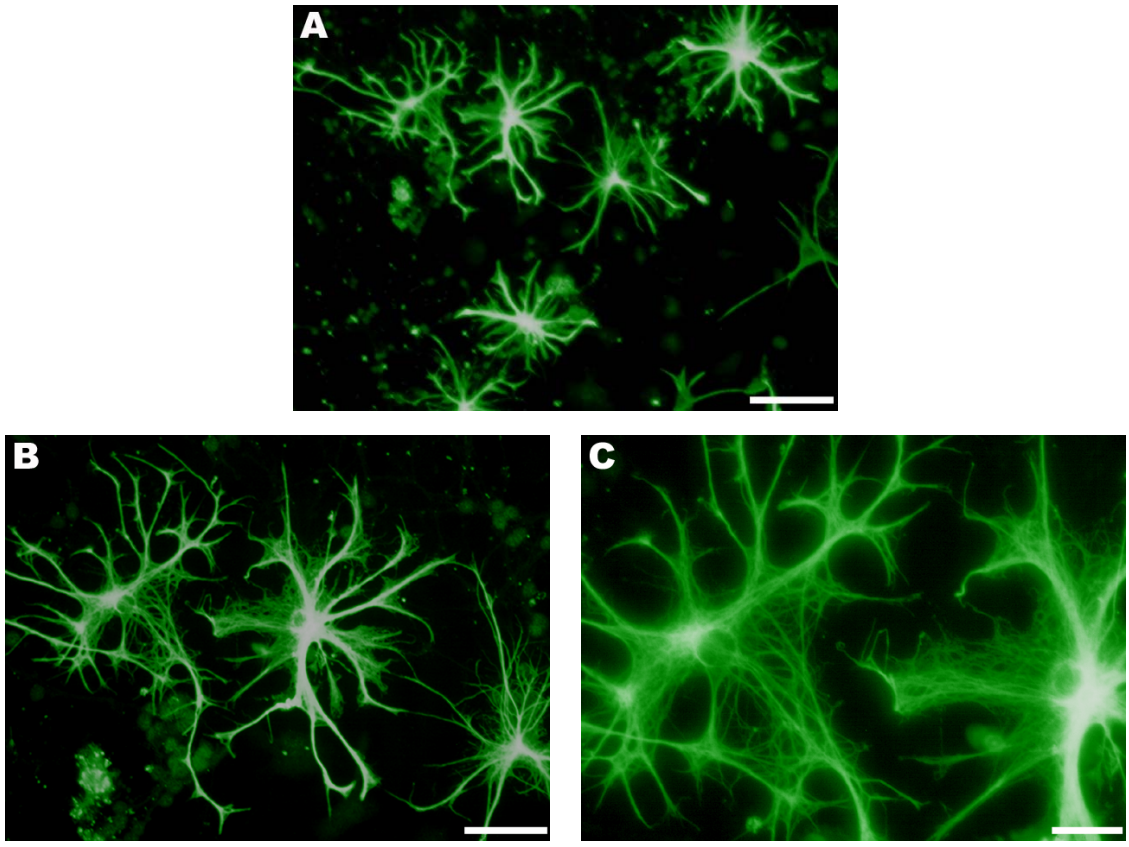

Figure 3.5 Immunocytochemical staining of non-neuronal cells (fixed at 9 DIV) immunostained with GFAP (from cultures not treated with cytosine arabinoside). Bars = 100μm (A), 50μm (B), 20μm (C). The contrast in appearance between these cells and those stained against β–tubulin$_{III}$ can be easily identified.

3.6 Assay results vary with cell plating density (FDA and Alamar blue)

To confirm that each of the viability assays used gave results consistent with the cell population density, results were compared from cultures plated at a range of densities ($500x10^5$ to $1.5x10^6$ cells/ml). The FDA assay dye was applied for 10 minutes and the Alamar blue assay dye for 4 and 6 hours, with all assays performed at 10 DIV (the time to be used during most subsequent experiments).

Both assays (and indeed at both time points for Alamar blue) produced a linear reading increase proportional to the increase in cell plating density, confirming the suitability of both in quantifying viable cell numbers in this culture system (Figs 3.6, 3.7 and 3.8).

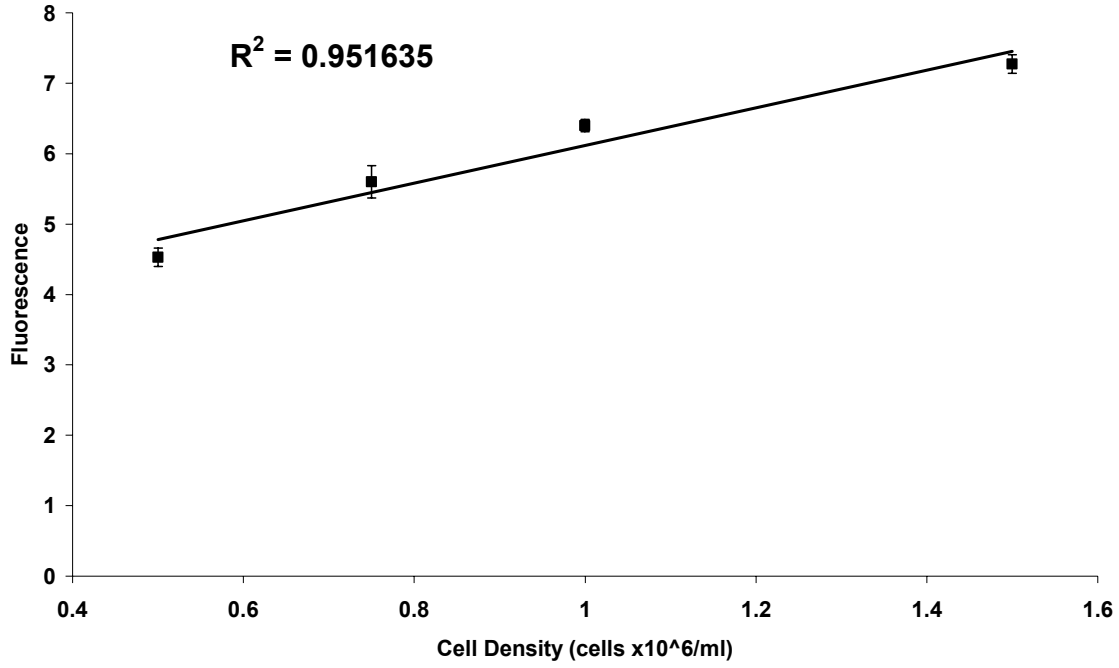

Figure 3.6 Cell density versus FDA reading (excitation at 485nm, emission at 538nm). Mean +/- standard error of mean (SEM), n=5. A linear increase in the quantity of fluorescein produced with increasing cell number is seen.

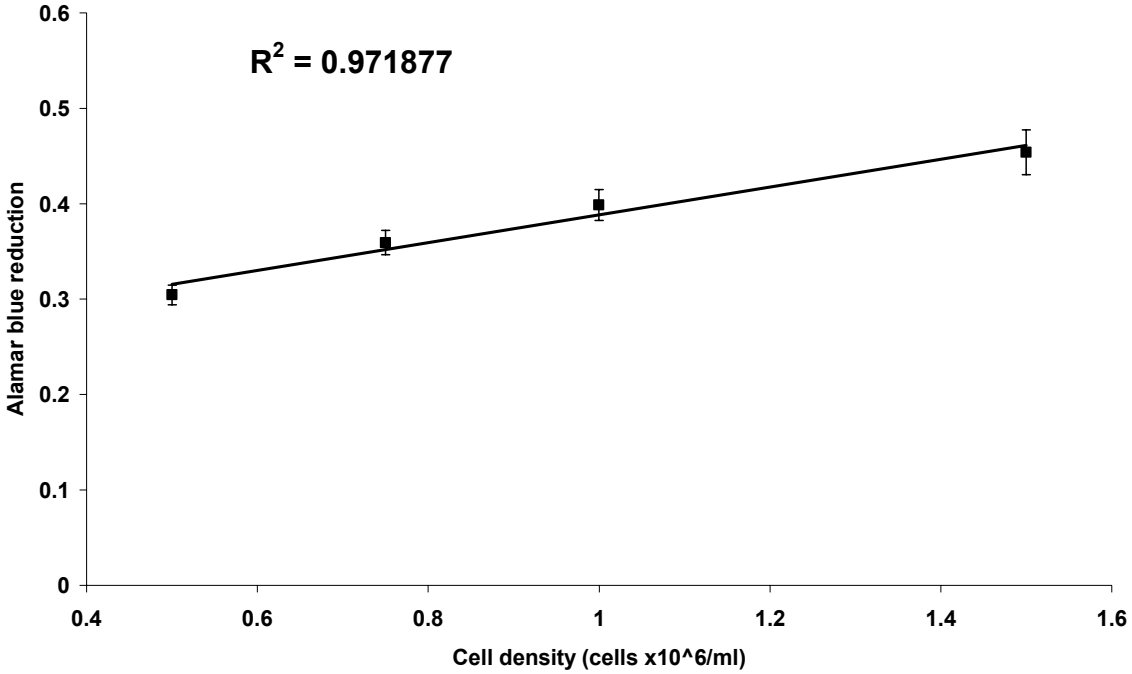

Figure 3.7 Cell density versus Alamar blue readings at 4 hours (colorimetric readings at 540nm and 595nm). Mean +/- SEM, n=5. A linear increase in the quantity of Alamar blue reduction with increasing cell number is seen.

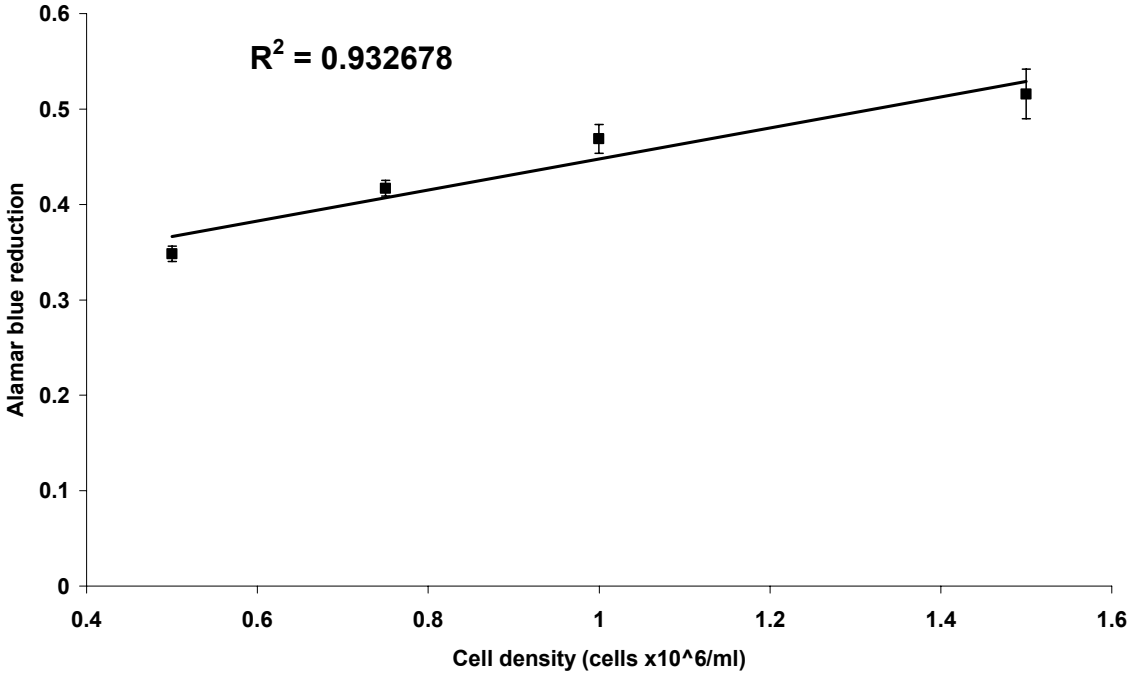

Figure 3.8 Cell density versus Alamar blue readings at 6 hours (colorimetric readings at 540nm and 595nm). Mean +/- SEM, n=5. A linear increase in the quantity of Alamar blue reduction with increasing cell number is seen.

3.7 Assay comparison (FDA and Alamar blue)

Having established that both viability assays give results consistent with a linear increase in cell population, it was of interest to establish whether the results attained with each were directly comparable. Viability readings were quantified as a percentage of those from sham controls, which were subjected to medium changes to replicate the mechanical stresses encountered by treated cultures during aspiration and replacement of medium, and hence compensate for this potential source of variation. This method was used as the standard for assessing viability in the remainder of the study (with occasional exceptions, identified as such in the relevant figures).

In all studies, the two assays provided results which were comparable and analysis of variance (ANOVA) followed by Tukey's post-hoc test for each set of three results (of each individual compound at each concentration) showed no significant differences in any case, with the p value determined to be ≥ 0.5 in each (Fig 3.9, 3.10 and 3.11).

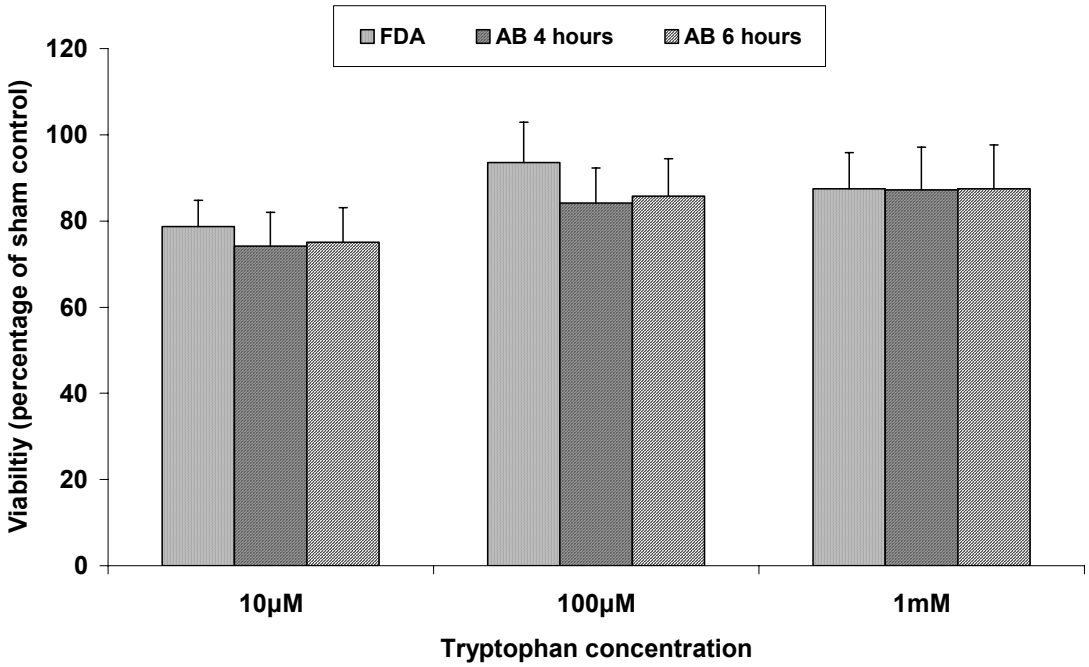

Figure 3.9 Comparison of FDA and Alamar blue in assaying tryptophan toxicity (applied for 1 hour at 9 DIV) in cultured CGNs. Mean +/- SEM, n=5; ANOVA followed by Tukey's test (in each set of three assay results) found no significant difference, indicating that the assays provide comparable data.

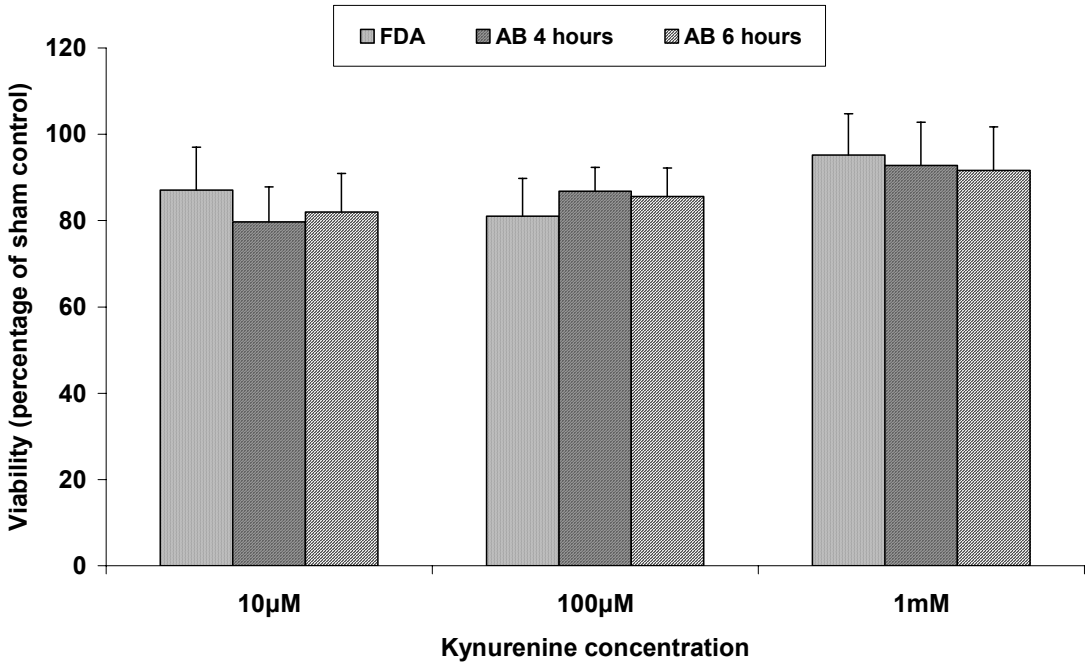

Figure 3.10 Comparison of FDA and Alamar blue in assaying kynurenine toxicity (applied for 1 hour at 9 DIV) in cultured CGNs. Mean +/- SEM, n=5; ANOVA followed by Tukey's test (in each set of three assay results) found no significant difference, indicating that the assays provide comparable data.

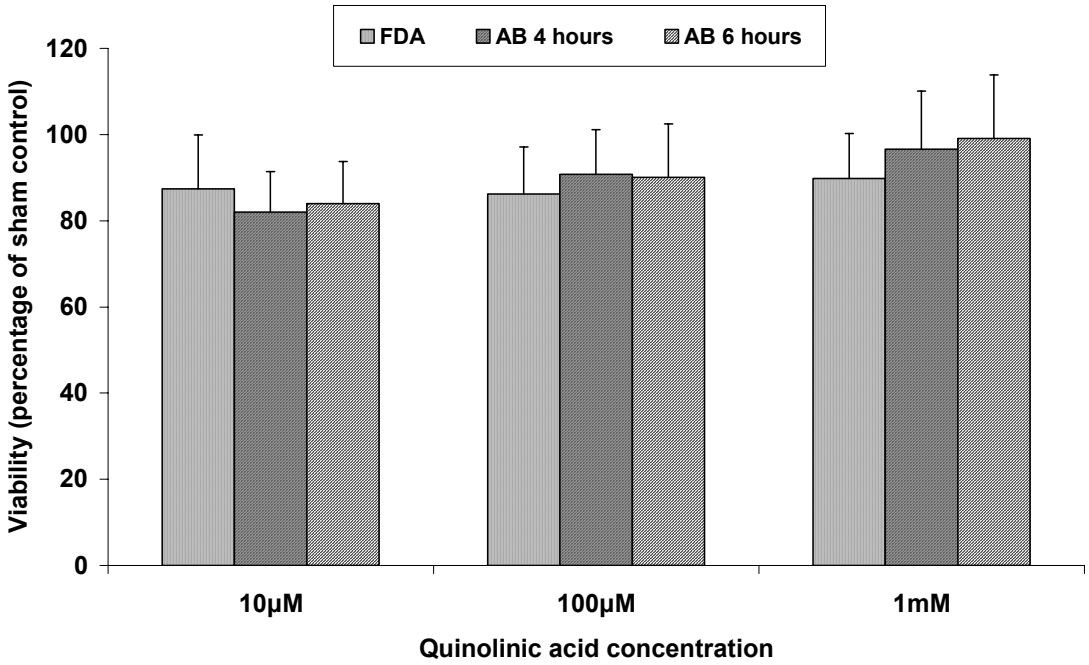

Figure 3.11 Comparison of FDA and Alamar blue in assaying QA toxicity (applied for 1 hour at 9 DIV) in cultured CGNs. Mean +/- SEM, n=5; ANOVA followed by Tukey's test (in each set of three assay results) found no significant difference, indicating that the assays provide comparable data.

3.8 Fluorescein staining and cell morphology comparison

With the readings from each assay consistent with cell number and with each other, further confirmation of assay accuracy was obtained by investigating whether the viability data provided by the assays were consistent with phenotypic appearances indicating viability. Fluorescein produced from FDA is visible under fluorescent light at a wavelength of 480nm, hence cells stained with FDA were examined under both white light and at 480nm (Fig 3.12).

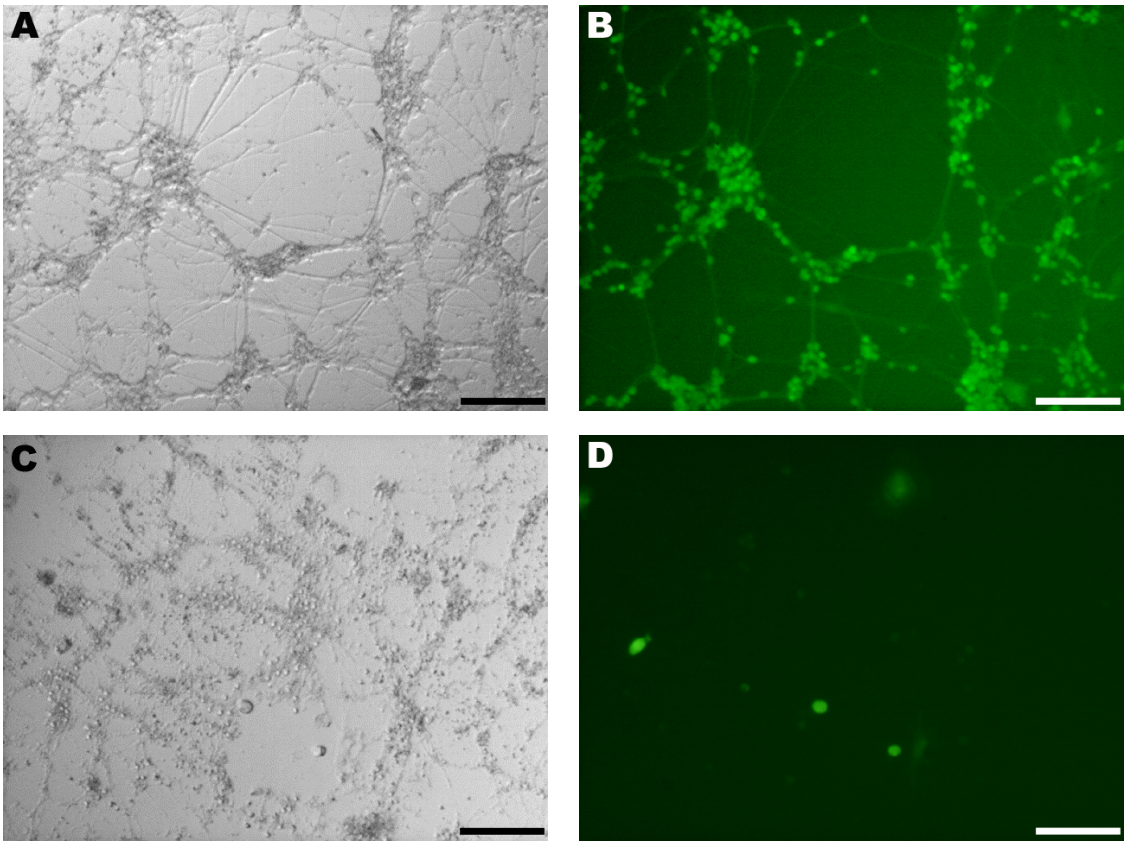

Figure 3.12 Staining of viable CGNs at 10 DIV with fluorescein: correlation with morphological appearances. A) Control CGNs, B) CGNs in A at wavelength 480nm, C) CGNs treated with 100μM 3-hydroxykynurenine for 5 hours at 9 DIV, D) CGNs in C; at wavelength 480nm. Bars = 100μm. A normal healthy morphology corresponds with increased fluorescein production, whereas no fluorescein staining is seen in dead cells.

There was a clear correlation between neurones with normal morphology and positive staining with fluorescein (Fig 3.12A and 3.12B), and between neurones with shrunken perikarya and destroyed neurites (features consistent with dead or dying neurones) and a lack of positive staining (Fig 3.12C and 3.12D). This demonstrated that the FDA assay provided an accurate assessment of neuronal viability in our culture system. Furthermore, as results obtained with both assays were consistent, Alamar blue also provided an accurate method of evaluating viability.

3.9 Fluorescein and PI co-staining

A common method of assessing viability is simultaneous staining with FDA and PI, marking viable and dead cells respectively. Further investigation of the specificity of intracellular de-esterified fluorescein as a viability marker was performed in a small comparative study, with both compounds applied simultaneously for 10 minutes and images recorded using both white light and at wavelengths of 480nm for fluorescein or 530nm for PI. Propidium iodide was shown to be an effective cell death marker and fluorescein staining a specific marker of viable cells (Fig 3.13).

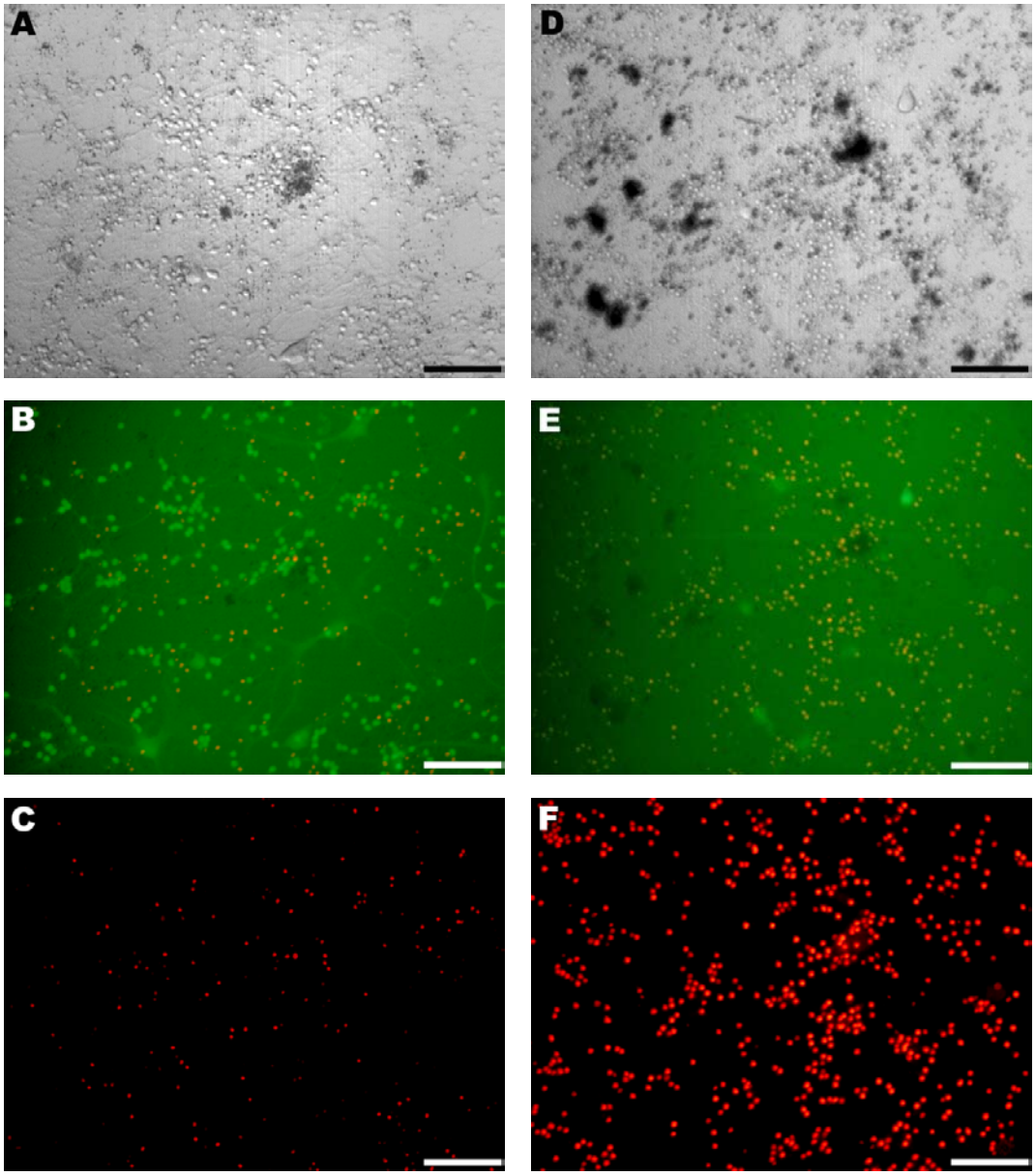

Figure 3.13 Comparison at 12 DIV of untreated CGNs (A, B, C) and CGNS treated with 50μM glutamate for 24 hours at 11 DIV (D, E, F) showing morphological appearance (A, D) fluorescein staining at 480nm (B, E) and PI staining at 530nm (C, F). Bars = 100μM. The morphological images show clearly that cells stained with PI are indeed dead, and that staining with PI and fluorescein are mutually exclusive.

3.10 Discussion of optimising culture conditions

3.10.1 Plating density

A major influence on survival in CGN cultures is the density at which cells are plated: it is well known that if plated at too low a concentration, then cells have a much lower chance of survival (Trenkner, 1998). This effect has been quantified in rat neonatal CGNs plated at densities of $1.1x10^5$, $2.2x10^5$, $4.4x10^5$, $8.8x10^5$, $17.6x10^5$ and $35.2x10^5$ cells/ml, with cell survival compared at 5 DIV (Young *et al.*, 2000). Of these densities, optimal survival proved to be at $8.8x10^5$ cells/ml. Survival rates at densities either below $4.4x10^5$ or above $17.6x10^5$ cells/ml were substantially reduced, although the addition of medium conditioned by CGNs at a density of $4.4x10^5$ cells/ml was shown to increase survival of CGNs plated at $2.2x10^5$ cells/ml (Young *et al.*, 2000). The range of densities used in this study was much narrower, between $0.75x10^5$ and $1.2x10^6$ cells/ml, nevertheless variation in the extent of the neurite network formed was appreciable in cultures plated at $0.75x10^5$ cells/ml compared to those at higher densities.

A significant factor to consider when selecting plating density is that higher densities may increase the vulnerability of CGNs to damage from changes in culture medium. Schramm and co-workers showed that Sprague-Dawley rat neonatal CGNs can be vulnerable to replenishment of culture medium with fresh serum after 14 DIV, with the medium change producing a neurotoxic effect. This effect was blocked by NMDA receptor antagonists 3-(2-carboxypiperazin-4-yl) propyl-1-phosphonate (CPP) or MK-801 (Schramm *et al.*, 1990), suggesting that serum supplementation caused an excitotoxic insult. Furthermore, the toxic effect of glutamate is of greater potency when CGNs were plated at higher densities (Ciotti *et al.*, 1996). Taken together, these results strongly indicate that CGNs plated at higher densities have greater vulnerability to an excitotoxic effect induced by glutamate or replenishment with fresh serum.

The increased susceptibility of higher-density CGN cultures to such an insult is unsurprising, as any excitotoxic stimulus (for example, glutamate in serum) causes an increase in neuronal firing, which in CGN cultures could lead to intracellular glutamate release. Therefore, increased extracellular glutamate

(above that causing neuronal firing) would be proportional to the CGN plating density, with toxicity rising proportionally above a certain threshold.

However, a more complicated process is implicated, since addition of medium conditioned by high-density CGN cultures after 8 DIV increased sensitivity of low-density CGN cultures to glutamate. This suggests that potentiation occurred due to a component within medium conditioned by high-density CGN cultures (Ciotti *et al.*, 1996). The effect of high-density plating on inducing a potential toxic quality to culture medium was also demonstrated by culturing CGNs at a lower density in a lower volume and was possibly mediated by increased expression of NMDAR1 receptor protein (Dus *et al.*, 1997).

Clearly these effects potentially complicate any studies concerning neuronal viability when culture medium changes are required, and particularly compromise those studies involving glutamate or any other excitotoxic stimuli. For these reasons, an excessively high plating density would be just as detrimental to culture survival over the course of the experimental protocol as an unduly low one. The study by Schramm *et al.* (1990) demonstrated vulnerability to serum replenishment used CGNs plated at $1.6x10^6$ cells/ml, a density considerably higher than in our experiments, with the exception of the cell density study. Additionally, the finding that reducing medium volume impacts significantly on the development of cultured CGNs underlines the necessity of excluding the outer rows of wells on the culture plate from experimental protocols due to the higher degree of evaporation (see Materials and Methods section).

These findings indicate that glutamate receptor stimulation levels, particularly of the NMDA subtype, are delicately balanced in CGNs, with the potential for induction of considerable damage by either excessive or insufficient receptor stimulation. Furthermore, this highlights that insufficient consideration of the precise plating density when using cultured CGNs risks significant undesirable effects, due to variations in plating density potentially adversely altering the levels of NMDA receptor stimulation.

3.10.2 Potassium concentration

Stimulation of NMDA receptors and its effect on CGN survival is also of relevance when considering the interaction between potassium concentration and neuronal survival, which is known to vary substantially depending on potassium (K^+) concentration. Neurones maintained in 25mM KCl, a depolarising concentration, showed greater cell survival and had more extensive neurite interconnections than those maintained in 5mM KCl. When neurones in 25mM KCl were switched to medium containing 5mM KCl, extensive apoptotic death occurred within 72 hours. Similarly, when CGNs were cultured in medium containing 5mM KCl from initiation of plating onwards, they suffered widespread apoptosis by 5 DIV (Gallo *et al.*, 1987, Kharlamov *et al.*, 1995).

The precise action of how the higher K^+ concentration produces greater cell survival is uncertain, although it is possible that the depolarisation it causes reduces or prevents excitotoxic damage or that it aids neuronal maturation. This second explanation is unlikely given that the replacement of 25mM KCl with 5mM KCl resulted in neuronal survival falling to levels similar to those in cultures that had been maintained in 5mM KCl since plating, i.e. growth in 25mM KCl did not confer irreversible protection. However, it is possible that such an explanation is correct, but that the duration of the neuronal maturation process is notably longer than the time interval usually used in culturing CGNs, i.e. full maturation may take longer than 14 DIV.

The depolarisation hypothesis was also examined using the depolarising agent veratridine, which was not protective, although notably this agent worked by opening sodium channels (Daniels and Brown, 2002). The protective effect of elevated K^+ is also not prevented by sodium channel blockade using either tetrodotoxin or xylocaine (Gallo *et al.*, 1987). Additionally, the extent of apoptosis induced by reduction of the extracellular K^+ concentration from 25mM to 5mM KCl was markedly reduced by co-applying the Na^+, K^+-ATPase inhibitor ouabain, an effect not blocked by application of MK-801 and the AMPA receptor antagonist CNQX (Isaev *et al.*, 2000). Isaev and co-workers also showed that ouabain protected CGNs subjected to oxidative stress by Fe^{2+} and ascorbic acid. If this is the mechanism of the protective action of ouabain against low K^+-mediated toxicity, this would also be consistent with the explanation of low K^+ toxicity as due to calcium influx, as protection against oxidative damage reduces

the vulnerability of mitochondria to damage from excessive intracellular calcium.

Investigations of effects of potassium concentration beyond simply monitoring cell survival have studied expression of NMDA receptor subunit proteins in CGNs, revealing that expression of mRNA coding for subunits NR1 and NR2A increased over 2-9 DIV, with greater increases in CGNs cultured in 25mM KCl relative to those in 10mM KCl (Resink *et al.*, 1995). Conversely, expression of mRNA for subunit NR2C increased over 2-9 DIV, with a greater increase with 10mM KCl than 25mM KCl (Resink *et al.*, 1995). This increase in NR1 expression due to high K^+ gives an interesting parallel with the 1997 finding of Dus *et al.* that culture of CGNs in a low volume of medium (comparable to high-density plating) also increased expression of NR1.

Previous studies with either higher (24.5mM) or lower (5.4mM) potassium have demonstrated clear differences in neuronal morphology. Cultured mouse CGNs maintained in both concentrations of K^+ (fixed at 8 DIV) were seen to form clusters of cells, which were more extensive in neurones cultured in 5.4mM KCl. Clusters consisted of neuronal soma predominantly at the outer edges, with extensive neuropil in the centre. However in cultures maintained in 5.4mM KCl, extensive neuropil degeneration was evident, particularly dendritic constituents, with pre-synaptic components relatively spared although synaptic vesicles were less developed (Peng *et al.*, 1991).

Plating and maintaining neonatal rat CGNs in 5mM KCl has also been shown to significantly reduce the expression of the dominant glucose transporter type GLUT3 to approximately a third of the levels seen with CGNs in 25mM KCl, although KCl concentrations above 25mM did not cause further increases in GLUT3 expression (Maher *et al.*, 1994). Expression of GLUT1 was also reduced, albeit less extensively than that of GLUT3, which is perhaps unsurprising as the expression of GLUT3 is 8-10 fold greater than GLUT1 in neonatal rat CGNs (Maher *et al.*, 1994).

Culturing CGNs in 5mM K^+ also caused significant reductions in PKC activity (Lin *et al.*, 1997). Activity increased in both 5mM KCl and 25mM KCl between 2-4 DIV, with PKC levels in CGNs in 25mM KCl continuing to rise until 8 DIV then remaining stable. However levels in CGNs cultured in 5mM KCl declined after 4

DIV, falling to below a third of the levels of 25mM CGNs by 8 DIV (Lin *et al.*, 1997). The range of roles of PKC, including involvement in neuroprotection, provides further evidence that CGNs in medium with a 5mM potassium concentration represent a neuronal type abnormally vulnerable to excitotoxic or oxidative damage.

The maintenance of CGNs in lower K^+ concentrations leads to significant levels of apoptotic cell death, associated alterations in expression of NMDA and GLUT3 receptors, PKC activity and an abnormal phenotype. This highlights the necessity of a depolarising concentration of K^+ in the medium and was borne out in the pilot qualitative study using a range of K^+ concentrations, in which optimal morphology was with a K^+ concentration of 25mM.

Both cell plating density and K^+ concentration and their consequent effects on NMDA receptor stimulation may mimic aspects of inter-neuronal signalling which occur during migration of CGNs into the external granular layer *in vivo*, specifically stimulation by mossy fibre neurones (Balázs *et al.*, 1988, Morán and Patel, 1989). It is known that failure to successfully migrate, with consequent lack of neuronal stimulation and depolarisation, is associated with DNA fragmentation and apoptosis during normal postnatal cerebellar development (Balázs *et al.*, 1988, Wood *et al.*, 1993). Consequently a plating density and K^+ concentration at the optimal levels will mimic the degree of NMDA receptor stimulation necessary for CGN survival, but without reaching excessive levels that risk excitotoxicity-mediated damage and cell death.

Application of NMDA to CGNs increased activity of the glutamate-synthesising enzyme glutaminase, an effect blocked by cycloheximide or actinomycin D and not replicated in cultured cerebellar astroglial cells (Morán and Patel, 1989). The loss of CGNs in a non-depolarising K^+ concentration can be prevented by the use of NMDA, an effect blocked by receptor antagonists. Furthermore, the use of these antagonists *in vivo* caused an increase in apoptotic death of CGNs (Balázs *et al.*, 1988, Monti *et al.*, 2002, Alvarez *et al.*, 2006).

Maturation of CGNs (both *in vivo* and *in vitro*) is associated with phosphorylation of the cAMP response-element binding protein (CREB), which is significantly reduced by blockade of the NMDA receptor *in vivo* or by the use of a non-depolarising potassium concentration *in vitro,* this latter effect prevented by the

application of NMDA (Monti *et al.*, 2002). It is of interest to note that CREB phosphorylation is also involved in differentiation of CGNs during development and that the extracellular matrix protein vitronectin (which acts to induce differentiation) induces CREB phosphorylation (Pons *et al.*, 2001). Furthermore, CGNs overexpressing CREB have a significantly higher rate of differentiation (Pons *et al.*, 2001).

In any exclusively neuronal culture system, an integral stage is the removal of non-neuronal cells, most commonly by pharmacological elimination, using an agent selectively toxic to mitotic cells. Cytosine arabinoside is frequently used in the preparation of CGN cultures, at doses ranging from 5μM to 50μM, with 10μM most commonly used for cultures prepared from 8-day old Sprague-Dawley rat neonates (Marini *et al.*, 1998, Trenkner, 1998, Wick *et al.*, 2002).

Cytosine arabinoside is a nucleotide analogue which eliminates proliferating cells, reducing DNA synthesis by inhibiting DNA polymerases, and which becomes incorporated into newly-formed DNA (Grant, 1998). The dose applied has to be at a non-toxic concentration for neurones as it has been reported to generate ROS, interfere with membrane lipid synthesis and can cause apoptosis in cultured neurones: this effect is dose-dependant and mediated by (although not dependant on) activation of Bax (Grant, 1998, Besirli *et al.*, 2003). It has been demonstrated however that 10μM cytosine arabinoside does not cause significant neuronal death when applied to neonatal rat CGN cultures (Courtney and Coffey, 1999).

Cerebellar granular neurones maintained in 5mM KCl are significantly more vulnerable to the toxic effects of cytosine arabinoside than cells grown in 25mM KCl. In experiments using rat and mouse CGNs, a clear increase in toxic effect was demonstrated as the concentration of cytosine arabinoside increased, with greater toxicity seen against neurones in 5mM KCl cultures than those in 25mM KCl cultures (Daniels and Brown, 2002). With 10μM cytosine arabinoside, the difference in survival rates was only ~10%, but at a concentration of 100μM, the disparity was ~20% and ~80% (Daniels and Brown, 2002). However, this group noted only a slight effect of K^+ withdrawal on CGN viability (using a normal 10μM concentration of cytosine arabinoside, in either rat or mouse CGNs). This is in

contrast to the extensive loss seen in our studies, so direct comparison with our system is uncertain.

The study of the effectiveness of cytosine arabinoside in our culture system was qualitative in nature and relied on immunocytochemical investigations using an antibody raised against ß-tubulin$_{III}$, a protein specific to neuronal cells including neonatal rat CGNs (Ankarcrona *et al.*, 1996, Cumming *et al.*, 1984), and an antibody raised against GFAP to stain for the presence of glial cells. Both antibodies were effective in labelling their respective target cell populations, and the presence of 10µM cytosine arabinoside 24 hours after plating effectively inhibited non-neuronal cells. Only a few cells stained positive for GFAP in cytosine arabinoside treated cultures. There were no evident differences in neuronal populations and neurite networks produced when cultures in the presence or absence of 10µM cytosine arabinoside were compared.

3.11 Discussion of viability assay reliability

A range of assays to quantify levels of cell viability or death have been used with cultured CGNs: Trypan blue, PI, FDA, 3-(4,5-dimethylthiazol-2-yl)-2,5-diphenyltetrazolium bromide (MTT), lactate dehydrogenase (LDH) and Alamar blue (Altman *et al.*, 1993, Budd and Nicholls, 1996, Marini and Paul, 1993, Morán *et al.*, 1999, Ward *et al.*, 2005, White *et al.*, 1996 respectively). The limitations of Trypan blue in assessing mature neuronal viability have been reported previously (Altman *et al.*, 1993), making either Alamar blue or FDA the most practical assay for use. These were compared initially to determine the most effective in our system. Alamar blue is a relatively recent non-toxic assay dye, initially used for quantification of cell proliferation rather than survival (Ahmed *et al.*, 1994). Fluorescein diacetate is well established, having been in use for more than forty years (Rotman and Papermaster, 1966).

The range of cell concentrations used to quantify the assays was limited by similar factors to those affecting the choice of cell plating density. The lowest concentration used was $500x10^5$ cells/ml, below which the risk of cell death due to apoptosis was too great. The highest density used was $1.5x10^6$ cells/ml, which was potentially vulnerable to damage from fresh serum in the medium used in the Alamar blue assay (Schramm *et al.*, 1990). However, the Alamar blue readings for this cell density and their positions relative to the final R^2 lines are

comparable to those achieved with FDA, which did not use any serum. This suggests that replenishment of the higher density cultures with fresh serum-containing medium was unlikely to have substantially impacted on cell survival in this experiment. However, the period over which any such insult could have taken place was limited to the 4 or 6 hours during which the Alamar blue was active, so it is possible that a density-related neurotoxic effect would have become more apparent over a longer period of time.

The lack of time for a potential neurotoxic effect to act is also a relevant factor when considering the effect of serum withdrawal, which is a feature of the fluorescein diacetate assay method. However, neurotoxicity resulting from the withdrawal of serum from the culture environment takes several hours to become apparent (Atabay *et al.*, 1996), whereas the FDA assay reading is taken after only 10 minutes. Therefore, although serum withdrawal could be a significant source of error if the assay duration was equivalent to that for Alamar blue, the withdrawal period used with this assay renders it immaterial.

When comparing results in a human hepatoma cell line, HepG2, following treatment with a range of 117 cytotoxic drugs, it was found that, excepting two drugs studied, Alamar blue appeared slightly more sensitive than MTT (Hamid *et al.*, 2004). Our study compared the results from Alamar blue and FDA assays in identically-treated CGN cultures exposed to tryptophan, kynurenine or QA at 10μM-1mM concentrations and clearly indicated that results using either assay were comparable. It is noteworthy that the statistical analysis used to exclude any significant difference was highly conservative, with the minimum number of comparisons used for ANOVA (three). Also, in each case there were very large p-values, indicating that the absence of any observed difference was extremely unlikely to be a type 2 error (false negative). Furthermore, this was observed in experiments using different compounds and a range of concentrations for each, and the analysis (a total of nine sets of three readings, each with a total of 5 repetitions) gave no significant difference. Nor is there any indication that one assay produced results that were consistently higher or lower than the other, even to a statistically insignificant degree.

Comparison of fluorescein staining with morphological characterisation gave clear evidence that the application of FDA for 10 minutes represented an

accurate assessment of neuronal viability in our system, with good correlation between fluorescein staining of cells and the presence of a viable phenotype. Fluorescein production is only possible in cells with functioning intracellular esterases to cleave the two acetate groups from the molecule (thus producing fluorescein: Rotman and Papermaster, 1966) and an intact cell membrane to retain the produced fluorescein. Therefore, positive staining is not possible in dead neurones, as was indeed evident.

Co-staining with PI, a DNA intercalating agent known to stain the nuclei of dead cells, also confirmed the efficacy of the FDA assay. Propidium iodide was excluded from the nuclei of viable cells by the intact cell membranes and hence provided an effective contrast with the viability marker of de-esterified intracellular fluorescein. This comparative study demonstrated that dead cells identified by positive staining with PI were not stained with fluorescein as further confirmation of the specificity of FDA as a marker of viable cells.

Co-application of FDA and PI, giving results for both viable and non-viable cells used, is an alternative method of viability analysis (Manev *et al.*, 1989, Scorziello *et al.*, 2001). With the effectiveness of FDA alone already clearly established, the double confirmation method was not necessary. An additional reason for not using this method was that (as is seen in the representative images), light at 480-485nm used to produce excitation of fluorescein also caused some response from PI, an effect that could potentially interfere with results taken via an automatic plate reader. The alternative method, to use representative images quantified by counting individual cells, was rejected due to increased potential for error, risk of observer bias and excessive time consumption for no appreciable gain.

The main drawback of FDA is that the fluorescein produced by viable cells gradually leaks out of the cellular cytoplasm into the medium, leading to potential increasing inaccuracy as this accumulates. In this study, the brief period of application of assay solution meant that this was minimal; however in studies necessitating a greater period of assay solution exposure, an analogue of fluorescein diacetate with a less membrane-permeable active product would be preferable. A wide range of such compounds is available, such as 5-carboxyfluorescein diacetate (Smith *et al.*, 2003), which could be of use in

studies investigating precisely when the loss of viability seen by the FDA assay at 24 hours occurs.

Having established the suitability of each of these methods for use as a viability assay, the choice between the two was primarily based on logistical factors. There is a higher potential for error if any inaccuracies in timing occur with the use of the FDA assay, as even a brief delay will cause significant alteration to the final result, and consideration of this factor is essential with use of this assay. However, the use of FDA was more efficient in terms of time (a ten minute incubation prior to assay period, compared to a four or six hour incubation for Alamar blue), and in cost effectiveness. Hence, although some early studies used Alamar blue, the vast majority of the subsequent viability studies in this study were carried out with FDA.

4 Excitotoxicity and Oxidative Stress

4.1 Introduction

The experiments in this chapter were concerned with the investigation of excitotoxic and oxidative damage to CGNs mediated by a variety of stressors, with a particular focus on the actions mediated by tryptophan and compounds of the kynurenine pathway, as this is known to produce neurotoxic compounds capable of generating excitotoxic or oxidative damage in neurones. The interaction of these toxic effects with increased levels of glucose was also considered. In addition, the effects of glutamate, NMDA, 3-nitropropionic acid (3-NPA) and OGD on CGN viability were examined.

These insults provided a range of stressors that have been identified as acting via excitotoxic NMDA receptor activation or generation of oxidative stress. The use of glutamate, increased glucose concentrations and tryptophan metabolites allowed examination of toxic effects due to endogenous agents of excitotoxicity or oxidative damage, with glutamate application and OGD also modelling aspects of damage to neurones during an ischaemic injury (for review see Lee *et al.*, 2000).

The investigation of the range of tryptophan metabolites subsequently focused on the neurotoxic effects of three compounds: 3-hydroxykynurenine (3-HK), 3-hydroxyanthranilic acid (3-HAA) and 5-hydroxyanthranilic acid (5-HAA). The mechanisms involved, concerning both the means of generating neurotoxic damage and the intracellular mechanisms leading to cell death, were explored. As published CGN culturing protocols use a variety of concentrations of glucose in medium, and increased concentrations of glucose can affect the toxicity of glutamate and 3-NPA (Fink *et al.*, 1996, Delgado-Esteban *et al.*, 2000), we set out to investigate whether the neurotoxic effects of tryptophan metabolites would be altered by a difference in glucose concentration.

Following the discovery of an altered ratio of anthranilic acid to 3-HAA concentrations found in stroke patients compared with those of healthy subjects (Darlington *et al.*, 2007), the effect of altering the concentration of anthranilic acid on the toxicity to CGNs of 3-HAA was also examined.

4.2 Aims and Objectives

- Demonstration of a dose-responsive neurotoxic effect of glutamate to CGNs

- Demonstration of reduced survival and increased vulnerability to glutamate in CGNs maintained in a non-depolarising potassium concentration

- Demonstration of a dose-responsive neurotoxic effect of 3-NPA on CGN viability

- Establishment of an effective system for delivering consistent OGD to cultured CGNs

- Investigation of mechanisms for OGD toxicity

- Investigation of the effects on CGN viability of increased glucose concentration

- Investigation of the effects on CGN viability of treatment with tryptophan and several metabolites, over a range of doses and exposure times, examined in both low and high glucose environments

- Effect of different medium glucose concentration on metabolism of tryptophan and selected metabolites in cultured CGNs

- Investigation of mechanisms involved in neurotoxic effects of selected tryptophan metabolites known to generate oxidative damage

- Investigation of effects on CGN viability of altered ratios of anthranilic acid and 3-HAA

4.3 Glutamate, *N*-methyl-D-aspartate and 3-nitropropionic acid toxicity

4.3.1 Glutamate toxicity

The application of glutamate, over a concentration range of 1μM to 10mM for 24 hours, at 9 DIV caused a dose-dependant reduction in neuronal viability up to a concentration of 5mM, beyond which no further damage due to glutamate-mediated toxicity was observed (Figure 4.1). It was notable that a relatively sharp drop in viability compared with the sham control was noted when applying the normally non-toxic concentration of 1μM glutamate, suggesting that the 'sham control' procedure may not have accounted for all of the damage inflicted by the treatment procedure. A possibility is that the presence of any supplementary glutamate in the medium causes a larger rise due to release of endogenous neuronal glutamate. It was also noted that even very high concentrations of glutamate did not completely eliminate viable cells: it is possible that a percentage of this is due to remaining glial cells, or neurones other than CGNs.

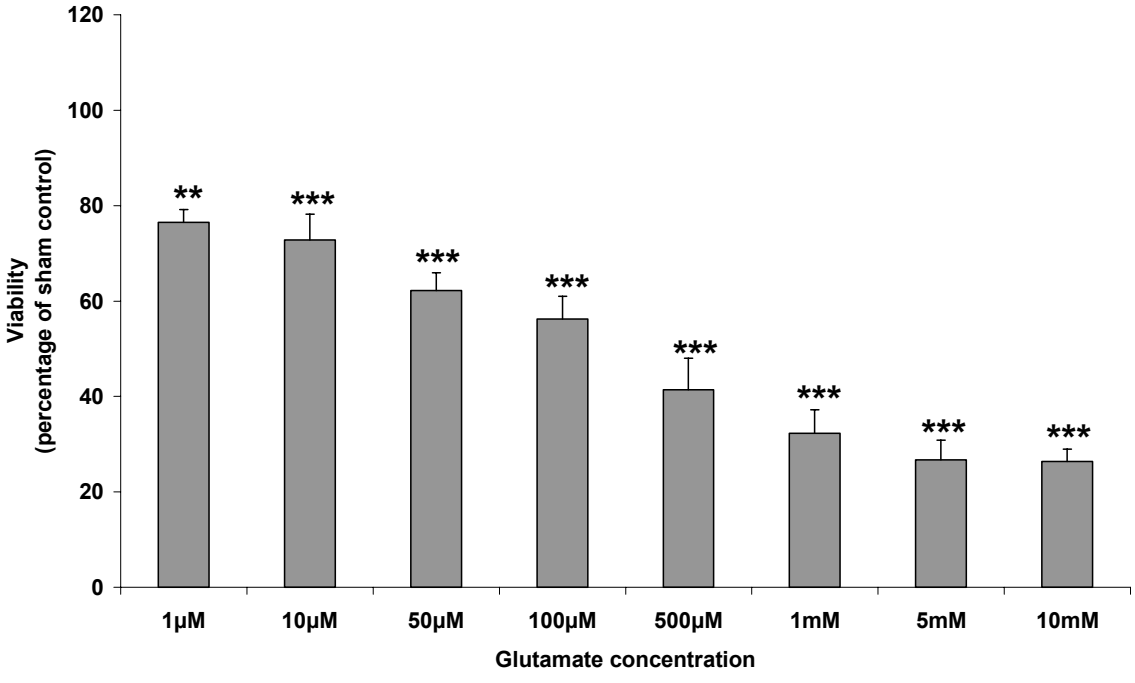

Figure 4.1 Effect of glutamate added in medium for 24 hours at 9 DIV on CGN viability (assessed by fluorescein diacetate assay), producing increased toxicity with increasing glutamate concentration. Mean +/- SEM, n=6; ANOVA plus Tukey's test, ** p<0.01, *** p<0.001.

4.3.2 Glutamate toxicity in low potassium medium

The survival of CGNs following glutamate treatment was reduced by switching the K^+ concentration to 5.5mM KCl 48 hours before treatment (Figure 4.2). The reduction in K^+ itself caused notable toxicity (cell viability was reduced to 45.5% of control values in 25mM KCl).

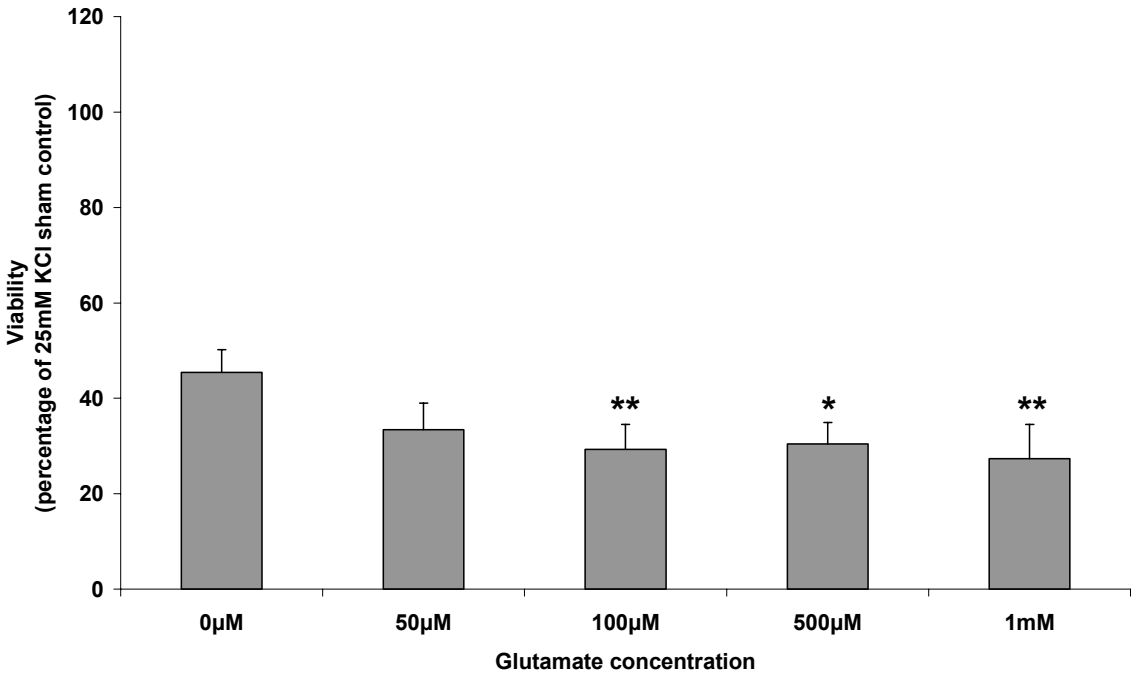

Figure 4.2 Effect of glutamate added in medium for 24 hours on viability of CGNs cultured in medium with 25mM KCl, then switched to 5.5mM KCl 48 hours before glutamate treatment (assessed by Alamar blue assay). Mean +/- SEM, n=5; ANOVA plus Tukey's test, * p<0.05, ** p<001 (relative to 0µM glutamate in 5.5mM KCl medium group). A striking decrease in viability occurred due to the switch to 5.5mM KCl, with maximum damage achieved using 100µM glutamate, as compared to 1mM in cultures maintained in 25mM KCl.

Although this demonstrated that this characteristic of CGN cultures was present in our system, further work using 5.5mM KCl medium was not continued since these cultures were clearly abnormal, with increased cell death due to K^+ withdrawal. Any damage by excitotoxic or oxidative insults therefore would have taken place against this background, making quantification of treatment damage difficult. Additionally, the significance of results from a culture system known to produce CGN networks with abnormal characteristics (Peng *et al.*, 1991, Resink *et al.*, 1995) would be uncertain.

4.3.3 3-Nitropropionic acid toxicity

The known excitotoxin and mitochondrial poison 3-NPA applied at concentrations of 1μM to 10mM for 24 hours at 9 DIV caused damage in a dose-dependant manner up to a concentration of 5mM, with no further damage observed beyond this point (Figure 4.3). This compound was studied to determine the effect on CGN viability of an excitotoxic insult complicated by metabolic compromise. As with glutamate, a percentage of cells survived this treatment, although the combined toxic effects of 3-NPA were evidently lethal to a larger number of cells.

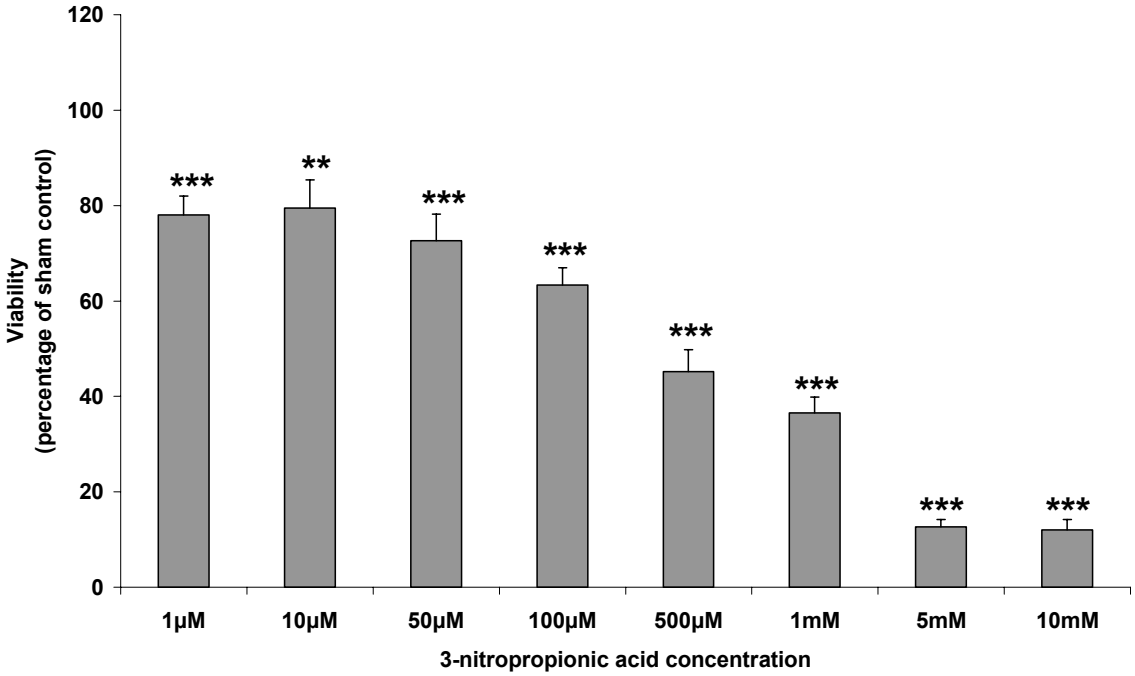

Figure 4.3 Effect of 3-NPA added in medium for 24 hours at 9 DIV on CGN viability (assessed by fluorescein diacetate assay), producing increased toxicity with increasing 3-NPA concentration. Mean +/- SEM, n=5; ANOVA plus Tukey's test, ** p<0.01, *** p<0.001.

4.3.4 Toxicity of glutamate or 3-NPA unaffected by glucose concentration

Despite the findings by others that glutamate-induced neurotoxicity is dependent on glucose levels (Delgado-Esteban *et al.*, 2000), and that increased glucose protects against the neurotoxic effect of 3-NPA (Fink *et al.*, 1996), there was no difference in effect seen when these compounds were applied in medium containing either 5.5 or 25mM glucose.

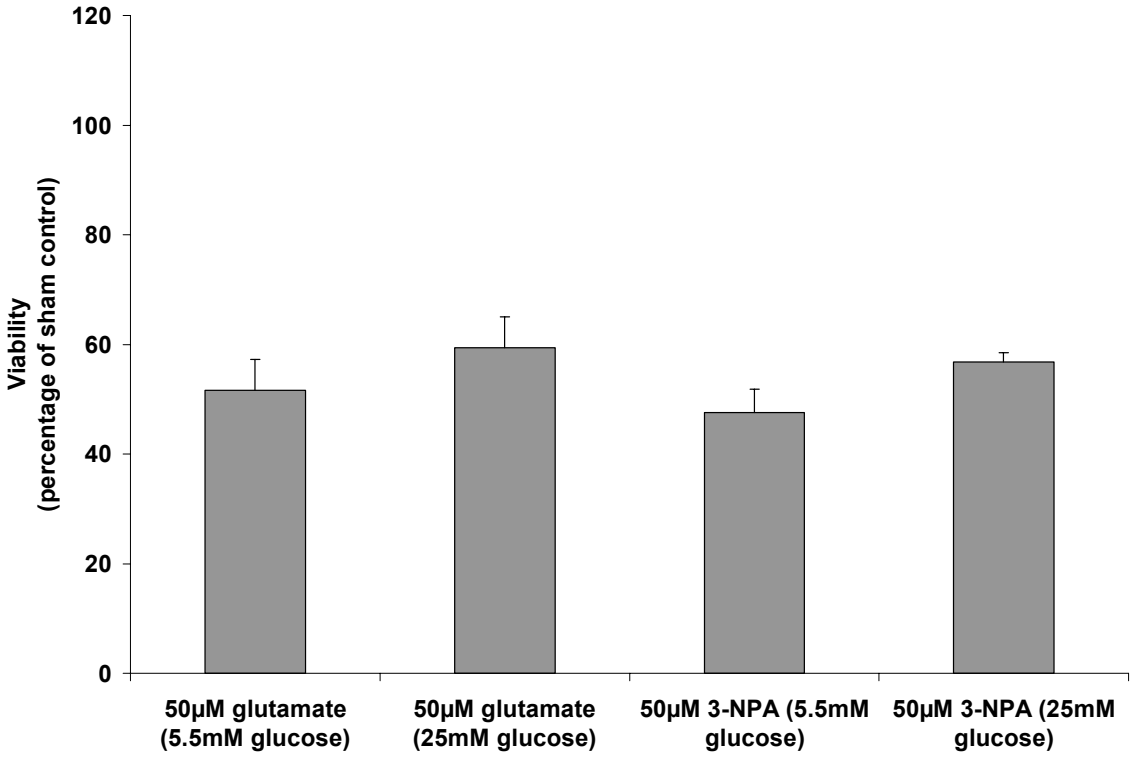

Figure 4.4 Toxicity of 100μM glutamate or 100μM 3-NPA unaffected by presence of either 5.5 or 25mM D-glucose (assessed by fluorescein diacetate assay). Mean +/- SEM, n=5; Student's T-test comparing paired columns identified no significant difference in the toxicity of either compound due to alteration of the glucose concentration.

4.3.5 Toxicity of glutamate, NMDA or 3-NPA unaffected by cycloheximide

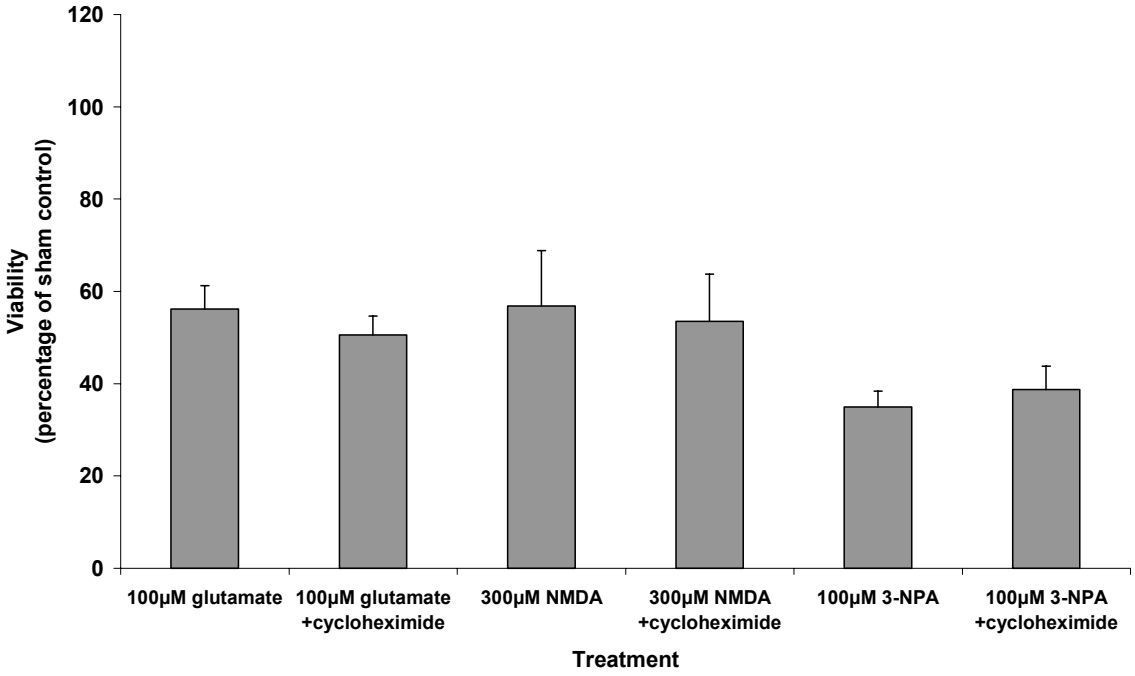

Figure 4.5 Toxicity of 100µM glutamate, 300µM *N*-methyl-D-aspartate or 100µM 3-NPA is unaffected by co-application of 0.05µg/ml cycloheximide (assessed by fluorescein diacetate assay). Mean +/- SEM, n=4; ANOVA followed by Tukey's test identified no significant protection by cycloheximide against the toxicity of any treatment.

Figure 4.5 showed that protein synthesis is not required to produce the neurotoxic effect mediated by 100µM glutamate, 300µM NMDA or 100µM 3-NPA (applied in medium for 24 hours at 9 DIV). This finding was confirmed by examination of neuronal morphology (Figure 4.6). It should be noted however, that this does not exclude the involvement of apoptotic mechanisms in these insults, only that the compounds' toxic effects are not dependent on protein synthesis: therefore increased production of death signalling proteins such as TNFα or Fas are not implicated.

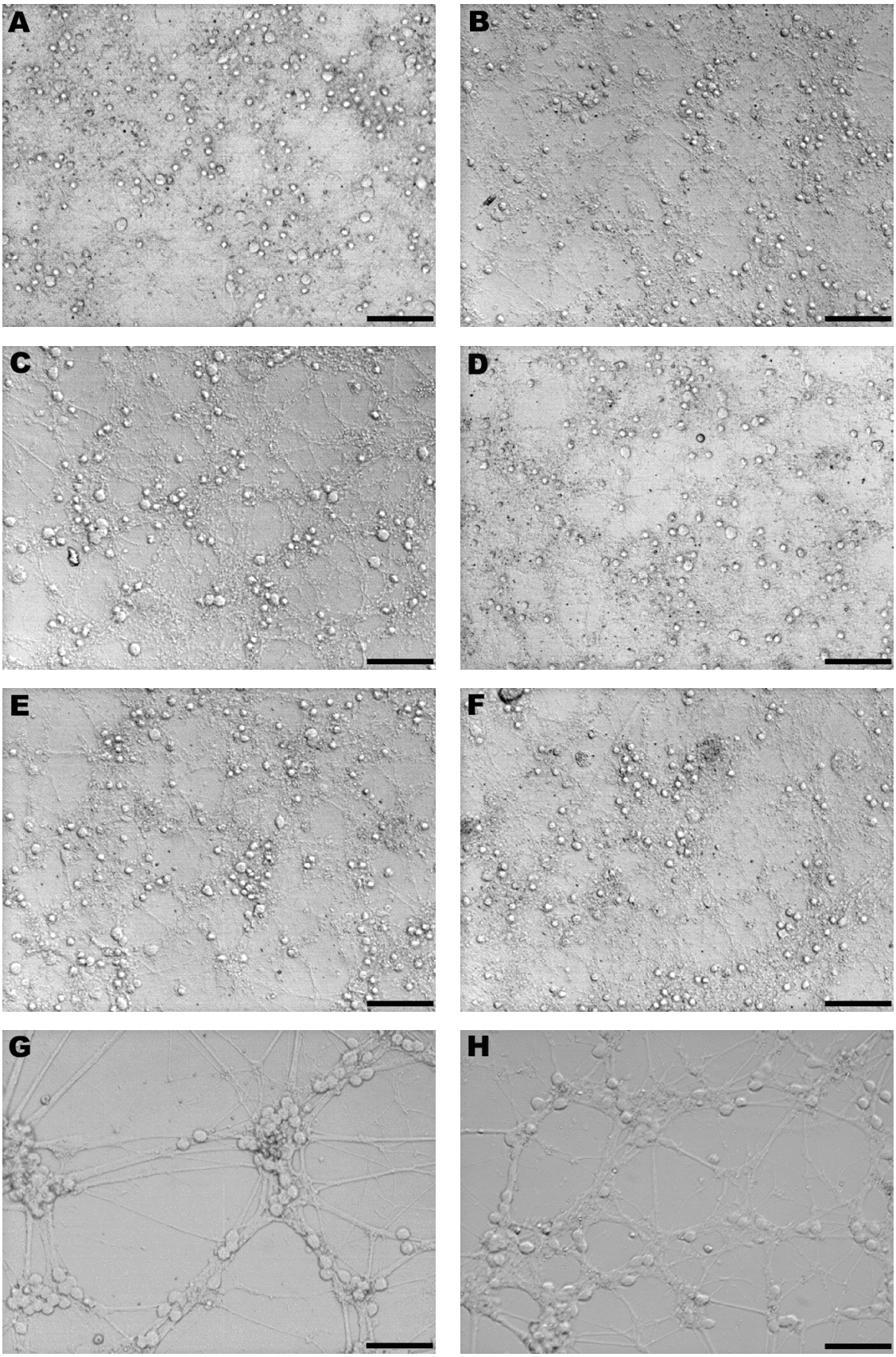

Figure 4.6 Effects of (A, B) 100μM glutamate, (C, D) 300μM NMDA and (E, F) 100μM 3-NPA applied for 24 hours at 9 DIV on morphology at 10 DIV. Effects shown with (B, D, F) and without (A, C, E) co-applied 0.05μg/ml cycloheximide. Also shown are controls (G) and cultures treated with 0.05μg/ml cycloheximide only (H). Bars = 50μm. Extensive neuronal death was induced by all three insults, with no protection given by cycloheximide.

4.4 Toxicity of oxygen-glucose deprivation

4.4.1 OGD toxicity – MK-801, kynurenic acid and nifedipine

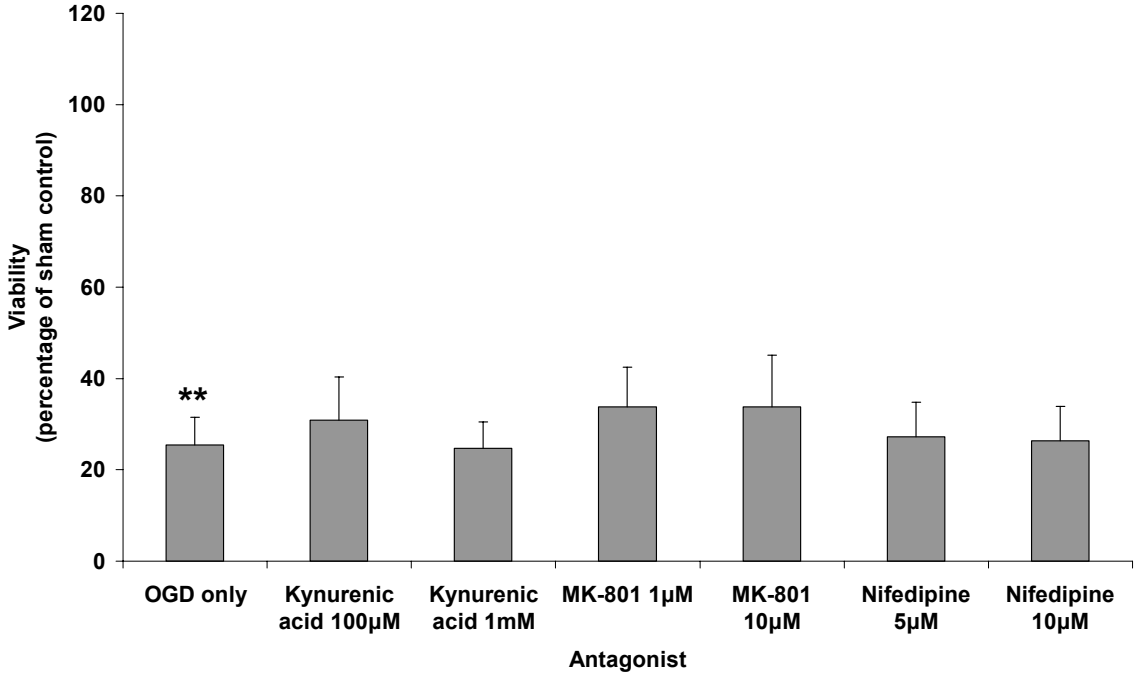

Figure 4.7 Effect of antagonists on toxicity of 5 hours OGD on CGNs at 9 DIV. Mean +/- SEM, n=4; Student's T-test, ** p<0.01 comparing OGD alone with sham control; ANOVA followed by Tukey's test identified no significant protection from any treatment, indicating that the toxic effect of OGD was not dependent on NMDA receptor stimulation or influx of calcium via voltage-gated calcium channels.

Oxygen-glucose deprivation for 5 hours at 9 DIV proved a potent method of inducing neuronal damage (Figure 4.7). The effects were not attenuated by the presence of the NMDA receptor antagonist MK-801, the glutamate receptor antagonist kynurenic acid or by the calcium channel blocker nifedipine (all applied throughout the period of OGD).

The role of protein synthesis in the neurotoxicity of OGD was also examined to determine if production of death signalling proteins was involved in the neuronal death mechanisms induced (Figure 4.8). Co-application of cycloheximide during or after OGD (or for both periods) was carried out to ascertain whether any such response was mediated during the OGD insult itself or during the period immediately after (with OGD as a model of ischaemia, this period would be comparable to the reperfusion stage). The use of cycloheximide in either or indeed both of these periods did not reduce the toxic effect seen either by viability assay (Figure 4.8) or with morphological observations (Figure 4.9).

4.4.2 OGD toxicity – effect of cycloheximide

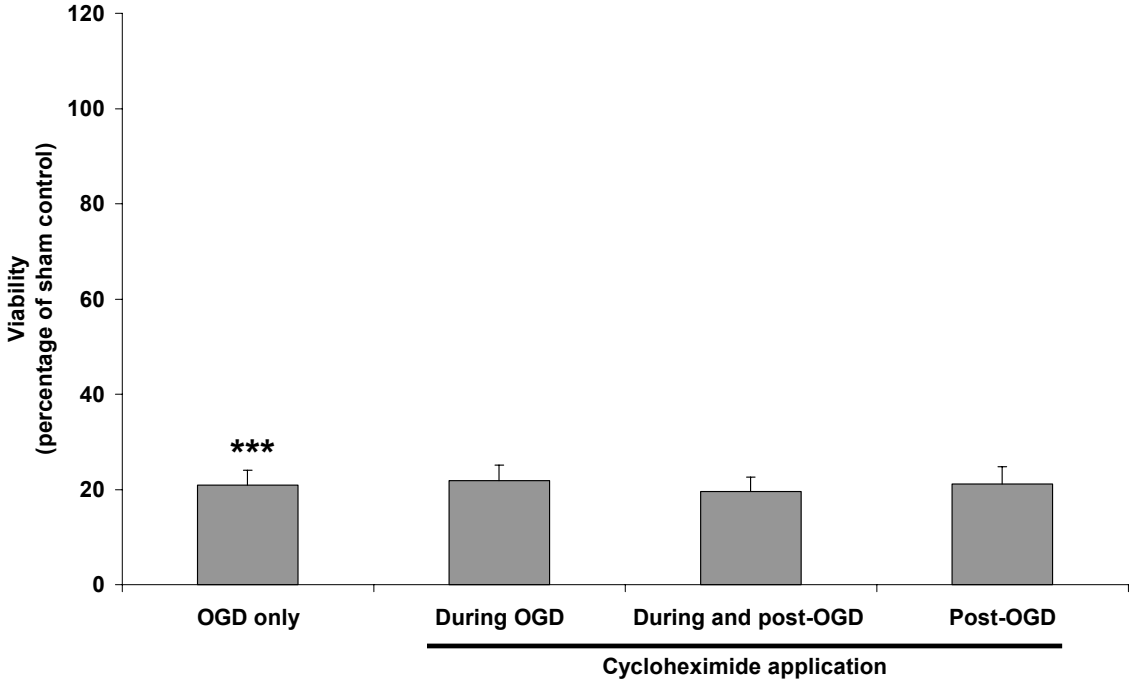

Figure 4.8 Effect of 0.05µg/ml cycloheximide application on toxicity of 5 hours OGD on CGNs at 9 DIV. Mean +/- SEM, n=4; Student's T-test, *** p<0.001 comparing OGD alone with sham control; ANOVA followed by Tukey's test identified no significant protection from cycloheximide treatment, whether applied during or after OGD.

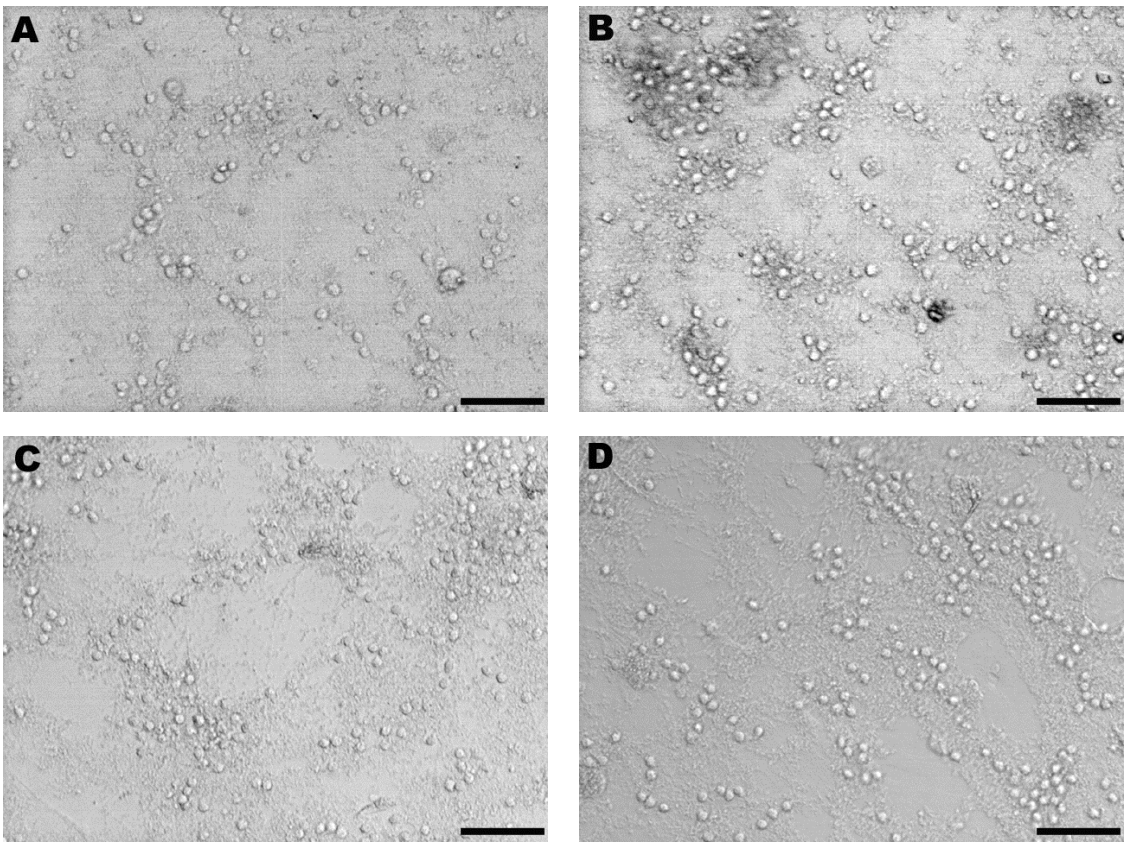

Figure 4.9 Effect of 5 hours oxygen-glucose deprivation at 9 DIV on CGN morphology at 10 DIV: A) OGD only, B) OGD with 0.05µg/ml cycloheximide, C) OGD with 1µM MK-801, D) OGD with 100µM kynurenic acid. Bars = 50µm. As can be seen, none of these treatments were able to reduce the toxicity of OGD for this duration.

4.5 Effect of increased glucose concentration

4.5.1 Effect of raised glucose in culture medium on viability

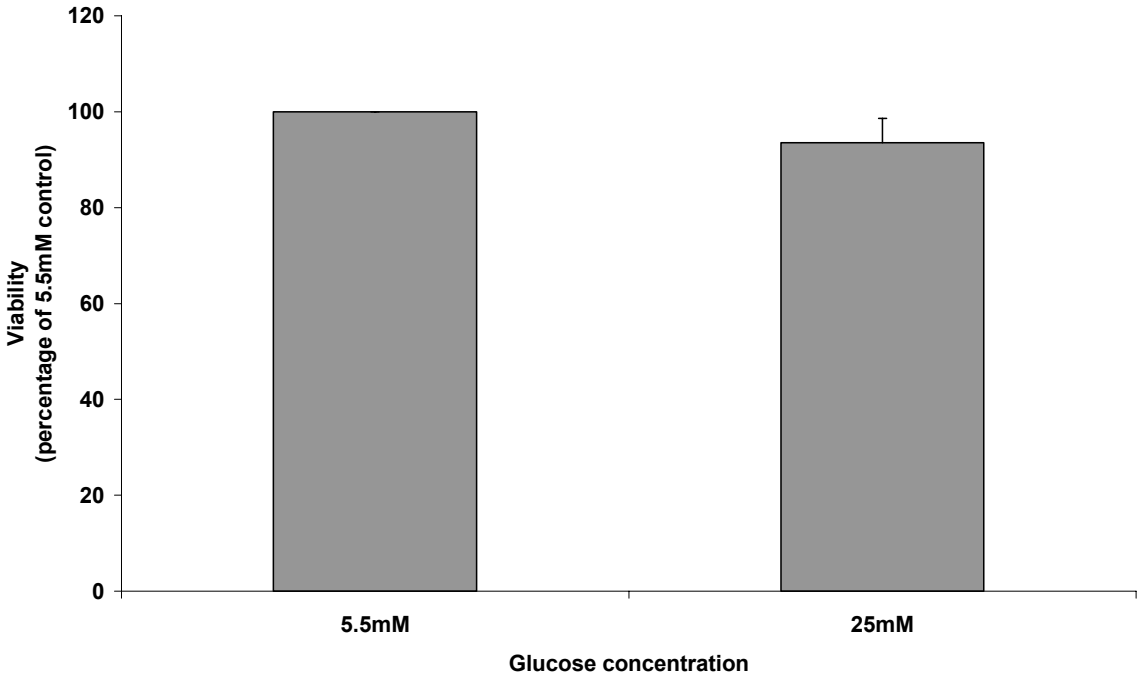

Figure 4.10 Effect of culturing in medium supplemented to 25mM D-glucose on viability of CGNs at 10 DIV. Mean +/- SEM, n=5; Student's one-sample t-test performed, with no significant difference seen in CGN viability with either concentration of glucose.

Figure 4.10 demonstrates that CGN cultures were maintained well in medium containing either 5.5 or 25mM glucose. Although previous studies have maintained CGNs in a range of glucose concentrations, and an increased glucose concentration *in vitro* or hyperglycaemia *in vivo* has been associated with several changes (Delgado-Esteban *et al.*, 2000, Sima, 2003, Vincent *et al.*, 2005), there was no significant neurotoxic effect in our system after 10 DIV. However, this does not exclude the possibility of the CGNs being exposed to a sub-lethal increase in oxidative stress.

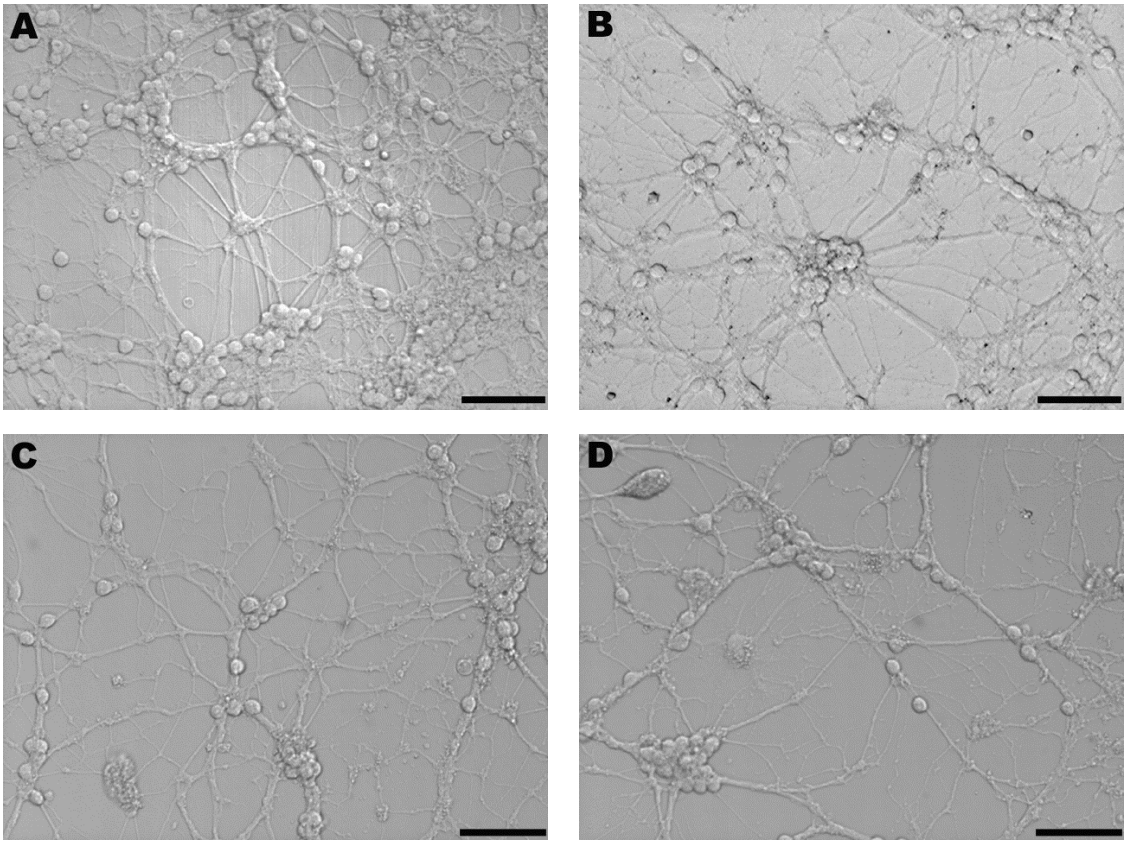

Figure 4.11 Morphological appearances of CGNs in medium containing (A, C) 5.5mM and (B, D) 25mM glucose at 12 DIV (A, B) and 31 DIV (C, D). Bars = 50µm. Neurones have a healthy appearance in both concentrations of glucose and at both 12 and 31 DIV, indicating a healthy phenotype can be maintained for long after the duration of our experimental protocols.

In addition to providing confirmation of the viability assay findings, observations of CGN morphology in medium containing 5.5 and 25mM glucose showed that over the period of 8-14 DIV, under either of these conditions, neuronal phenotype with extensive neurite networks were maintained (Figure 4.11 A-C), and could be sustained for over four weeks (Figure 4.11D). It is therefore clear that experiments performed within 14 DIV are well within the CGNs' normal period of survival.

4.6 Toxicity of tryptophan and kynurenine pathway compounds

Tryptophan and eight metabolites from various branches of the kynurenine pathway were included in the study. The compounds were selected as they together constitute the main products of the kynurenine pathway, and thus illustrate the major effects due to tryptophan metabolism via this route. The effects of the compounds on CGN viability were studied over a concentration range of 10μM to 1mM, and over time periods ranging from 1 to 9 hours. Additionally, each of the compounds was examined both in medium with a glucose concentration of 5.5mM and with 25mM, in order to demonstrate any differences in neurotoxic effect due to increased glucose concentration.

A positive correlation between concentration and toxicity for three compounds (3-HK – Figure 4.14, 3-HAA – Figure 4.15 and 5-HAA – Figure 4.20) was evident, although no consistent relationship with concentration occurred with the remaining six compounds (tryptophan - Figure 4.12, kynurenine – Figure 4.13, QA – Figure 4.16, kynurenic acid – Figure 4.18, anthranilic acid – Figure 4.19 and picolinic acid – Figure 4.21). However, a tendency towards an increase in toxicity with longer exposure times, although not at every concentration, was evident in all nine compounds.

In addition to assessment of cell viability levels using the FDA assay, neuronal morphological changes were recorded following treatment with each of the compounds for a comparable duration (Figure 4.17). These findings were consistent with the results achieved using the FDA assay.

4.6.1 Tryptophan toxicity

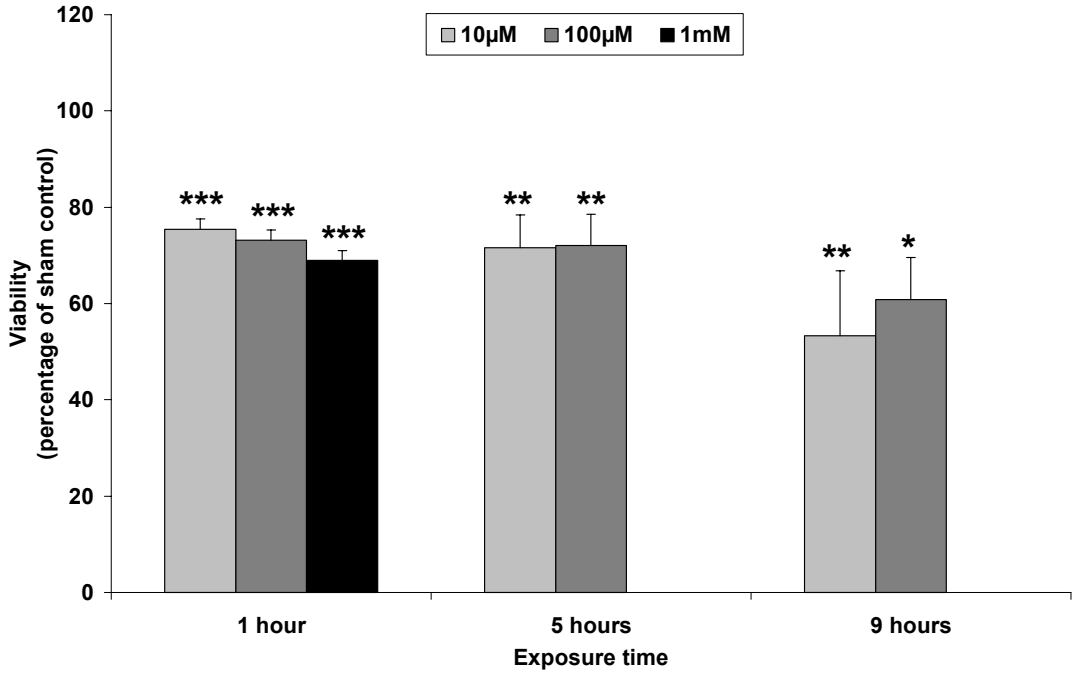

Figure 4.12a Toxicity of tryptophan in medium containing 5.5mM glucose to CGNs at 9 DIV. Mean +/- SEM, n=5; ANOVA followed by Tukey's test, * p<0.05, ** p<0.01, *** p<0.001. Tryptophan toxicity increased with exposure time, but was not affected by concentration.

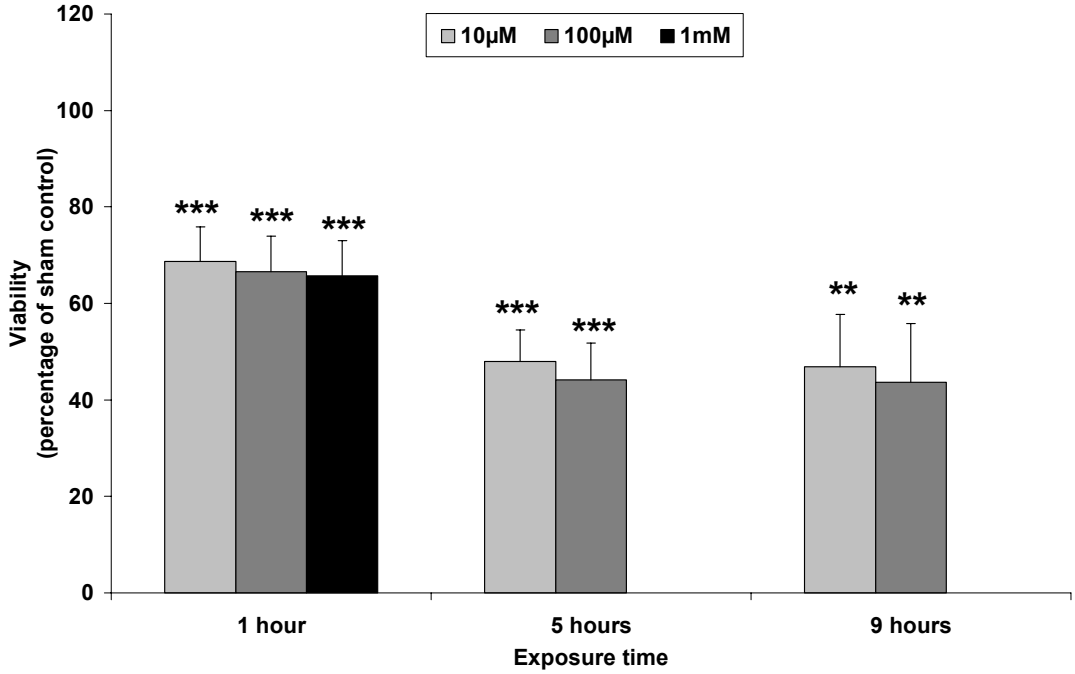

Figure 4.12b Toxicity of tryptophan in medium containing 25mM glucose to CGNs at 9 DIV. Mean +/- SEM, n=5; ANOVA followed by Tukey's test, ** p<0.01, *** p<0.001. Tryptophan toxicity increased with exposure time, but was not affected by concentration.

4.6.2 Kynurenine toxicity

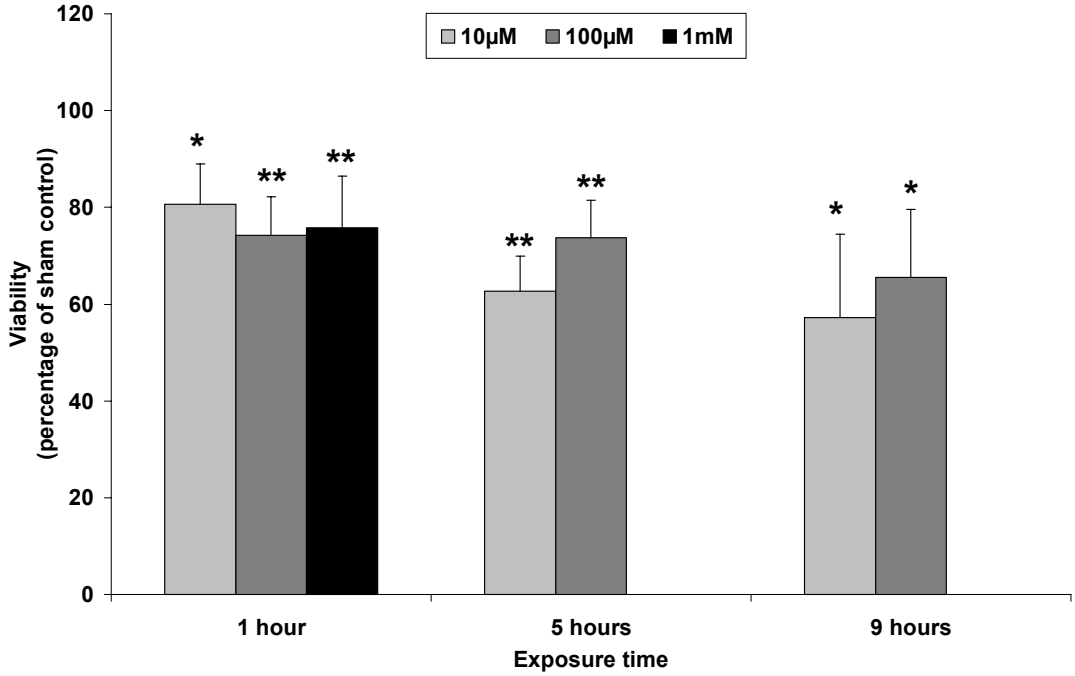

Figure 4.13a Toxicity of kynurenine in medium containing 5.5.mM glucose to CGNs at 9 DIV. Mean +/- SEM, n=5; ANOVA followed by Tukey's test, * p<0.05, ** p<0.01. Kynurenine toxicity increased with exposure time, but was not affected by concentration.

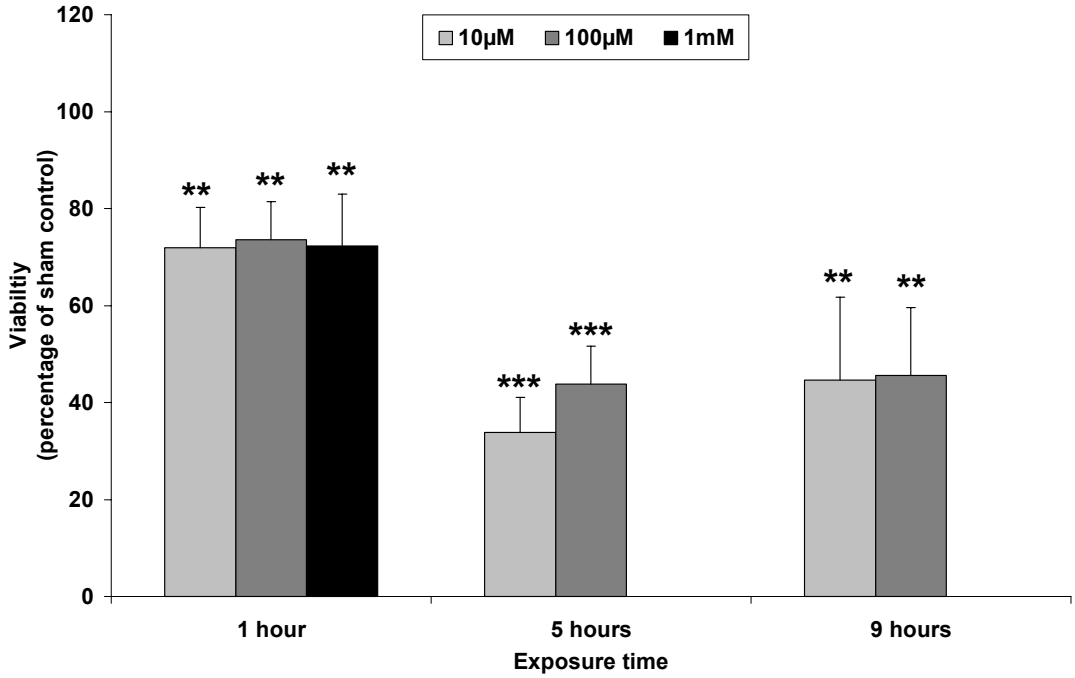

Figure 4.13b Toxicity of kynurenine in medium containing 25mM glucose to CGNs at 9 DIV. Mean +/- SEM, n=5; ANOVA followed by Tukey's test, ** p<0.01, *** p<0.001. Kynurenine toxicity increased with exposure time, but was not affected by concentration.

4.6.3 3-Hydroxykynurenine toxicity

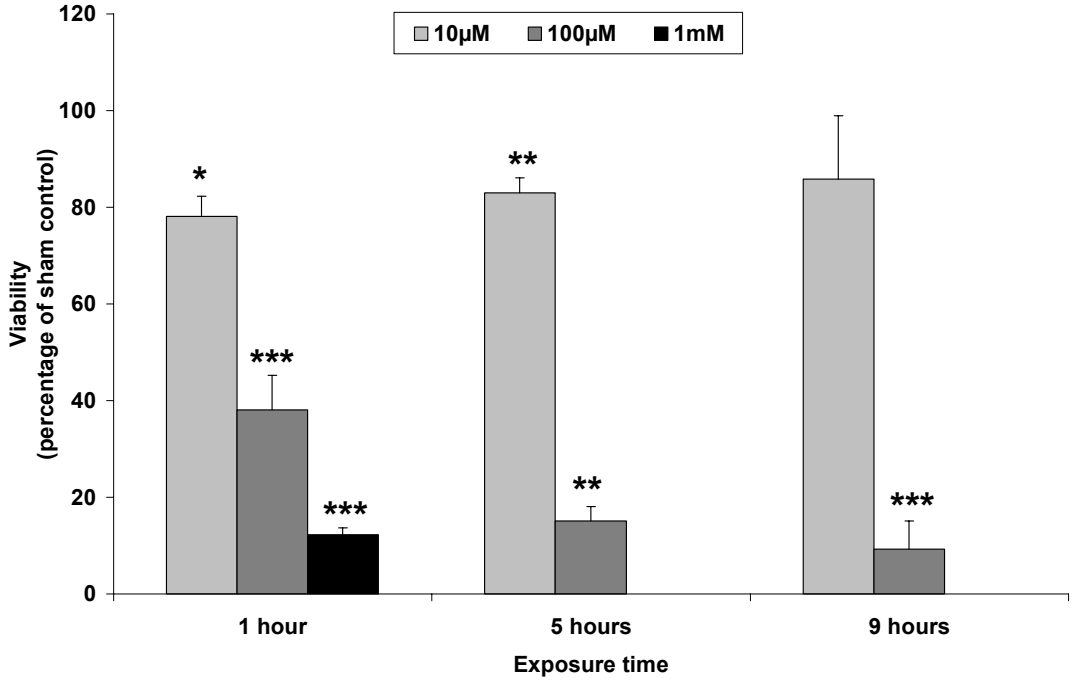

Figure 4.14a Toxicity of 3-HK in medium containing 5.5mM glucose to CGNs at 9 DIV. Mean +/- SEM, n=5; ANOVA followed by Tukey's test, * p<0.05, ** p<0.01, *** p<0.001. 3-Hydroxykynurenine toxicity increased with exposure time (although this was not evident at 10μM) and with concentration.

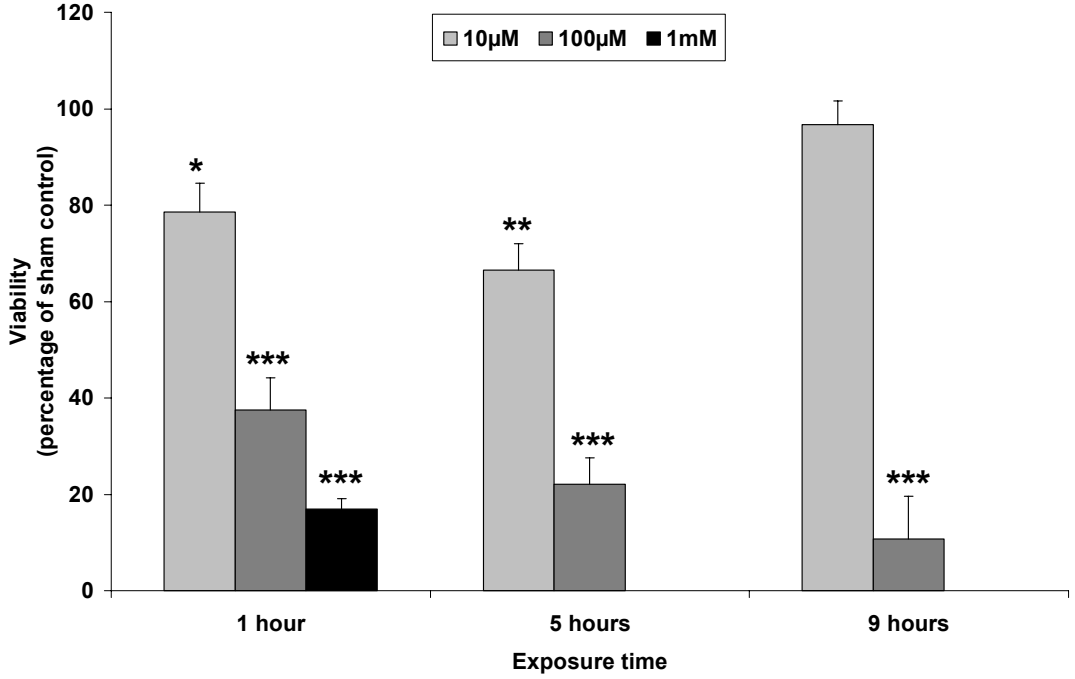

Figure 4.14b Toxicity of 3-HK in medium containing 25mM glucose to CGNs at 9 DIV. Mean +/- SEM, n=5; ANOVA followed by Tukey's test, * p<0.05, ** p<0.01, *** p<0.001. 3-Hydroxykynurenine toxicity increased with exposure time (although this was not evident at 10μM) and with concentration.

4.6.4 3-Hydroxyanthranilic acid toxicity

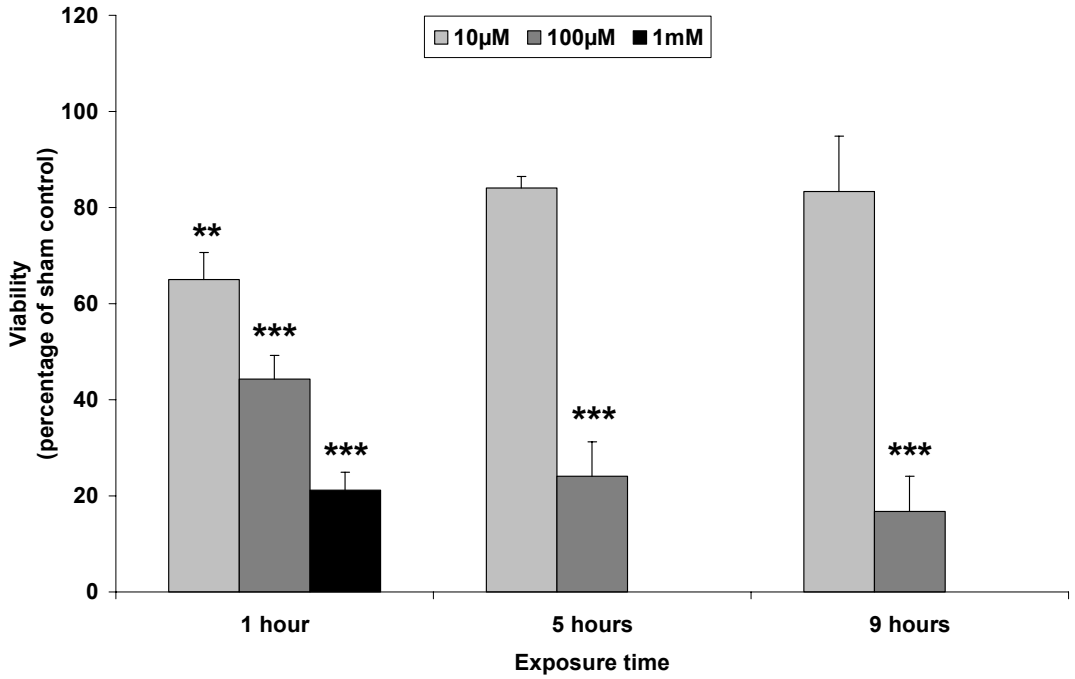

Figure 4.15a Toxicity of 3-HAA in medium containing 5.5mM glucose to CGNs at 9 DIV. Mean +/- SEM, n=5; ANOVA followed by Tukey's test, ** p<0.01, *** p<0.001. 3-Hydroxyanthranilic acid toxicity increased with exposure time (although this was not evident at 10μM) and with concentration.

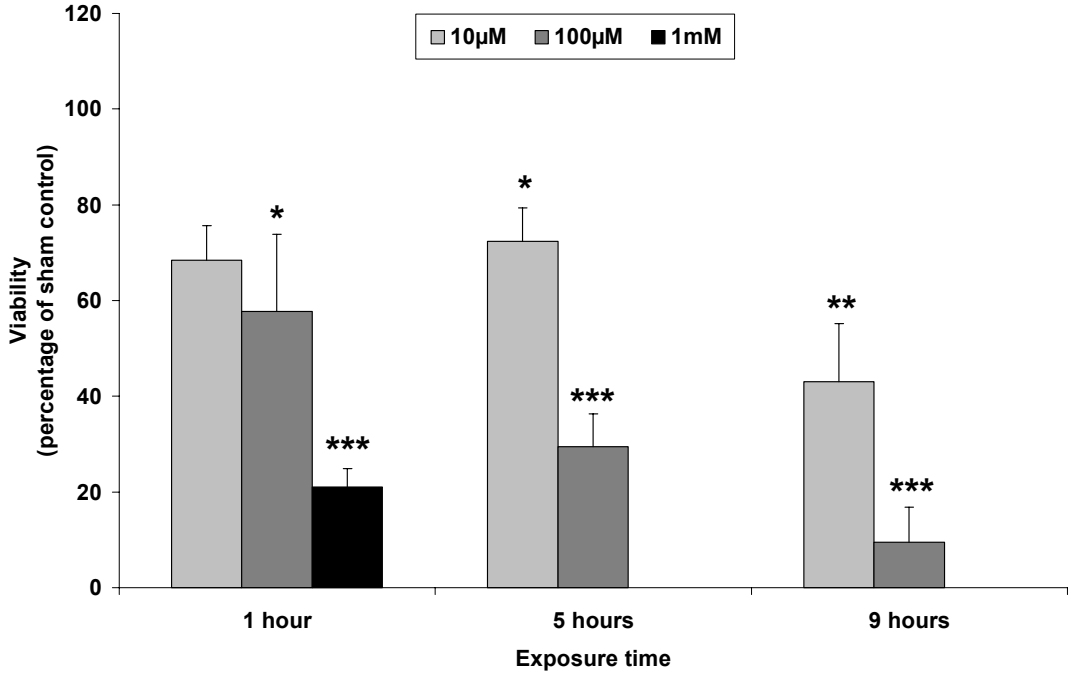

Figure 4.15b Toxicity of 3-HAA in medium containing 25mM glucose to CGNs at 9 DIV. Mean +/- SEM, n=5; ANOVA followed by Tukey's test, * p<0.05, ** p<0.01, *** p<0.001. 3-Hydroxyanthranilic acid toxicity increased with exposure time and with concentration.

4.6.5 Quinolinic acid toxicity

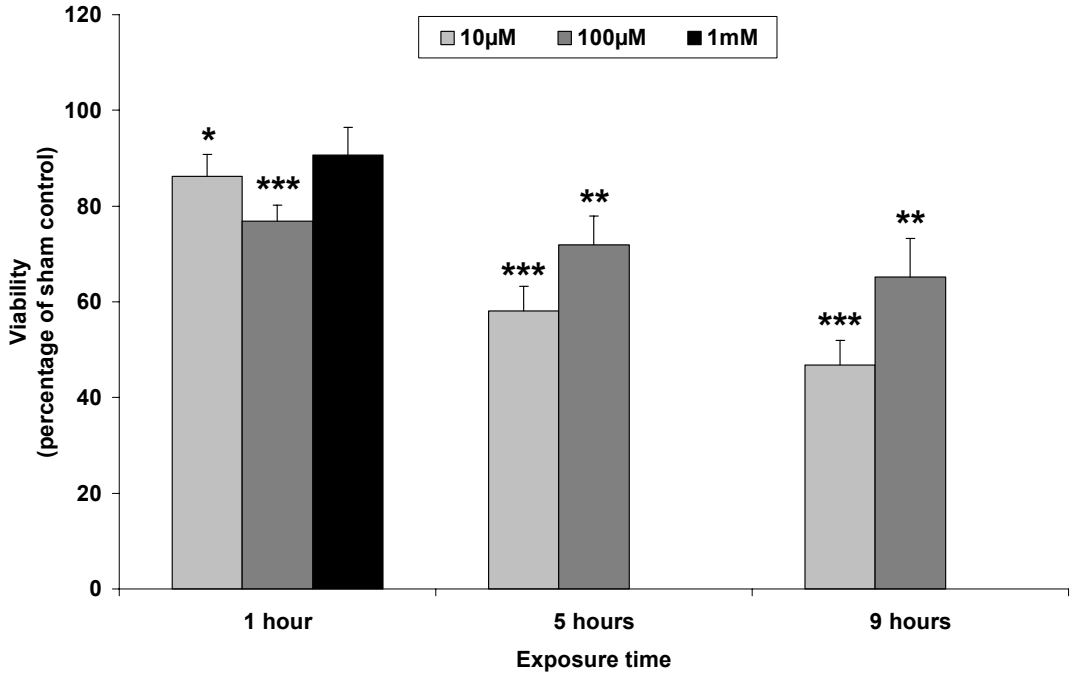

Figure 4.16a Toxicity of QA in medium containing 5.5mM glucose to CGNs at 9 DIV. Mean +/- SEM, n=5; ANOVA followed by Tukey's test, * p<0.05, ** p<0.01, *** p<0.001. Quinolinic acid toxicity increased with exposure time, but was not affected by concentration.

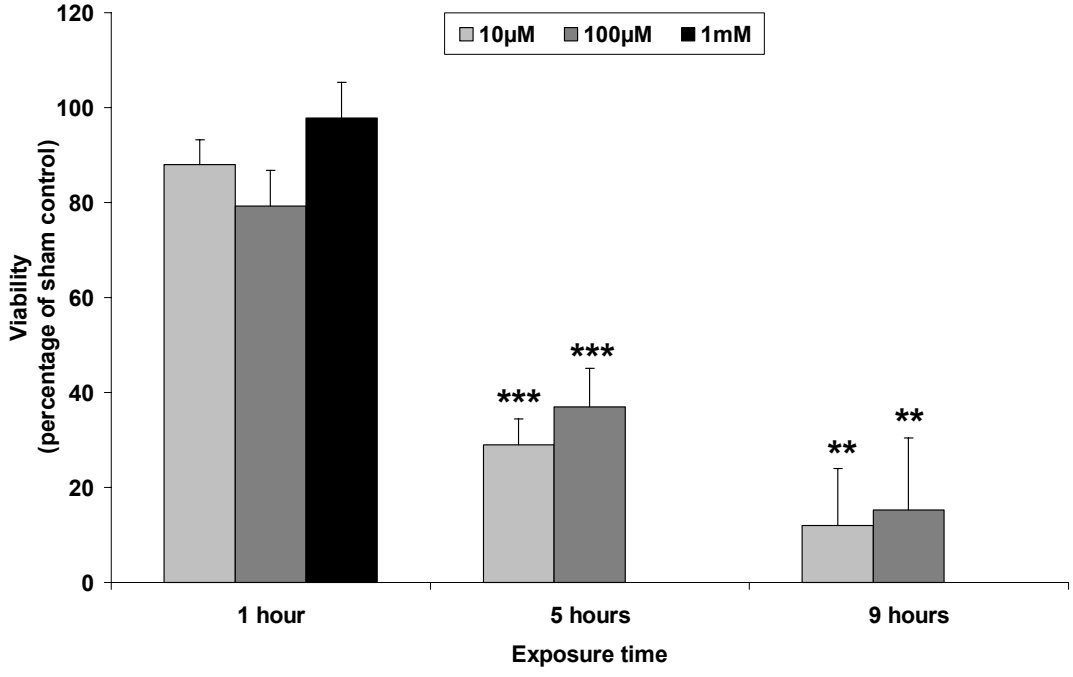

Figure 4.16b Toxicity of QA in medium containing 25mM glucose to CGNs at 9 DIV. Mean +/- SEM, n=5; ANOVA followed by Tukey's test, ** p<0.01, *** p<0.001. Quinolinic acid toxicity increased with exposure time, but was not affected by concentration.

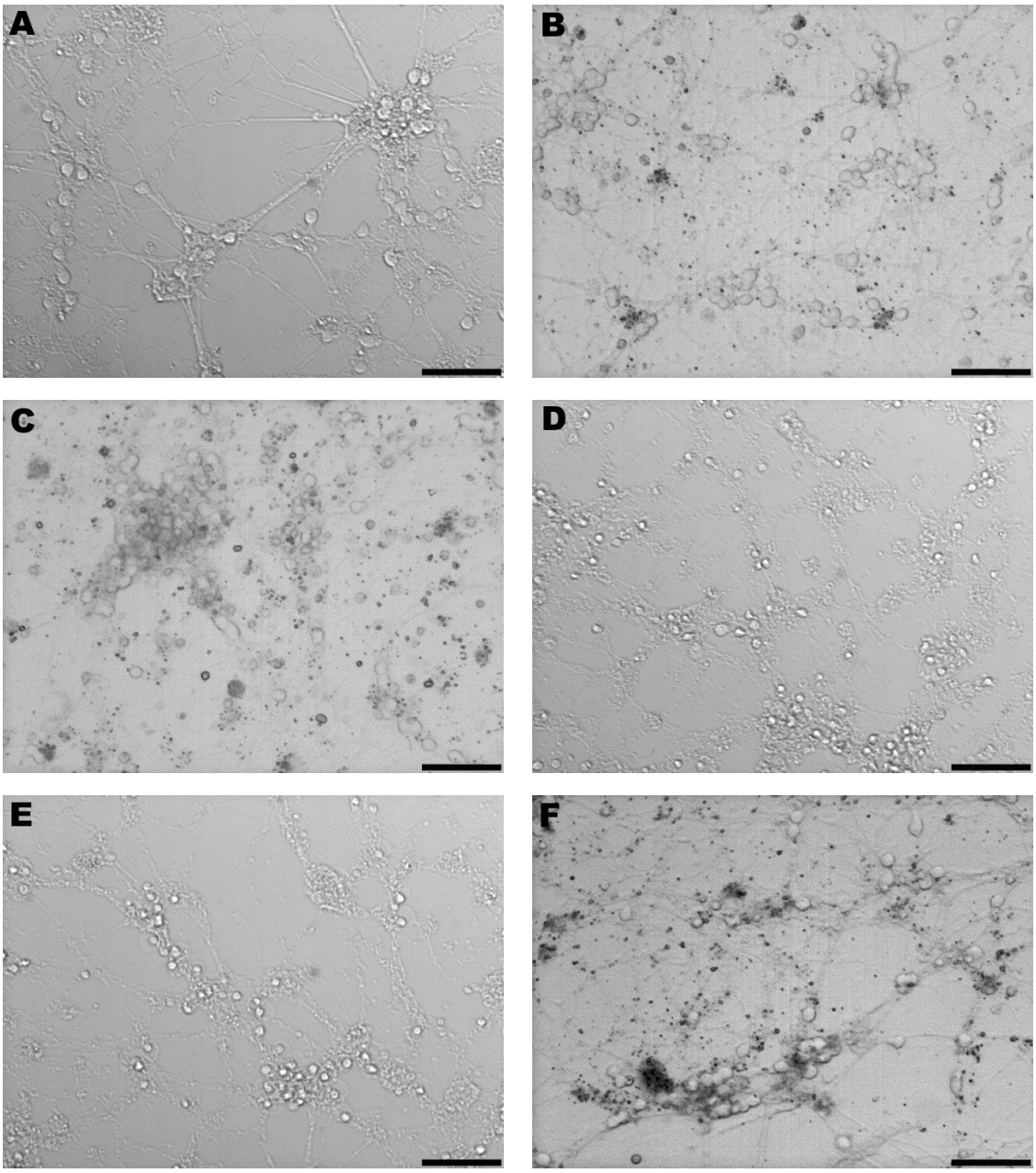

Figure 4.17a Cerebellar granule neurone morphology at 10 DIV after treatments at 9 DIV: A) Control, B) 1mM tryptophan for 1 hour, C) 1mM kynurenine for 1 hour, D) 100µM 3-HK for 1 hour, E) 100µM 3-HAA for 1 hour, F) 1mM QA for 1 hour. Bars = 50µm. Although panels B, C and F are somewhat obscured by debris, a higher level of surviving CGNs compared with panels D and E can be seen, with all treatments decreasing the number of viable cells in comparison with the control (A).

As shown in Figure 4.17a, the neurotoxic effect identified by the FDA viability assay was also evident in the morphological appearances of treated CGNs, with moderate damage due to tryptophan, kynurenine and quinolinic acid, and more extensive damage apparent following treatment with 3-HK and 3-HAA.

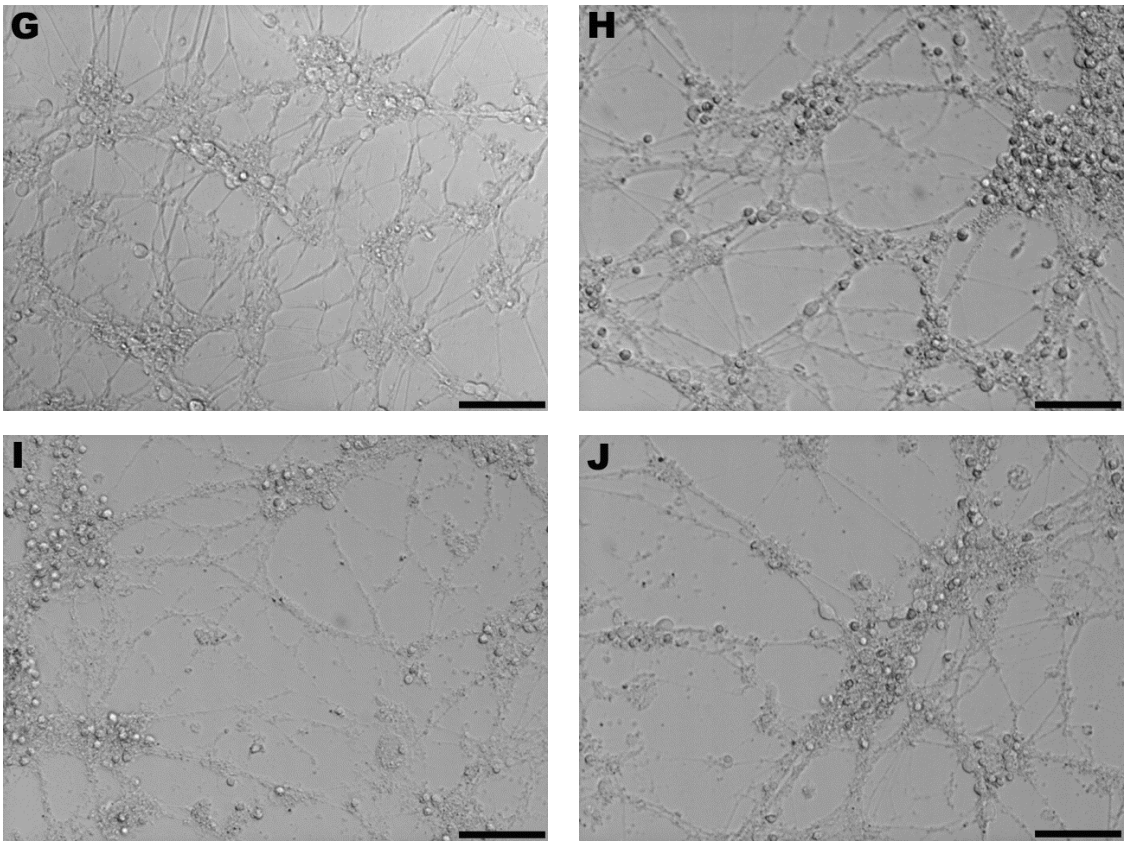

Figure 4.17b Cerebellar granule neurone morphology at 10 DIV after treatments at 9 DIV: G) 100µM kynurenic acid for 1 hour, H) 100µM anthranilic acid for 1 hour, I) 100µM 5-HAA for 1 hour, J) 100µM picolinic acid for 1 hour. Bars = 50µm. Kynurenic acid for 1 hour was not toxic and the toxicity of 5-HAA was more extensive than that of anthranilic acid or picolinic acid.

The notably less neurotoxic effect of kynurenic acid treatment for 1 hour is confirmed by morphological observations (Figure 4.17b, G), with appearances of treated neurones found to be comparable to controls (Figure 4.17a, A). All other treatments (anthranilic acid, picolinic acid, 5-HAA) induced obvious neuronal damage, with the effect of 5-HAA most pronounced, which is a finding that is again consistent with FDA assay results.

4.6.6 Kynurenic acid toxicity

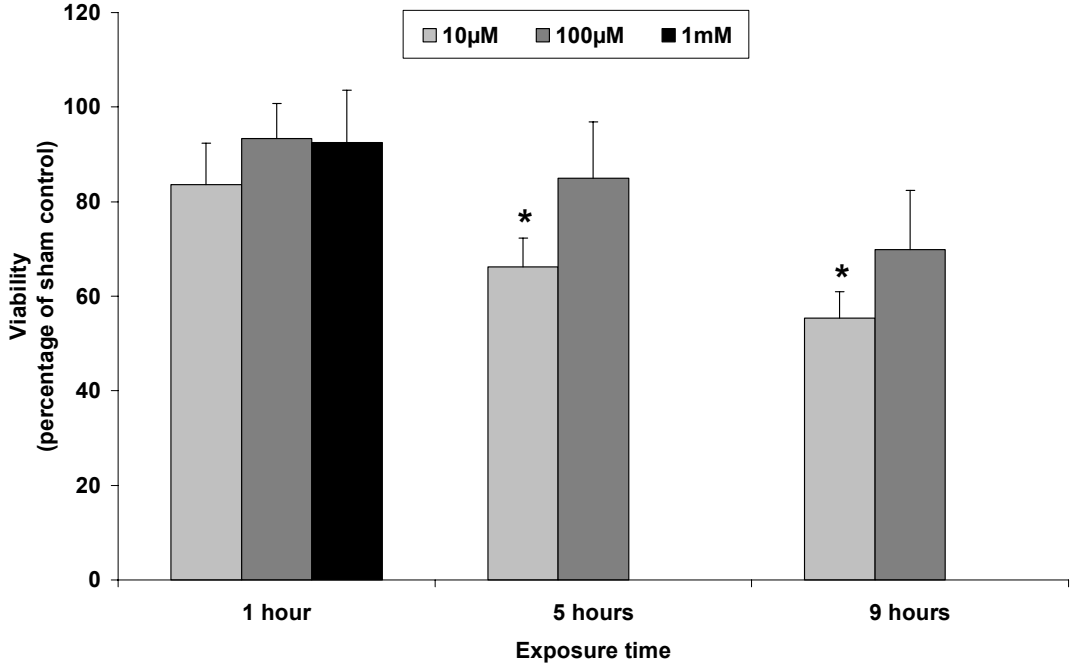

Figure 4.18a Toxicity of kynurenic acid in medium containing 5.5mM glucose to CGNs at 9 DIV. Mean +/- SEM, n=5; ANOVA followed by Tukey's test, * p<0.05. Kynurenic acid toxicity was initially limited, but increased with exposure time, but was not affected by concentration.

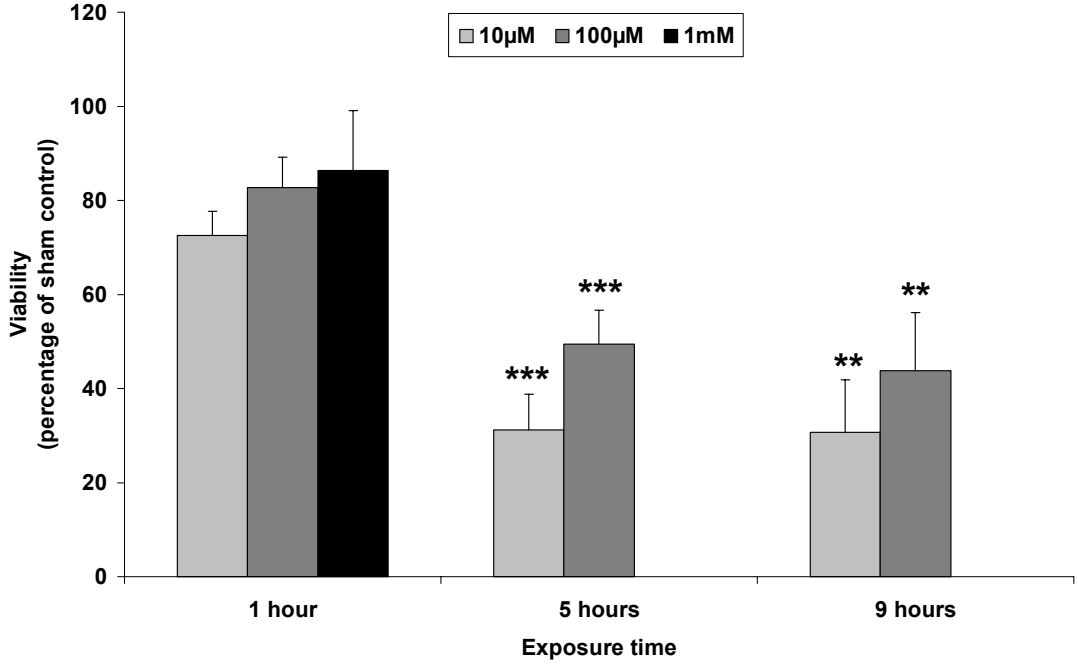

Figure 4.18b Toxicity of kynurenic acid in medium containing 25mM glucose to CGNs at 9 DIV. Mean +/- SEM, n=5; ANOVA followed by Tukey's test, ** p<0.01, *** p<0.001. Kynurenic acid toxicity was initially limited, but increased with exposure time, but was not affected by concentration.

4.6.7 Anthranilic acid toxicity

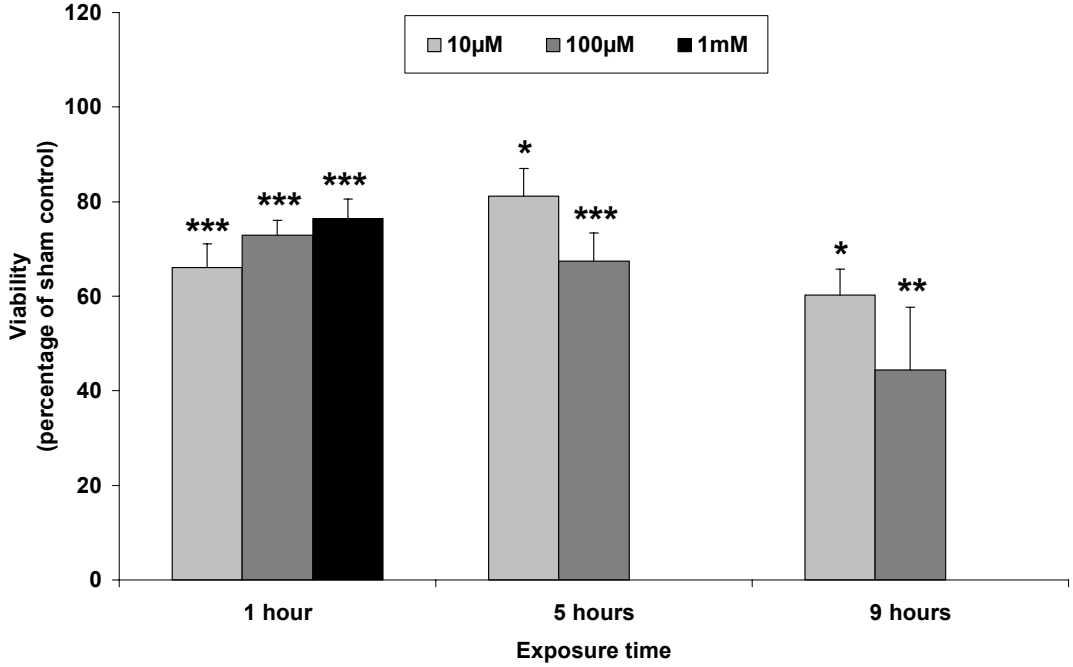

Figure 4.19a Toxicity of anthranilic acid in medium containing 5.5mM glucose to CGNs at 9 DIV. Mean +/- SEM, n=5; ANOVA followed by Tukey's test, * p<0.05, ** p<0.01, *** p<0.001. Anthranilic acid toxicity increased with exposure time to 9 hours, but was not affected by concentration.

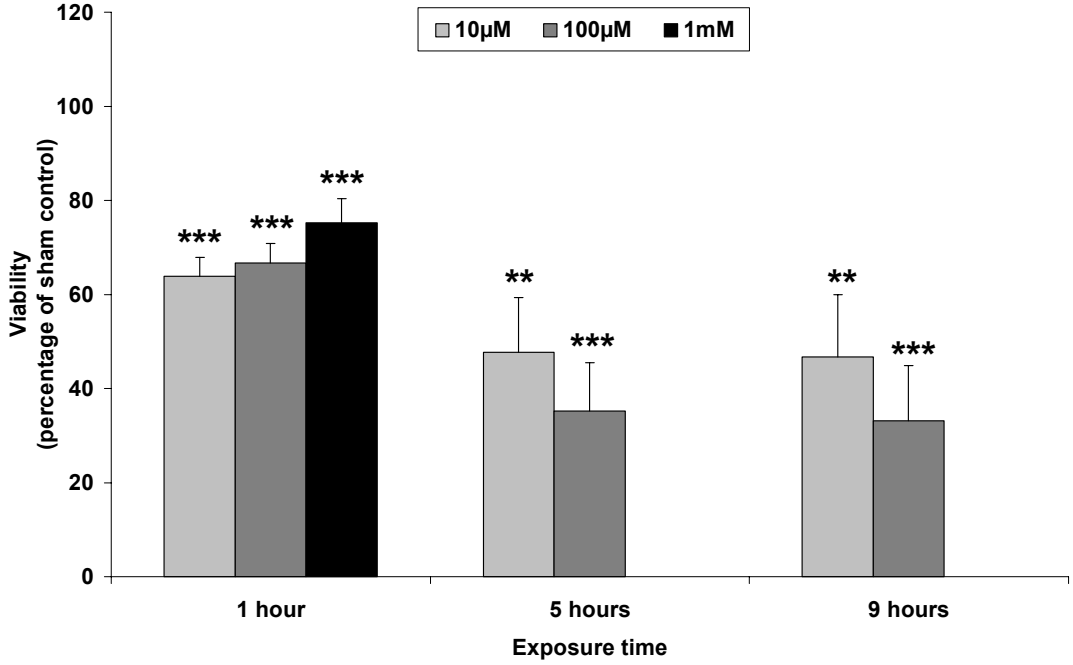

Figure 4.19b Toxicity of anthranilic acid in medium containing 25mM glucose to CGNs at 9 DIV. Mean +/- SEM, n=5; ANOVA followed by Tukey's test, ** p<0.01, *** p<0.001. Anthranilic acid toxicity increased with exposure time, but was not affected by concentration.

4.6.8 5-Hydroxyanthranilic acid toxicity

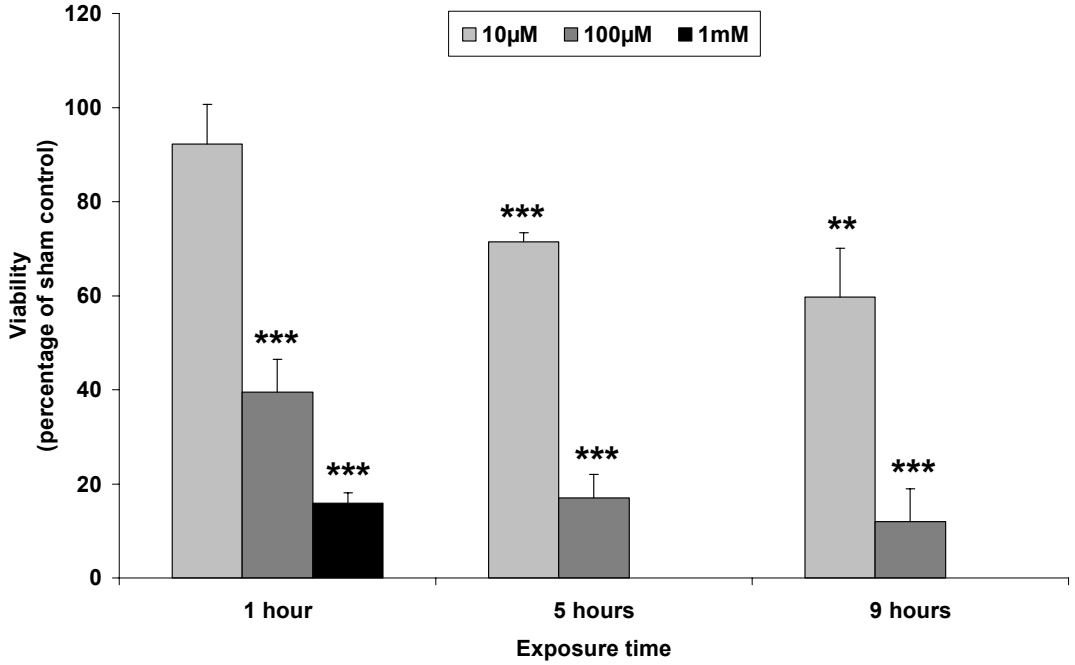

Figure 4.20a Toxicity of 5-HAA in medium containing 5.5mM glucose to CGNs at 9 DIV. Mean +/- SEM, n=5; ANOVA followed by Tukey's test, ** p<0.01, *** p<0.001. 5-Hydroxyanthranilic acid toxicity increased with exposure time and with concentration.

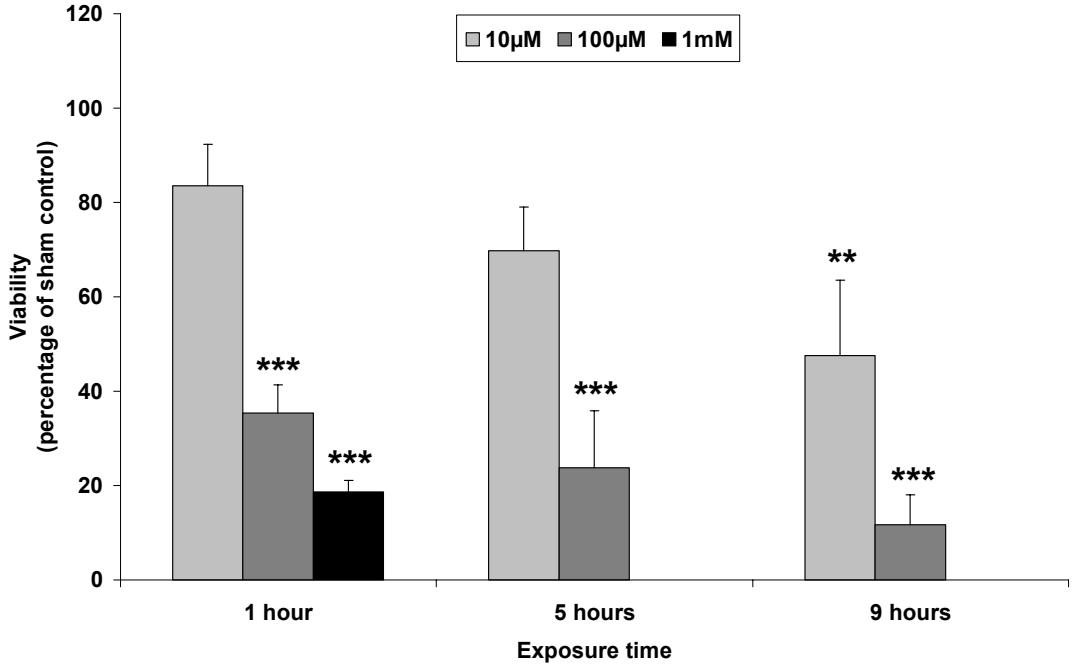

Figure 4.20b Toxicity of 5-HAA in medium containing 25mM glucose to CGNs at 9 DIV. Mean +/- SEM, n=5; ANOVA followed by Tukey's test, ** p<0.01, *** p<0.001. 5-Hydroxyanthranilic acid toxicity increased with exposure time and with concentration.

4.6.9 Picolinic acid toxicity

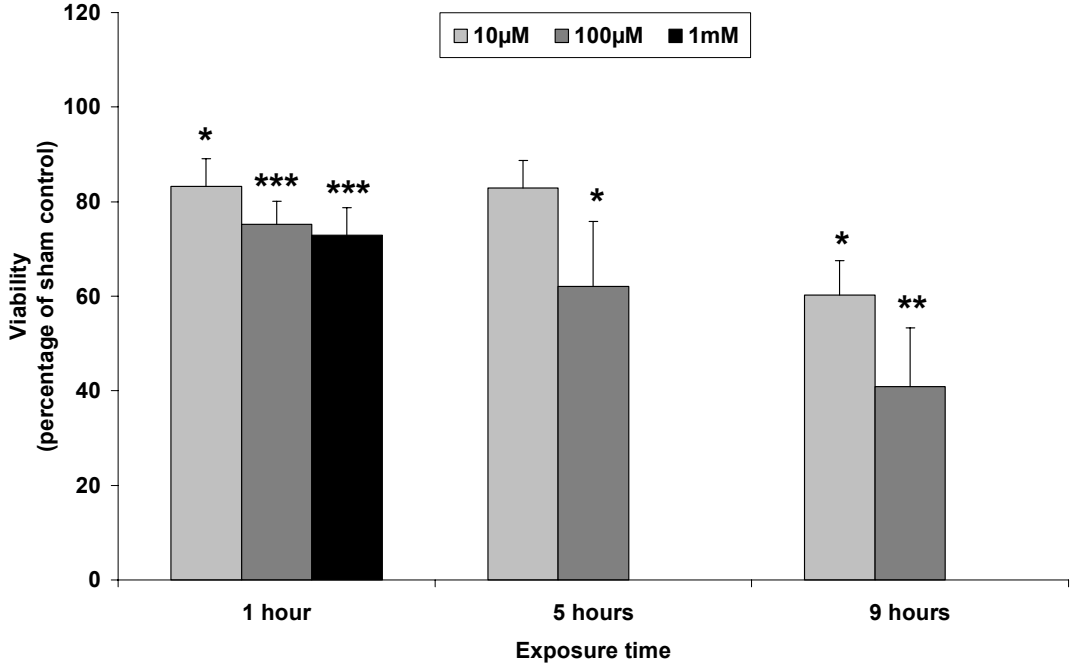

Figure 4.21a Toxicity of picolinic acid in medium containing 5.5mM glucose to CGNs at 9 DIV. Mean +/- SEM, n=5; ANOVA followed by Tukey's test, * p<0.05, ** p<0.01, *** p<0.001. Picolinic acid toxicity increased with exposure time, but was not affected by concentration.

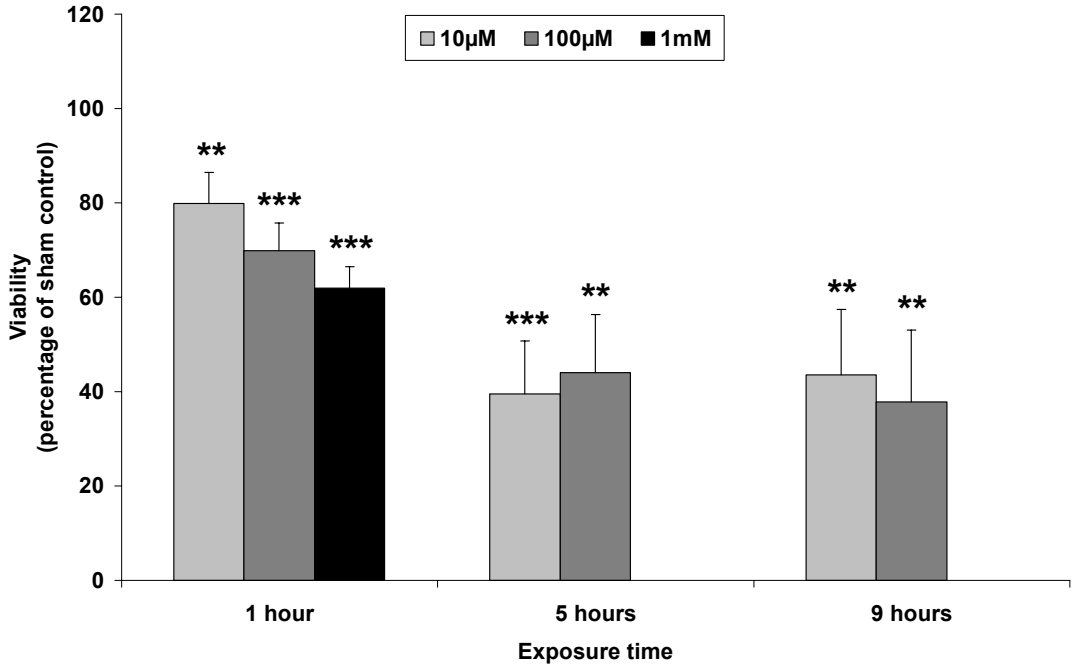

Figure 4.21b Toxicity of picolinic acid in medium containing 25mM glucose to CGNs at 9 DIV. Mean +/- SEM, n=5; ANOVA followed by Tukey's test, ** p<0.01, *** p<0.001. Picolinic acid toxicity increased with exposure time, but was not affected by concentration.

Comparison of the neurotoxic effect of the tryptophan metabolites in medium containing 5.5 and 25mM glucose showed that a significant potentiation in neurotoxic effect occurred in cultures in higher glucose, when applied for 5 hours (Figure 4.22). This was evident for most of the compounds studied (the exceptions being 3-HK, 3-HAA and 5-HAA), raising the question of the underlying mechanism. Possible explanations included: that potentiation was due to increased catabolism or an osmotic effect of the additional glucose in the treatment medium; increased vulnerability due to pre-existing sub-lethal oxidative stress (caused by additional glucose in the plating medium); metabolism of the additional glucose altered metabolism of the compounds themselves. Therefore, the difference in toxicity identified in the two groups was compared directly, and each possible explanation explored.

The first question considered was whether the increased vulnerability was due to plating and maintenance in a higher glucose concentration or to an effect that occurred during the treatment period.

Switching over the glucose concentrations used for culturing and treatment caused a reduction in toxicity, but for several compounds there was still a significant potentiation (Figure 4.23). This suggested that much of the potentiation resulted from the treatments being applied in 25mM glucose-containing medium, raising the further question of whether this was due to an osmotic effect or to metabolism of the additional glucose during the 5 hour treatment period.

To investigate this question, a metabolically inert compound (providing the osmotic actions of glucose but not its metabolic properties), 3-*O*-methyl-D-glucose, was added to an equivalent concentration of 25mM. This showed that the degree of toxicity seen in the groups supplemented with either D-glucose or 3-*O*-methyl-D-glucose was comparable, and therefore that metabolism of the D-glucose was not the cause of the potentiated toxicity (Figure 4.24).

4.6.10 Comparison of effects in 5.5 and 25mM glucose

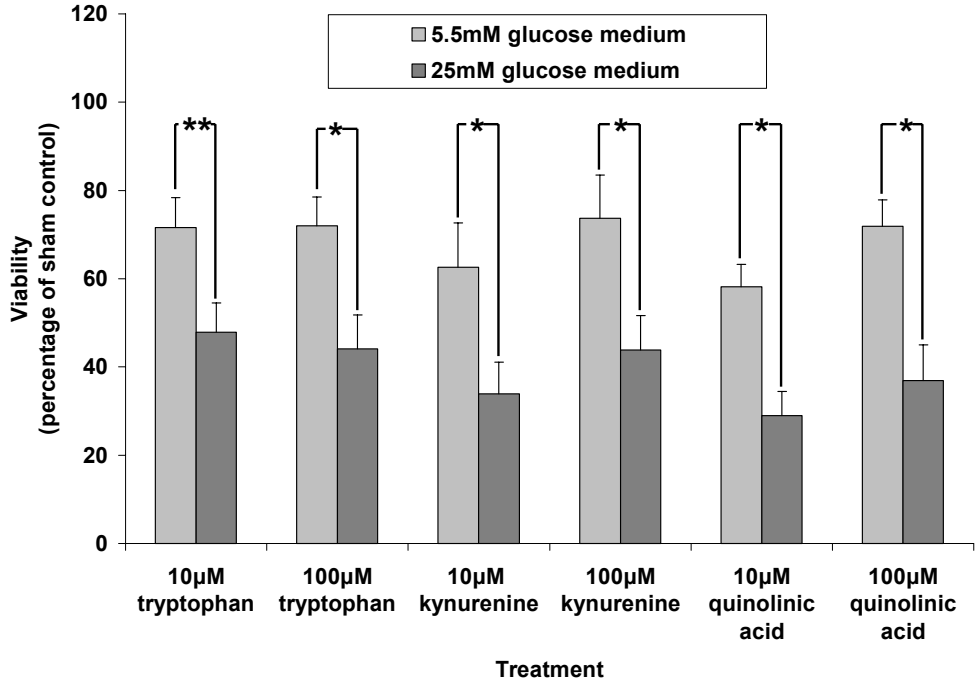

Figure 4.22a Toxicity of tryptophan, kynurenine and QA to cultured CGNs is potentiated by increased medium glucose when applied for 5 hours at 9 DIV. Mean +/- SEM, n=5; Student's t-test comparing groups, * p<0.05, ** p<0.01. Increased toxicity due to all compounds is apparent when they are applied in 25mM glucose.

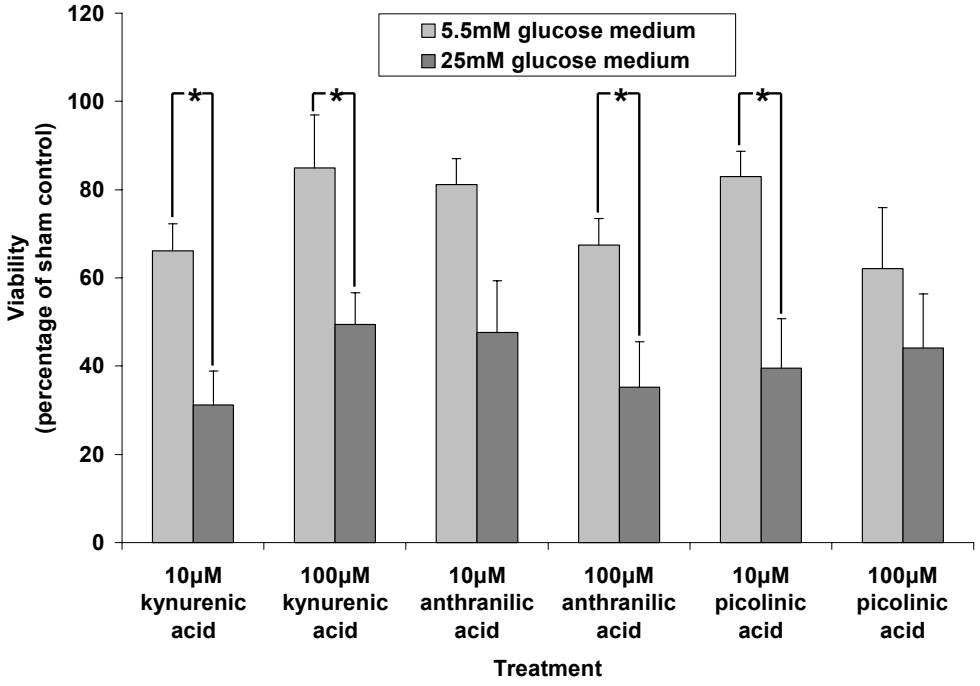

Figure 4.22b Toxicity of kynurenic acid, anthranilic acid and picolinic acid to cultured CGNs is potentiated by increased medium glucose when applied for 5 hours at 9 DIV. Mean +/- SEM, n=5; Student's t-test comparing groups, * p<0.05. Increased toxicity due to all compounds (although not all concentrations) is apparent when they are applied in 25mM glucose.

4.6.11 Switchover of 5.5 and 25mM glucose

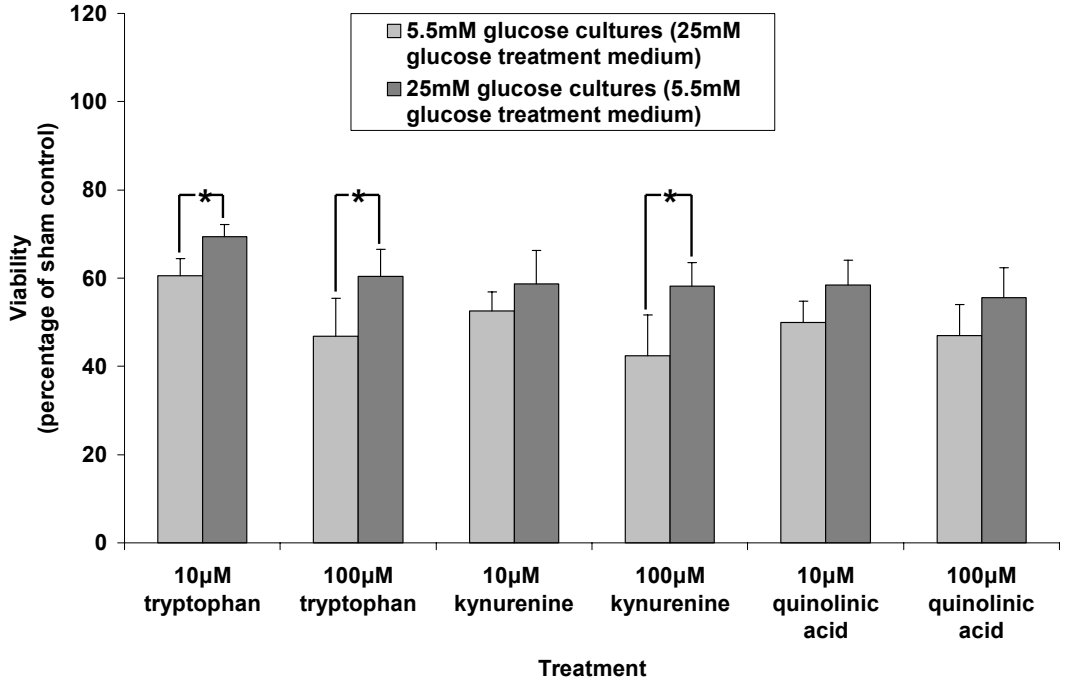

Figure 4.23a Toxicity of tryptophan, kynurenine and QA applied for 5 hours at 9 DIV to cultured CGNs with glucose in treatment medium increased or decreased in relation to glucose concentration in culturing medium. Mean +/- SEM, n=5; Student's t-test comparing paired groups, * p<0.05. The toxic effect was more pronounced in CGNs maintained in 25mM glucose, although this was not significant in the case of quinolinic acid treatment.

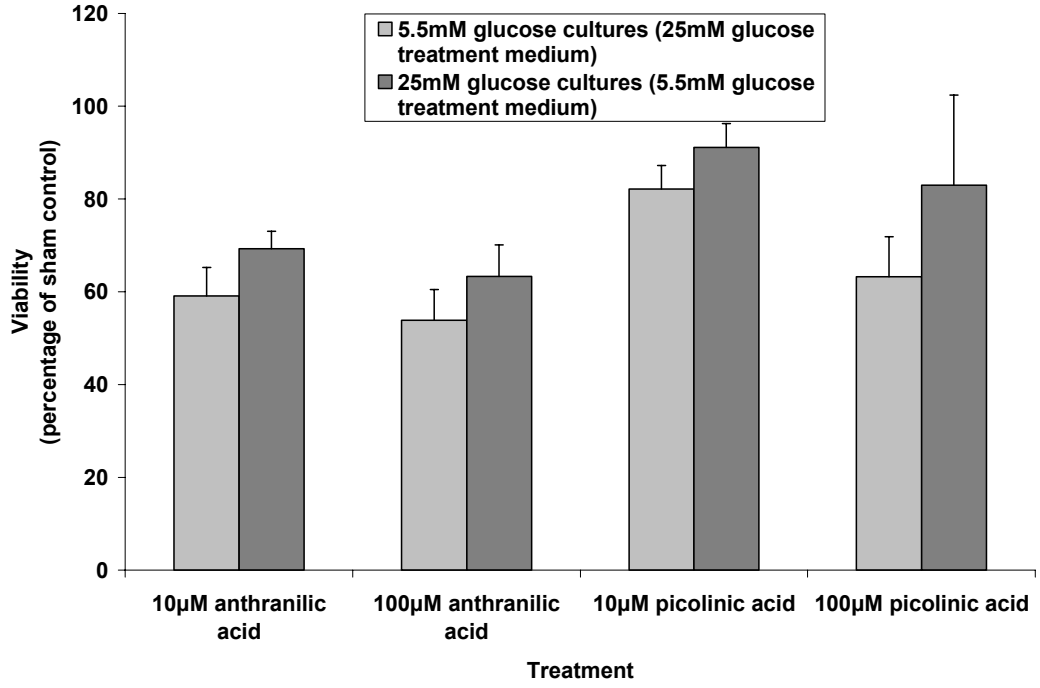

Figure 4.23b Toxicity of anthranilic acid and picolinic acid applied for 5 hours at 9 DIV to cultured CGNs with glucose in treatment medium increased or decreased in relation to glucose concentration in culturing medium. Mean +/- SEM, n=5; Student's t-test comparing paired groups showed no significant difference. No significant variation between the two alteraytions in glucose concentration were seen regarding their effects on the toxic effects of kynurenine pathway compounds.

4.6.12 Toxicity with D-glucose or 3-O-methyl-D-glucose

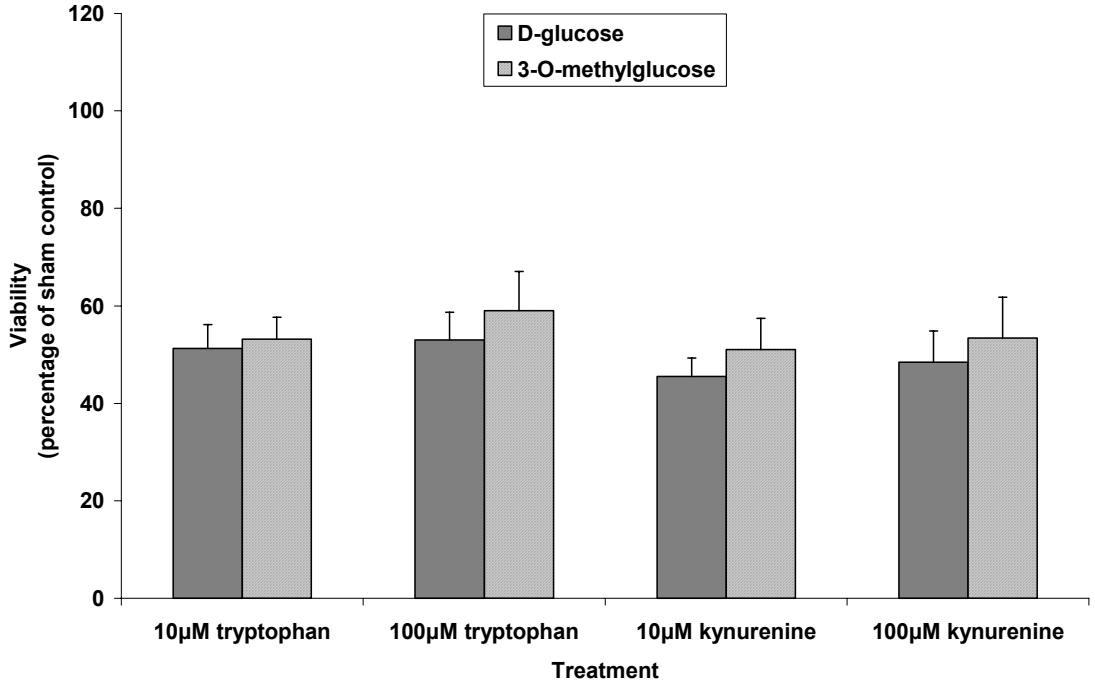

Figure 4.24a Toxicity of tryptophan and kynurenine in 5.5mM glucose medium supplemented with either 19.5mM D-glucose or 19.5mM 3-O-methylglucose. Mean +/- SEM, n=5; Student's t-test comparing paired groups showed no significant difference. No difference was seen when treatments were applied in medium supplemented with D-glucose or 3-O-methylglucose, indicating that the potentiating effect of adding treatments in 25mM glucose-containing medium was not due to an effect caused by increased glucose metabolism.

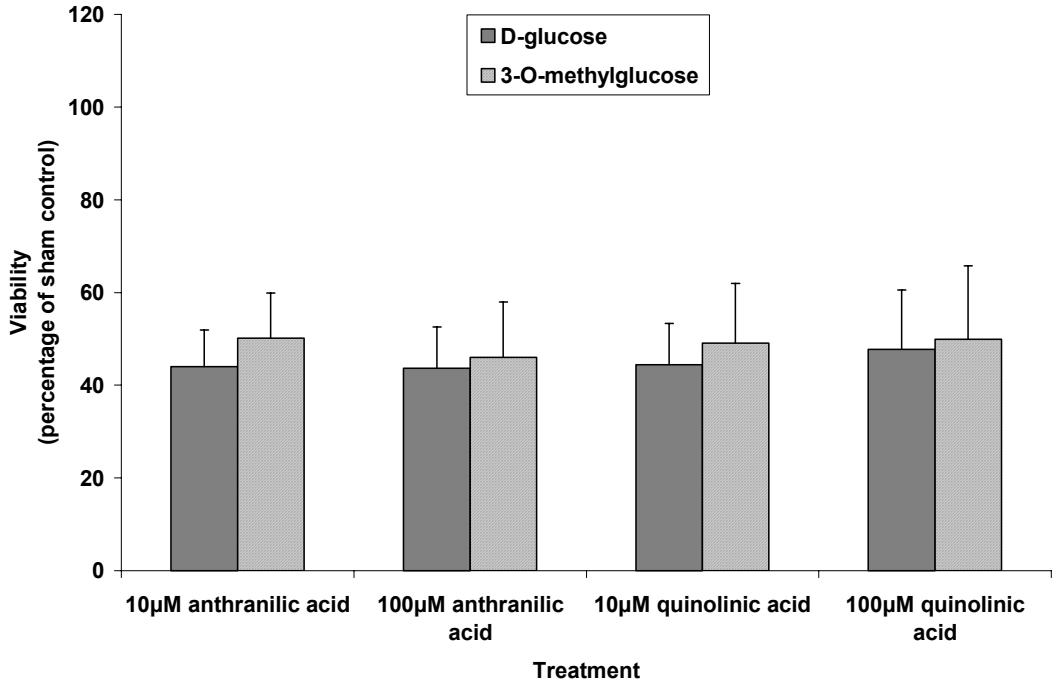

Figure 4.24b Toxicity of anthranilic acid and QA in 5.5mM glucose medium supplemented with either 19.5mM D-glucose or 19.5mM 3-O-methylglucose. Mean +/- SEM, n=5; Student's t-test comparing paired groups showed no significant difference. No difference was seen when treatments were applied in medium supplemented with D-glucose or 3-O-methylglucose, indicating that the potentiating effect of adding treatments in 25mM glucose-containing medium was not due to an effect caused by increased glucose metabolism.

4.6.13 HPLC of tryptophan metabolite products

Sample (5.5mM glucose)	Tryptophan (μM)	Kynurenine (μM)	Kynurenic acid (nM)	Anthranilic acid (nM)
Control	57.83	0.49	48.46	139.17
Tryptophan 1 hour	44.94	0.50	40.35	110.01
Tryptophan 5 hours	44.75	0.52	38.25	119.42
Tryptophan 9 hours	49.48	0.54	42.03	121.92
Kynurenine 1 hour	54.06	-21.66	42.11	116.85
Kynurenine 5 hours	54.03	-21.68	46.26	119.97
Kynurenine 9 hours	55.65	-18.61	48.90	129.79
Anthranilic acid 1 hour	53.65	0.52	39.38	109.44
Anthranilic acid 5 hours	54.25	0.55	40.79	117.45
Anthranilic acid 9 hours	52.80	0.53	37.21	108.36

Table 4.1 High-performance liquid chromatography analysis of tryptophan, kynurenine, kynurenic acid and anthranilic acid levels in medium containing 5.5mM D-glucose from CGN cultures treated with 100μM tryptophan, 100μM kynurenine or 100μM anthranilic acid for the indicated periods at 9 DIV. Mean value from two separate experiments.

Sample (25mM glucose)	Tryptophan (μM)	Kynurenine (μM)	Kynurenic acid (nM)	Anthranilic acid (nM)
Control	65.22	0.52	54.57	197.63
Tryptophan 1 hour	45.82	0.53	50.05	128.28
Tryptophan 5 hours	55.11	0.57	49.85	131.26
Tryptophan 9 hours	46.85	0.55	47.94	126.85
Kynurenine 1 hour	53.26	-17.51	51.59	125.30
Kynurenine 5 hours	52.14	-19.44	52.69	129.83
Kynurenine 9 hours	54.96	-12.65	59.54	170.34
Anthranilic acid 1 hour	54.04	0.69	48.37	137.52
Anthranilic acid 5 hours	52.73	0.79	52.96	100.69
Anthranilic acid 9 hours	53.36	0.73	46.82	135.08

Table 4.2 High-performance liquid chromatography analysis of tryptophan, kynurenine, kynurenic acid and anthranilic acid levels in medium containing 25mM D-glucose from CGN cultures treated with 100μM tryptophan, 100μM kynurenine or 100μM anthranilic acid for the indicated periods at 9 DIV. Mean value from two separate experiments.

Sample (5.5mM glucose)	3-HK (μM)	3-HAA (nM)	5-HAA (nM)
Control	0	5.494829	1.370648
Kynurenine 5 hours	0	0.8691	0
Anthranilic acid 5 hours	0	0	0
3-HK 5 hours	22.60704	2.381419	2.736635
3-HK 9 hours	22.008.62	3.927136	0.67824
3-HAA 5 hours	0	43200.53	5.990729
3-HAA 9 hours	0	40843.5	12.12206

Table 4.3 High-performance liquid chromatography analysis of 3-HK, 3-HAA and 5-HAA levels in medium containing 5.5mM D-glucose from CGN cultures treated with 100μM kynurenine, 100μM anthranilic acid, 50μM 3-HK or 50μM 3-HAA for the indicated periods at 9 DIV. Mean value from two separate experiments, with no compound metabolism evident.

Sample (25mM glucose)	3-HK (μM)	3-HAA (nM)	5-HAA (nM)
Control	0	2.552336	0
Kynurenine 5 hours	0	1.833821	0
Anthranilic acid 5 hours	0	1.86033	0
3-HK 5 hours	30.13986	3.141345	0
3-HK 9 hours	28.87514	3.912287	0
3-HAA 5 hours	0	44509.97	4.388807
3-HAA 9 hours	0	40461.74	9.828422

Table 4.4 High-performance liquid chromatography analysis of 3-HK, 3-HAA and 5-HAA levels in medium containing 25mM D-glucose from CGN cultures treated with 100μM kynurenine, 100μM anthranilic acid, 50μM 3-HK or 50μM 3-HAA for the indicated periods at 9 DIV. Mean value from two separate experiments, with no compound metabolism evident.

Additionally, examining the metabolism of compounds in medium from neurones cultured in both 5.5mM and 25mM D-glucose did not show any differences between the two groups (Tables 4.1 to 4.4). Therefore, the most likely cause of potentiation was the osmotic effect of the additional glucose in the treatment medium. However, the reduced potentiation seen when cultures were plated in medium containing 5.5mM glucose prior to treatment in medium with 25mM glucose suggested there was a heightened vulnerability in CGNs plated and maintained in 25mM glucose to this neurotoxic effect. It should also be noted that several of the compounds studied may have degraded during analysis.

4.7 Investigation of mechanisms of toxicity of selected kynurenine pathway compounds

As 3-HK, 3-HAA and 5-HAA are capable of significant neurotoxicity, the mechanisms behind these effects were investigated. The effects of exogenously applied antioxidant enzymes during application of each of these three compounds were studied since 3-HK has been previously shown to generate H_2O_2 and superoxide, using metal ions for electron exchange (Goldstein *et al.*, 2000). Therefore, the effect on toxicity of the co-application of catalase (to remove H_2O_2) and of SOD (to remove superoxide) was studied.

Neuronal survival was greatly enhanced when catalase was added, providing protection against toxicity and may be compared with the extensive death in cultures with SOD present in treatments with 3-HK (Figure 4.25, 4.28), 3-HAA (Figures 4.26, 4.28) and 5-HAA (Figures 4.27, 4.28). It is therefore apparent that the generation of H_2O_2 is of critical importance in the generation of neurotoxic damage by these three compounds.

4.7.1 3-Hydroxykynurenine toxicity – effects of antioxidant enzymes

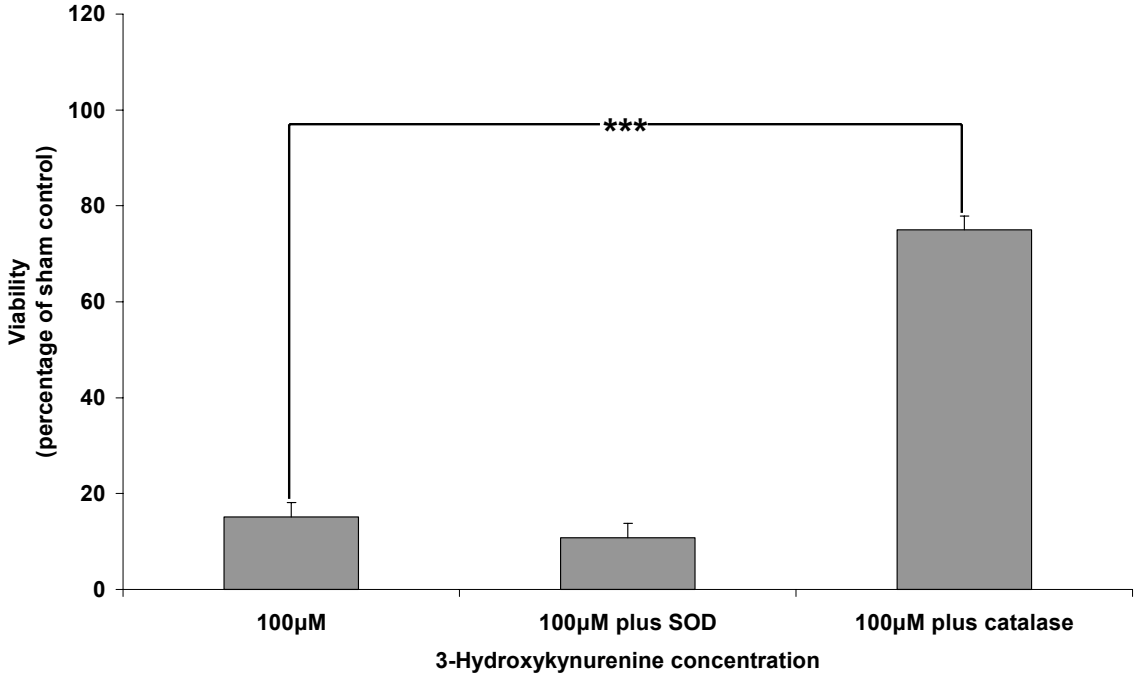

Figure 4.25 Effect of co-application of 200U/ml SOD or 200U/ml catalase with 100µM 3HK for 5 hours at 9 DIV. Mean +/- SEM, n=5; ANOVA followed by Tukey's test, *** p<0.001. A very significant protective effect was seen due to catalase, although SOD was neither protective nor significantly potentiating.

4.7.2 3-Hydroxyanthranilic acid toxicity – effects of antioxidant enzymes

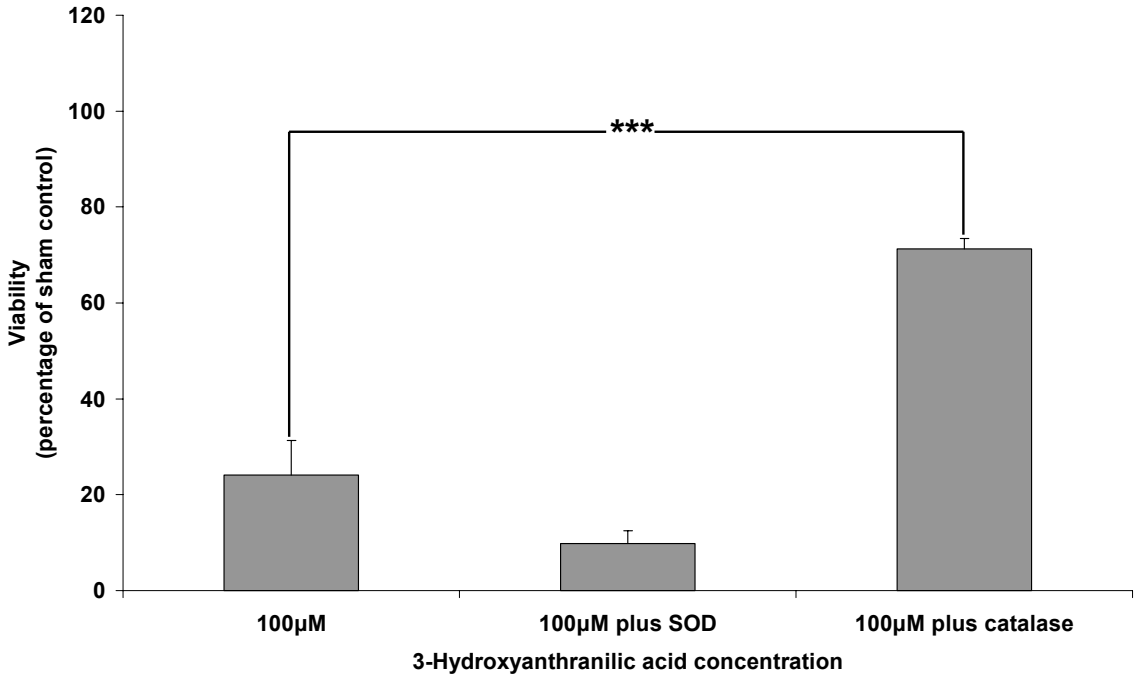

Figure 4.26 Effect of co-application of 200U/ml SOD or 200U/ml catalase with 100µM 3-HAA for 5 hours at 9 DIV. Mean +/- SEM, n=5; ANOVA followed by Tukey's test, *** p<0.001. A very significant protective effect was seen due to catalase, although SOD was neither protective nor significantly potentiating.

4.7.3 5-Hydroxyanthranilic acid toxicity – effects of antioxidant enzymes

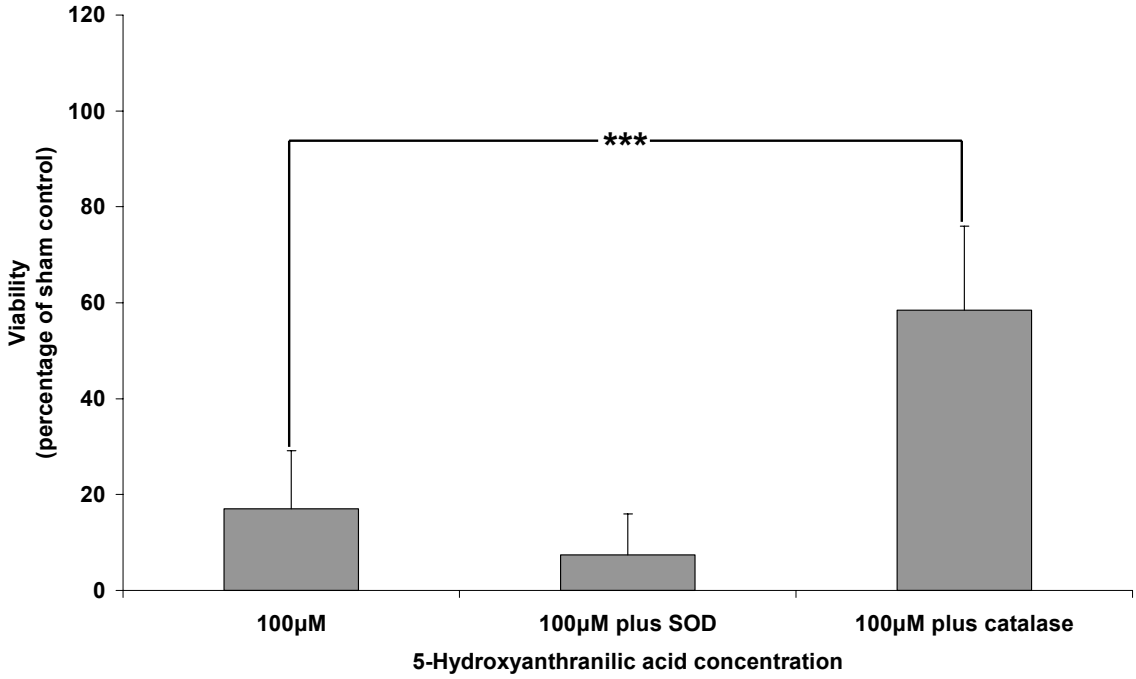

Figure 4.27 Effect of co-application of 200U/ml SOD or 200U/ml catalase with 100µM 5-HAA for 5 hours at 9 DIV. Mean +/- SEM, n=5; ANOVA followed by Tukey's test, *** p<0.001. A very significant protective effect was seen due to catalase, although SOD was neither protective nor significantly potentiating.

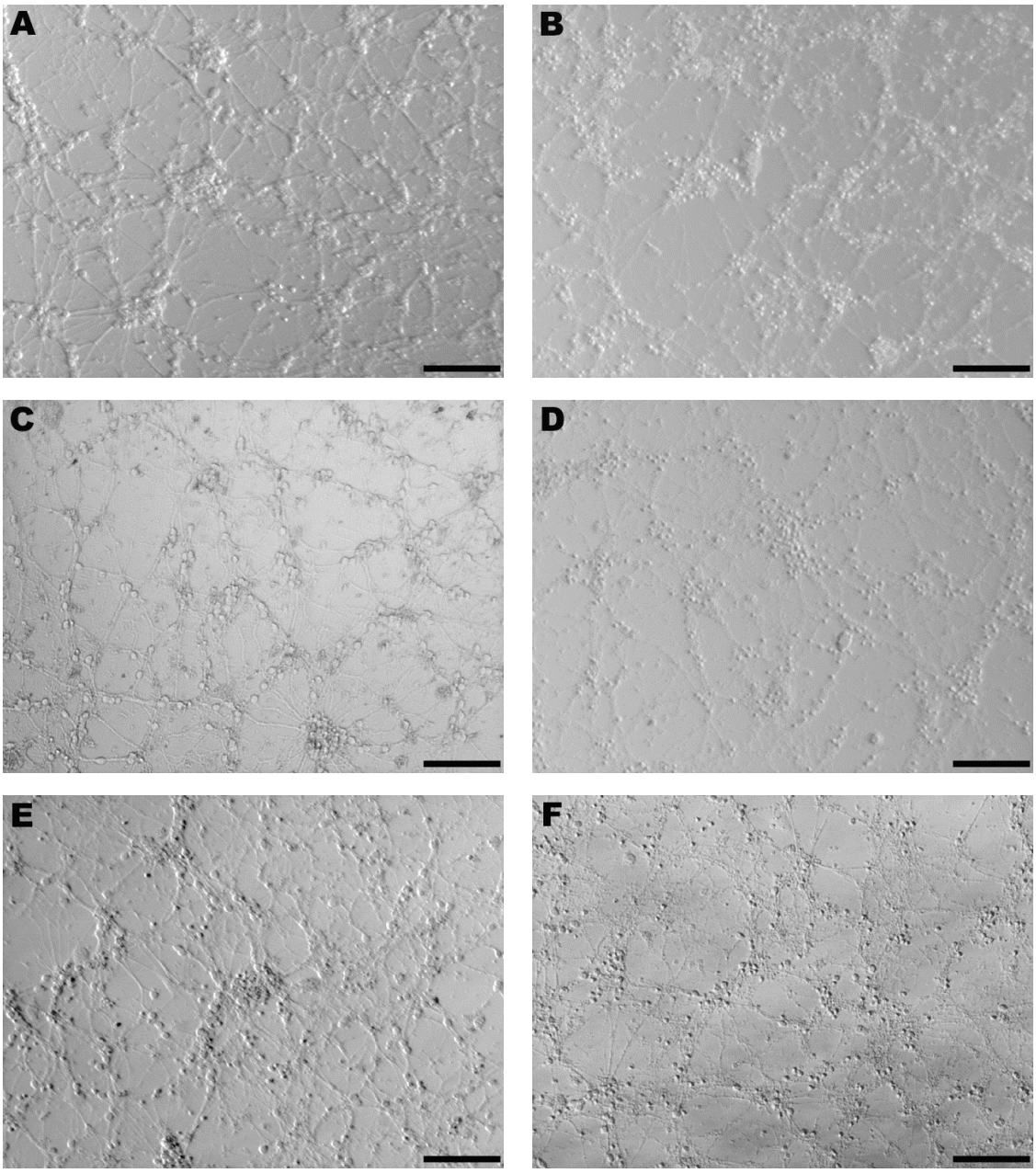

Figure 4.28 Effects of 100µM 3-HK (A, B), 100µM 3-HAA (C, D) or 100µM 5-HAA (E, F) applied for 5 hours at 9 DIV on CGN morphology at 10 DIV. Effects shown with 200U/ml catalase (A, C, E) or 200U/ml SOD (B, D, F) co-applied. Bars = 100µm. The protective effect of catalase co-application against the neurotoxicity of all three compounds is clearly seen, whereas the co-application of SOD did not reduce damage.

As shown in Figure 4.28, co-application of catalase caused an extensive reduction in the neurotoxic effects of 3-HK, 3-HAA and 5-HAA, whereas SOD co-application did not provide any protection against the effects of any of these compounds.

4.7.4 3-Hydroxykynurenine toxicity – effect of desferrioxamine

In order to establish the effect of removal of iron (which may act as an electron donor during ROS generation by the compounds studied), the iron chelating agent desferrioxamine was co-applied with treatments. Desferrioxamine was unable to afford protection against the toxicity of any of the compounds over the range of concentrations tested, 1-100μM (Figures 4.29, 4.30, 4.31). Replication of this experiment with the compounds and desferrioxamine applied for 5 hours was also unable to demonstrate protection due to desferrioxamine.

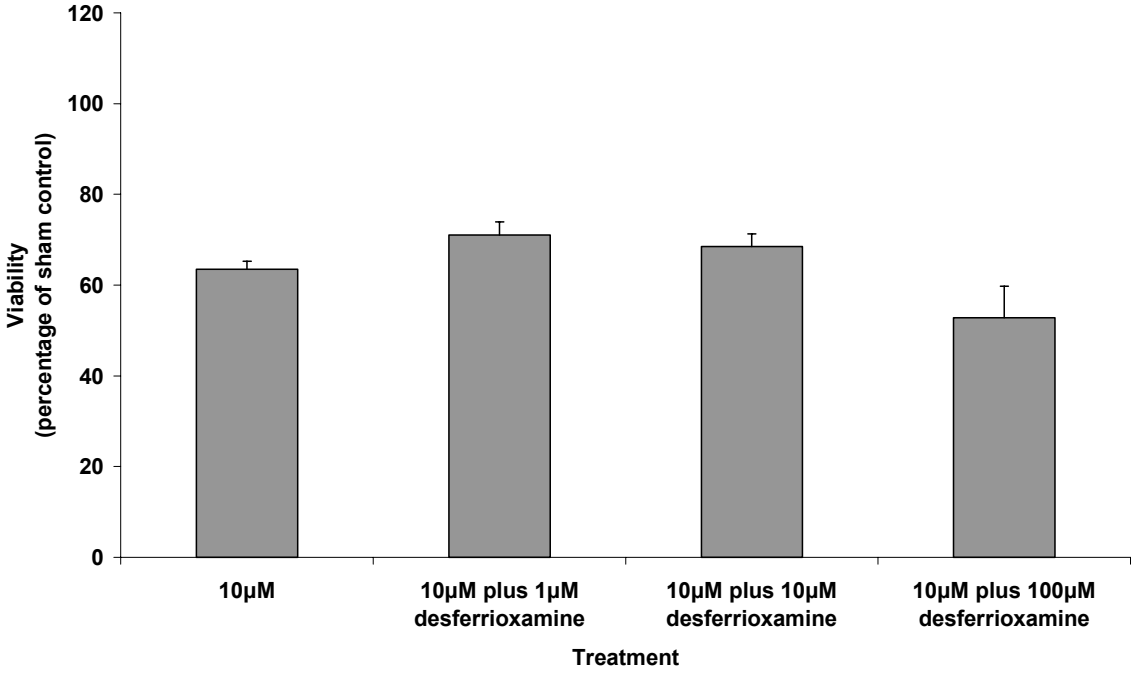

Figure 4.29 Effect of 1-100μM desferrioxamine on toxicity of 10μM 3-HK applied for 48 hours from 9 DIV. Mean +/- SEM, n=5; ANOVA followed by Tukey's test identified no significant protection at any concentration of desferrioxamine used.

4.7.5 3-Hydroxyanthranilic acid toxicity – effect of desferrioxamine

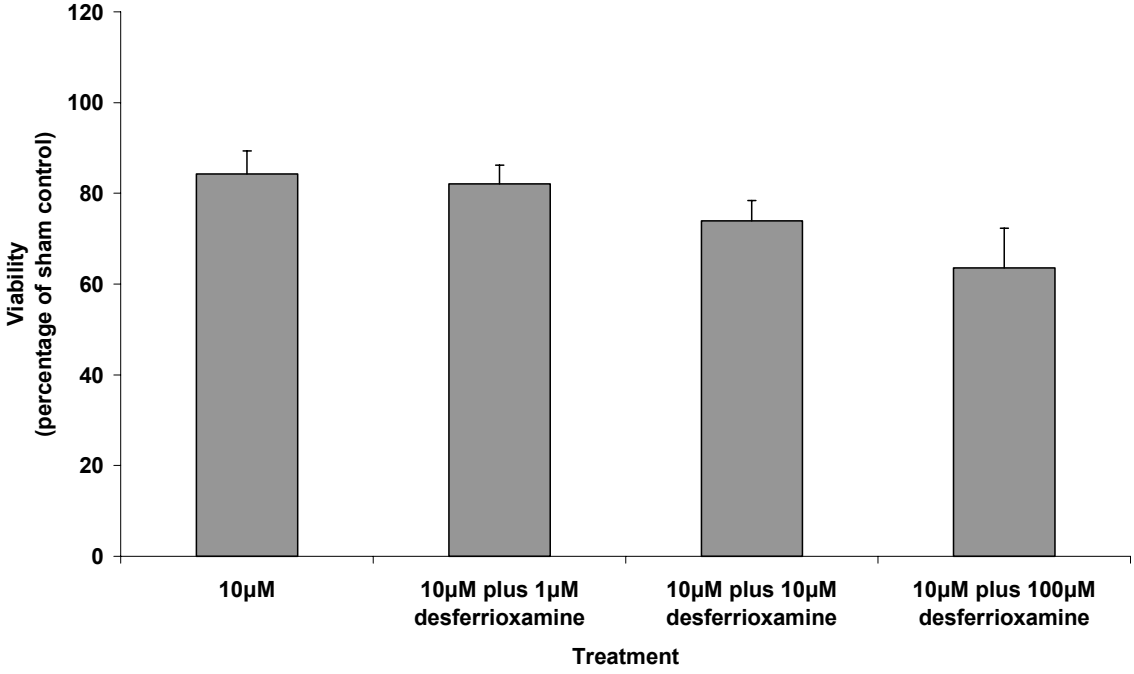

Figure 4.30 Effect of 1-100μM desferrioxamine on toxicity of 10μM 3-HAA applied for 48 hours from 9 DIV. Mean +/- SEM, n=5; ANOVA followed by Tukey's test identified no significant protection at any concentration of desferrioxamine used.

4.7.6 5-Hydroxyanthranilic acid toxicity – effect of desferrioxamine

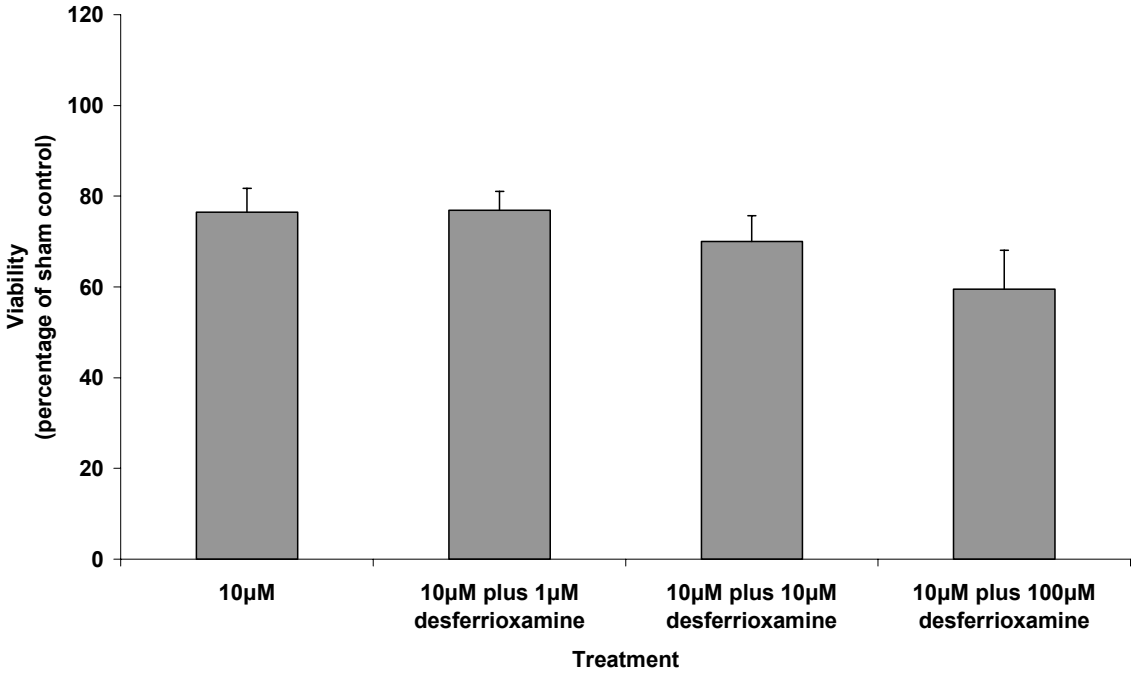

Figure 4.31 Effect of 1-100μM desferrioxamine on toxicity of 10μM 5-HAA applied for 48 hours from 9 DIV. Mean +/- SEM, n=5; ANOVA followed by Tukey's test identified no significant protection at any concentration of desferrioxamine used.

4.7.7 Effects of cycloheximide on 3-HK, 3-HAA and 5-HAA toxicity

Cycloheximide at 0.05µg/ml also failed to provide protection against the effects of 3-HK, 3-HAA and 5-HAA (Figures 4.32, 4.33). It was therefore concluded that protein synthesis was not necessary for the mechanism of neuronal death caused by treatment with these compounds, suggesting that an inflammatory response leading to increased production of TNFα and subsequent activation of death receptor-mediated pathways was not involved in the mediation of neuronal death that was mediated by treatment with any of these compounds.

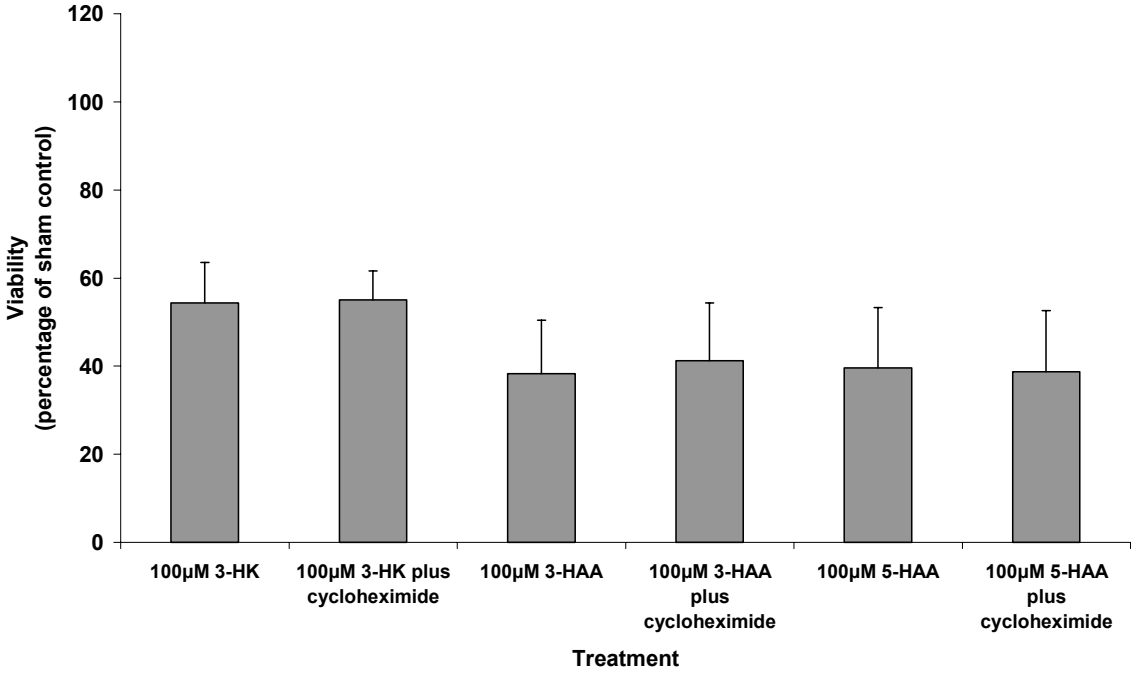

Figure 4.32 Effect of 0.05µg/ml cycloheximide on toxicity of 3-HK, 3-HAA and 5-HAA for 5 hours at 9 DIV. Mean +/- SEM, n=4; ANOVA followed by Tukey's test identified no significant protection by cycloheximide co-application against the neurotoxicity of any of the compounds tested.

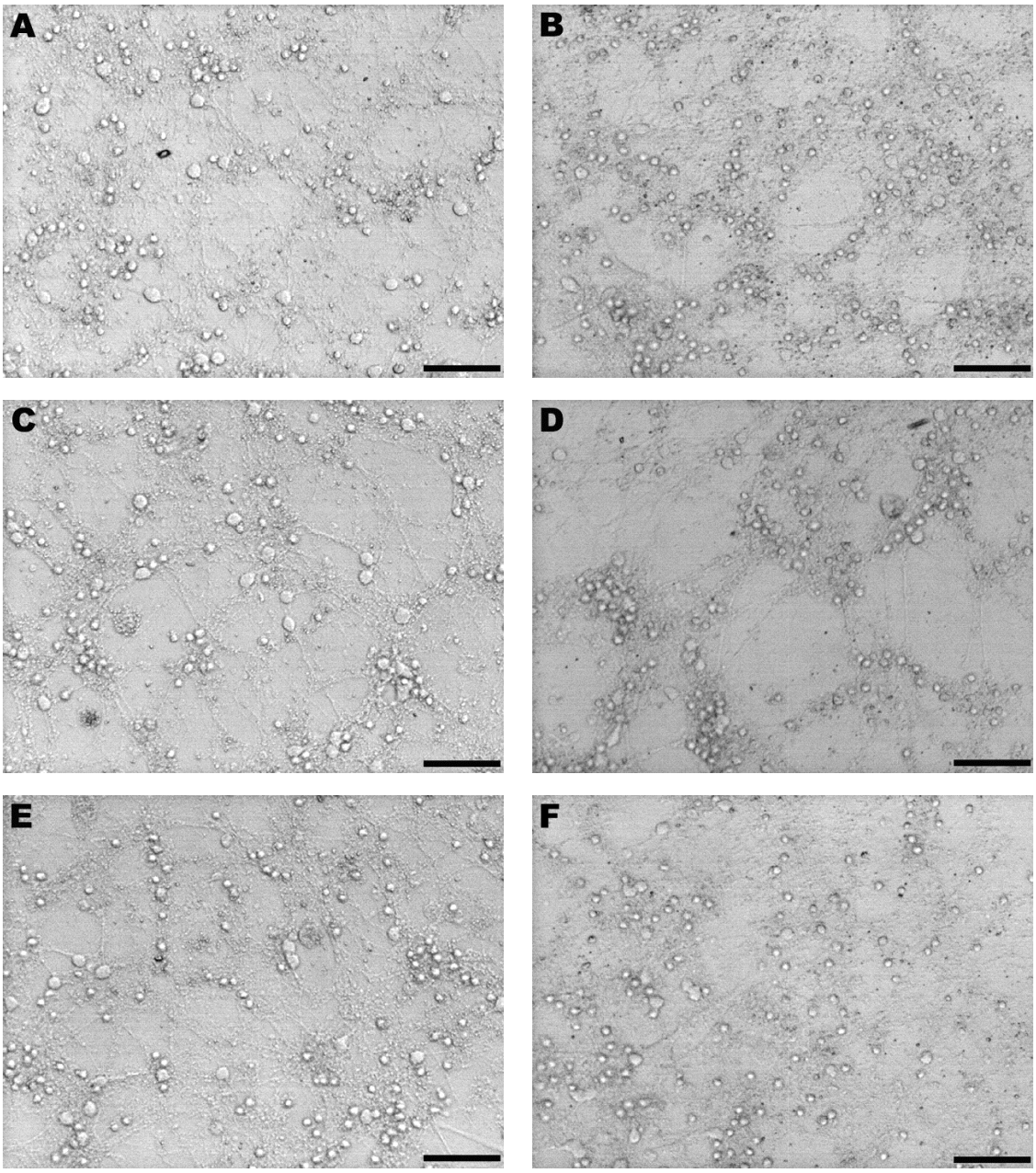

Figure 4.33 Effects of (A, B) 100μM 3-HK, (C, D) 100μM 3-HAA and (E, F) 100μM 5-HAA applied for 5 hours at 9 DIV on CGN morphology at 10 DIV. Effects shown with (B, D, F) and without (A, C, E) co-applied 0.05μg/ml cycloheximide. Bars = 50μm. Co-application of cycloheximide caused no reduction in damage due to treatment with any of the compounds tested.

The co-application of cycloheximide at 0.05μg/ml was not protective against the neurotoxic effects of 3-HK, 3-HAA or 5-HAA, with morphological images clearly showing no alteration in the extent of CGN death induced by treating with these compounds in either the presence or absence of cycloheximide (Figure 4.33).

4.7.8 3-Hydroxykynurenine – p38 phosphorylation

Western blots revealed that 100μM 3-hydroxykynurenine caused phosphorylation of the p38 signalling protein (Figure 4.34), with activity raised over the period 0.5 to 9 hours, although reduced to normal levels by 24 hours. The numbers of samples (n=2) however were insufficient for statistical analysis of densitometric data (Figure 4.35).

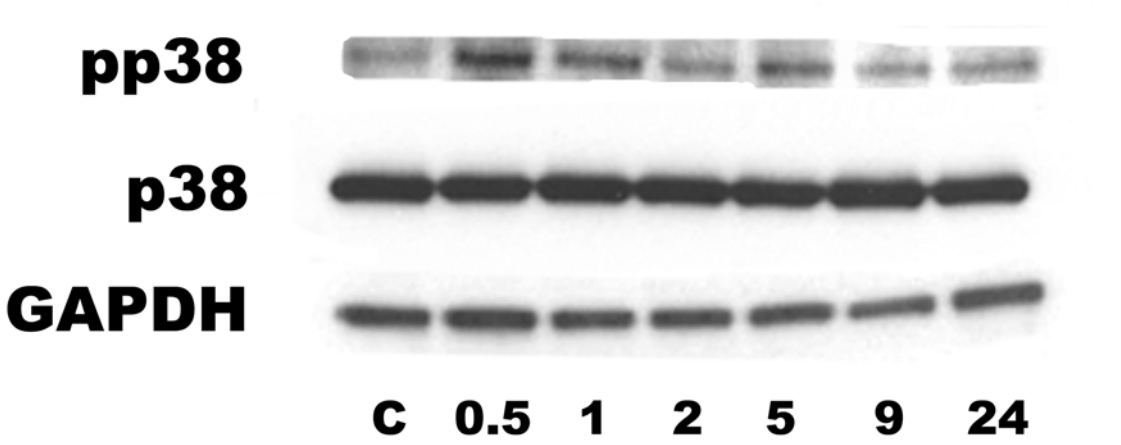

Figure 4.34 Representative blots of p38 and phosphorylated p38 (pp38) in samples from cultures treated with 100μM 3-HK for different time periods: C = control, 0.5 = 0.5 hours, 1 = 1 hour, 2 = 2 hours, 5 = 5 hours, 9 = 9 hours, 24 = 24 hours. An increase in p38 phosphorylation at 0.5 and 1 hours is evident in this sample blot.

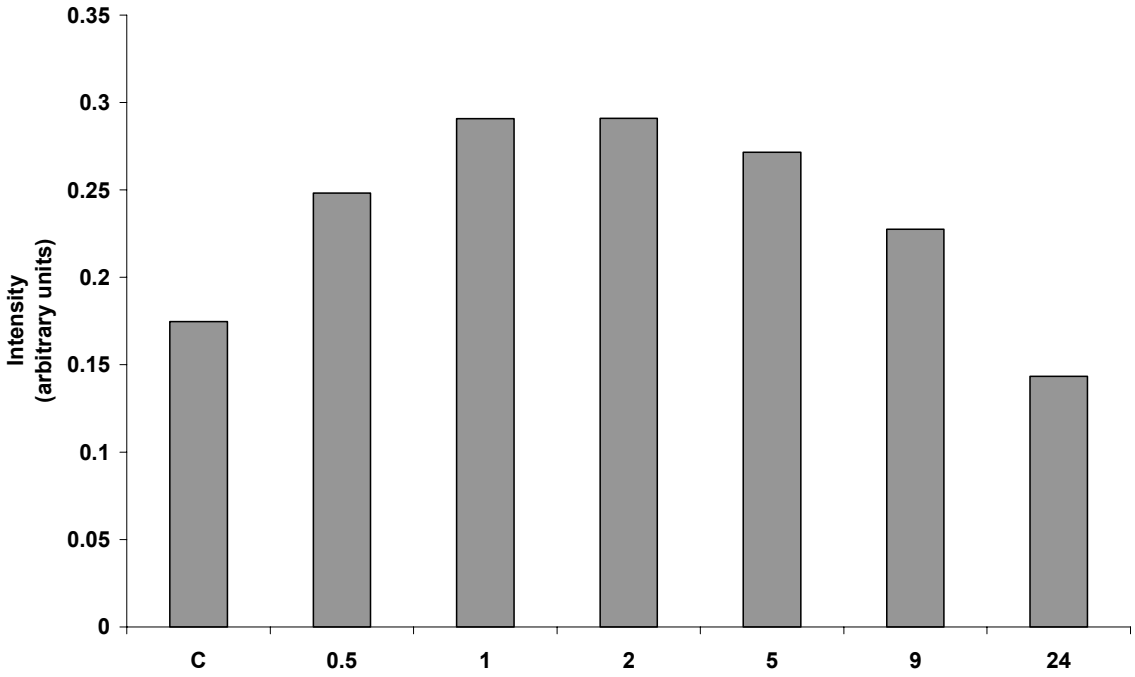

Figure 4.35 Quantification of phosphorylation of p38 in samples from cultures treated with 100μM 3-HK for different time periods: C = control, 0.5 = 0.5 hours, 1 = 1 hour, 2 = 2 hours, 5 = 5 hours, 9 = 9 hours, 24 = 24 hours. Mean value of samples taken from two separate experiments. An increase in p38 phosphorylation at 0.5 to 5 hours is evident.

4.7.9 3-Hydroxykynurenine – caspase-3 activation

No increase in caspase-3 activation was seen in Western blots of samples treated with 100μM 3-HK (Figures 4.36, 4.37). This finding suggests that p38 activation in these neurones leads to activation of an alternative route to cell death, possibly activation of caspase-6 or -7.

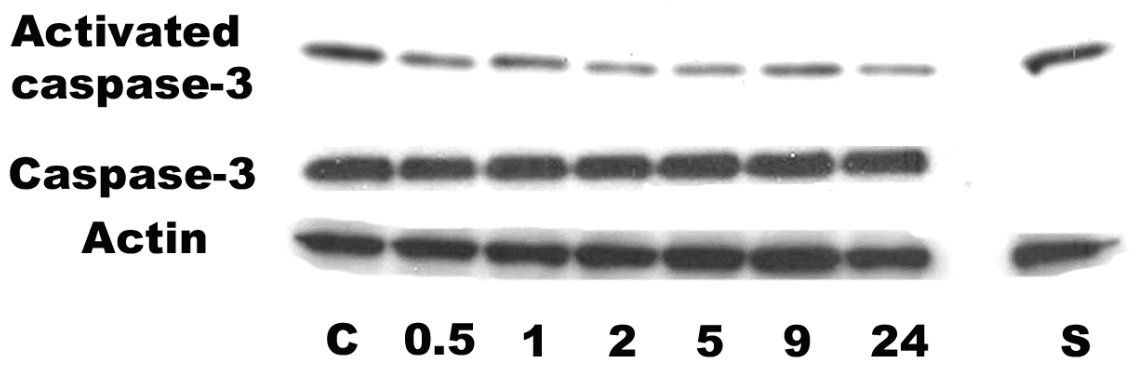

Figure 4.36 Representative blots of activated and non-activated caspase-3 in samples from cultures treated with 100μM 3-HK for different time periods: C = control, 0.5 = 0.5 hours, 1 = 1 hour, 2 = 2 hours, 5 = 5 hours, 9 = 9 hours, 24 = 24 hours, S = 1μM staurosporine for 6 hours at 9 DIV (positive control). No increase in caspase-3 activation is seen in this blot due to 3-HK treatment, although a staurosporine-induced increase is apparent.

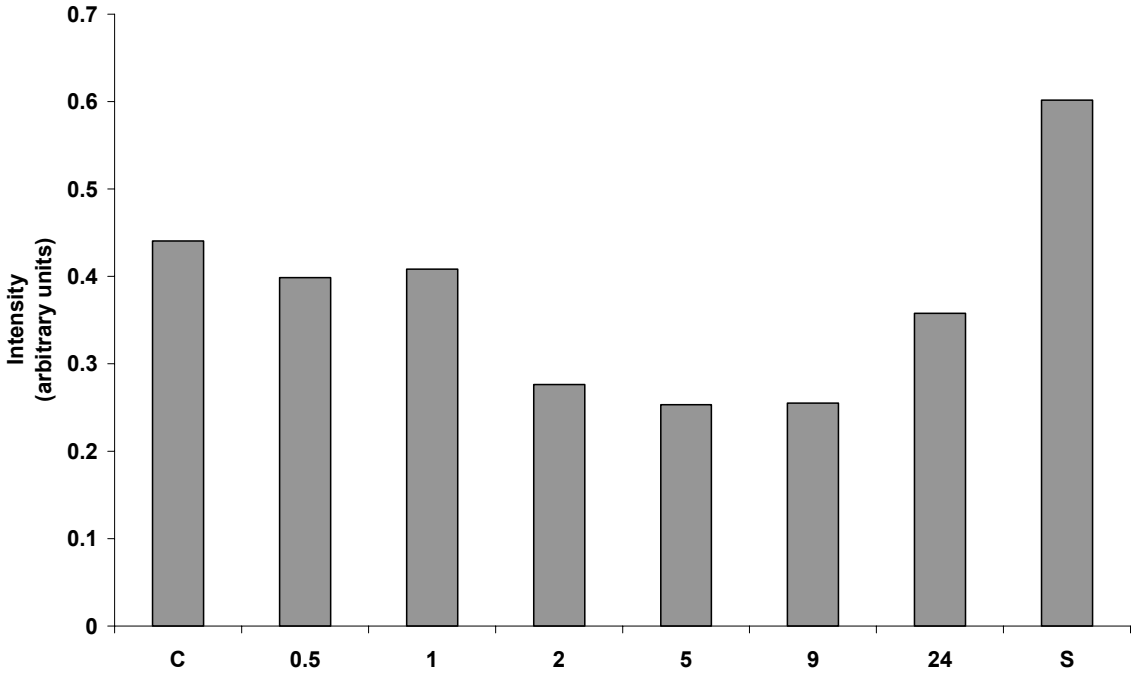

Figure 4.37 Quantification of caspase-3 activation in samples from cultures treated with 100μM 3-HK for different time periods: C = control, 0.5 = 0.5 hours, 1 = 1 hour, 2 = 2 hours, 5 = 5 hours, 9 = 9 hours, 24 = 24 hours, S = 1μM staurosporine for 6 hours at 9 DIV (positive control). Mean value of samples taken from two separate experiments. No increase in caspase-3 activation is seen due to 3-HK treatment, although a staurosporine-induced increase is apparent.

4.7.10 5-Hydroxyanthranilic acid – p38 phosphorylation

There was evidence that treatment with 100μM 5-HAA caused phosphorylation of the p38 signalling protein in CGNs, with a rise in activity over the period of 0.5 to 9 hours after exposure to 5-HAA (Figure 4.38), although the numbers were insufficient for statistical analysis of densitometric data (Figure 4.39).

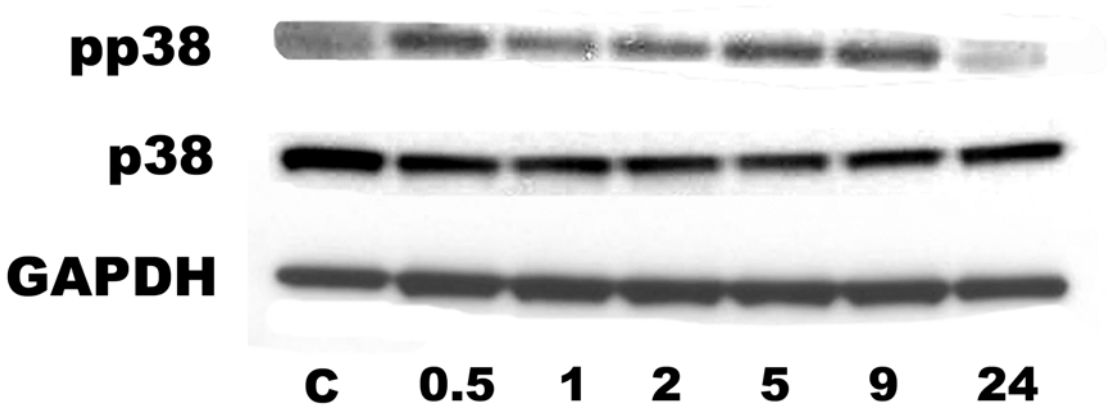

Figure 4.38 Representative blots of p38 and phosphorylated p38 (pp38) in samples from cultures treated with 100μM 5-HAA for different time periods: C = control, 0.5 = 0.5 hours, 1 = 1 hour, 2 = 2 hours, 5 = 5 hours, 9 = 9 hours, 24 = 24 hours. An increase in p38 phosphorylation at 0.5 to 9 hours is evident in this sample blot.

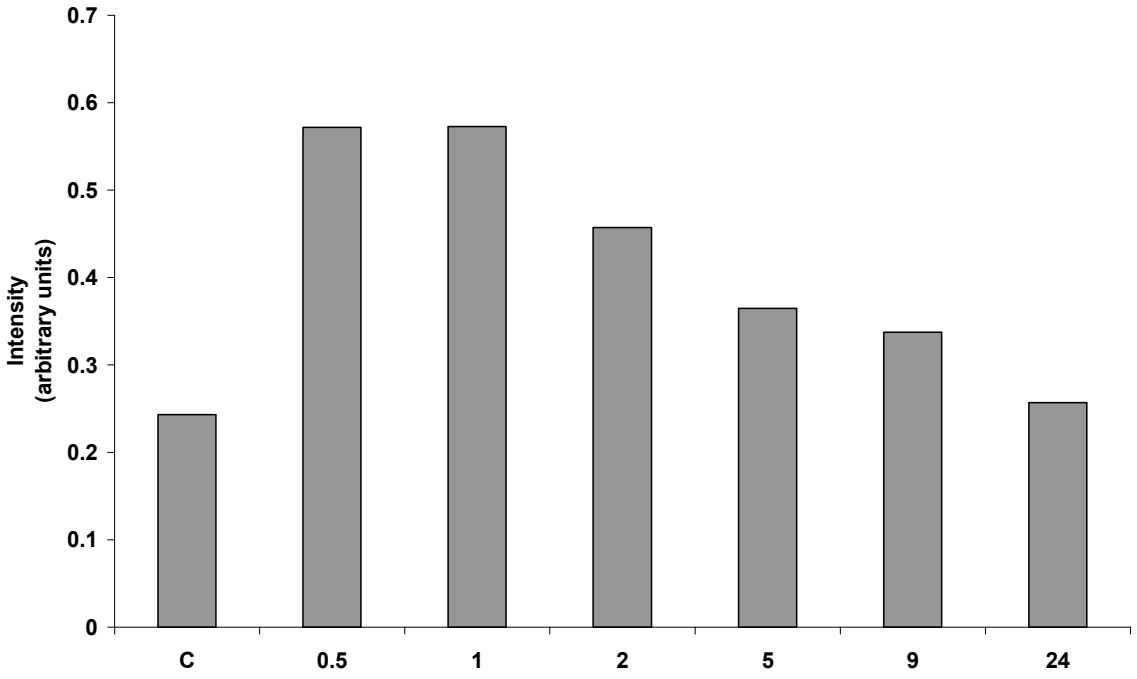

Figure 4.39 Quantification of phosphorylation of p38 in samples from cultures treated with 100μM 5-HAA for different time periods: C = control, 0.5 = 0.5 hours, 1 = 1 hour, 2 = 2 hours, 5 = 5 hours, 9 = 9 hours, 24 = 24 hours. Mean value of samples taken from two separate experiments. An increase in p38 phosphorylation at 0.5 and 1 hours is evident.

4.7.11 5-Hydroxyanthranilic acid – caspase-3 activation

Treatment with 100μM 5-HAA did not lead to an increase in caspase-3 activation (Figures 4.40, 4.41), a finding again indicating that p38 activation in CGNs in our system leads to an alternative route to cell death.

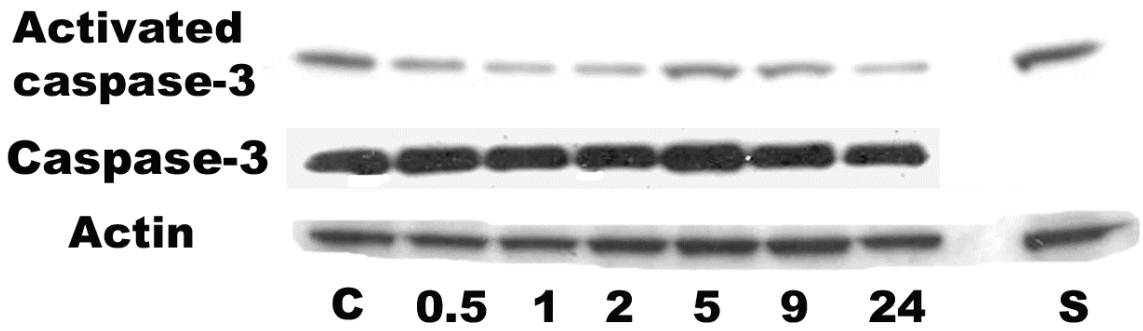

Figure 4.40 Representative blots of activated and non-activated caspase-3 in samples from cultures treated with 100μM 5-HAA for different time periods: C = control, 0.5 = 0.5 hours, 1 = 1 hour, 2 = 2 hours, 5 = 5 hours, 9 = 9 hours, 24 = 24 hours, S = 1μM staurosporine for 6 hours at 9 DIV (positive control). No increase in caspase-3 activation is seen in this blot due to 5-HAA treatment, although a staurosporine-induced increase is apparent.

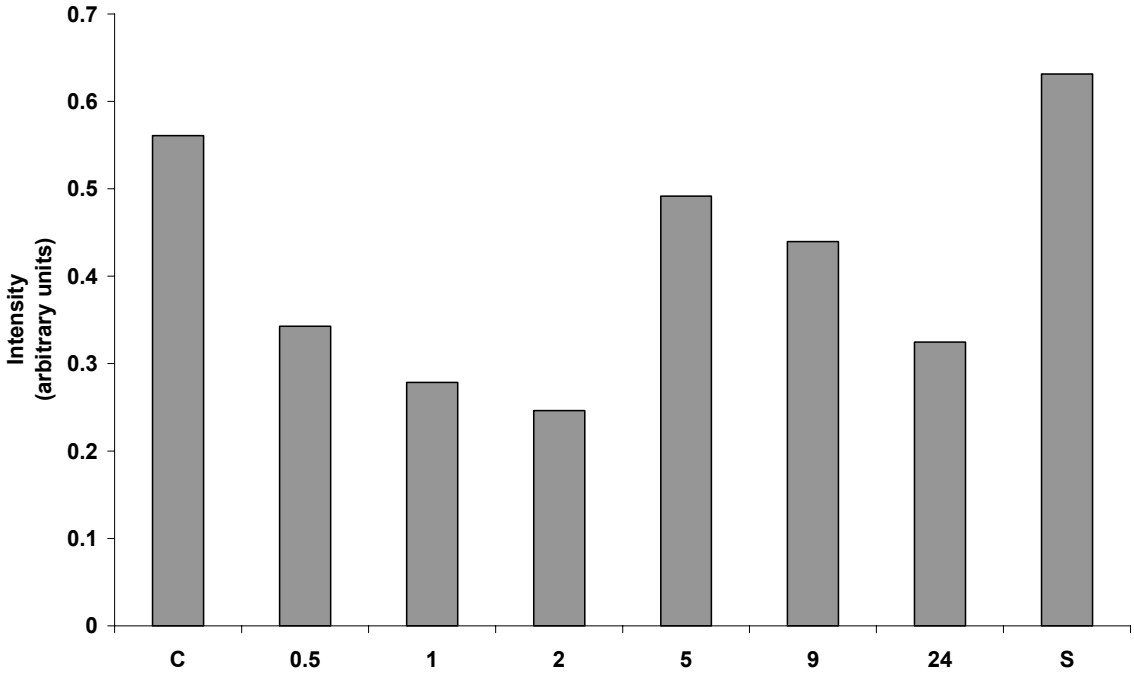

Figure 4.41 Quantification of caspase-3 activation in samples from cultures treated with 100μM 5-HAA for different time periods: C = control, 0.5 = 0.5 hours, 1 = 1 hour, 2 = 2 hours, 5 = 5 hours, 9 = 9 hours, 24 = 24 hours, S = 1μM staurosporine for 6 hours at 9 DIV (positive control). Mean value of samples taken from two separate experiments. No increase in caspase-3 activation is seen due to 5-HAA treatment, although a staurosporine-induced increase is apparent.

4.7.12 3-Hydroxykynurenine – p38 phosphorylation (ICC)

The activation of p38 in CGNs exposed to 3-HK for 0.5 to 5 hours was also investigated immunocytochemically by staining with antibodies raised to both p38 and phosphorylated p38 (Figure 4.42). This was successful to a limited extent, but it was not as effective as Western blotting and therefore was not continued beyond a pilot study.

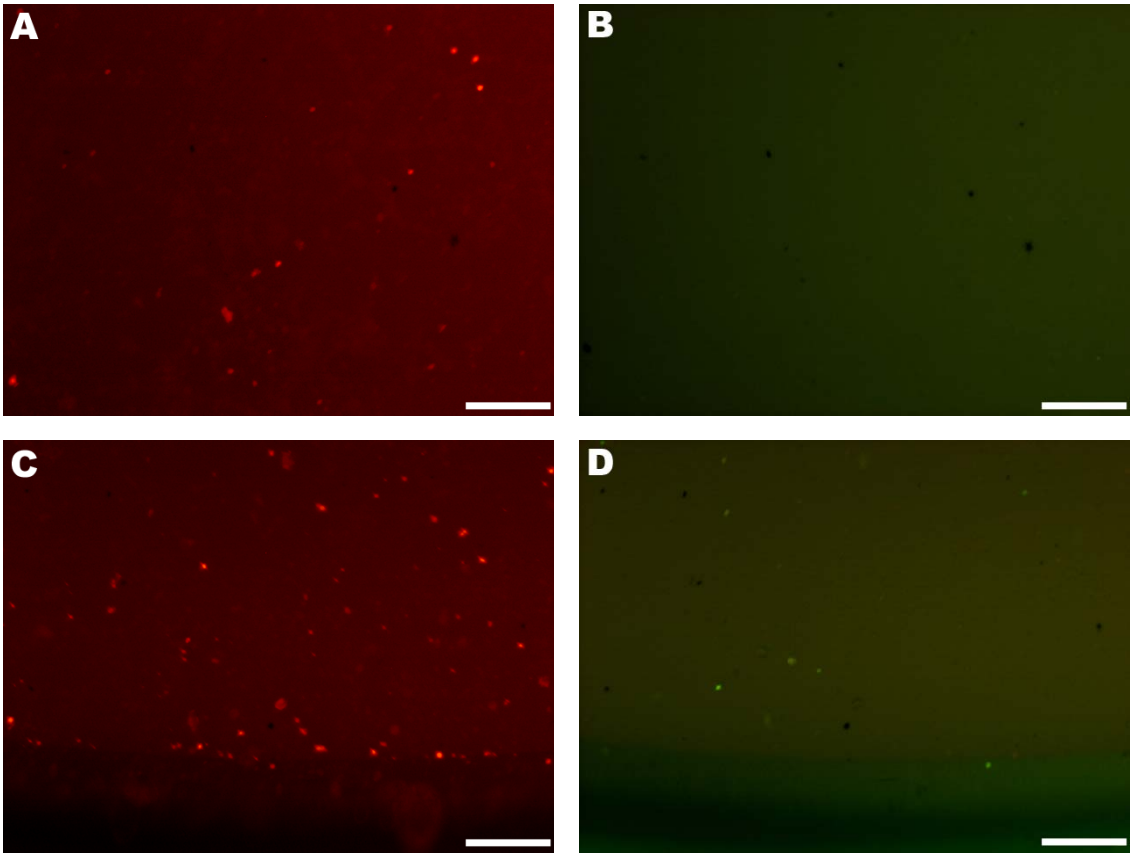

Figure 4.42 ICC staining of CGNs with antibody against p38 (A, C) and phosphorylated p38 (B, D) in untreated cultures (A, B) and cultures treated with 100μM 3-HK for 1 hour (C, D). Bars = 100μm. Staining for p38 can be seen in both treated and untreated cultures, with positive staining for phosphorylated p38 visible in treated CGNs.

Both treated and untreated cultures show positive staining for non-activated p38 (Figure 4.42A and C). Untreated cultures were negative for phosphorylated p38 (Figure 4.42B), whereas there was occasional positive staining in cultures treated with 3-HK (Figure 4.42D).

4.8 Effect of altering ratios of anthranilic acid and 3-hydroxyanthranilic acid concentrations

4.8.1 Anthranilic acid and 3-hydroxyanthranilic acid ratios

As previously described, an association between an increased ratio of anthranilic acid to 3-HAA has been demonstrated in stroke patients (Darlington *et al.*, 2007); the effect of directly altering the ration of exogenous anthranilic acid to 3-HAA was therefore studied. Increasing the ratio of anthranilic acid to 3-hydroxyanthranilic acid did not provide a significant attenuation of 3-hydroxyanthranilic acid toxicity (Figure 4.43). When the concentration of anthranilic acid was increased, a slight additive toxic effect was noted, a finding in keeping with earlier studies of the effect of anthranilic acid applied alone (Figure 4.19). A similar result was seen if the experiment was performed in medium containing 25mM glucose.

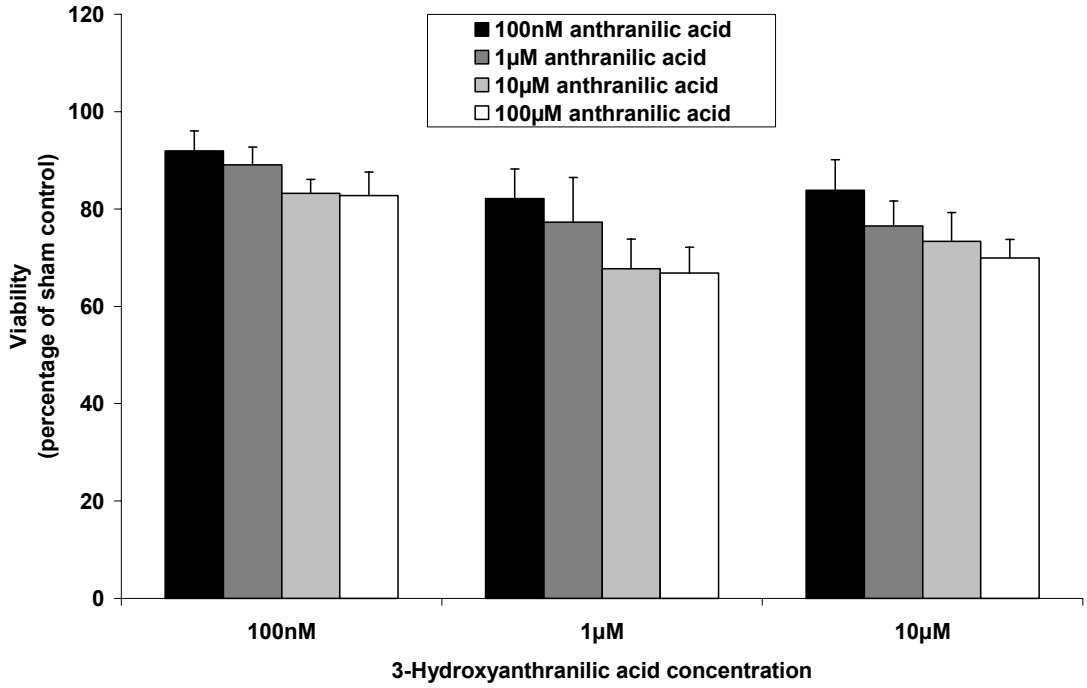

Figure 4.43 Effect of 100nM-10µM anthranilic acid on the toxicity of 100nM-10µM 3-HAA for 5 hours at 9 DIV. Mean +/- SEM, n=4-7. No protective effect is seen on 3-HAA toxicity if anthranilic acid is co-applied, indicating that an increased anthranilic acid-3HAA ration is not protective against 3-HAA toxicity in CGNs. It therefore appears most unlikely that an increased ration of anthranilic acid to 3-HAA provides any protective function in neurones.

4.9 Discussion of glutamate, NMDA, 3-NPA and OGD results

4.9.1 Glutamate neurotoxicity

Excessive glutamate exposure has long been recognised as a source of neurotoxic damage via excitotoxicity, which mediates damage by causing over-stimulation of neurones with excitatory amino acids (Olney and de Gubareff, 1978). Hypoxia or ischaemia trigger release of intracellular glutamate, bringing the glutamate concentration to high micromolar or millimolar levels, with excessive glutamate (100μM) destroying neurones after only 5 minutes exposure (Choi and Rothman, 1990). Taken together, these factors explain why glutamate-mediated excitotoxicity following ischaemia results in a much more rapid onset of cell death in the CNS compared to other regions. It also accounts for the regional differences in sensitivity to ischaemia seen within the brain, such as the hippocampal CA1 region and dorsolateral striatum (Sims and Zaidan, 1995).

Glutamate treatment in cultured mouse CGNs increased levels of cleaved collapsin response mediator protein 3 (CRMP-3), prevented by calpain inhibitors or small interfering RNA strands that down-regulated CRMP-3 production (Hou *et al.*, 2006). It was also determined that CRMP-3 was normally predominantly cytoplasmic, whereas in glutamate-treated neurones, CRMP was mainly nuclear (Hou *et al.*, 2006).

Damage due to glutamate increases proportional to concentration due to the greater excitotoxic effect and calcium influx magnitude, with resultant loss of mitochondrial calcium regulation and damage to plasma membrane calcium pumps. Therefore the dose-response effect of glutamate was examined, which produced a series of results over a range of 1μM to 10mM glutamate, demonstrating an increasing degree of neurotoxicity up to a maximum reached at 5mM (with approximately 70% cell death).

Cultures maintained in 25mM KCl-containing medium and then switched to 5mM KCl medium at 7 DIV for 48 hours prior to glutamate application were examined to assess whether lowering the KCl concentration to a non-depolarising level increased vulnerability of CGNs to glutamate. Higher levels of cell death were seen over a range of glutamate concentrations (50μM to 1mM), although the high

degree of background cell death (CGNs switched to 5mM KCl but untreated with glutamate suffered over 50% death relative to controls maintained in 25mM KCl throughout) overshadowed the additional damage due to glutamate. Nevertheless, the apparent maximum level in our system for glutamate-induced damage (70% cell death) was reached by 100μM glutamate, with no further increase up to 1mM glutamate: a lower maximally toxic dose than was seen in CGNs in 25mM KCl.

Co-application of 0.05μg/ml cycloheximide did not affect the neurotoxicity of 100μM glutamate applied for 24 hours, consistent with the findings of Dessi *et al.* in 1993, who demonstrated that glutamate neurotoxicity in CGNs was not blocked by co-application of 100μg/ml cycloheximide, or associated with DNA fragmentation. The cycloheximide dose initially selected (0.1μg/ml) had been shown to prevent caspase-3 activation in rat neonatal CGNs (Morán *et al.*, 1999), but this dose damaged CGNs in our system; hence the lower concentration of 0.05μg/ml was preferred. The reason for this toxicity was uncertain: it is unlikely that the exposure time of 24 hours was relevant, as this had been used previously (Morán *et al.*, 1999).

Glutamate toxicity evidently involves activation of more than one cell death mechanism (Fatokun *et al.*, 2008a). Exposure of rat cortical neurones to 100*μ*M glutamate for 5 minutes caused neurotoxicity due to necrosis (48% versus 15% in controls) and apoptosis (14% versus 8% in controls), caused an increase in cyclic GMP (a marker of endogenous NO formation) and could be blocked by the NMDA receptor antagonist APV at 100*μ*M or by the NOS inhibitor *N*-nitro-L-arginine methyl ester (NAME). The neurotoxic effects induced by glutamate were paralleled by reductions in ATP levels 24 hours post-glutamate and it was also shown that glutamate affected mitochondrial respiratory chain complex enzymes. Although no alterations were seen to the activity of either NADH-CoQ reductase or cytochrome *c* oxidase, a significant reduction in succinate-cytochrome c reductase was seen, with levels of NADH also reduced (Delgado-Esteban *et al.*, 2000).

Five to 60 minutes glutamate treatment resulted in upregulation of p38 expression in neonatal rat CGNs, with toxicity inhibited by the specific p38 inhibitor SB203580. The increased p38 expression was shown to be calcium-

dependent, as it was blocked by pre-treating with 5mM EGTA (ethylene glycol tetra-acetic acid) and replicated by the calcium ionophore A23187. Pre-treatment with verapamil or nifedipine was not protective however, suggesting L-type voltage-gated calcium channels are not involved in p38 induction by glutamate (Kawasaki *et al.*, 1997). Blockade of NMDA receptors with AP5 caused a dose-dependant reduction in p38 activation, whilst NMDA itself was also shown to increase p38 expression (Kawasaki *et al.*, 1997). Glutamate-induced excitotoxicity has also been linked to p38 activity in neonatal rat cerebral cortex *in vivo* (Rivera-Cervantes *et al.*, 2004).

As the greatest part of glutamate-mediated neurotoxicity is mediated by the NMDA receptor and damage via this receptor was of most interest, it was necessary to establish a dose of this compound that provided an equivalent degree of excitotoxicity to 50-100μM glutamate. An equal degree of neurotoxicity to 100μM glutamate for 24 hours was achieved using 300μM NMDA. As with glutamate, this insult was not prevented by addition of 0.05μg/ml cycloheximide, indicating little dependence on protein expression to induce neurotoxicity.

4.9.2 3-NPA neurotoxicity

The excitotoxin and mitochondrial poison 3-NPA has been used to explore neurotoxicity in CGNs in several studies (Hassel and Bråthe, 2000, Olsen *et al.*, 1999, Weller and Paul, 1993). 3-Nitropropionic acid was shown to exert neurotoxicity by NMDA receptor activation and calcium influx, as blockade with MK-801 caused significant reduction in both neuronal death and the associated calcium influx, although did not provide complete protection when the treatment period was increased from 3 to 24 hours (Olsen *et al.*, 1999). Additionally, 3-NPA acts to inhibit succinate dehydrogenase (due to its close structural resemblance to succinic acid), causing a dose-related reduction in activity and an associated reduction in neurone (although not astrocyte) viability (Alexi *et al.*, 1998, Olsen *et al.*, 1999).

The first step in our investigation of 3-NPA's neurotoxic action on CGNs was to establish that the toxicity was concentration-dependent, as reported in previous work with cultured rat CGNs (Weller and Paul, 1993, Fink *et al.*, 1996, Olsen *et al.*, 1999). This was demonstrated over a range of 1μM to 10mM, with the

maximum effect (approximately 90% cell death) reached at 5mM. As with glutamate and NMDA, co-application of 0.05µg/ml cycloheximide with 3-NPA did not affect its ability to induce neurotoxic damage.

Neurones from different regions of embryonic rat brain were found by Fink and colleagues to differ in their sensitivity to 3-NPA, with cerebellar neurones less sensitive than hypothalamic or hippocampal neurones. The reason for this apparent lack of sensitivity was not however a lack of sufficiently matured NMDA receptors, as blockade with MK-801 (but not kynurenic acid) was effective in significantly reducing 3-NPA-mediated toxicity in striatal neurones in this study (Fink *et al.*, 1996). 3-Nitropropionic acid toxicity was also reduced by the presence of 20mM glucose, a protective effect not mediated against glutamate toxicity (Fink *et al.*, 1996). Our findings, with 3-NPA used as a toxic insult at 11 DIV in medium with 5.5mM and 25mM glucose, showed a slight but non-significant decrease in 3-NPA toxicity in the higher glucose concentration.

It has been suggested that the interaction between the NMDA receptor-mediated and the mitochondrial poison actions of 3-NPA may combine to generate a 'lethal triplet' of actions, which accentuates excitotoxicity, oxidative stress and metabolic compromise (Alexi *et al.*, 1998). Certainly, the inhibition of succinate dehydrogenase will reduce ATP formation, reducing the sodium-calcium exchange pump's ability to remove excess calcium and will increase ROS generation in the mitochondria. Both of these effects will hamper the neurone's ability to cope with the effects of NMDA receptor activation and hence 3-NPA provides a model of a simultaneously excitotoxic and oxidative insult.

4.9.3 OGD-induced neurotoxicity

Oxygen-glucose deprivation has been used as a more representative model for ischaemia than hypoxia alone, although it does not fully characterise an ischaemic episode. Anoxia alone causes depolarisation of neuronal membranes due to increased conductance of potassium channels, with depolarisation enhanced during OGD by reduced ATP formation and consequent failure of the Na,K-ATPase pump (Martin *et al.*, 1994). In addition to increasing extracellular glutamate levels, this causes rises in intracellular levels of sodium, chloride and calcium.

The use of OGD as a toxic insult in our cultures necessitated considerable method development, with an initial trial of hypoxia only, followed by the introduction of a glucose-free buffer which could be applied to CGNs without causing cell death due to buffer toxicity. A suitable buffer formula was obtained from Dr. Joseph Tauskela (Tauskela *et al.*, 2003) and a gas mixture of 95% nitrogen/5% carbon dioxide replaced the normoxic environment. The gas mixture and buffer were assayed to confirm accuracy of composition and that the procedure was effective in reducing pO_2 (by approximately 40%) in the OGD buffer, this latter finding comparable to previously published work (Scorziello *et al.*, 2001). Following this, the optimum period of OGD to effect neurotoxic damage was determined, with most consistent results achieved with 5 hours' exposure, a finding consistent with previous demonstrations of OGD toxicity in neonatal rat CGNs of ~25% death after 3 hours and ~60% death after 6 hours (Wick *et al.*, 2002).

The NMDA receptor antagonist MK-801, the NMDA and AMPA receptor antagonist kynurenic acid and the calcium channel blocker nifedipine failed to significantly protect against damage due to OGD for 5 hours, despite using different concentrations for each agent. Involvement of protein synthesis in the mediation of damage by OGD toxicity was also investigated by adding cycloheximide during OGD treatment, during the 24 hour period between exposure and assay (the equivalent of the reperfusion period following ischaemia) and for both of these periods. However, cycloheximide did not protect in any of these periods, indicating that increased production of cell death signalling proteins (such as Fas) is not involved. This does not exclude the involvement of apoptosis or the possibility that apoptotic mechanisms were activated and superseded by necrotic cell death. Certainly, in rat CGN cultures a shorter duration of OGD (90 minutes) induced cell death via both pathways, with notable secondary necrosis (Kalda *et al.*, 1998).

Considerable evidence links NMDA receptor activation to OGD-related neurotoxicity: OGD damage to cultured hippocampal neurones depends on synaptic connections, with attenuation of damage by NMDA receptor antagonists and high-dose magnesium, although this protection may be limited to preventing damage from mild to moderate severity OGD (Choi and Rothman, 1990). Hypoxia–induced loss of evoked field potentials in rat dentate gyrus slices,

attenuated by removal of extracellular calcium has also been reported (Kass and Lipton, 1982). Application of OGD to rat cerebral cortical neurones was not significantly reduced by the AMPA receptor antagonist CNQX, but was reduced by MK-801, with co-application of MK-801 and CNQX causing a reduction in cell death equal to that produced by MK-801 alone. These reductions in cell death were paralleled by reduced calpain expression (Tauskela *et al.*, 2001).

N-methyl-D-aspartate and kainate receptor channels change in response to hypoxia. In foetal guinea pig neurones, NMDA receptors demonstrated enhanced MK-801 binding when subjected to hypoxia and kainate channel desensitisation. This led to prolonged sodium influx and contributed to increased calcium influx due to greater sodium-calcium exchange (Mishra and Delivoria-Papadopoulos, 1999). Increased calcium influx was also mediated via NMDA receptors in response to NMDA or glutamate stimulation. This altered receptor function may result from cycles between phosphorylation and dephosphorylation (Mishra and Delivoria-Papadopoulos, 1999). Another aspect of glutamate involvement in OGD-related damage to CGNs concerned blockade of metabotropic glutamate receptors, which attenuated damage induced by OGD in neonatal rat CGNs (Kalda *et al.*, 2000).

Scorziello and co-workers (2001) undertook a comparison of effects of OGD on neonatal rat CGNs and embryonic rat cortical neurones. After 1 hour of OGD, CGNs were unaffected but by 2 hours showed significant mitochondrial damage (assayed by MTT production), reduced ATP formation and increased lipid peroxidation (assayed by malondialdehyde production) were evident (Scorziello *et al.*, 2001). Additionally, lipid peroxidation and LDH release in CGNs were increased by 24 hours reoxygenation and commenced prior to reoxygenation. By comparison, both 1 and 2 hours' OGD caused cell death in cortical neurones, with lipid peroxidation again made more severe by 24 hours of reoxygenation. However, cortical neurones did not show LDH release following either 1 or 2 hours' OGD, with or without subsequent reoxygenation, nor was ATP production reduced.

Further evidence of mitochondrial damage in neurotoxicity induced in neonatal rat CGNs by OGD was demonstrated by the use of melatonin, which caused a dose-dependent reduction in cytochrome c release, caspase-3 activation and

maintenance of mitochondrial membrane potential (Han *et al.*, 2006). Two hours of OGD with 24 hours reoxygenation in CGNs has also been shown to cause a calcium-dependent increase in nitric oxide synthase activity and consequent nitric oxide production (Scorziello *et al.*, 2004). Nitric oxide synthase inhibitors or intracellular Ca^{2+} removal were partially protective against this OGD-induced cell death, although a nitric oxide donor abolished the effect (Scorziello *et al.*, 2004).

4.10 Discussion of findings concerning kynurenine pathway compounds and glucose

4.10.1 Increased glucose concentration

Hyperglycaemia or raised exogenous glucose causes a variety of effects both *in vivo* and *in vitro*, with increased neurotoxic effects seen due to hyperglycaemia directly and also heightened vulnerability to oxidative damage (see section 1.3.6).

Hyperglycaemia *in vivo* enhances vulnerability to ischaemia, with ischaemia in hyperglycaemic animals demonstrated to cause significant increases in mitochondrial cytochrome *c* release into the cytosol at 0.5, 1 or 3 hours of reperfusion, positive caspase-3 staining after 1 and 3 hours and positive TUNEL staining after 3 hours (Li *et al.*, 2001, Muranyi *et al.*, 2003). There was also correlation between staining for cytochrome c release and increased TUNEL-positive staining compared to normoglycaemic animals subjected to ischaemia (Li *et al.*, 2001, Muranyi *et al.*, 2003). Another study of ischaemia in rats with streptozotocin-induced diabetes mellitus found that a high-dose of insulin was effective in reducing infarct volume significantly in hyperglycaemic animals (Rizk *et al.*, 2006). It should be noted however, that insulin can induce AMPA receptor encocytosis (Ahmadian *et al.*, 2004) and GABA receptor recruitment (Wan *et al.*, 1997), so these effects may not be entirely due to alterations in glucose levels.

Transient ischaemia (30 minutes of MCA occlusion) in rats with streptozotocin-induced diabetes caused more extensive damage 3 and 6 hours after occlusion in diabetic than non-diabetic rats (Muranyi *et al.*, 2003). Examination at 7 days post-occlusion showed that damage had continued to develop beyond 6 hours' reperfusion in non-diabetic but not diabetic animals, although infarct volume in

diabetic animals was significantly larger (39% vs. 16%), therefore not only was ischaemic damage in diabetic animals more extensive, but onset was also more rapid (Muranyi *et al.*, 2003).

Comparable *in vitro* data exist: a study of the effects of increased glucose on embryonic rat dorsal root ganglion (DRG) neurones cultured in medium with 25mM glucose in which 'hyperglycaemia' was induced by raising the concentration to 45mM) found that 45mM glucose caused a range of effects. These included: increased NADH oxidase activity, increased ROS generation, mitochondrial swelling and disruption of inner cristae, caspase-3 cleavage and TUNEL staining, with similar levels of neuronal death induced by increased glucose exposure for 6 or 24 hours (Vincent *et al.*, 2005). The exposure to high glucose led to increased expression of SOD and more markedly of catalase (Vincent *et al.*, 2005).

Increased apoptosis was evident in neuroblastomal cells (SH-SY5Y), hippocampal neurones and primary DRG neurones due to hyperosmolar conditions caused by glucose or mannitol (Pittenger *et al.*, 1997, Sima, 2003). Glucose has an effect beyond hyperosmolarity and in DRG neurones of diabetic rats a progressive increase in intracellular calcium is evident (Ristic *et al.*, 1996). A possible mechanism for hyperglycaemic neurotoxicity is that increased glycation of axonal structural proteins (tubulin, neurofilament and actin) leads to axonal atrophy and degeneration. Additionally, increased glucose levels induce alterations in redox status, dysregulation of glutathione synthesis and glucose autoxidation, generating ROS (Sima, 2003).

A study of cultured rat cortical neurones, returned to medium with 5.5mM glucose, 20mM D-glucose or 20-mM L-glucose following glutamate application revealed that glutamate-induced neurotoxic effects (necrosis and apoptosis) were significant in control cultures and those with added L-glucose but not in neurones replenished with medium containing 20mM D-glucose (Delgado-Esteban *et al.*, 2000). The reduction in succinate-cytochrome c reductase and NADH levels by glutamate were abolished by D-glucose supplementation post-glutamate. The protective effect of D-glucose was unlikely to be due to ability to scavenge peroxynitrite, as L-glucose should also have had this ability (Delgado-Esteban *et al.*, 2000).

Activation of NMDA receptors in neonatal rat CGNs by glutamate also caused a concentration-dependent increase in glucose uptake which increased from 2 DIV, reaching its maximum by 8 DIV and increases were also seen with kainate and AMPA receptor stimulation (Minervini *et al.*, 1997).

It is perhaps unsurprising that increasing the concentration of exogenous glucose in this study failed to cause any obvious damage due to increased oxidative activity. It has been shown previously in cultured mouse cortical neurones that that rate of glucose oxidation becomes saturated when the extracellular concentration of glucose reaches 1.4mM, with no further rise when this concentration was increased up to 16.7mM in the study (Gorus *et al.*, 1984). Using radio-labelled 2-deoxyglucose in neonatal rat CGNs to study uptake rates, saturation was found to occur at 4mM (Minervini *et al.*, 1997). 2-Deoxyglucose undergoes phosphorylation, the rate-limiting step of glucose utilisation, and therefore makes a good model for this, although it should be noted that its phosphorylation uses ATP rather than generates it (Whitesell *et al.*, 1995).

However, as with the *in vivo* studies, the absence of any obvious increase in cell death does not exclude the possibility of hyperglycaemia (or an *in vitro* equivalent) causing an increased underlying vulnerability to subsequent damage from a neurotoxic stimulus.

4.10.2 Kynurenine pathway compounds

The finding that tryptophan and a number of kynurenine pathway metabolites were more neurotoxic in CGNs maintained in a higher glucose environment raised the question of whether this was due to elevation in glucose during plating and maintenance, or during treatment. To answer this, further studies were carried out: the glucose concentration for cultures plated in 5.5mM glucose was raised to 25mM in treatment medium and vice versa for cultures plated in 25mM glucose. An increased toxicity when the treatment medium contained 25mM glucose, applied to CGNs plated in 5mM glucose was observed, although the disparity was less clear than when using CGNs plated in 25mM glucose, with significance lost for several of the comparisons. This suggests that the potentiated toxicity was mainly mediated by the increased glucose in the treatment medium, although it was still uncertain whether this was due to an osmotic effect or its effects on cellular metabolism.

To answer this, a compound capable of mimicking the osmotic actions of the supplementary D-glucose, but without metabolic effects was required. Mannitol has been previously used (Vincent *et al.*, 2005), although this was not a suitable replacement in our study since it protects against oxidative stress by scavenging hydroxyl radical (Ohkuna *et al.*, 1998). Alternatives included a variety of modified forms of D-glucose, such as L-glucose, 2-deoxyglucose and 3-*O*-methyl-D-glucose, although there were clear indications as to which compound would provide the most suitable model for metabolically inert D-glucose.

Application of D-glucose to cultured CGNs leads to rapid uptake via GLUT1 and GLUT3 receptors (Maher *et al.*, 1994). This D-glucose uptake effect was not mimicked by L-glucose in a study using cerebellar slice cultures (Renkawek *et al.*, 1978). A study of the hyperosmotic stimulation of neuromuscular junction membranes found that the action of D-glucose was mimicked by either 2-deoxyglucose or 3-*O*-methyl-D-glucose, but not by L-glucose (Shimoni *et al.*, 1978). The use of 2-deoxyglucose was unsuitable however, as it undergoes phosphorylation (the first stage of D-glucose metabolism, although it is not metabolised further), the metabolic step that rate-limits the utilisation of D-glucose (Heidenreich *et al.*, 1989). Furthermore, 2-deoxyglucose has been shown to precondition hippocampal neurones against subsequent glutamate treatment (Lee *et al.*, 1999). For both of these reasons, 2-deoxyglucose was considered not to be an appropriate osmotic substitute for D-glucose. 3-*O*-methyl-D-glucose was selected as it is a metabolically inert compound which accurately mimics patterns of D-glucose uptake and retention and hence the osmotic effects of D-glucose (Maher *et al.*, 1996, Whitesell *et al.*, 1995), and has no known anti-oxidative or neuroprotective properties.

The comparison of the neurotoxicity of tryptophan and selected kynurenine pathway compounds in treatment medium supplemented with either 19.5mM D-glucose or 19.5mM 3-*O*-methyl-D-glucose demonstrated no significant difference, indicating that neurotoxicity was not potentiated by metabolism or utilisation of the increased glucose in the treatment medium. Having thus demonstrated a non-metabolic effect, it was concluded that the potentiation was primarily mediated by osmotic effects of the additional D-glucose in treatment medium, although plating and maintenance of CGNs in 25mM glucose contributed slightly.

A further possible effect of the additional glucose was that metabolism of the kynurenine pathway compounds themselves was altered. High-performance liquid chromatography (HPLC) was therefore carried out to study the metabolism of the compounds. It should be noted at this point that analysis of QA and picolinic acid levels would have been highly desirable, but was not possible due to technical limitations regarding which compounds could be accurately assayed using our equipment. The addition of 3-HK and 3-HAA, the toxicity of which had not been potentiated by higher glucose, was used to study whether these compounds were substantially metabolised during a 5 hour exposure (which was the secondary reason for the study of the other compounds by HPLC). No difference in the metabolism of any of the compounds due to the presence of a higher concentration of glucose was observed, nor was there any sign of extensive metabolic breakdown of any of the compounds: although a substantial drop in the concentrations of 3-HK and 3-HAA were seen, these did not alter between 5 and 9 hours, suggesting that this was due to compound instability and breakdown on addition to the culture medium rather than an ongoing metabolic effect. This was consistent with the other experiments in the study and indeed gave reassurance that treatments of 5 hours duration were treatments with the compound applied. The study was therefore sufficient with two sets of samples, as it was unlikely that any further relevant information would be gained from further repeats. A possible explanation for the lack of identifiable metabolism during the time periods studied was the absence of glial cells from the culture preparation, so it is possible that these findings would be at variance with equivalent *in vivo* studies.

Concerning the neurotoxic effects of tryptophan and its metabolites themselves, 3-HK and 3-HAA have been shown to cause a dose-related reduction in cell survival in cultured neurones, but no effect was seen with AA, kynurenine, QA or xanthurenic acid over the same range of concentrations (1-100μM) and time period (48 hours) (Okuda *et al.*, 1998). Our findings for tryptophan, kynurenine, QA, kynurenic acid, anthranilic acid and picolinic acid are considered initially.

Tryptophan produced a neurotoxic effect that was time-dependent but not concentration-dependent and was potentiated by 25mM glucose when applied for 5 hours. High performance liquid chromatography analysis did not reveal any reduction in tryptophan over the course of 1-9 hours, indicating that the toxic

effects were due to tryptophan itself rather than its metabolites. An *in vivo* study of induced hypertryptophanaemia in adult Wistar rats produced plasma tryptophan levels ten times higher than normal and demonstrated that the hypertryptophanaemia increased tryptophan levels in cortical neural tissue one hour after subcutaneous tryptophan injection. This was associated with a reduction in pyruvate kinase activity of ~20%, a finding reproduced *in vitro*, but prevented by co-application of alanine (which alone did not affect pyruvate kinase activity)(Feksa *et al.*, 2003). The question arises of whether the inhibitory effect was due to the tryptophan itself, or to a product of its metabolism, but there was no significant difference in pyruvate kinase inhibition between tissues samples taken 1 hour and 12 hours after tryptophan injection (Feksa *et al.*, 2003).

Pyruvate can reduce neurotoxicity induced by H_2O_2, in addition to an inhibition of glycolysis, in mouse neuroblastoma (N-2A) cells: preincubating cultures with pyruvate at concentrations of 1-10mM for 1 hour prior to addition of H_2O_2 caused a significant reduction in H_2O_2–mediated damage (Mazzio and Soliman, 2003). The inhibition of pyruvate kinase by excess tryptophan may have contributed to the potentiation due to higher glucose concentrations. In the current study, the potentiation was largely due to the higher glucose concentration in treatment medium, but a greater degree of damage was seen when CGNs were plated and maintained in 25mM glucose: the excess tryptophan may therefore have augmented any background oxidative stress, which although not sufficient to cause cell death alone, was more damaging due to suppression of pyruvate kinase.

Kynurenine caused a very similar neurotoxic effect to that seen with tryptophan, with a slight but not significant increase in toxicity over time. There was no significant increase with concentration or notable potentiation due to higher glucose levels when applied for 5 hours. In Huntington's disease patients, increased levels of plasma kynurenine occur (Stoy *et al.*, 2005) and cross the blood-brain barrier using the same neutral amino acid transporter as tryptophan (Fukui *et al.*, 1991, Chiarugi *et al.*, 1996). It is notable that although there was no significant metabolism of kynurenine in our study, other studies using injection of kynurenine into the striatum of adult rats *in vivo*, showed a significant reduction in radio-labelled kynurenine after 4 hours (Guidetti *et al.*,

1995). A slight increase in kynurenic acid was also reported, suggesting the presence of kynurenine aminotransferase, which is known to be present in neonatal rat cerebral cortex (Rzeski *et al.*, 2005).

Establishing whether the neurotoxic effects of kynurenine in CGN cultures could be replicated in mixed neuronal and glial cultures would be an interesting future avenue of study, as kynurenine is known to significantly increase the expression of nerve growth factor (NGF) when applied to cultured mouse astroglial cells at micromolar concentrations (Dong-Ruyl *et al.*, 1998). Also, given the previous findings relating to the metabolism of kynurenine in the striatum *in vivo*, it would be of interest to determine whether the relative lack of kynurenine metabolism seen in our system was due to absence of glial cells or to a regional variation.

Quinolinic acid (QA) produced a time-dependent neurotoxic effect, but again without any concentration-response correlation. Quinolinic acid has long been recognised as a neurotoxin, with injection of QA at concentrations of 20nM or above into rat striatum *in vivo* producing an axon-sparing neurodegenerative lesion, the volume of which increased in proportion to the QA dose applied (Guidetti and Schwarcz, 1999).

Intracerebral injection of 1µl of 34nM QA *in vivo* caused a transient increase in expression of c-Jun N-terminal kinase (JNK) and p38 in the core of the lesion, which were no longer evident at 24 hours, but which correlated with areas of subsequent cell death. TUNEL-positive cells were also identified, although there was no evidence of an increase in active caspase-3 expression (Ferrer *et al.*, 2001). Injection of QA also caused increased expression of mitogen-activated protein kinase (MAPK) in the penumbra of the resultant lesion, with increased MAPK expression associated with subsequent cell survival (Ferrer *et al.*, 2001).

Quinolinic acid neurotoxicity appears to be closely related to its known NMDA receptor agonist action and oxidative stress, with application to rat brain homogenates shown to cause a significant increase in lipid peroxidation, an effect lessened by co-application of kynurenic acid with QA, suggesting the effect was mediated by the NMDA receptor agonist action of QA (Rios and Santamaria, 1991).

A finding comparable to glutamate-induced mitochondrial damage was that QA neurotoxicity in rat hippocampus was significantly reduced by co-administration of the antioxidant melatonin and that QA-induced lipid peroxidation in rat brain homogenates was reduced in a dose-dependant manner by melatonin (Behan *et al.*, 1999). A further link between QA and oxidative damage was evident following co-application of the free radical generator xanthine oxidase, which significantly potentiated QA neurotoxicity in rat hippocampus *in vivo*, but with only minor loss caused by either of the two compounds alone. Notably co-application of kynurenic acid significantly reduced the toxicity of QA alone but not of QA and xanthine oxidase combined (Behan and Stone, 2002).

The co-application of either APV, MK-801, the NOS inhibitor nitroindazole or the poly(ADP-ribose) polymerase (PARP) inhibitor DPQ was effective in significantly reducing damage due to 10μM QA applied for 48 hours, but QA toxicity was not reduced by co-application of cyclosporine and the pan-caspase inhibitor Z-VAD-fmk (Chiarugi *et al.*, 2001). This reconfirms the links with NMDA receptor activation and oxidative stress, but further indicates that the cell death mechanism most likely to be involved in QA neurotoxicity is necrosis rather than apoptosis.

Kynurenic acid caused less toxicity than was seen with the other compounds, with only prolonged exposure times causing damage, particularly in the presence of higher glucose concentrations, where osmotic effects will also contribute. The compound is more noted for possession of neuroprotective properties than neurotoxic ones, with the glutamate receptor antagonist properties of kynurenic acid have been used to protect against a variety of excitotoxic insults. Kynurenic acid protected adult rat dopaminergic subtantia nigra neurones against injection of 60nmoles of QA or 15nmoles of NMDA, with endogenous kynurenic acid generated by administering kynurenine with the kynureninase inhibitor nicotinylalanine, thus ensuring that an increased quantity of the administered kynurenine was converted into kynurenic acid (Miranda *et al.*, 1997). Kynurenic acid was also shown to reduce infarct volume in neonatal rats subjected to left carotid artery occlusion, despite being applied after ischaemia was already of two hours' duration (Andine *et al.*, 1988).

Little has been published with regard to anthranilic acid as a potential neurotoxin, although one study has previously reported damaging effects on cultured insect neurones (Cerstiaens *et al.*, 2003). This was not however reproduced in a study using cultured rat striatal neurones, where no toxicity occurred despite using concentrations up to 100μM and for 48 hours (Okuda *et al.*, 1998). Although this is in contrast to our findings, there was no toxicity seen in the Okuda group's 1998 study using the same concentration range and exposure time with kynurenine or QA either, suggesting that a substantial difference exists between these neurones and CGNs. Anthranilic acid caused neurotoxicity in a time-dependent but not concentration-related manner, with toxicity at 5 hours again potentiated by the use of higher glucose levels.

Picolinic acid also demonstrated time-dependent neurotoxicity with a slight concentration-related effect at 1 hour. Picolinic acid has also been relatively little studied, although it has been linked with cerebral malaria in both clinical and animal studies (Medana *et al.*, 2003, Clark *et al.*, 2005). It is notable that while a significant effect on neuronal viability was not identified with picolinic acid alone, it did reduce QA neurotoxicity, although interestingly it does not affect excitation of neurones, in contrast to the protection given by kynurenic acid against QA (Jhamandas *et al.*, 1990). A possible mechanism is via picolinic acid's known action as a zinc chelator, as this has been shown to protect against excitotoxic and ischaemic damage with other compounds (Jhamandas *et al.*, 1998).

This was also demonstrated in an *in vivo* study of the effect of QA on NADPH diaphorase-containing rat striatal neurones, where picolinic acid infusion protected the neurones against an otherwise neurotoxic dose of QA, while picolinic acid alone did not affect neuronal viability (Kalisch *et al.*, 1994).

The discovery of a significant switch over in the ratio of anthranilic acid to 3-HAA in patients suffering from stroke, with an increased anthranilic acid to 3-HAA, raised the question of what role this finding may play in the generation of the associated pathology (Darlington *et al.*, 2007). To investigate this question, a series of combinations of anthranilic acid and 3-HAA were applied to CGNs for 5 hours at 9 DIV, to examine whether this caused any significant alterations in neurotoxicity.

No protection was evident by an increased ratio of anthranilic acid to 3-HAA with a 3-HAA concentration range of 100nM to 10μM and with anthranilic acid concentrations ranging from 100nM to 100μM. There was a slight potentiation in toxicity, although this was predictable given the toxicity of anthranilic acid applications for 5 hours. This experiment was also performed in cultures plated and maintained in medium containing 25mM glucose, although results were the same as those found using 5.5mM glucose.

4.10.3 Oxidative stress generation by kynurenine pathway compounds

Treatment with 10μM-1mM 3-HK, 3-HAA or 5-HAA over 1 to 9 hours caused a time- and concentration-dependent neurotoxic effect. A previous study in cultured striatal neurones showed that an accumulation of intracellular peroxides and a significant reduction in viability resulted from application of 1μM 3-HK 24 or 48 hours (Okuda *et al.*, 1996). Co-application of catalase prevented peroxide accumulation and toxicity from 1-100μM 3-HK, but SOD had no protective effect; the iron chelating agent desferrioxamine reduced 3-HK toxicity in a concentration-dependent fashion. Allopurinol pre-treatment for 24 hours was highly protective against 10μM 3-HK but was less effective against higher concentrations (Okuda *et al.*, 1996).

It has also been shown that 3-HK uptake was by large amino acid transporters in striatal neurones, as co-application of neutral amino acids or blockade of the sodium-dependant neutral amino acid uptake prevented 3-HK neurotoxicity. A dose-dependant reduction in tryptophan uptake occurred following 3-NK treatments, an effect not seen with 3-HAA, which is probably not taken up by the transporter (Okuda *et al.*, 1998).

3-Hydroxykynurenine in striatal neurones caused death with features of apoptosis, with cycloheximide or actinomycin-D almost entirely preventing neuronal death (Okuda *et al.*, 1998). The neurotoxic effect involved generation of ROS. A range of antioxidants (ascorbic acid, 2,3,5,5-tetramethyl-pyridine-*N*-oxide(TMPO), α-tocopherol, trolox) prevented neurotoxicity induced by 3-HK at 1 and 10μM, although not 100μM and *N*-acetylcysteine was effective against all three concentrations: *N*-acetylcysteine is an effective scavenger of the hydroxyl

radical and to a lesser extent of hydrogen peroxide, but a poor scavenger of superoxide (Okuda *et al.*, 1998).

However, CGNs have been shown to be vulnerable to 3-HK, although less severely than striatal neurones, and with different characteristics to those identified by the Okuda group. As in striatal neurones and osteoblast cells (Fatokun *et al.*, 2008b), co-application of catalase significantly reduced the neurotoxicity of 3-HK, whereas SOD co-application increased death; co-application of SOD and catalase had the same effect as catalase alone. Although 3-HK was shown to reduce tryptophan uptake through the neutral amino acid transporter, blockade of this transporter was not protective in CGNs, nor was there any protective effect seen with the pre-treatment of the cultures with xanthine oxidase inhibitors (Wei *et al.*, 2000). Additionally, NMDA antagonists or the neurotrophic factors BDNF, neurotrophin-3 or neurotrophin-4 did not provide protection (Wei *et al.*, 2000).

3-Hydroxykynurenine, 3-HAA and 5-HAA were all capable of generating a concentration- and time-dependent neurotoxic effect, and therefore warranted investigation of the mechanisms involved. It has previously been shown that 3-HK and 3-HAA are both capable of generating the ROS H_2O_2 and superoxide when added to phosphate buffer solution (Goldstein *et al.*, 2000).

Catalase caused a significant reduction in the neurotoxic effects of all three compounds, with a similar reduction in cell death for each. Superoxide dismutase failed to provide any protection, although neither was further cell death induced. Co-application of denatured superoxide and denatured catalase did not alter the toxicity of any of these compounds.

Desferrioxamine has been used as a chelator of Fe^{2+} ions in a previous study of where addition of 1-100μM desferrioxamine provided significant dose-related protection to culture striatal neurones treated with 10μM 3-HK 48 hours (Okuda *et al.*, 1996). Our initial trials using desferrioxamine (over the same concentration range) against 3-HK, 3-HAA and 5-HAA for 5 hours at 9 DIV did not produce a protective effect, hence the concentrations and exposure times of the previous study were replicated. Even under these circumstances however, there was no protection induced by desferrioxamine over a concentration range of 1-100μM in our work.

It is perhaps not entirely surprising that desferrioxamine failed to protect against oxidative damage induced by 3-HK or 3-HAA, as it has been previously shown that the compounds can generate ROS alone. The chemical actions of 3-HK and 3-HAA generate H_2O_2 and superoxide: either 3-HK or 3-HAA caused reduction of Cu^{2+} to Cu^{+}, and of Fe^{3+} to Fe^{2+}, in an environment with a physiological pH (Goldstein *et al.*, 2000). These effects were not replicated by tryptophan, kynurenine, kynurenic acid, anthranilic acid, QA, nicotinic acid or xanthurenic acid, although xanthurenic acid caused reduction of Cu^{2+} to Cu^{+} only (Goldstein *et al.*, 2000).

A further aspect of the neurotoxicity induced by these three compounds of interest was whether or not the cell death they produced was dependent on protein synthesis. The levels of toxicity during treatments with the compounds for 5 hours at 9 DIV were not altered by addition of 0.05µg/ml cycloheximide, which would suggest that apoptotic mechanisms triggered by neuronal production of death proteins were not the major cause of cell death in CGNs. This was pursued folowing the findings of a previous study using striatal neurones, where chromatin condensation and protein synthesis were shown to be involved in cell death following 3-HK exposure (Okuda *et al.*, 1996), although the responses of different neuronal types are not always consistent and indeed variations between striatal neurones and CGNs have been noted (Okuda *et al.*, 1998). Glutamate toxicity in CGNs has been shown not to be associated with DNA fragmentation (Dessi *et al.*, 1993), although it was present in PC12 cells, again highlighting different responses to excitotoxicity between cell types.

The finding that the neurotoxic effects of 3-HK, 3-HAA and 5-HAA are not primarily mediated through the action of superoxide is of interest when considering the possible cell death mechanisms involved. It has been demonstrated using neonatal rat CGNs that production of superoxide and molecular oxygen were associated with chromatin condensation and activation of caspases 3, 8 and 9, indicating apoptosis. In contrast, production of hydrogen peroxide caused no increase in any of these markers, while still producing comparable levels of cell death, suggesting a necrotic mechanism (Valencia and Morán, 2004).

Western blotting of protein extracted from CGNs subjected to 100μM 3-HK or 100μM 5-HAA for 0.5 to 24 hours showed no increase in expression of activated caspase-3 in the present study. However, increases in phosphorylation of p38 MAPK following both 3-HK and 5-HAA treatments were also observed. Phosphorylation of p38 MAPK has been reported in neurones exposed to glutamate or QA (Ferrer *et al.*, 2001, Kawasaki *et al.*, 1997), linking this signalling molecule and neuronal cell death induced by excitotoxic or oxidative stress stimuli. The current evidence of phosphorylation of this molecule by 3-HK and 5-HAA further strengthens this association.

Application of 250μM 3-HK to human neuroblastoma SK-N-SH cells caused a significant increase in ERK1/2 phosphorylation between 0.5 and 2 hours' exposure, returning to normal after 3 and 6 hours. Co-application of the ERK pathway inhibitor PD98059 caused a significant increase in cell death (Lee *et al.*, 2004). 3-Hydroxykynurenine caused a progressive loss of mitochondrial membrane potential over 3-12 hours, with release of cytochrome *c* from the mitochondrial matrix and associated activation of caspase-9 and activity of caspase-3: these effects were also exacerbated by PD98059 (Lee *et al.*, 2004).

In summary, it is clear that the metabolism of tryptophan causes the formation of a number of potentially significant neurotoxins, and that three of these (3-HK, 3-HAA and 5-HAA) are capable of inducing extensive oxidative damage. The damage thus caused involves activation of cell death pathways, but does not depend on apoptotic processes to induce cell death.

5 Preconditioning

5.1 Introduction

Having established the suitability of our culture system for models of excitotoxic and oxidative neuronal damage, it was of interest to investigate the protection which could be provided against this damage by preconditioning. Initially, a relatively brief preconditioning period with a toxic insult applied 24 hours later was examined. Later work was concerned with investigating the protection provided by preconditioning neurones for a considerably longer period, with a toxic insult again applied 24 hours subsequent to preconditioning.

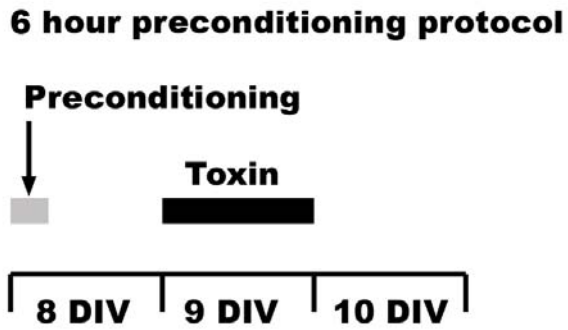

Figure 5.1 Diagram representing protocol used for preconditioning with NMDA, 3-NPA and H_2O_2 at 8 DIV.

The brief preconditioning regimen consisted of 6 hours treatment with NMDA (added to culture medium), after which medium was aspirated and replaced with fresh medium for 18 hours, then medium containing the toxic compound was applied for 24 hours. This model formed the basis for all studies using a brief period of preconditioning with NMDA, 3-NPA or H_2O_2.

A small number of studies involved preconditioning at 12 DIV: in these experiments the same durations of treatment, recovery and toxin application were used, with the protocol commencing at 12 DIV instead of 8 DIV. In studies with shorter preconditioning treatments, the relevant preconditioning periods commenced at the same point as their equivalents in the 6 hour preconditioning studies.

The choice of 8 DIV and the 6 hour period of preconditioning were based on extensive review of the previously published NMDA preconditioning protocols and represented the times most likely to be successful with CGN cultures (Chuang *et al.*, 1992, Damschroder-Williams *et al.*, 1998, Lipsky *et al.*, 2001). Some difficulties were encountered in extending the range of insults for which protection by NMDA preconditioning was effective, therefore the alternative of preconditioning at 12 DIV was investigated. Two alternative stimuli, 3-NPA and H_2O_2, were also tested, as these have been previously shown to precondition neurones against subsequent neurotoxic damage (Weih *et al.*, 1999, Tang *et al.*, 2005a).

The preconditioning protocol for 3-NPA preconditioning was essentially the same as with NMDA; however the toxicity of H_2O_2, even at very low doses, necessitated a much shorter period of preconditioning (5-15 minutes) (Fatokun *et al.*, 2007).

An alternative method, previously successful for cultures of both hippocampal and cerebral cortical neurones using the $GABA_A$ receptor antagonist bicuculline, supplemented by the potassium channel blocker 4-aminopyridine (4-AP), to provide protection by preconditioning neurones for a longer period (24-48 hours) (Papadia *et al.*, 2005, Tauskela *et al.*, 2008) was investigated.

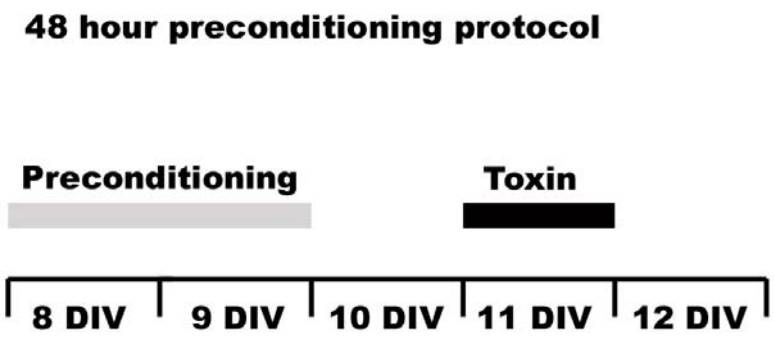

Figure 5.2 Diagram representing protocol used for preconditioning with 4-aminopyridine and bicuculline at 8-10 DIV.

The initial experiments with this protocol in our system failed to protect when using bicuculline alone, although the protection induced by 4-AP (in either the presence or absence of bicuculline) was highly effective and was investigated further.

The methods used for 48 hour preconditioning experiments were similar to those in earlier preconditioning studies, with 4-AP (with or without bicuculline) added to medium and left to act over 48 hours. The medium was then aspirated and replaced by fresh medium for 24 hours before switching to medium containing the toxin, or to the OGD buffer.

5.2 Aims and Objectives

- Establishment of effective protocol for preconditioning with NMDA against glutamate based on findings from previous studies

- Investigating efficacy of this protocol in protecting against alternative methods of neurotoxic damage

- Replicate protection achieved with NMDA preconditioning in cerebral cortical neurone cultures

- Study of effectiveness of 3-NPA in preconditioning against neurotoxic insults

- Investigation of effectiveness of H_2O_2 in preconditioning against neurotoxic insults

- Establishment of successful preconditioning protocol based on prolonged stimulation with bicuculline and 4-AP

- Investigation of efficacy of this protocol in protecting against various methods of neurotoxic damage

- Investigation of mechanisms of action involved in prolonged preconditioning model using both pharmacological and molecular techniques

5.3 Preconditioning with *N*-methyl-D-aspartate

5.3.1 NMDA preconditioning protects against glutamate toxicity

The use of NMDA to precondition at a moderately high concentration (100μM) for 6 hours at 8 DIV provided a significant degree of protection against a range of concentrations of glutamate applied 24 hours subsequent to commencement of the preconditioning stimulus (Figure 5.3). Additionally, when the preconditioning stimulus alone was applied (i.e. without any subsequent toxic insult) there was no loss of viability detected; indeed the stimulus seemed to cause a mild (although not significant) trophic effect (Figure 5.3).

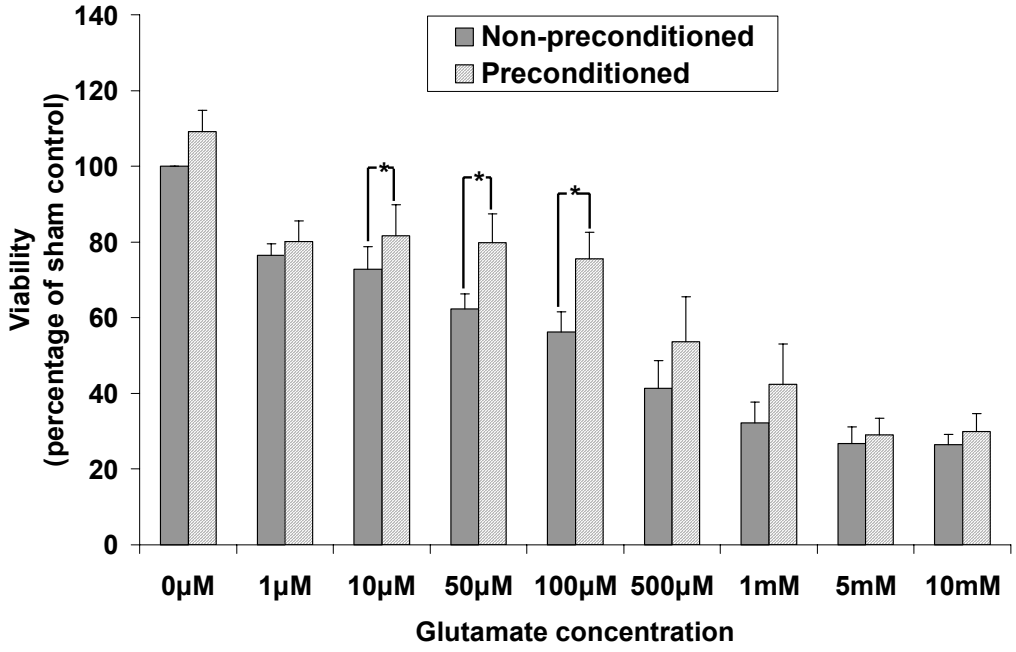

Figure 5.3 Effect of preconditioning with 100μM NMDA for 6 hours at 8 DIV on toxicity of 100μM glutamate for 24 hours at 9 DIV. Mean +/- SEM, n=5; Student's t-test comparing preconditioned and non-preconditioned groups, * $p<0.05$. Effective preconditioning was induced by NMDA against the toxicity of 10-100μM glutamate.

5.3.2 NMDA preconditioning protects against 3-nitropropionic acid toxicity

Further to previous findings demonstrating protection against glutamate, it was also established that preconditioning with NMDA for 6 hours at 8 DIV provided a significant degree of protection against subsequent application of a range of concentrations of 3-NPA (notably, significant protection against 3-NPA was effective over a wider range of concentrations of the toxin) (Figure 5.4). Again the preconditioning stimulus itself had no evident detrimental result, causing a slight (but again not significant) trophic effect (Figure 5.4).

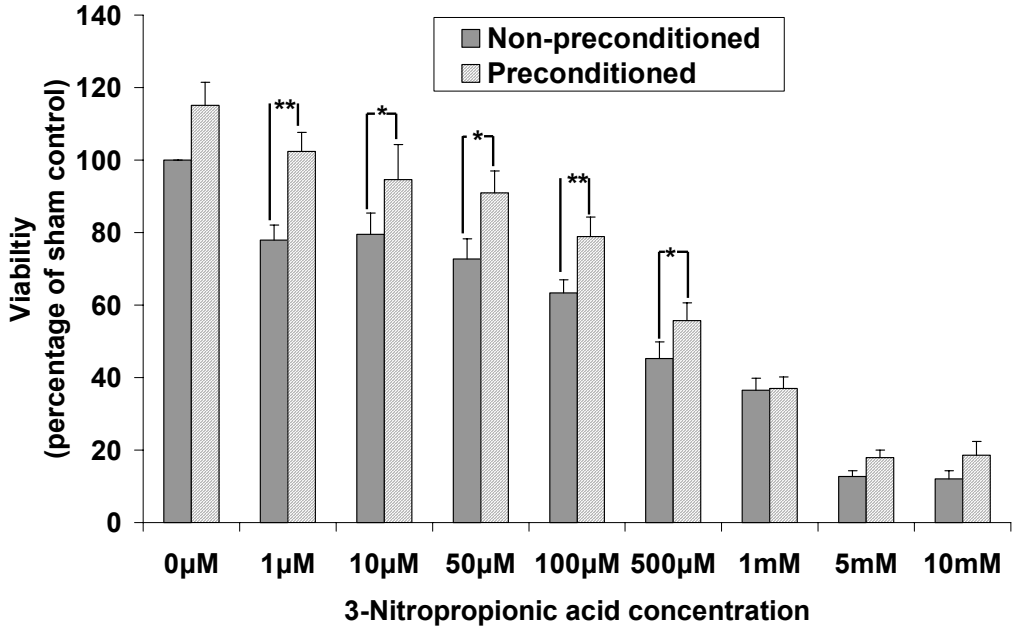

Figure 5.4 Effect of preconditioning with 100μM NMDA for 6 hours at 8 DIV on toxicity of 100μM 3-NPA for 24 hours at 9 DIV. Mean +/- SEM, n=5; Student's t-test comparing preconditioned and non-preconditioned groups, * p<0.05, ** p<0.01. Effective preconditioning was induced by NMDA against the toxicity of 1-500μM 3-NPA.

The protective effect of NMDA at a moderately high dose (100μM) for 6 hours at 8 DIV against both glutamate and 3-NPA was identified in viability assay readings, and confirmed by the morphological observations of preconditioned cultures, compared to positive controls (Figure 5.5). Furthermore, study of CGN morphology, again showed no evidence of notable damage due to the preconditioning stimulus.

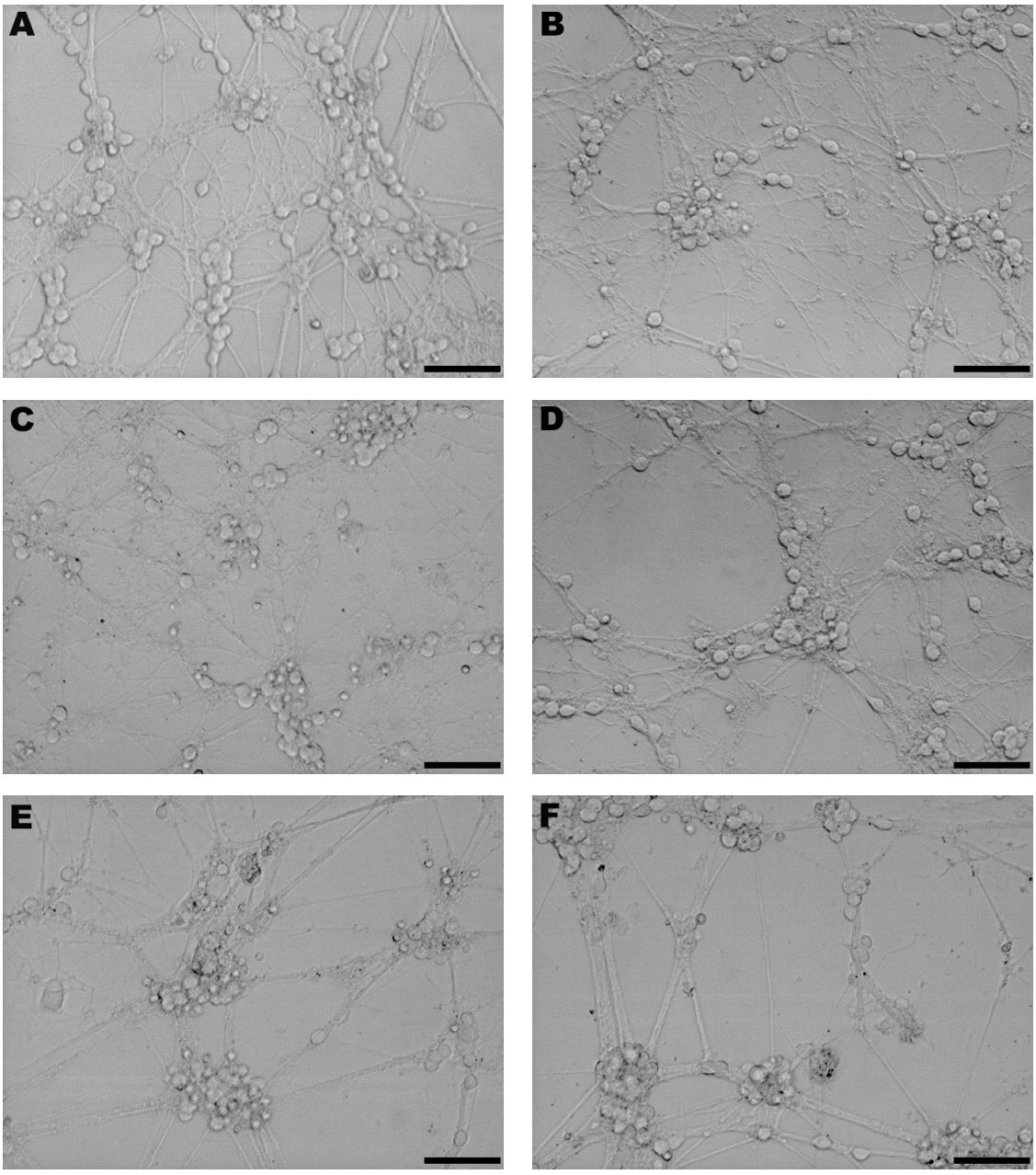

Figure 5.5 Phase contrast microscopic images of CGNs at 10 DIV: untreated control (A), effect of preconditioning with 100μM NMDA for 6 hours at 8 DIV without subsequent toxic treatment (B), following exposure to 100μM glutamate (C) or 100μM 3-NPA (E) for 24 hours at 9 DIV. Also shown: cultures preconditioned with 100μM NMDA prior to exposure to 100μM glutamate (D) or 100μM 3-NPA (F) for 24 hours at 9 DIV. Bars = 50μm. Preconditioning with NMDA did not cause any morphological changes, and was protective against the damage caused by treatment with either glutamate or 3-NPA.

5.3.3 NMDA preconditioning against hypoxia

The ability of NMDA preconditioning to protect against other aspects of ischaemia was also investigated. Initial experiments involved hypoxia alone due to difficulty in developing a buffer which was non-toxic to CGNs (Figure 5.6a, b).

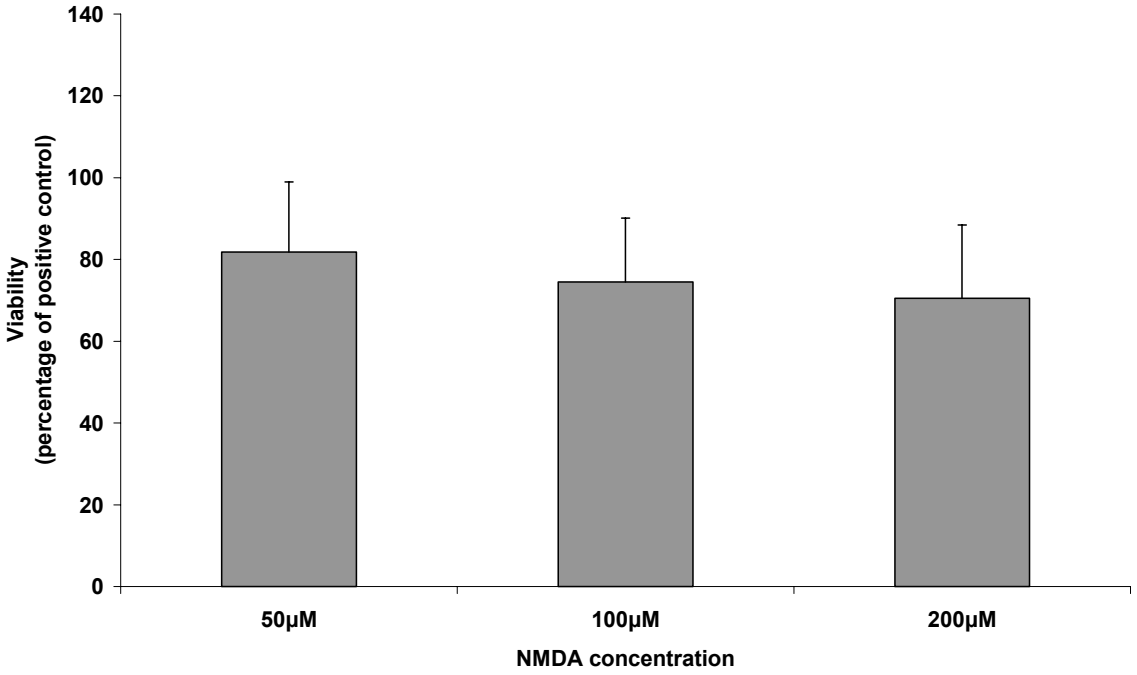

Figure 5.6a Effect of preconditioning with 50-200µM NMDA for 6 hours at 8 DIV on toxicity of hypoxia for 1 hour at 9 DIV. Mean +/- SEM, n=5; ANOVA followed by Tukey's test identified no significant protection by NDMA at any concentration.

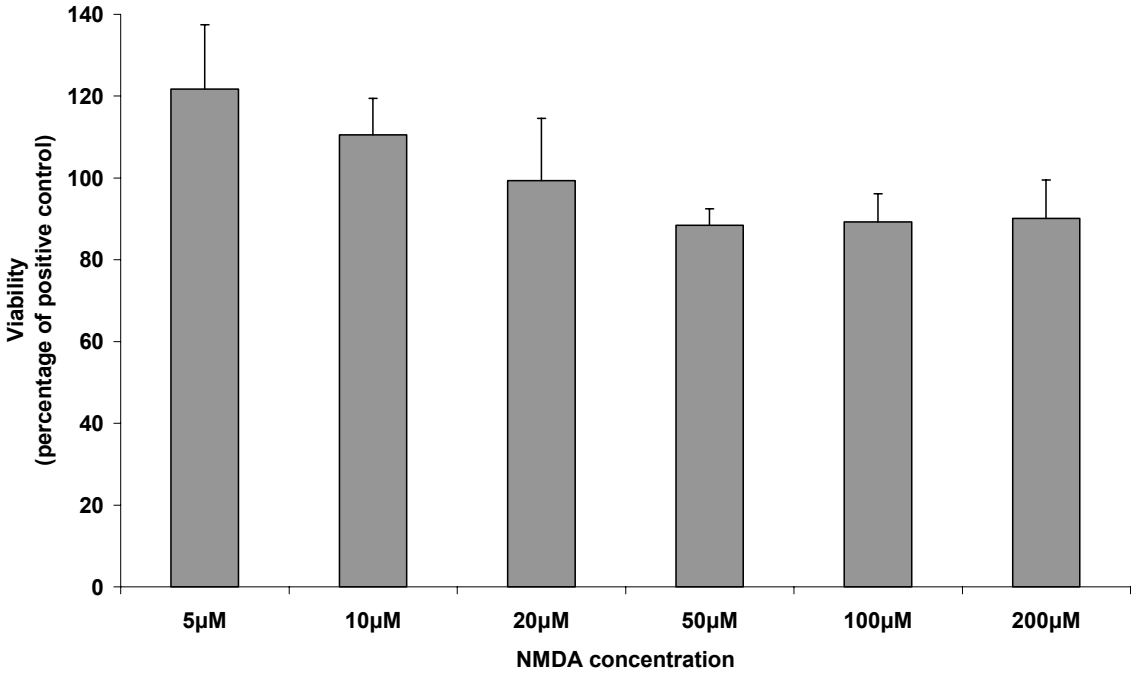

Figure 5.6b Effect of preconditioning with 5-200µM NMDA for 6 hours at 12 DIV on toxicity of hypoxia for 2 hours at 13 DIV. Mean +/- SEM, n=4-6; ANOVA followed by Tukey's test identified no significant protection by NMDA at any concentration.

5.3.4 NMDA preconditioning against OGD

Once a suitable buffer had been identified, the representative model combining oxygen and glucose deprivation simultaneously was used. *N*-methyl-D-aspartate preconditioning from 10-200μM was not effective against toxicity due to hypoxia in cultures of any of the ages used, nor was any protection seen against oxygen-glucose deprivation (Figure 5.7), which was consistent with the findings that NMDA did not protect against hypoxia at either 8 or 12 DIV (Figure 5.6a, 5.6b).

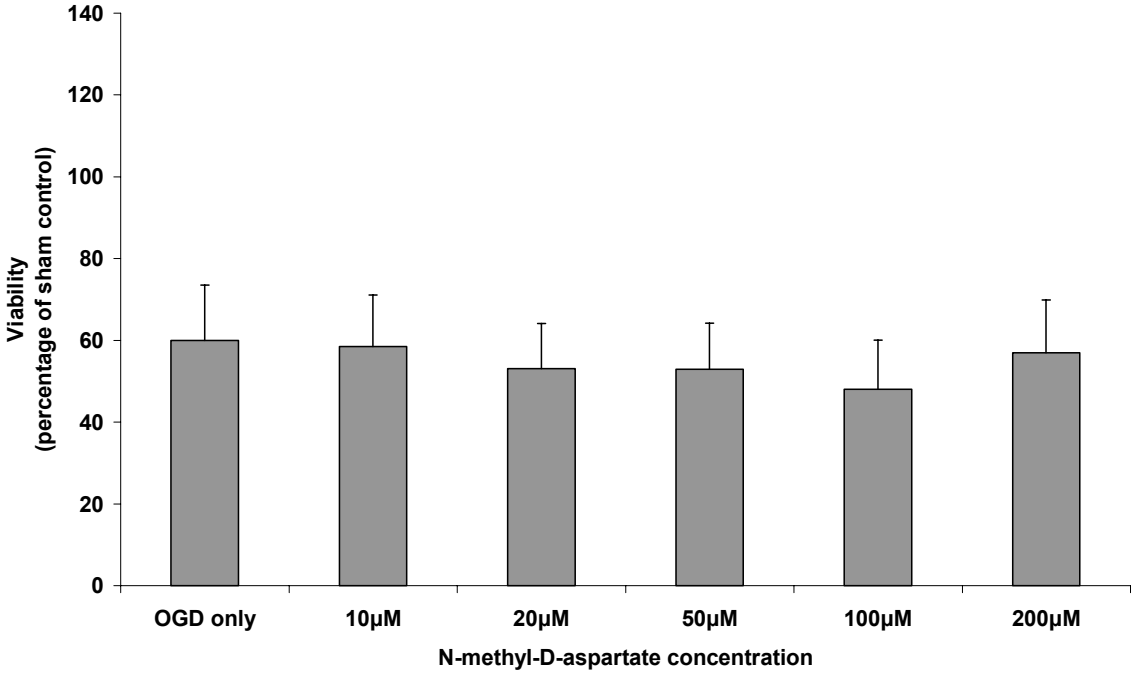

Figure 5.7 Effect of preconditioning with 10- 200μM NMDA for 6 hours at 8 DIV on toxicity of 4 hours OGD at 9 DIV. Mean +/- SEM, n=5; ANOVA followed by Tukey's test identified no significant protection by any concentration of NMDA against the toxicity of OGD for 4 hours.

5.4 Preconditioning with hydrogen peroxide and 3-nitropropionic acid

5.4.1 Hydrogen peroxide preconditioning against hypoxia

An investigation of preconditioning against hypoxia at 12 DIV was also attempted using a low concentration of H_2O_2 as a potential preconditioning stimulus. As with the lower concentrations of NMDA used prior to hypoxia (Figure 5.6b), there was a slight, but non-significant increase in viability relative to positive controls; although even this was lost if either the concentration or preconditioning period were increased (Figure 5.8).

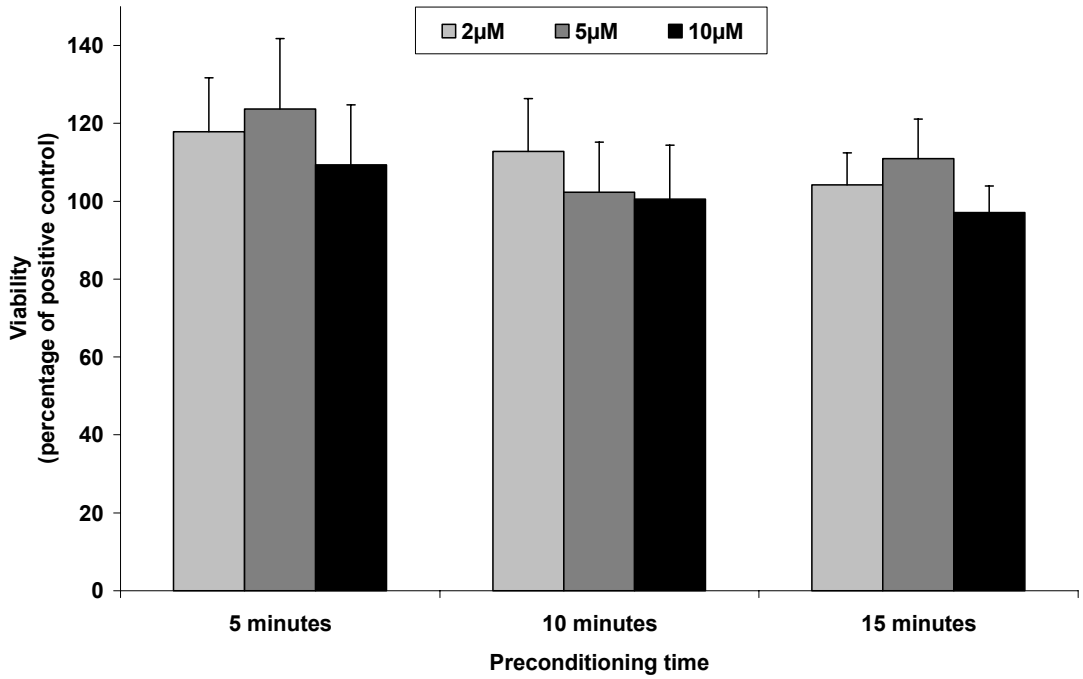

Figure 5.8 Effect of preconditioning with 2-10µM H_2O_2 for 5-15 minutes at 12 DIV on toxicity of 2 hours hypoxia at 13 DIV. Mean +/- SEM, n=5; ANOVA followed by Tukey's test identified no significant protection by 2-10µM H_2O_2, all applied for 5-15 minutes, against hypoxia for 2 hours.

5.4.2 3-Nitropropionic acid preconditioning against glutamate and NMDA

Although 3-NPA had been successfully used to precondition by others (Weih *et al.*, 1999), we were unable to provide protection against 100μM glutamate (Figure 5.9a) or 300μM NMDA (Figure 5.9b) despite using a range of concentrations of 3-NPA.

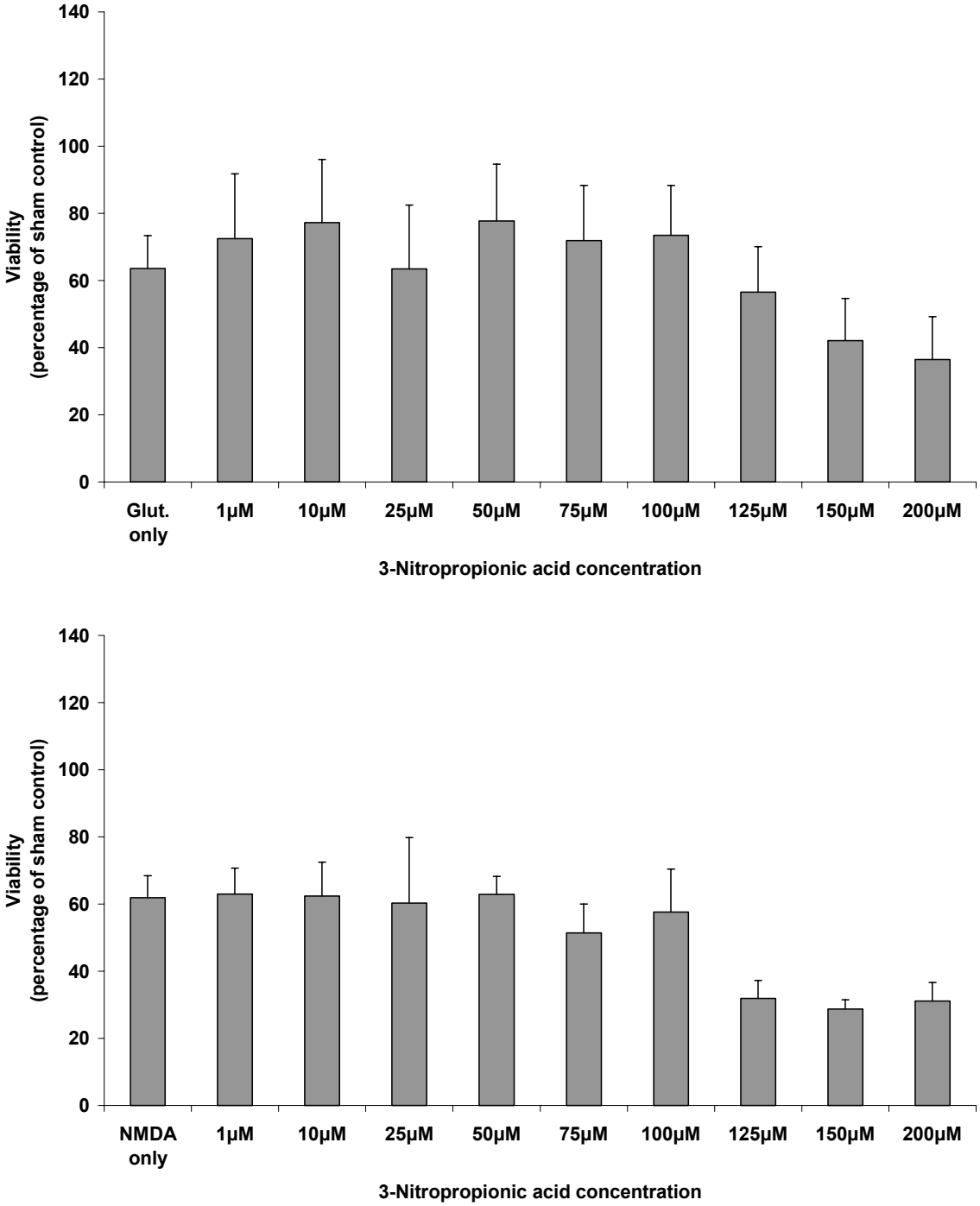

Figure 5.9 Effect of preconditioning with 3-NPA for 6 hours at 8 DIV on toxicity of a) 100μM glutamate or b) 300μM NMDA applied for 1 hour in HBSS buffer at 9 DIV. Mean +/- SEM, n=5; ANOVA followed by Tukey's test identified no significant protection from 3-NPA preconditioning at any of the concentrations trialled, against subsequent treatment with either glutamate or NMDA.

5.5 48-hour preconditioning with 4-aminopyridine and bicuculline

Although preconditioning using 100μM NMDA for 6 hours at 8 DIV had provided successful protection against glutamate and 3-NPA, this failed to protect against either hypoxia or OGD. Additionally, the uses of alternative preconditioning regimens using H_2O_2 or 3-NPA were less successful, with a considerable degree of variation in response from one experiment to the next.

Following communication with Dr. Joseph Tauskela, who has developed a method of protection against neurotoxic insults by stimulating neurones with bicuculline and 4-AP for extended periods of time (24 to 48 hours) (Tauskela *et al.*, 2008), a similar protocol was adopted, capable of effectively preconditioning CGNs against several neurotoxic insults.

We initially established that the protocol was effective against subsequent glutamate application (Figures 5.10, 5.11, and then investigated whether the protection was dependent on neuronal electrical activity, NMDA receptor stimulation or calcium channel opening. Therefore the protocol was tried in the presence of the sodium channel blocker tetrodotoxin (TTX), the NMDA receptor antagonist MK-801 or the calcium channel blocker nifedipine (Figures 5.12, 5.13, 5.14, 5.15, Table 5.2). In order to explore the effectiveness of this protective mechanism against a range of alternative toxic insults, several alternative methods of producing neurotoxicity were used, specifically: NMDA (Figures 5.16, 5.17, 5.18, 5.19, 5.20, 5.21), 3-NPA (Figures 5.22, 5.23) and OGD (Figures 5.24, 5.25).

The possible molecular mechanisms underlying this protection were also studied, with CREB phosphorylation (Figure 5.30, 5.31), bcl-2 expression (Figure 5.32, 5.33) and caspase-3 activation (Figure 5.34, 5.35) examined by Western blotting.

It was found that preconditioning with 2500μM 4-AP for 48 hours gave complete protection against the toxicity of 50μM glutamate, 300μM NMDA or 50μM 3-NPA, although was unable to protect against the damage induced by 5 hours OGD. Co-application of bicuculline did not improve the protection, and in fact was detrimental to it.

The use of TTX during preconditioning caused a reduction in 4-AP protection, with the protection afforded by preconditioning with 50μM 4-AP against 50μM glutamate eliminated entirely, and the protection given by 2500μM 4-AP reduced notably. This indicated that the generation of neuronal excitation is a key component of this mechanism of protection.

Co-application of the NMDA receptor antagonist MK-801 during preconditioning did not reduce precontiioning, indicating that activation of these receptors is not required for the establishment of this protection. Although MK-801 'preconditioning' itself did not provide significant protection against glutamate, there was significant protection given against NMDA treatment, although the protection given by 4-AP (at all concentrations) was still far greater. Another interesting effect of co-applying MK-801 was that the detrimental effect on 4-AP preconditioning induced by bicuculline co-treatment was eliminated, indicating that this damaging effect involved NMDA receptor stimulation.

In order to establish whether calcium influx via voltage-gated calcium channels was involved in 4-AP protection, the L-type calcium channel antagonist nifedipine was co-applied also. Unfortunately, the use of nifedipine for 48 hours was highly toxic in itself, preventing any useful information being gained from this part of the study.

The examination of CREB phosphorylation, bcl-2 expression and activation of caspase-3 by Western blotting found that although CREB phosphorylation appeared raised by 4-AP preconditioning relative to untreated controls, this effect was not statistically significant when analysed by quantification. There was no alteration in bcl-2 expression by either 4-AP of glutamate treatments, suggesting that this protein is not the mechanism by which 4-PA protection acted in this study. Activation of caspase-3 was not significantly altered by 4-AP treatment or glutamate application relative to negative controls.

5.5.1 48-hour preconditioning against glutamate

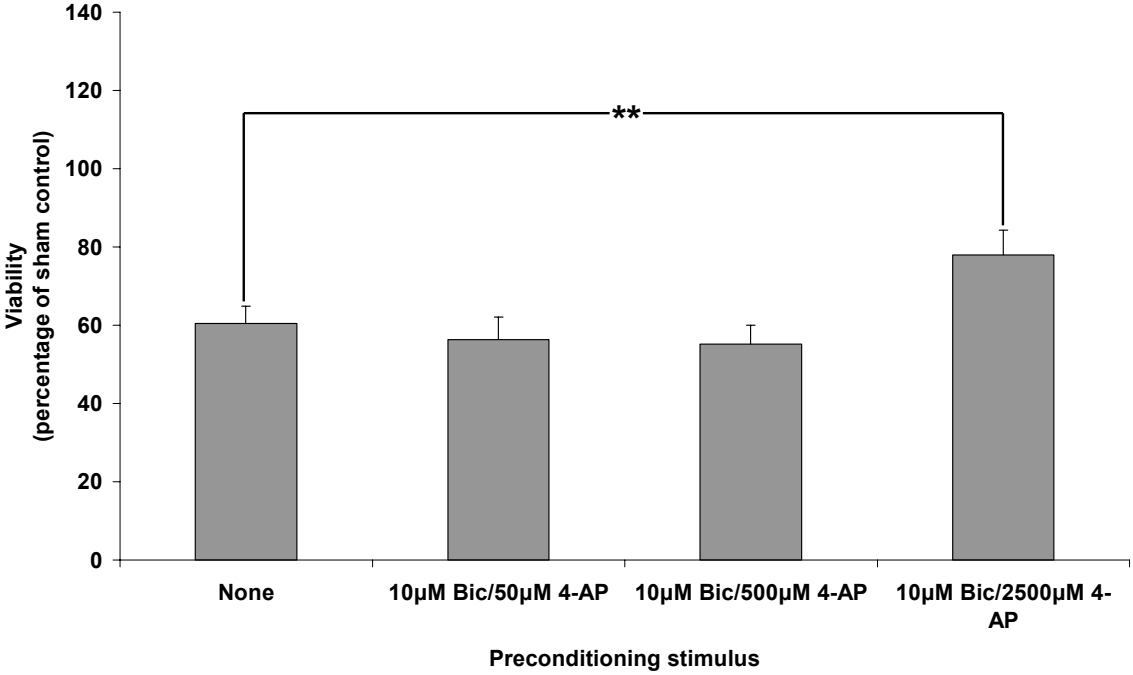

Figure 5.10 Effect of preconditioning with 10μM bicuculline (Bic) and 50-2500μM 4-AP for 48 hours at 8-10 DIV on toxicity of 50μM glutamate applied for 24 hours at 11 DIV. Mean +/- SEM, n=5; ANOVA followed by Tukey's test, ** p<0.01. Bicuculline and 2500μM 4-AP co-treatment was protective against glutamate toxicity.

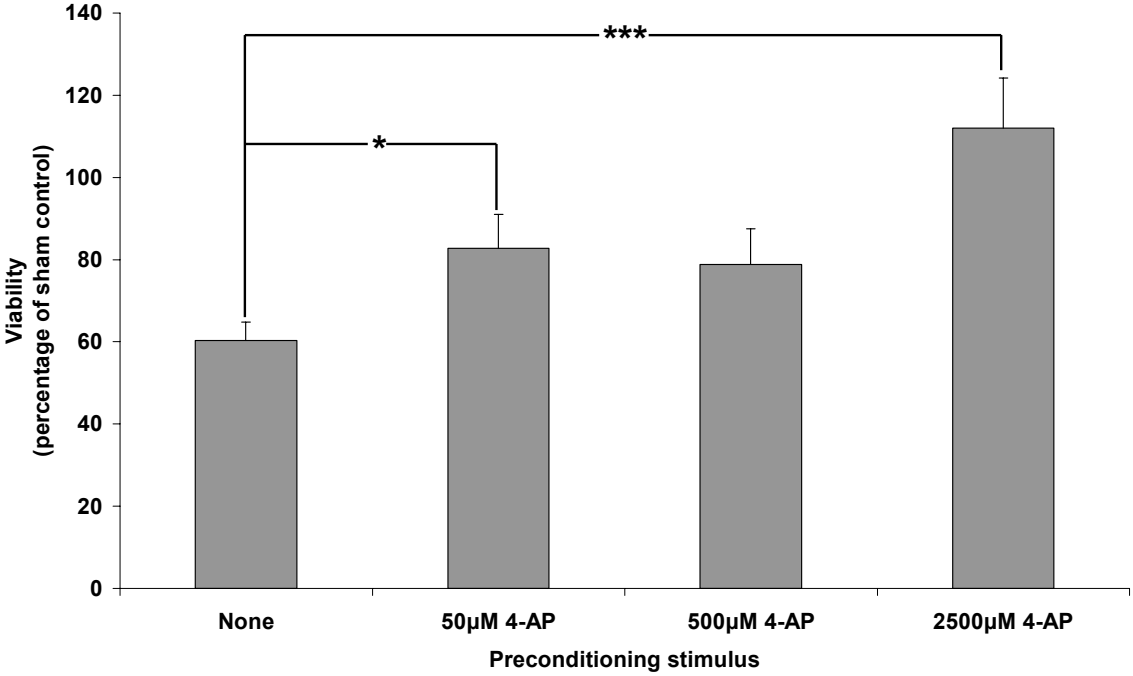

Figure 5.11 Effect of preconditioning with 50-2500μM 4-AP for 48 hours at 8-10 DIV on toxicity of 50μM glutamate applied for 24 hours at 11 DIV. Mean +/- SEM, n=5; ANOVA followed by Tukey's test, * p<0.05, *** p<0.001. Preconditioning with 50 or 2500μM 4-AP was protective against glutamate toxicity.

5.5.2 48-hour preconditioning (with TTX) against glutamate

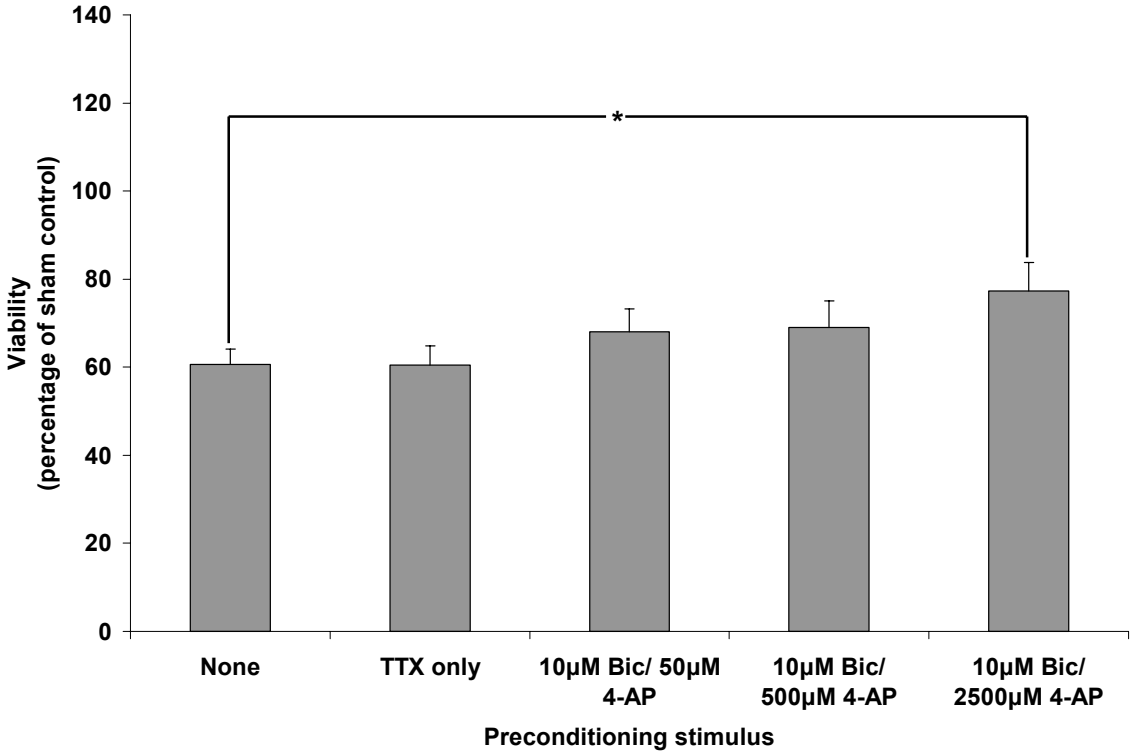

Figure 5.12 Effect of preconditioning with 10μM bicuculline and 50-2500μM 4-AP in the presence of 1μM TTX for 48 hours at 8-10 DIV on toxicity of 50μM glutamate applied for 24 hours at 11 DIV. Mean +/- SEM, n=5; ANOVA followed by Tukey's test, * p<0.05. Co-application of TTX reduced the protection provided by preconditioning with bicuculline and 2500μM 4-AP, although this still provided significant protection.

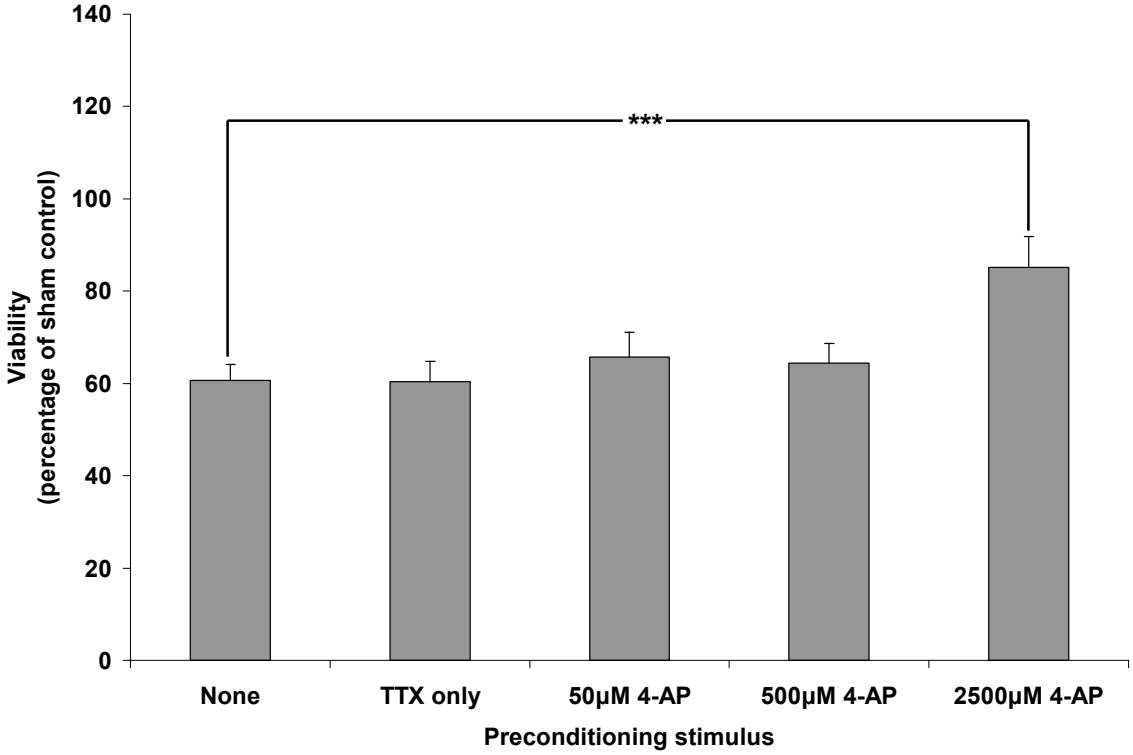

Figure 5.13 Effect of preconditioning with 50-2500μM 4-AP in the presence of 1μM TTX for 48 hours at 8-10 DIV on toxicity of 50μM glutamate applied for 24 hours at 11 DIV. Mean +/- SEM, n=5; ANOVA followed by Tukey's test, *** p<0.001. Co-application of TTX reduced the protection provided by preconditioning with 2500μM 4-AP, although this still provided significant protection; protection due to 50μM 4-AP was lost by TTX co-treatment.

5.5.3 48-hour preconditioning (with MK-801) against glutamate

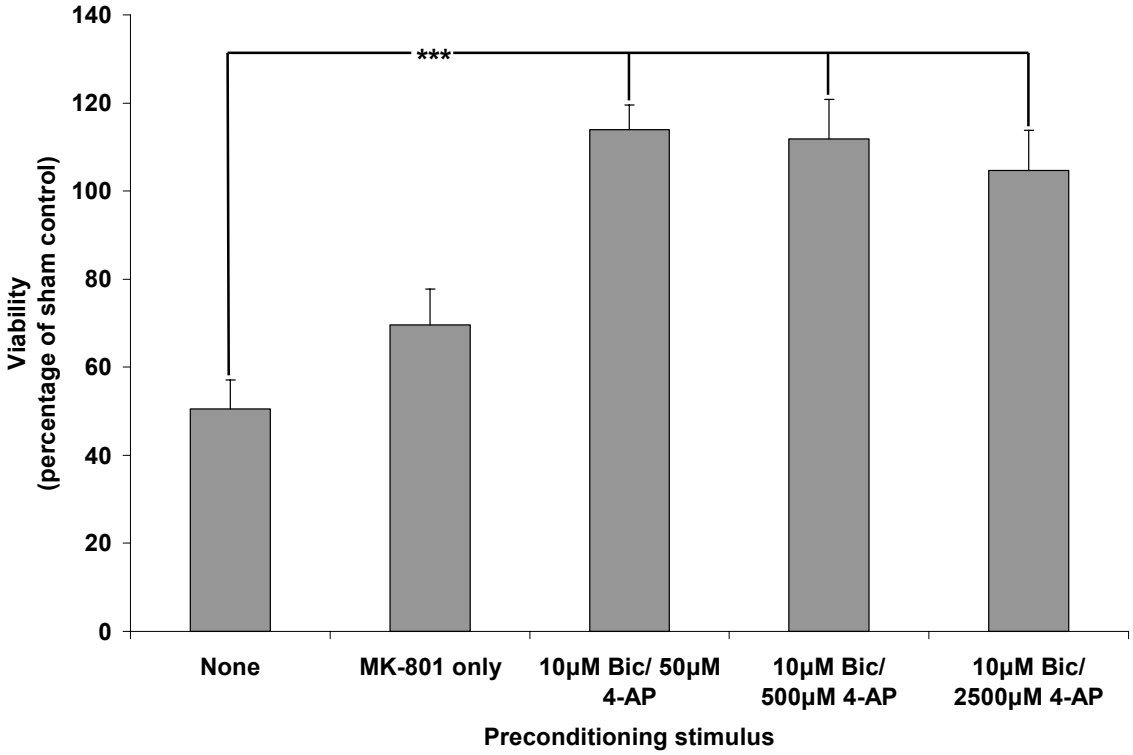

Figure 5.14 Effect of preconditioning with 10μM bicuculline and 50-2500μM 4-AP in the presence of 1μM MK-801 for 48 hours at 8-10 DIV on toxicity of 50μM glutamate applied for 24 hours at 11 DIV. Mean +/- SEM, n=5; ANOVA followed by Tukey's test, *** p<0.001. Co-application of MK-801 with bicuculline/4-AP preconditioning caused a potentiation in the protective effect.

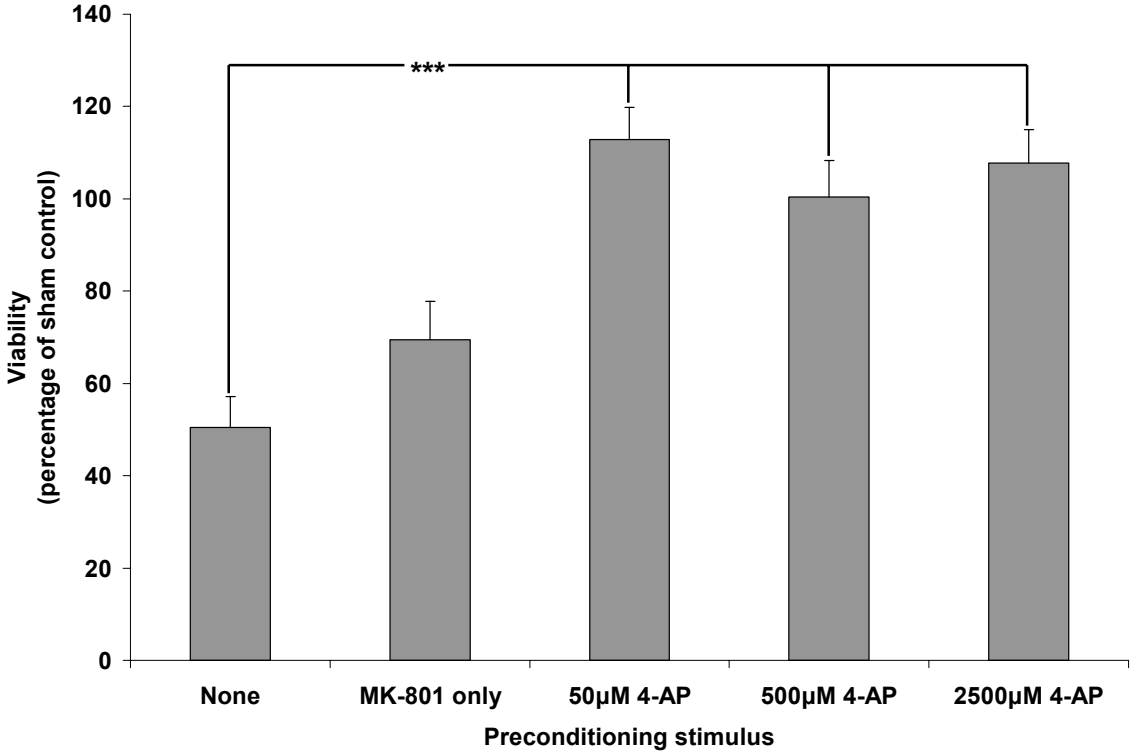

Figure 5.15 Effect of preconditioning with 50-2500μM 4AP in the presence of 1μM MK-801 for 48 hours at 8-10 DIV on toxicity of 50μM glutamate applied for 24 hours at 11 DIV. Mean +/- SEM, n=5; ANOVA followed by Tukey's test, *** p<0.001. Co-application of MK-801 with 4-AP preconditioning caused a potentiation in the protective effect.

5.5.4 48-hour preconditioning against NMDA

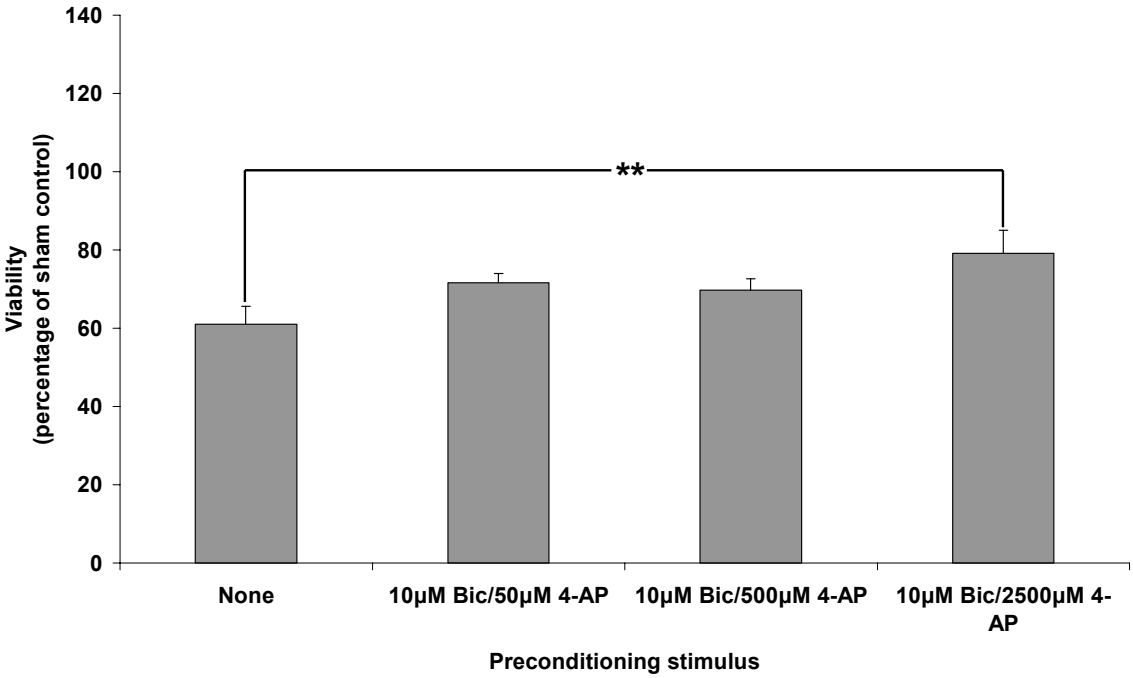

Figure 5.16 Effect of preconditioning with 10μM bicuculline and 50-2500μM 4-AP for 48 hours at 8-10 DIV on toxicity of 300μM NMDA applied for 24 hours at 11 DIV. Mean +/- SEM, n=5; ANOVA followed by Tukey's test, ** p<0.01. Bicuculline and 2500μM 4-AP co-treatment was protective against NMDA toxicity.

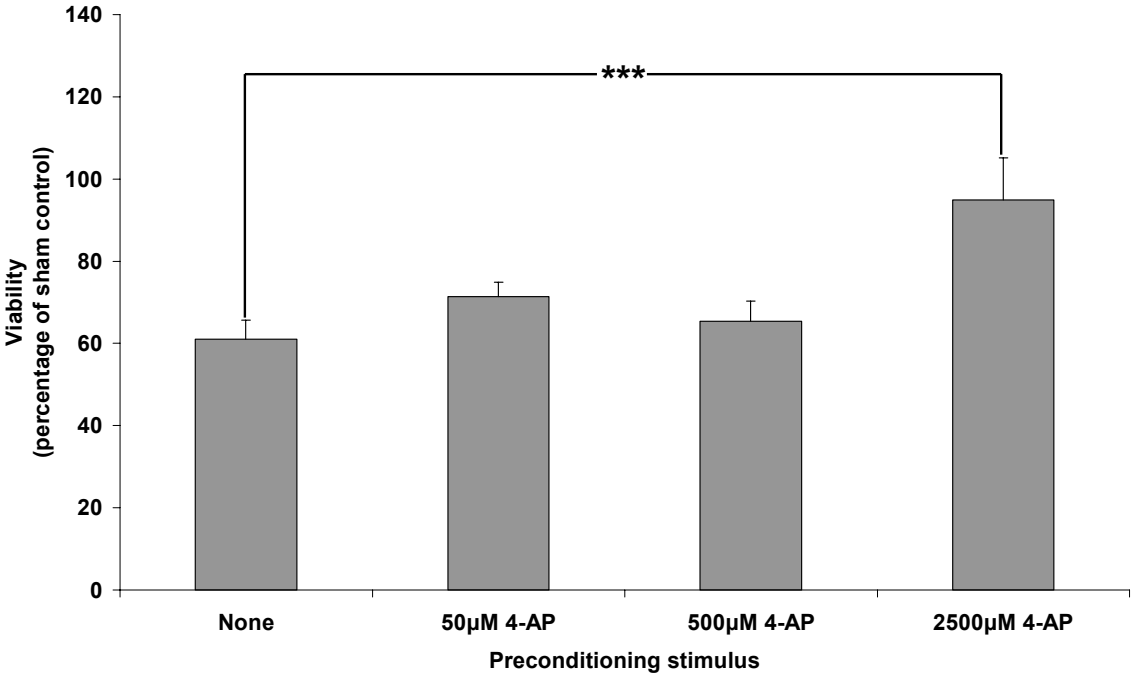

Figure 5.17 Effect of preconditioning with 50-2500μM 4-AP for 48 hours at 8-10 DIV on toxicity of 300μM NMDA applied for 24 hours at 11 DIV. Mean +/- SEM, n=5; ANOVA followed by Tukey's test, *** p<0.001. Treatment with 2500μM 4-AP was protective against NMDA toxicity.

5.5.5 48-hour preconditioning (with TTX) against NMDA

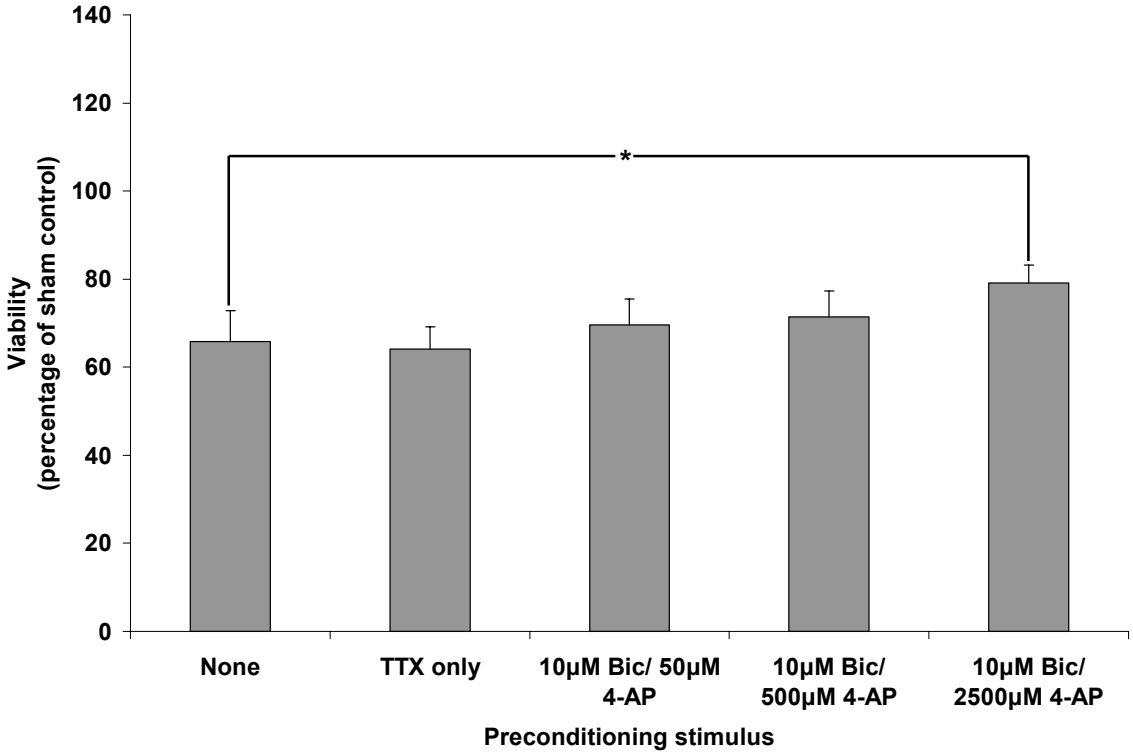

Figure 5.18 Effect of preconditioning with 10μM bicuculline and 50-2500μM 4-AP in the presence of 1μM TTX for 48 hours at 8-10 DIV on toxicity of 300μM NMDA applied for 24 hours at 11 DIV. Mean +/- SEM, n=5; ANOVA followed by Tukey's test, * p<0.05. Co-application of TTX reduced the protection provided by preconditioning with bicuculline and 2500μM 4-AP, although this still provided significant protection.

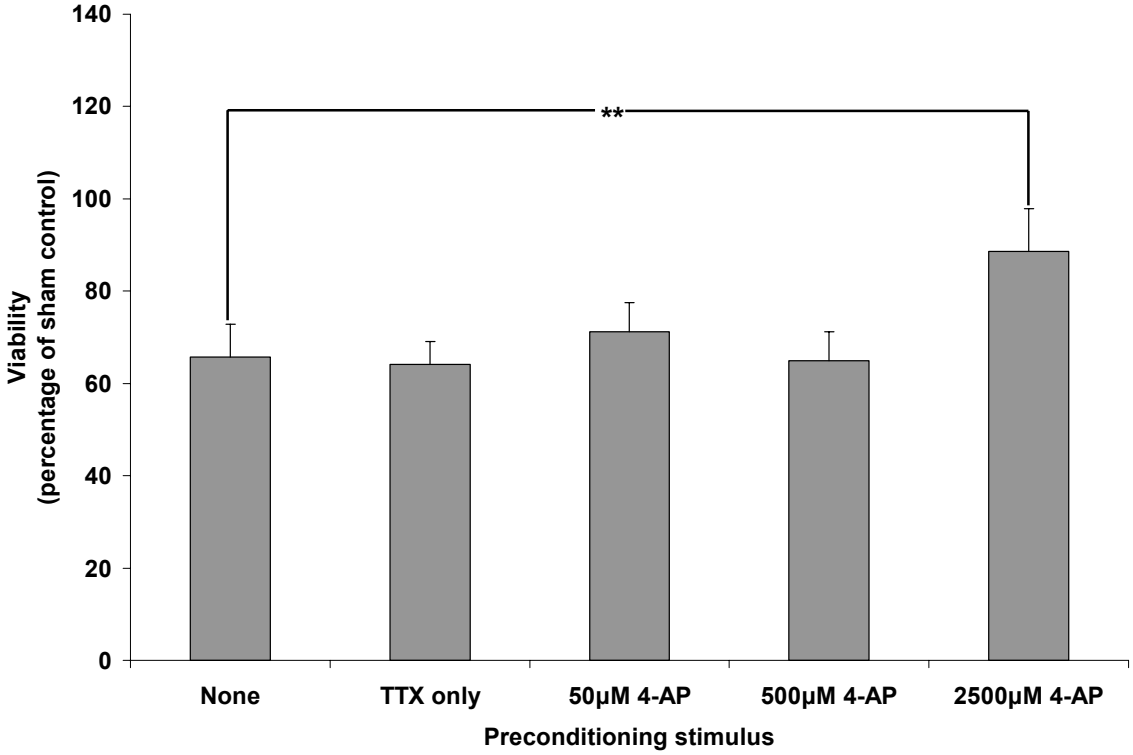

Figure 5.19 Effect of preconditioning with 50-2500μM 4-AP in the presence of 1μM TTX for 48 hours at 8-10 DIV on toxicity of 300μM NMDA applied for 24 hours at 11 DIV. Mean +/- SEM, n=5; ANOVA followed by Tukey's test, ** p<0.01. Co-application of TTX reduced the protection provided by preconditioning with 2500μM 4-AP, although this still provided significant protection.

5.5.6 48-hour preconditioning (with MK-801) against NMDA

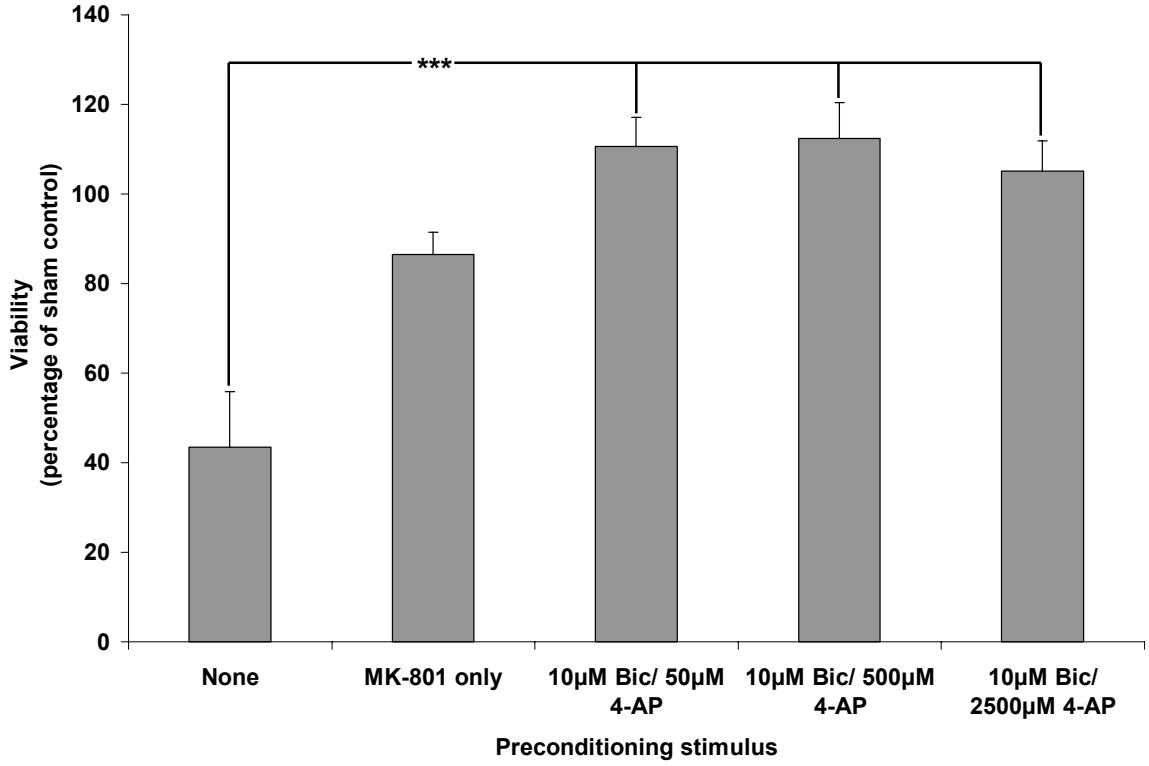

Figure 5.20 Effect of preconditioning with 10μM bicuculline and 50-2500μM 4-AP in the presence of 1μM MK-801 for 48 hours at 8-10 DIV on toxicity of 300μM NMDA applied for 24 hours at 11 DIV. Mean +/- SEM, n=5; ANOVA followed by Tukey's test, *** p<0.001. Co-application of MK-801 with bicuculline/4-AP preconditioning caused a potentiation in the protective effect.

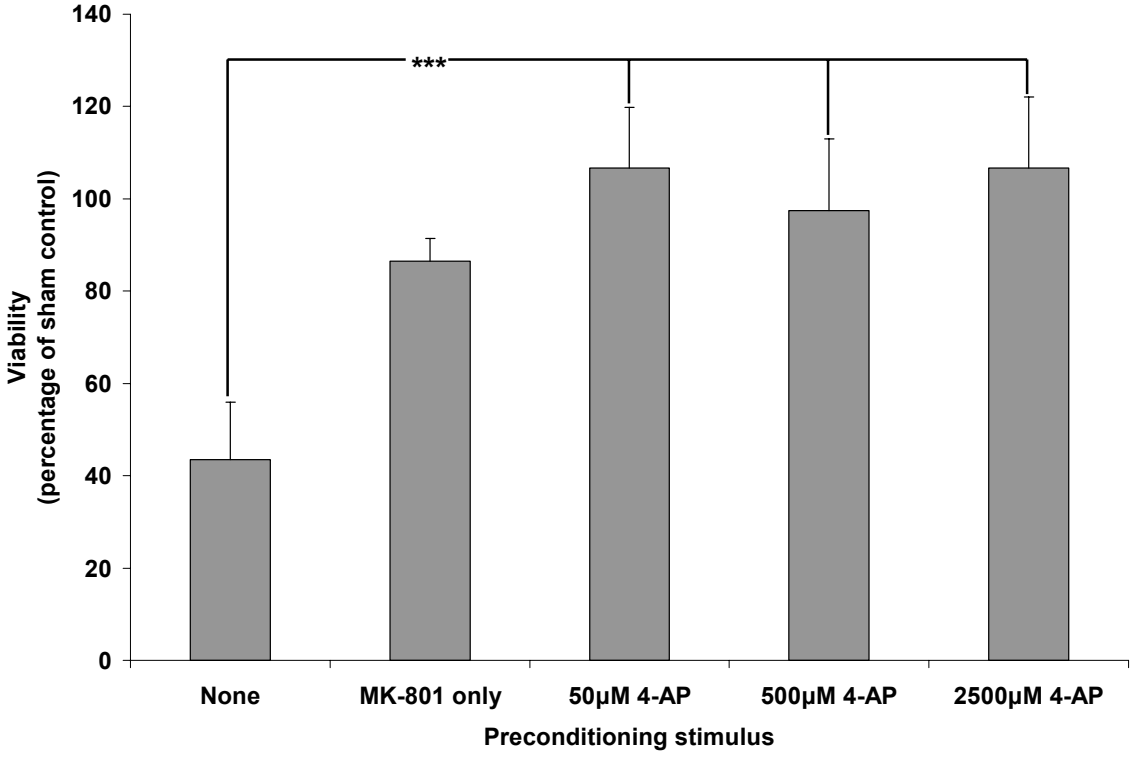

Figure 5.21 Effect of preconditioning with 50-2500μM 4-AP in the presence of 1μM MK-801 for 48 hours at 8-10 DIV on toxicity of 300μM NMDA applied for 24 hours at 11 DIV. Mean +/- SEM, n=5; ANOVA followed by Tukey's test, *** p<0.001. Co-application of MK-801 with 4-AP preconditioning caused a potentiation in the protective effect.

5.5.7 48-hour preconditioning against 3-NPA

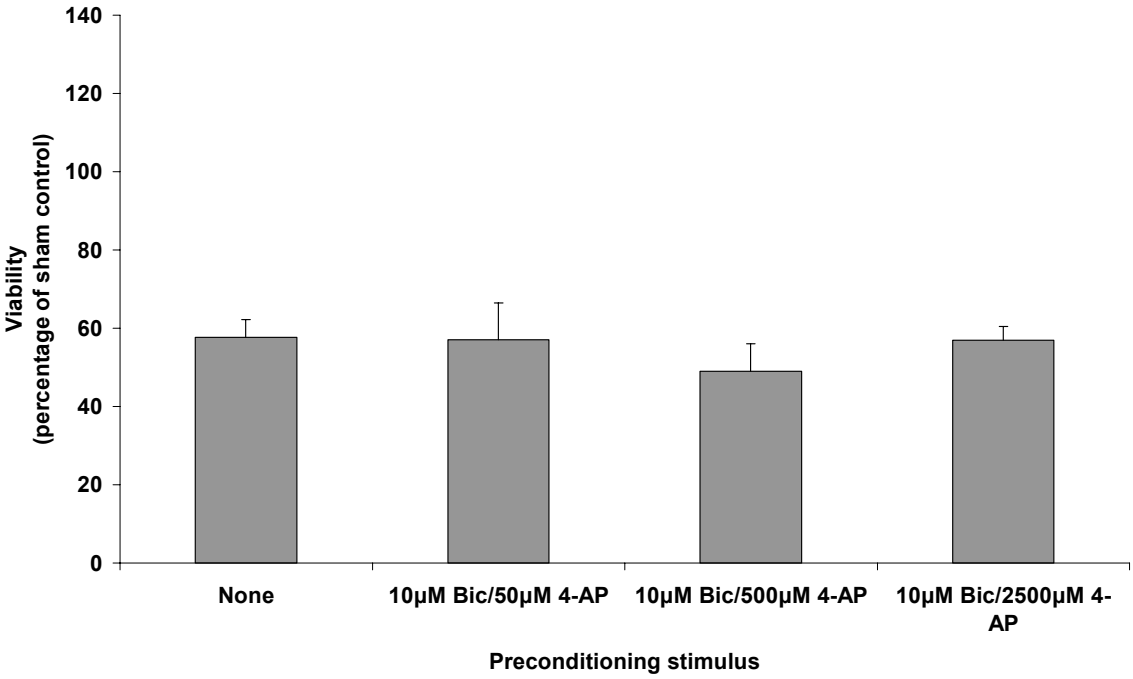

Figure 5.22 Effect of preconditioning with 10μM bicuculline and 50-2500μM 4-AP for 48 hours at 8-10 DIV on toxicity of 50μM 3-NPA applied for 24 hours at 11 DIV. Mean +/- SEM, n=5; ANOVA followed by Tukey's test identified no significant protection provided against the toxicity of 3-NPA.

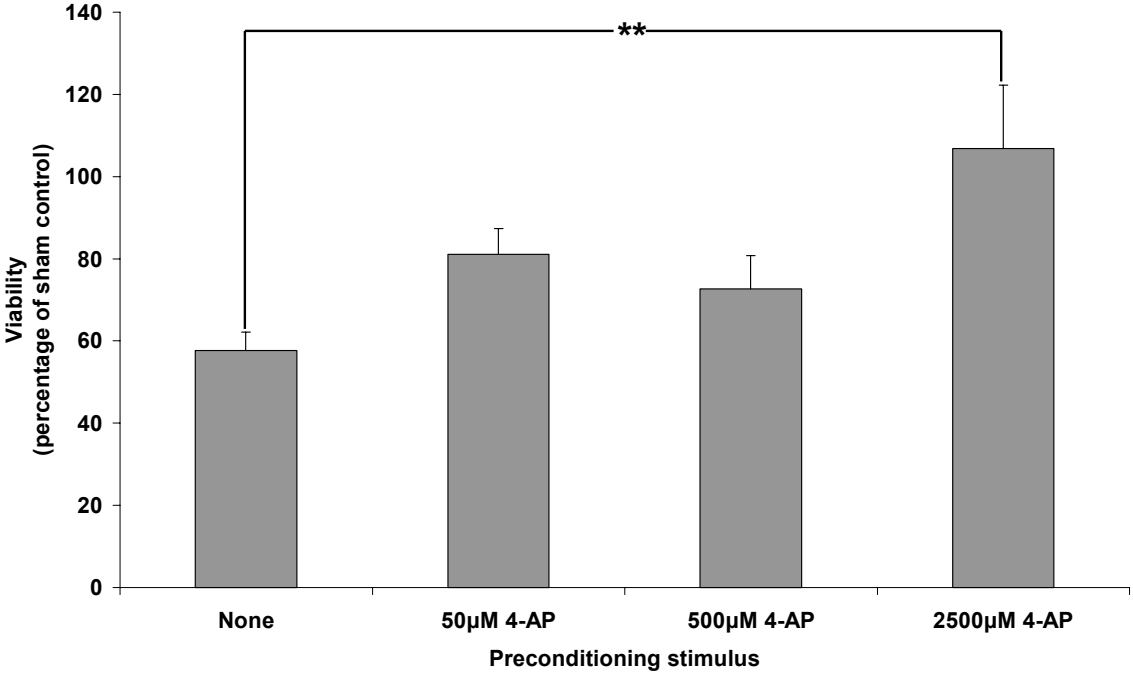

Figure 5.23 Effect of preconditioning with 50-2500μM 4-AP for 48 hours at 8-10 DIV on toxicity of 50μM 3-NPA applied for 24 hours at 11 DIV. Mean +/- SEM, n=5; ANOVA followed by Tukey's test, ** $p<0.01$. Preconditioning with 2500μM 4-AP provided very significant protection against the neurotoxic effect of 3-NPA.

5.5.8 48-hour preconditioning against OGD

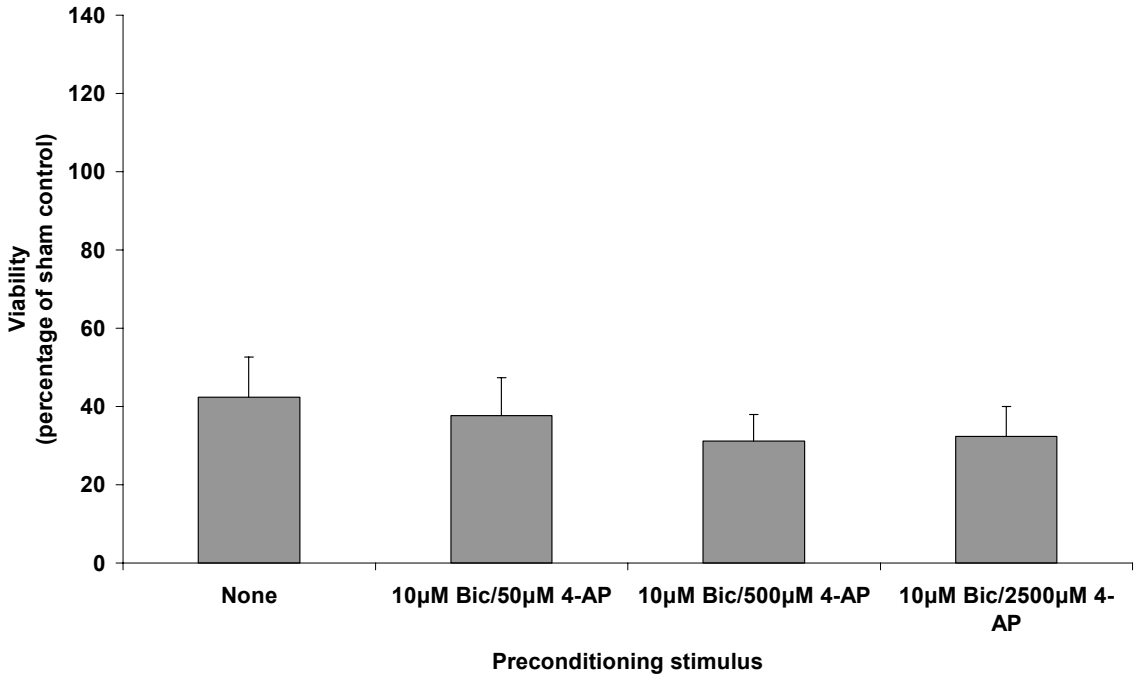

Figure 5.24 Effect of preconditioning with 10μM bicuculline and 50-2500μM 4-AP for 48 hours at 8-10 DIV on toxicity of 5 hours OGD at 11 DIV. Mean +/- SEM, n=5; ANOVA followed by Tukey's test identified no significant protection by preconditioning with bicuculline and 4-AP against the toxicity of OGD for 5 hours.

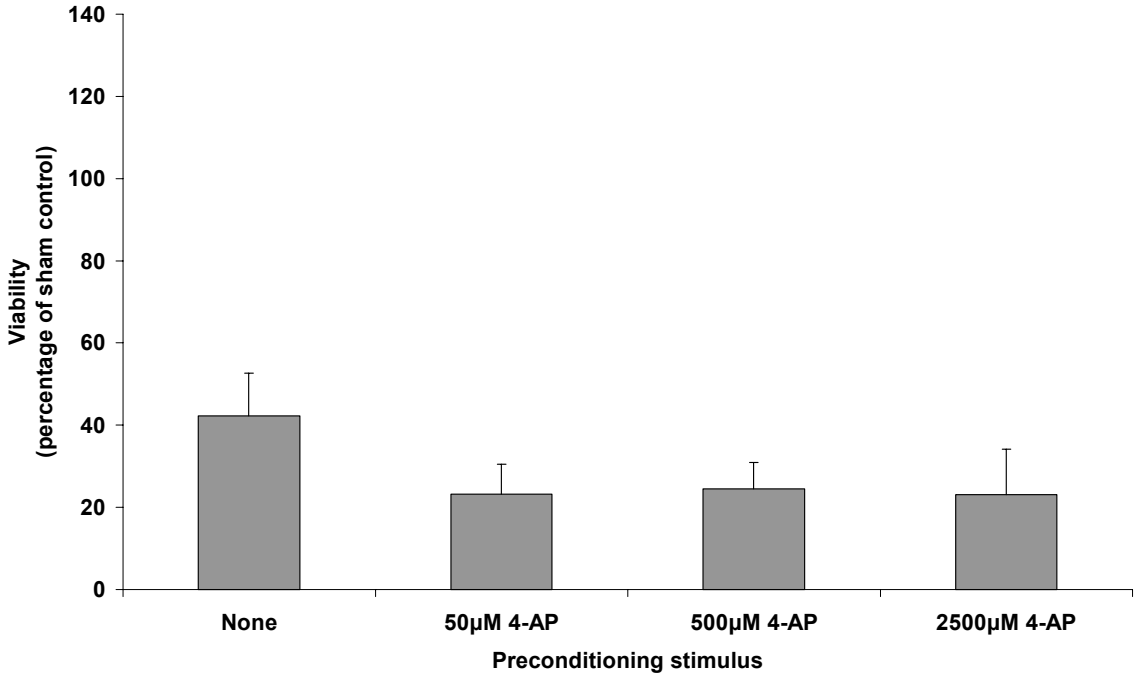

Figure 5.25 Effect of preconditioning with 50-2500μM 4-AP for 48 hours at 8-10 DIV on toxicity of 5 hours OGD at 11 DIV. Mean +/- SEM, n=5; ANOVA followed by Tukey's test identified no significant protection by preconditioning with 4-AP against the toxicity of OGD for 5 hours.

5.5.9 48-hour preconditioning stimuli: control series

To establish the effects of preconditioning stimuli on viability and of TTX, MK-801 and nifedipine on glutamate or NMDA toxicity, a series of control experiments were performed. Preconditioning with 4-AP alone caused no significant neurotoxicity, whereas co-application of bicuculline was detrimental to protection from 2500μM 4-AP). Tetrodotoxin caused no significant effects on glutamate or NMDA toxicity but reduced viability; MK-801 did not affect viability or glutamate toxicity but significantly reduced NMDA neurotoxicity (Table 5.1).

Preconditioning stimulus	Toxic insult	Viability (% of control)	Significance (vs. neg. control unless stated)
10μM Bic + 50μM 4-AP	None	77.4	None
10μM Bic + 500μM 4-AP	None	75.1	None
10μM Bic + 2500μM 4-AP	None	83.5	None
10μM Bic + 50μM 4-AP	None	77.4	None (versus 4-AP)
10μM Bic + 500μM 4-AP	None	75.1	None (versus 4-AP)
10μM Bic + 2500μM 4-AP	None	83.5	** (versus 4-AP)
50μM 4-AP	None	86.8	None
500μM 4-AP	None	89.4	None
2500μM 4-AP	None	102.9	None
1μM Tetrodotoxin	None	71.1	*
1μM Tetrodotoxin	Glutamate	60.4	None (vs. glutamate)
1μM Tetrodotoxin	NMDA	64.1	None (vs. NMDA)
1μM MK-801	None	109.9	None
1μM MK-801	Glutamate	69.5	None (vs. glutamate)
1μM MK-801	NMDA	86.5	* (vs. NMDA)
None	Glutamate	60.6	***
None	NMDA	61.6	**
None	3-NPA	57.6	***

Table 5.1 Effect of preconditioning stimuli on viability, and effect of TTX, MK-801 and nifedipine on viability and toxicity of 50μM glutamate and 300μM NMDA (average value of 5 repetitions).

5.5.10 48-hour preconditioning: effect of nifedipine

In order to identify the part played in 4-AP preconditioning by calcium uptake via voltage-gated calcium channels, the L-type calcium channel blocker nifedipine was applied during preconditioning. Unfortunately, nifedipine caused a significant reduction in viability, comparable to that induced by glutamate or NMDA and hence did not clarify the role of calcium currents via these channels in inducing protection (Table 5.2).

Preconditioning stimulus	Toxic insult	Viability (% of control)	Significance (vs. neg. control unless stated)
5μM Nifedipine	None	59.1	**
5μM Nifedipine	Glutamate	43.6	None (vs. glutamate)
5μM Nifedipine	NMDA	31.3	None (vs. NMDA)
5μM Nifedipine + 50μM 4-AP	Glutamate	37.1	***
5μM Nifedipine + 500μM 4-AP	Glutamate	26.8	***
5μM Nifedipine + 2500μM 4-AP	Glutamate	36.7	***
5μM Nifedipine + 10μM Bic + 50μM 4-AP	Glutamate	35.1	***
5μM Nifedipine + 10μM Bic + 500μM 4-AP	Glutamate	33.6	***
5μM Nifedipine + 10μM Bic + 2500μM 4-AP	Glutamate	29.5	***
5μM Nifedipine + 50μM 4-AP	NMDA	26.4	***
5μM Nifedipine + 500μM 4-AP	NMDA	18.8	***
5μM Nifedipine + 2500μM 4-AP	NMDA	30.3	***
5μM Nifedipine + 10μM Bic + 50μM 4-AP	NMDA	28.3	***
5μM Nifedipine + 10μM Bic + 500μM 4-AP	NMDA	33.1	***
5μM Nifedipine + 10μM Bic + 2500μM 4-AP	NMDA	27.8	***

Table 5.2 Effect of preconditioning stimuli in presence of nifedipine on viability and toxicity of 50μM glutamate and 300μM NMDA (average value of 5 repetitions), showing that nifedipine treatment caused a very significant drop in viability when applied for 48 hours at a concentration of 5μM.

5.5.11 48-hour preconditioning: morphological appearances

Preconditioning with 4-AP for 48 hours did not cause any adverse effects to CGN phenotypes, as both cell bodies and neurite networks appeared as control morphology (Figure 5.26). It was also clear that the co-application of either tetrodotoxin or MK-801 for 48 hours had no evident damaging effect on CGN morphology.

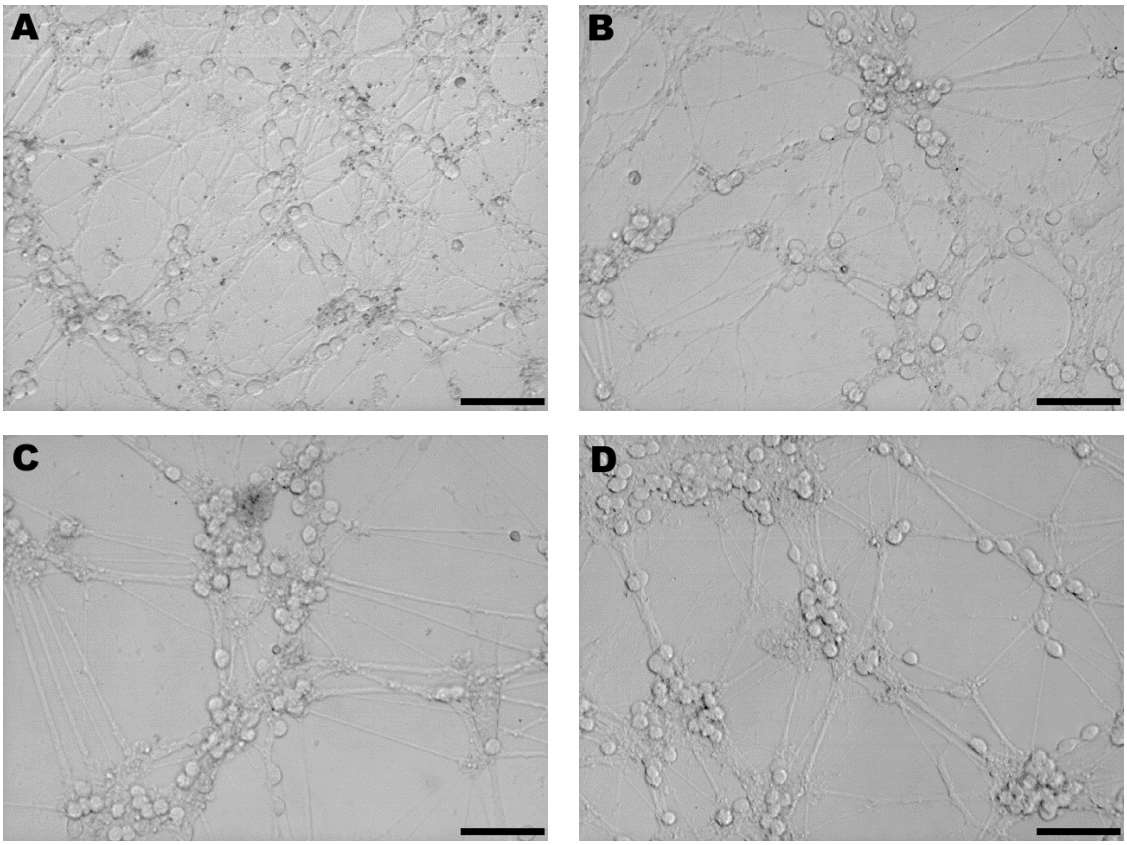

Figure 5.26 Phase contrast microscopic images of CGNs at 10 DIV after 48-hour preconditioning stimulus: control (A), treated with 2500μM 4-AP for 48 hours (B), treated with 2500μM 4-AP and 1μM TTX for 48 hours (C) and treated with 2500μM 4-AP and 1μM MK-801 for 48 hours (D). Bars = 50μm. It is shown that 4-AP preconditioning did not cause any morphological abnormalities, whether applied alone or with TTX or MK-801.

The protective effect of 2500μM 4-AP against the damage by 50μM glutamate treatment is seen in Figure 5.27. Glutamate caused an increase in both neuronal death and neurite loss, with these effects almost completely attenuated by preconditioning with 2500μM 4-AP. Additionally, this protection (at this higher dose) was also apparent in the presence of either 1μM TTX or 1μM MK-801 was also apparent (Figure 5.27).

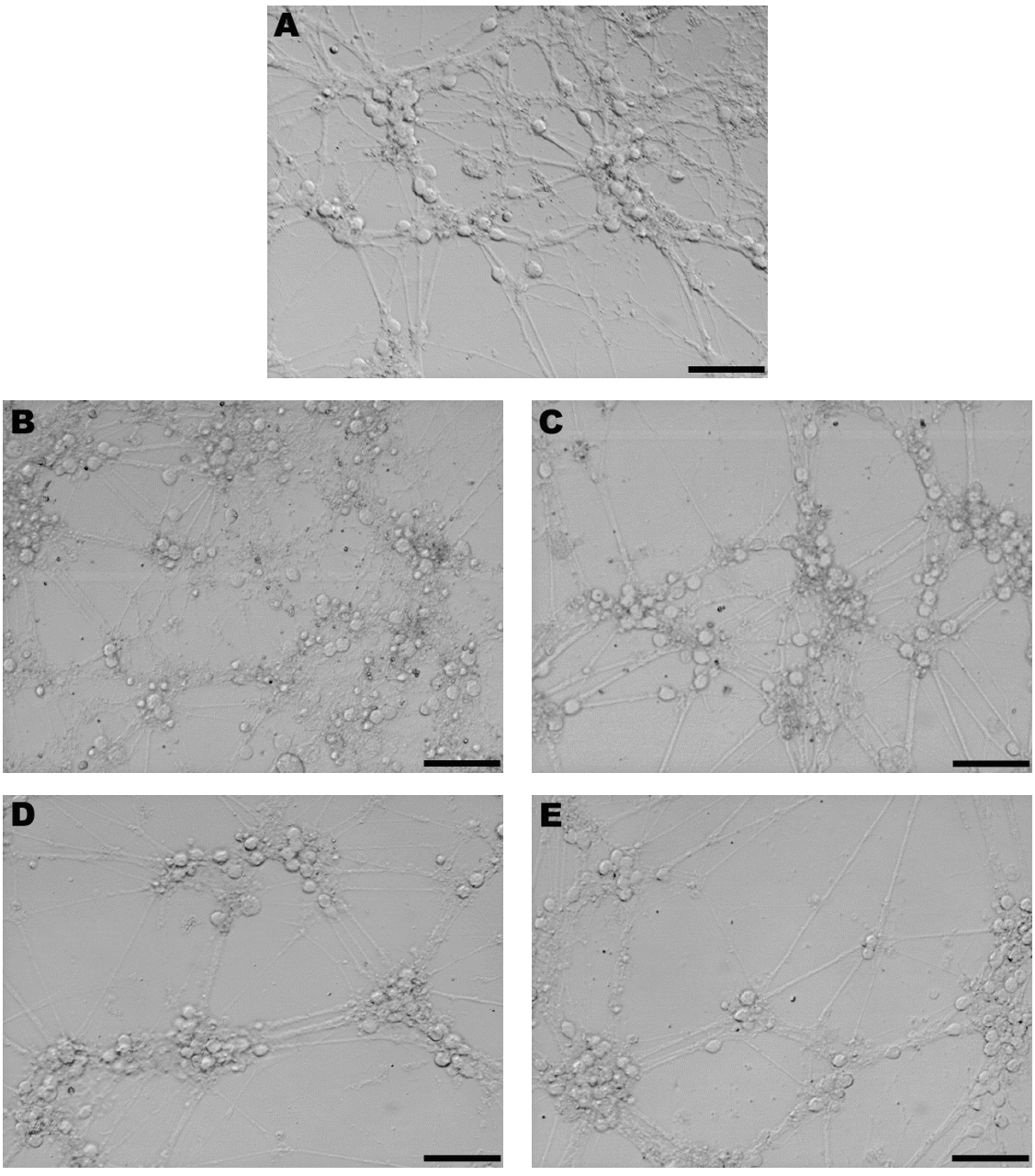

Figure 5.27 Morphology of CGN cultures at 12 DIV: control (A), following exposure to 50μM glutamate for 24 hours at 11 DIV (B), treated with 2500μM 4-AP for 48 hours prior to glutamate exposure (C), treated with 2500μM 4-AP and 1μM TTX for 48 hours prior to glutamate exposure (D) and treated with 2500μM 4-AP and 1μM MK-801 for 48 hours prior to glutamate exposure (E). Bars = 50μm. The damaging effect of treatment with glutamate was completely prevented by treatment with 2500μM 4-AP, an effect maintained in the presence of either TTX or MK-801.

Although the neurotoxic effect of 300μM NMDA was less than with glutamate, again cell death and neurite network destruction was apparent (Figure 5.28B). The protective effect of 2500μM 4-AP against NMDA toxicity was also evident, and also in the presence of 1μM TTX or 1μM MK-801 (Figure 5.28).

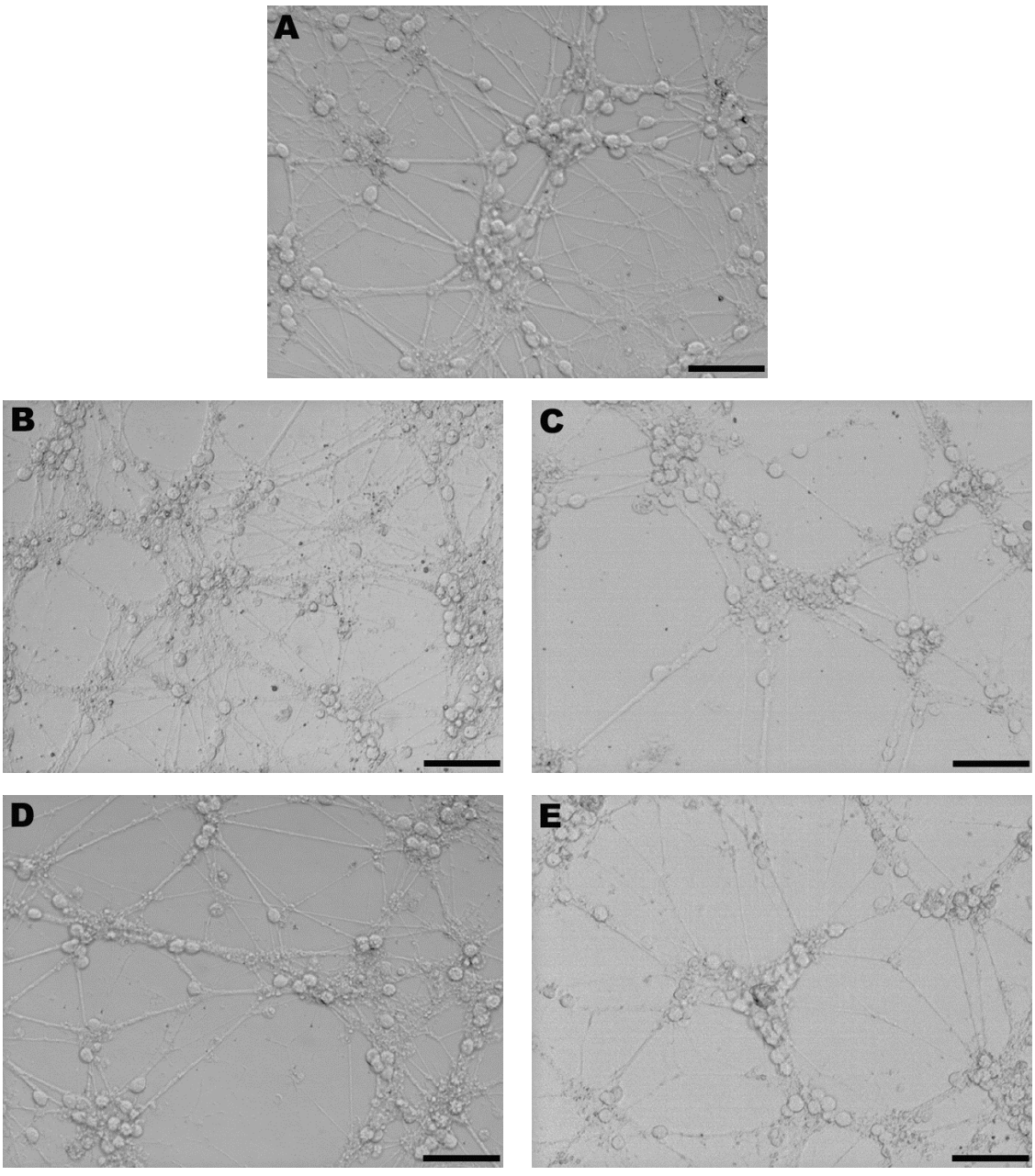

Figure 5.28 Morphology of CGNs at 12 DIV: control (A), following exposure to 300μM NMDA for 24 hours at 11 DIV (B), treated with 2500μM 4-AP for 48 hours prior to NMDA exposure (C), treated with 2500μM 4-AP and 1μM TTX for 48 hours prior to NMDA exposure (D) and treated with 2500μM 4-AP and 1μM MK-801 for 48 hours prior to NMDA exposure (E). Bars = 50μm. The damaging effect of treatment with NMDA was completely prevented by treatment with 2500μM 4-AP, an effect maintained in the presence of either TTX or MK-801.

100μM 3-NPA also produced clear morphological evidence of neuronal death and again 2500μM 4-AP has provided extensive protection against this insult, an effect that was not lost by co-application of either 1μM TTX or 1μM MK-801 (Figure 5.29).

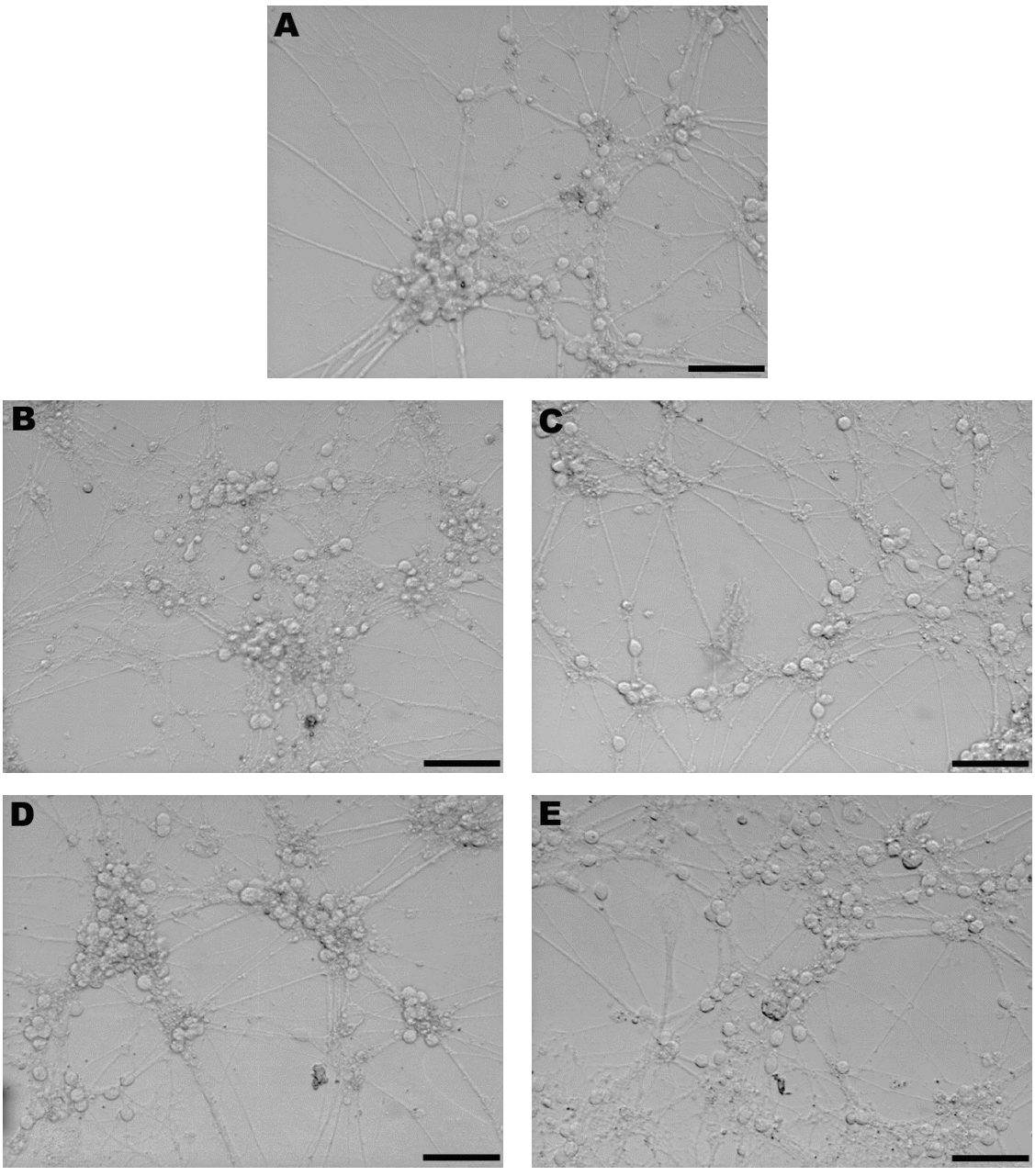

Figure 5.29 Morphology of CGN cultures at 12 DIV: control (A), following exposure to 50μM 3-NPA for 24 hours at 11 DIV (B), treated with 2500μM 4-AP for 48 hours prior to 3-NPA exposure (C), treated with 2500μM 4-AP and 1μM TTX for 48 hours prior to 3-NPA exposure (D) and treated with 2500μM 4-AP and 1μM MK-801 for 48 hours prior to 3-NPA exposure (E). Bars = 50μm. The damaging effect of treatment with 3-NPA was completely prevented by treatment with 2500μM 4-AP, an effect maintained in the presence of either TTX or MK-801.

5.5.12 48-hour preconditioning – CREB phosphorylation

Stimulation of CGNs with 2500μM 4-AP increased CREB phosphorylation compared with untreated controls when samples were analysed (Figure 5.30). This contrasted to the reduced CREB phosphorylation in preconditioned CGNs relative to untreated controls when both were exposed to 50μM glutamate. Densitometric analysis did not show statistical significance, although this may have been due to the limited sample size (Figure 5.31).

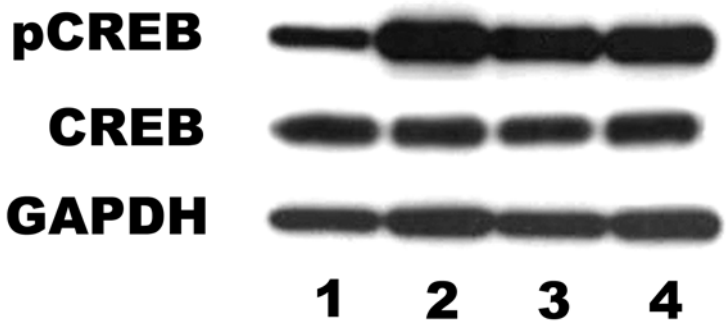

Figure 5.30 Representative blots of CREB and phosphorylated CREB in samples from cultures treated with 1 = control, 2 = 2500μM 4-AP for 48 hours at 8-10 DIV, 3 = 50μM glutamate at 11 DIV, 4 = 2500μM 4-AP for 48 hours at 8-10 DIV followed by 50μM glutamate at 11 DIV. Samples collected at 11 DIV (1 and 2) and 12 DIV (3 and 4) at points corresponding with beginning or end of toxic insult. Increased CREB phosphorylation due to 4-AP treatment is apparent in this sample blot.

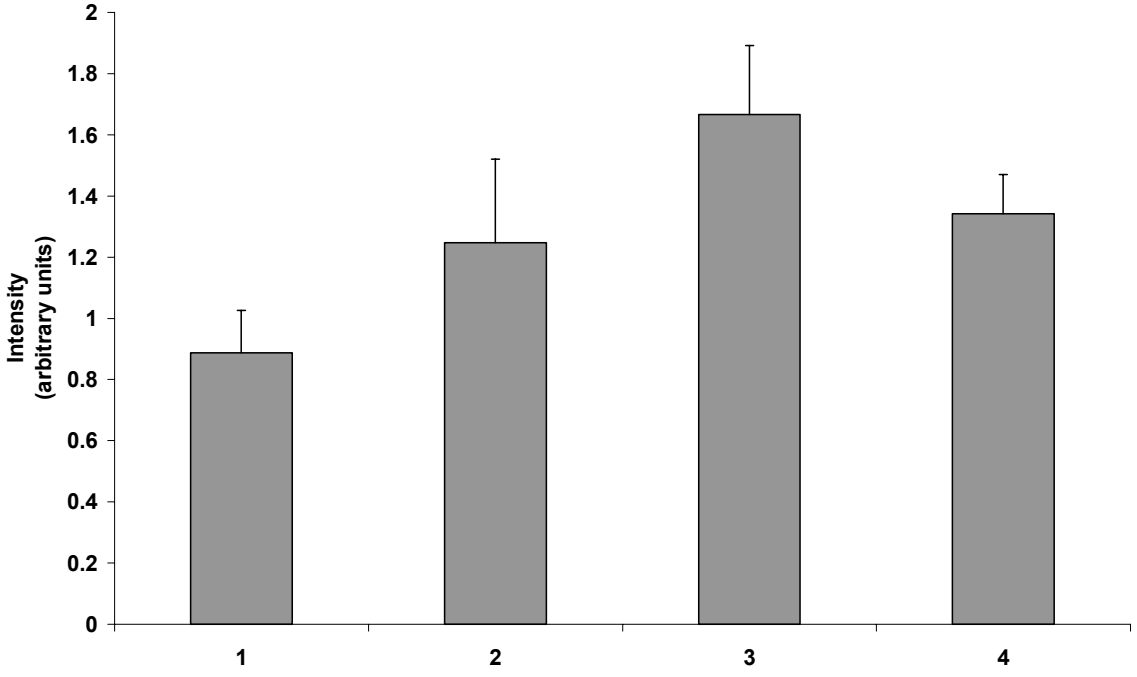

Figure 5.31 Quantification of CREB phosphorylation in samples from cultures treated with: 1 = control, 2 = 2500μM 4-AP for 48 hours at 8-10 DIV, 3 = 50μM glutamate at 11 DIV, 4 = 2500μM 4-AP for 48 hours at 8-10 DIV followed by 50μM glutamate at 11 DIV. Samples collected at 11 DIV (1 and 2) and 12 DIV (3 and 4)) at points corresponding with beginning or end of toxic insult. Mean +/- SEM, n=3. No statistically significant difference was seen.

5.5.13 48-hour preconditioning – bcl-2 expression

Although bcl-2 has been associated with CREB activation and is known to act as an effective protector against either apoptotic or necrotic cell death, there was no evidence to suggest its involvement in the 4-AP-mediated preconditioning protection that was seen in our culture system (Figures 5.32, 5.33).

Figure 5.32 Representative blots of bcl-2 in samples from cultures treated with 1 = control, 2 = 2500µM 4-AP for 48 hours at 8-10 DIV, 3 = 50µM glutamate at 11 DIV, 4 = 2500µM 4-AP for 48 hours at 8-10 DIV followed by 50µM glutamate at 11 DIV. Samples collected at 11 DIV (1 and 2) and 12 DIV (3 and 4) at points corresponding with beginning or end of toxic insult. No variation in bcl-2 expression is seen following either 4-AP preconditioning of glutamate treatment in this sample blot.

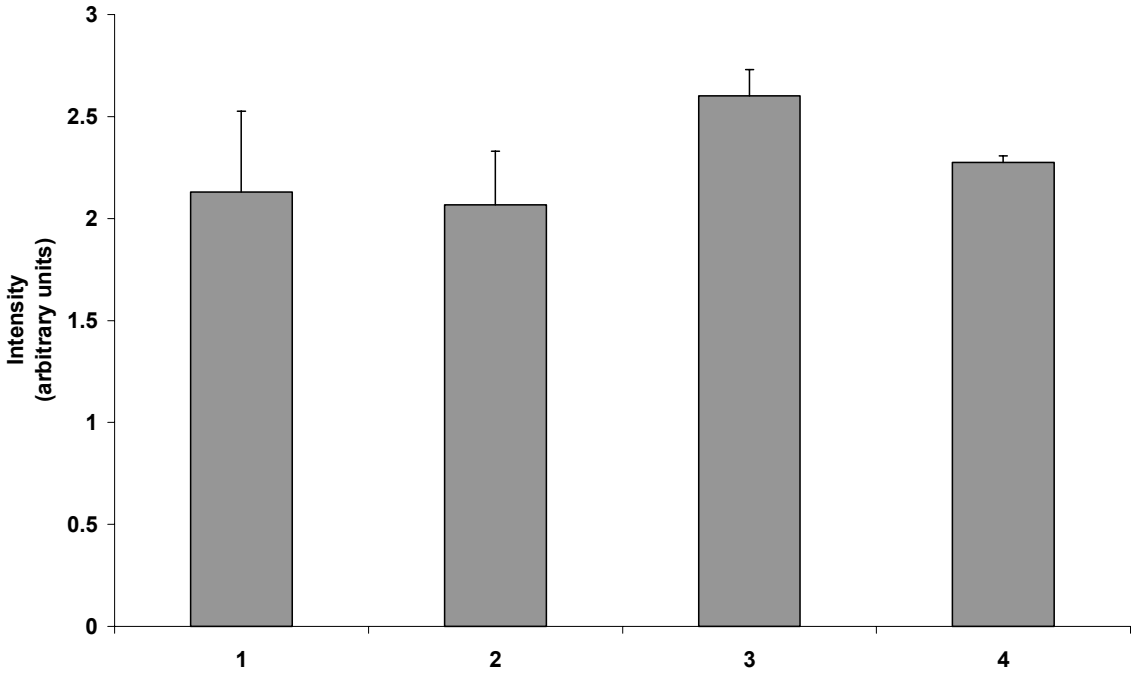

Figure 5.33 Quantification of bcl-2 in samples from cultures treated with: 1 = control, 2 = 2500µM 4-AP for 48 hours at 8-10 DIV, 3 = 50µM glutamate at 11 DIV, 4 = 2500µM 4-AP for 48 hours at 8-10 DIV followed by 50µM glutamate at 11 DIV. Samples collected at 11 DIV (1 and 2) and 12 DIV (3 and 4) at points corresponding with beginning or end of toxic insult. Mean +/- SEM, n=3. No alteration in bcl-2 expression due to either preconditioning or glutamate treatment is seen.

5.5.14 48-hour preconditioning – caspase-3 activation

Although again not significant, preconditioning with 2500μM 4-AP appeared to mediate an interesting effect on the activation of caspase-3, with a reduction in activation seen when compared to both negative and positive (glutamate-treated) controls (Figures 5.34, 5.35).

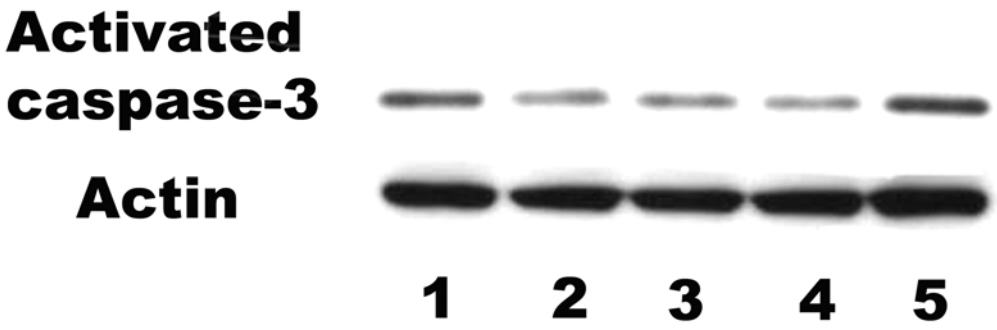

Figure 5.34 Representative blots of activated caspase-3 in samples from cultures treated with 1 = control, 2 = 2500μM 4-AP for 48 hours at 8-10 DIV, 3 = 50μM glutamate at 11 DIV, 4 = 2500μM 4-AP for 48 hours at 8-10 DIV followed by 50μM glutamate at 11 DIV, 5 = 1μM staurosporine for 6 hours at 9 DIV (positive control). Samples collected at 11 DIV (1 and 2), 12 DIV (3 and 4) at points corresponding with beginning or end of toxic insult; and 9 DIV (5). No variation in caspase-3 activation is seen following either 4-AP preconditioning of glutamate treatment in this sample blot.

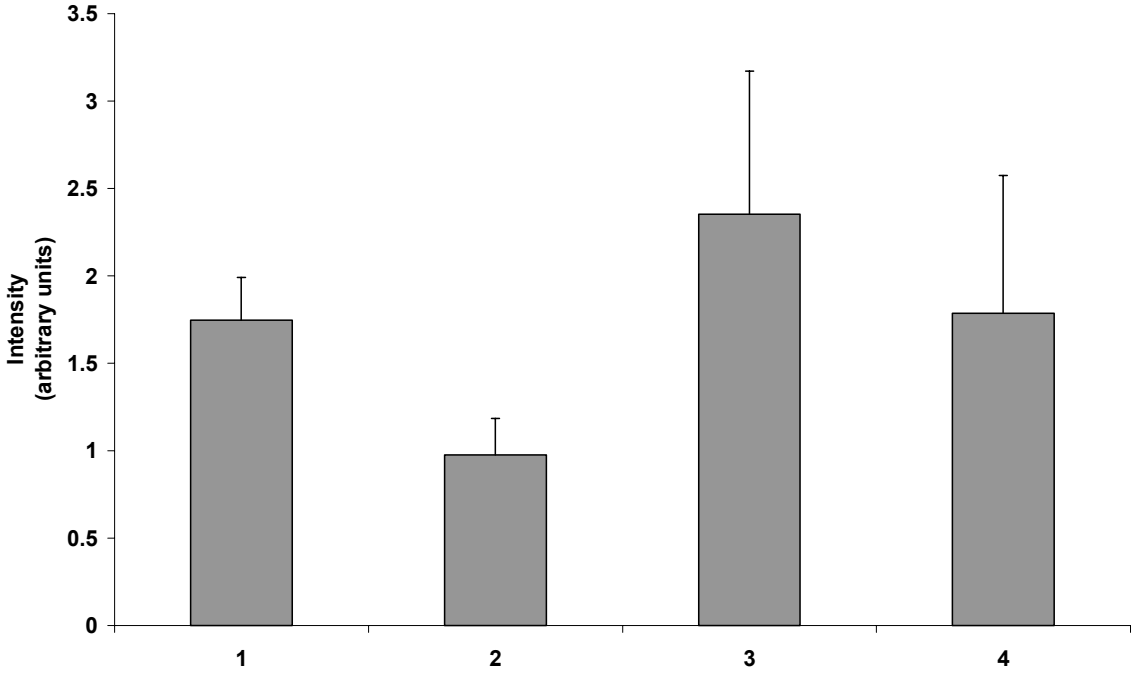

Figure 5.35 Quantification of activated caspase-3 in samples from cultures treated with: 1 = control, 2 = 2500μM 4-AP for 48 hours at 8-10 DIV, 3 = 50μM glutamate at 11 DIV, 4 = 2500μM 4-AP for 48 hours at 8-10 DIV followed by 50μM glutamate at 11 DIV. Samples collected at 11 DIV (1 and 2) and 12 DIV (3 and 4) at points corresponding with beginning or end of toxic insult. Mean +/- SEM, n=3. No significant variation in caspase-3 activation is seen following either 4-AP preconditioning of glutamate treatment.

5.6 Discussion of NMDA, hydrogen peroxide and 3-nitropropionic acid preconditioning

5.6.1 Preconditioning with NMDA

Preconditioning with NMDA has previously been shown to confer protection against subsequent glutamate toxicity in neonatal rat CGNs (Marini and Paul, 1993). This method was therefore employed in the current study to protect against the neurotoxic effects of glutamate, 3-NPA, hypoxia and OGD. Previously published data suggested that the NMDA concentration and exposure duration most likely to be effective in CGNs was 100μM NMDA for 6 hours at 8 DIV, with a toxic stimulus applied 24 hours after commencing the preconditioning stimulus (Chuang *et al.*, 1992, Damschroder-Williams *et al.*, 1998, Lipsky *et al.*, 2001).

This preconditioning regimen used here provided a significant degree of protection not only against a range of concentrations of glutamate (10μM to 100μM) applied in medium for 24 hours, but also against 3-NPA over the concentration range 1μM to 500μM. For NMDA preconditioning, protein and RNA synthesis have been shown to be necessary since protection was blocked by the presence of either cycloheximide or actinomycin D (Marini and Paul, 1993).

In our system however, this protocol was unable to provide significant protection against exposure to either hypoxia or OGD. Altering the preconditioning procedure by applying NMDA stimulation at 12 DIV 24 hours prior to 2 hours of hypoxia was also not effective in inducing protection, although a slight, non-significant shift in the concentration at which NMDA was most trophic was seen.

The period over which a sub-toxic concentration of NMDA protects against a toxic glutamate insult has been demonstrated as being over the range of 12-48 hours, with protection not apparent outside this period (Damschroder-Williams *et al.*, 1995). Additionally, NMDA treatments of cultured CGNs for 4 hours, followed by removal and replacement with control medium for 8 hours was not significantly less protective than treatment with NMDA for the full 12 hour period (Damschroder-Williams *et al.*, 1995).

The mechanism of NMDA preconditioning in CGNs was not via reduced calcium influx secondary to NMDA receptor down-regulation, as calcium influx caused by

NMDA receptor stimulation was not significantly lower in preconditioned neurones than in controls (Damschroder-Williams *et al.*, 1995). Nor is it likely that preconditioning acts via alterations to NMDA receptor subunit composition, as *in vivo* ischaemic preconditioning in rats did not affect expression levels of subunits NR1, NR2A or NR2B in hippocampal CA1 or neocortex synaptosomes fractions (Shamloo and Wieloch, 1999).

Levels of extracellular glutamate during toxic OGD are reduced by preconditioning with KCl or NMDA in cultured cortical neurones or by OGD-preconditioning of brain slices (Johns *et al.*, 2000, Tauskela *et al.*, 2001, Grabb *et al.*, 2002). Furthermore, ischaemia in rat hippocampus *in vivo* caused a significant rise in extracellular glutamate, which did not occur with ischaemic preconditioning, although a significant rise in extracellular GABA was noted (Dave *et al.*, 2005). In both neurones and slices, GABA release in preconditioned neurones was enhanced during normally-lethal OGD and tolerance could be eliminated by blockade of GABA receptors during lethal OGD (Johns *et al.*, 2000, Grabb *et al.*, 2002).

Effects of NMDA preconditioning on mitochondria are not limited to altered calcium levels, as mitochondrial decouplers blocked calcium influx into mitochondria, but did not prevent NMDA-induced reductions in mitochondrial movement in neuronal dendrites and morphological changes (Rintoul *et al.*, 2003).

Ischaemic preconditioning *in vivo*, or OGD preconditioning in cortical cultures, caused expression of the mitochondrial uncoupler protein UCP-2, located on the mitochondrial inner membrane and induced membrane depolarisation, by reducing mitochondrial calcium uptake or by generation of ROS (Diano *et al.*, 2003, Mattiasson *et al.*, 2003, Sullivan *et al.*, 2003). Also, ischaemic preconditioning caused mitochondrial calcium levels to increase, in hippocampal CA1 neurones, while cytosolic levels decreased; the demonstrated ischaemic preconditioning-induced increase in bcl-2 could explain the ability of the mitochondria to hold greater amounts of calcium without damage (Shimazaki *et al.*, 1994). Ischaemic preconditioning has been shown to reduce cytochrome c release following normally lethal cerebral ischaemia in rats, whilst isolated

mitochondria from preconditioned neurones were shown to release less cytochrome c after exposure to elevated calcium (Zhan *et al.*, 2002).

N-methyl-D-aspartate receptor stimulation causes release of brain-derived neurotrophic factor (BDNF), with a subsequent increase in neurotrophin receptor TrkB tyrosine phosphorylation due to BDNF binding with and activating TrkB (Marini *et al.*, 1998). This neuroprotection was prevented by blockade of either the NMDA receptor or the TrkB receptor and replicated by treatment of the CGNs with BDNF before glutamate exposure, but not by nerve growth factor (NGF) or neurotrophin-3 (Marini *et al.*, 1998).

The involvement of the transcription factor nuclear factor kappa B (NF-κB) was also demonstrated (Lipsky *et al.*, 2001). Nuclear factor kappa B is normally found in the cytosol, in an inactive complex with the inhibitory protein IκBα, which goes through phosphorylation and degradation upon activation and subsequent release of active NF-κB. *N*-methyl-D-aspartate preconditioning was completely lost if cells were pre-treated with NF-κB target DNA which acted as a 'decoy' for the transcription factor, thus blocking any protein synthesis that would otherwise have been mediated by NF-κB (Blondeau *et al.*, 2001, Lipsky *et al.*, 2001, Ravati *et al.*, 2001).

When NF-κB translocates to the nucleus, it up-regulates genes involved in anti-apoptotic pathways, including the production of Mn-SOD and inhibitors of apoptosis-related proteins (Hou and MacManus, 2002, Sapolsky *et al.*, 2001). Glutamate-induced calcium rises are one of the signals which can lead to activation of NF-κB in neurones (Kaltschmidt *et al.*, 1995). *N*-methyl-D-aspartate preconditioning is also effective at protecting against seizure activity and neuronal death in hippocampal neurones exposed to QA 24-48 hours later (Boeck *et al.*, 2004).

Stimulation of NMDA receptors with bicuculline and 4-AP increased neuronal survival when a period of neuronal electrical inactivity intervened between this stimulus and a toxic insult: this protection was blocked by the use of the CREB pathway inhibitor inducible cAMP early repressor (ICER), although protection against an insult applied immediately after stimulation was not CREB-dependent (Papadia *et al.*, 2005).

The activation of CREB was associated with increased production of bcl-2 protein in cerebral cortical, hippocampal and hypothalamic neurones, in response to OGD-induced preconditioning, toxic exposure to glutamate and hypoxic preconditioning respectively (Mabuchi *et al.*, 2001, Wu *et al.*, 2004, Meller *et al.*, 2005). These increases in bcl-2 were blocked by use of a CRE decoy oligonucleotide (Mabuchi *et al.*, 2001, Meller *et al.*, 2005) and associated with retardation of loss of mitochondrial membrane potential during severe anoxia or toxic H_2O_2 application (Wu *et al.*, 2004, Tang *et al.*, 2005b).

5.6.2 Preconditioning with 3-NPA

Preconditioning with 3-NPA has been shown *in vitro*, with rat cortical neurones preconditioned against subsequent OGD 24-48 hours later (Weih *et al.*, 1999). The current study set out to investigate further the mechanisms involved in mediating this effect, such as whether the abilities of 3-NPA to activate NMDA receptors or inhibit succinate dehydrogenase were involved. *N*-methyl-D-aspartate receptor stimulation in 3-NPA-mediated preconditioning is of particular interest, as blockade of the adenosine A_1 receptor during preconditioning in gerbil hippocampal slices prevents protection, A_1 receptor involvement in preconditioning having been previously noted (see section 1.4.1) (Aketa *et al.*, 2000).

A range of concentrations (1μM to 10mM) of 3-NPA for 6 hours was proved ineffective, failing to protect against either 100μM glutamate or 300μM NMDA, applied for 1 hour in Hank's balanced salt solution (HBSS) buffer in this study. The concentrations range was comparable with that used by Weih *et al.* (1999), although was at the upper range of concentrations, since CGNs are known to be less sensitive than cerebral cortical neurones to neurotoxic stimuli of comparable severity (Okuda *et al.*, 1998, Scorziello *et al.*, 2001).

Administration of 3-NPA to adult rats as a preconditioning stimulus 3 days prior to a cerebral infarct induced by MCA occlusion caused infarct volumes to be reduced relative to controls (Horiguchi *et al.*, 2003). This protection was lost if either the mitochondrial K_{ATP} blocker 5-hydroxydecanoate (5-HD) or the non-selective K_{ATP} channel blocker glibenclamide were co-applied with 3-NPA. Application of 3-NPA to cultured cerebral cortical neurones caused mitochondrial depolarisation, which could be prevented by the presence of 5-HD (Horiguchi *et*

al., 2003). 3-Nitropropionic acid preconditioning was also blocked by a free radical scavenger or protein synthesis inhibitor, which caused an increase in the bcl-2/bax ratio (Wiegand *et al.*, 1999, Brambrink *et al.*, 2000).

There are similarities between the preconditioning induced by 3-NPA and that induced by NMDA, notably the involvement of ROS formation, mitochondrial depolarisation and protein synthesis. Differences also exist however, such as the failure of 3-NPA preconditioning in cerebral cortical neurones to induce translocation of the transcription factors NF-κB or hypoxia-inducible factor (HIF) (Weih *et al.*, 1999).

5.6.3 Preconditioning with H_2O_2

Preconditioning against excitotoxic and oxidative insults was also investigated in the rat phaeochromocytoma cell line PC12 by using exogenous H_2O_2 (10μM for 90 minutes) to protect against the toxicity of H_2O_2 itself or dopamine administered 24 hours after preconditioning (Tang *et al.*, 2005a, Tang *et al.*, 2005c). Protection was shown to involve over-expression of bcl-2 and the prevention of increased ROS formation and mitochondrial membrane potential alterations, although protection was not dependent on K_{ATP} channel activation (Tang *et al.*, 2005a, Tang *et al.*, 2005b, Tang *et al.*, 2005c).

As exogenous H_2O_2 can induce severe cell damage in CGN cultures, at even lower micromolar concentrations (Fatokun *et al.*, 2007), the period of preconditioning was reduced substantially, to 5, 10 and 15 minute periods against 2 hours' hypoxia in the current study. This however did not produce significant protection, and therefore was not continued.

As protection induced by H_2O_2 preconditioning in other studies involved ROS production, it may have involved similar mechanisms to those in NMDA receptor preconditioning. However, although levels of viability seen in CGNs preconditioned by H_2O_2 were slightly raised, variability made this difference insignificant. This further underlines the problems of the previous method of preconditioning; where a relatively severe (albeit subtoxic) stimulus is used to induce protection.

This may be a limitation inherent in this model of preconditioning, as suggested by the finding that ischaemic preconditioning for 3 minutes (but not shorter durations) induced tolerance in rat brain *in vivo*, while even slightly longer durations caused cell death and that the preconditioning stimulus does indeed require toxic potential to be effective (Shamloo and Wieloch, 1999).

5.7 Discussion of 4-aminopyridine and bicuculline preconditioning

5.7.1 Preconditioning with 4-AP

As the earlier studies using relatively high doses of NMDA to stimulate CGNs had been of limited success, development of a method of neuronal stimulation that was effective in generating protection, but did not induce even sub-lethal excitatory or oxidative stress, was investigated.

A highly significant degree of protection resulted from application of 2500μM 4-AP for 48 hours at 8-10 DIV against 50μM glutamate, 50μM 3-NPA or 300μM NMDA applied for 24 hours at 11 DIV, but was ineffective at protecting against 5 hours' exposure to OGD at 11 DIV. Preconditioning with 50μM 4-AP was effective at protecting against 50μM glutamate. Co-application of bicuculline with either concentration of 4-AP reduced the protection against glutamate and NMDA, although a significant effect was still present. Protection against 3-NPA was eliminated by bicuculline co-application and again failed to protect against OGD.

The neuronal population in our system differed from those used by the Tauskela group, with a higher concentration of purely glutamatergic neurones. For this reason, the effect of preconditioning with 50, 500 or 2500μM 4-AP alone was investigated alongside a combination of 10μM bicuculline with 50, 500 or 2500μM 4-AP, the concentrations used based on previous studies (Mei *et al.*, 2000, Lange-Asschenfeldt *et al.*, 2005, Hu *et al.*, 2006, Tauskela *et al.*, 2008). Stimulation with 4-AP alone gave more extensive protection than was achieved using combined treatment with bicuculline and 4-AP. The use of 4-AP alone to induce preconditioning has been previously demonstrated against kainate (Ogita *et al.*, 2005), but here we also demonstrated effective protection against glutamate, NMDA and 3-NPA. This is evidence that the protection induced by 4-

AP is effective against a wide range of neurotoxic insults, including excitotoxicity complicated by oxidative stress and metabolic compromise.

The finding that non-toxic excitatory stimulation with a low (5-10μM) concentration of NMDA for 12-24 hours was found to effectively precondition hippocampal neurones against subsequent glutamate or staurosporine exposure was of great interest (Soriano *et al.*, 2006), suggesting a potential method for inducing preconditioning without any risk of neurotoxicity. The use of this method in rat hippocampal neurones caused CREB-dependent gene expression, increased BDNF mRNA expression and TrkB phosphorylation (Soriano *et al.*, 2006). This protected (depending on AP production) against glutamate, staurosporine or trophic deprivation in both acute and long-lasting forms and was still evident 48 hours after termination of the NMDA stimulus (Soriano *et al.*, 2006).

Preconditioning with 5 or 10μM NMDA did not affect mitochondrial membrane potential, although higher concentrations caused a dose-related loss of mitochondrial membrane potential and an associated increase in toxicity. Additionally, NMDA preconditioning caused transient increases in mitochondrial calcium levels, whereas toxic levels of NMDA resulted in sustained mitochondrial calcium rises (Soriano *et al.*, 2006). Tetrodotoxin prevented NMDA-induced AP firing, and significantly reduced the neuroprotection resulting from CREB-dependent gene expression, BDNF mRNA expression and phosphorylation of TrkB, the BDNF receptor (Soriano *et al.*, 2006).

A similar method of stimulation using the $GABA_A$ receptor antagonist bicuculline also protected against trophin withdrawal, this protection potentiated by co-application of bicuculline and the potassium channel blocker 4-AP (Papadia *et al.*, 2005, Mei *et al.*, 2000). A comparable protocol had been effective in providing protection against excitotoxicity in embryonic cerebral cortical neurones, using a combination of bicuculline and 4-AP (Tauskela *et al.*, 2008) and was considered in our experiments in order to develop a more prolonged, but lower intensity, stimulus capable of protecting against excitotoxic and oxidative damage. The fact that 4-AP was a more effective preconditioning stimulus than bicuculline suggests there are significant differences between our CGN cultures and the hippocampal and cerebral cortical cultures of other

groups. It is possible that both receptor stimulation and membrane stimulation are capable of generating the pro-survival signalling induced by this method of preconditioning, but that the former is of less importance in CGNs while being of critical importance in other neuronal types.

Jonas *et al.* (2001) showed that an extremely low concentration of glutamate protected cultures of cerebellar granule, spinal or cortical neurones against subsequent, otherwise lethal exposure to 25μM glutamate, with protection evident following exposure to 10^{-20}M or 10^{-30}M glutamate for 72 hours. However, although this indicated that prolonged, low-intensity stimulation provided protection against excitotoxic and oxidative neuronal damage, the degree of protection was limited, with viability increased by only approximately 10%. Furthermore, as there was no apparent concentration-response relationship, this model provides a less reliable method of inducing neuroprotection than could be achieved using the methods previously described.

5.7.2 Mechanisms of 4-AP preconditioning

The pharmacological and molecular mechanisms involved in 4-AP preconditioning were investigated. Tetrodotoxin, MK-801 and the L-type calcium channel blocker nifedipine were all co-applied with the preconditioning stimuli to determine the contribution of depolarisation, NMDA receptor activation and calcium channel opening respectively. The effects of the preconditioning procedure and exposure to a toxic glutamate insult on expression of bcl-2, phosphorylation of cAMP response-element binding protein (CREB) and activation of caspase-3 were also studied using Western blotting.

Protection against glutamate and NMDA was reduced by co-application of 1μM TTX but was still significant at the most effective dose of 4-AP (2500μM), although protection attained by 50μM 4-AP against glutamate was abolished by TTX. That the highest used dose of 4-AP was able to protect despite the effect of TTX (albeit to a lesser extent) is not surprising, as 4-AP has been successfully used *in vivo* to counteract the effects of TTX poisoning in guinea pigs (Chan *et al.*, 1997). This reduction in 4-AP protective effect indicates that generation of neuronal electrical activity is integral to this protection. The use of a higher concentration of TTX against 2500μM 4-AP would clarify the extent to which this protection is dependant upon depolarisation.

Co-application of MK-801 in the present study had little effect on the protection by 4-AP, showing that the mechanism involved was not dependent on NMDA receptor activation. The adverse effect of co-application of bicuculline on 4-AP-induced protection was prevented by MK-801, indicating that the effect of bicuculline was dependent on NMDA receptor stimulation. Although co-application of MK-801 alone caused a significant degree of protection against NMDA neurotoxicity, this was not equivalent to the protective effect seen with co-administration of MK-801 and 4-AP.

Furthermore, 'preconditioning' with MK-801 alone failed to protect against glutamate treatment and the increased protective effect of MK-801 co-application during 4-AP preconditioning was still present, which excluded the possibility that the protective effect of MK-801 co-application in cultures treated with toxic NMDA was due to inadequate washing out of MK-801 from the cultures. Given that such an effect was not seen against glutamate toxicity, it appears unlikely to have been due to inadequate washout, so may be an example of MK-801-induced preconditioning, which has previously been reported (Tremblay *et al.*, 2000). The difference between the effect of MK-801 on NMDA and glutamate toxicity may be due to kainate receptor activation, as although MK-801-induced preconditioning was demonstrated against both NMDA and AMPA (Tremblay *et al.*, 2000), the effect on kainate toxicity is unknown as yet.

The independence of the 4-AP-induced protective effect from NMDA receptor stimulation clearly indicated a different mechanism from those involved in the relatively high-intensity preconditioning studies considered previously, suggesting that although the broad method (bicuculline or 4-AP-induced neuronal stimulation) may be similar, the precise component (receptor stimulation or membrane depolarisation) which induces protection varies in different neuronal types. A possibility is that involvement of AMPA receptors is a critical component, a possibility which could be addressed by further study.

4-Aminopyridine has been shown previously as pharmacologically active, as 1-5mM 4-AP blocked potassium flow and sodium influx triggered by depolarisation in a dose-dependant fashion in rat neonatal CGNs at 1-7 DIV. These effects occurred rapidly and were completely reversed by 4-AP washout (Mei *et al.*, 2000). 4-Aminopyridine did not alter the voltage level required for sodium

channel activation and was insensitive to alterations in frequency of the triggering electrical pulses (Mei *et al.*, 2000). 4-Aminopyridine caused glutamate release and an increase in intracellular calcium in synaptosomes from rat cerebral cortical neurones (Zoccorato *et al.*, 2001).

The L-type calcium channel blocker nifedipine was used to test the involvement of non-NMDA receptor-mediated calcium currents on the induction of 4-AP preconditioning. Nifedipine alone however, caused significant neuronal death, greater than that induced by subsequent glutamate or NMDA, so that it was not possible to discern the effects on 4-AP preconditioning of L-type calcium channel blockade with this agent. The mechanism by which nifedipine caused increased neuronal death was unclear, although it is notable that exposure to 1μM nifedipine for 8 hours caused increased caspase-3 activation in rat CGNs (Morán *et al.*, 1999). Cerebellar granule neurone death *in vivo* caused by L-2-chloropropionic acid (acting via NMDA receptors) was increased by nifedipine and several other L-type calcium channel antagonists (Widdowson *et al.*, 1997), and as previously noted, nifedipine also potentiated the neurotoxicity of kainate (Leski *et al.*, 1999).

Inhibition of L-type calcium channels by nifedipine may have disrupted the normal responses to calcium influx due to NMDA receptor activation, resulting in a critical impairment to cytosolic calcium homeostasis or an excessive reduction of intracellular calcium. Although MK-801 did not eliminate its protective effect, 4-AP preconditioning evidently induced neuronal electrical activity, hence NMDA receptor stimulation was quite certain. As a result, the potential disruptive effect of nifedipine on calcium homeostasis during NMDA-induced calcium influx could still have occurred in our study. It has been previously noted that CGNs in high K^+ can be vulnerable to nifedipine treatment of 48 hours' duration, due to effects on levels of calcium influx via L-type calcium channels (Galli *et al.*, 1995). It is therefore clear that the sensitivity of CGNs to nifedipine prevents its use as a tool for investigating the role of calcium in 4-AP preconditioning.

Nifedipine reduced intracellular calcium in CGNs as shown by Courtney *et al.* (1990) and although in our study this may have occurred during NMDA receptor activation-mediated increases, the prolonged period of L-type calcium channel inhibition could have resulted in an excessive reduction in intracellular calcium,

triggering neuronal death. Another aspect of this specific to CGNs is that as glutamate exocytosis is calcium dependent (Section 1.2.1). Although nifedipine does not reduce calcium influx due to depolarisations itself (Galli *et al.*, 1995), the reduced intracellular calcium may inhibit glutamate release to such an extent that, as seen in CGNs maintained in 5mM KCl, depolarisation is suppressed to such an extent that apoptosis ensues. The lack of neuronal death induced by exposure to MK-801 for 48 hours indicates that lack of NMDA receptor activity was not the cause of death. However, it remains possible that the depolarisation itself was the critical factor in averting death, which would still have occurred due to AMPA and kainate receptor activity.

The mechanism of protection involved in our study could be related to the depolarisation seen in neonatal rat cerebral cortical neurones and astrocytes where treatments with KCl or 4-AP caused an increase in synthesis of kynurenic acid of about 75% (Rzeski *et al.*, 2005). Although this property would be likely to protect against OGD, the failure of 4-AP to protect against 5 hours' OGD exposure in our study could be due to the severity of the insult itself.

Injection of 5mg/kg 4-AP in mice *in vivo* induced c-Fos expression in both hippocampus and cerebral cortices, providing protection in hippocampal CA1 and CA3b regions against kainate injection between 2 and 7 days after 4-AP preconditioning, but were abolished by co-administration of MK-801 with 4-AP (Ogita *et al.*, 2005). These findings are comparable with ours, particularly the effective protection noted over 2-7 days, which encompasses the time between preconditioning and toxic insult used in our experiments. The blockade of this protection by co-application of MK-801 in the study by Ogita and co-workers does however differ from our findings.

In relation to c-Fos activation by 4-AP, increases in intracellular calcium (due to NMDA receptor stimulation, L-type calcium channel opening or release of intracellular calcium stores, all of which increase nuclear and cytoplasmic calcium) cause up-regulated expression of c-Fos (Hardingham *et al.*, 1998).

C-Fos contains two elements, a cAMP response element (CRE) and a serum response element, activated by increased nuclear and cytoplasmic calcium respectively. Transcription activated by calcium and mediated via the CRE and cAMP-response-element-binding protein (CREB) is dependent on an increase in

nuclear calcium, with the CREB activity also contingent upon its phosphorylation by Ser133, present in CGNs, and primary hippocampal neurones (Hardingham *et al.*, 1998).

Western blot analysis in the current study indicated that preconditioning with 2500μM 4-AP increased CREB phosphorylation relative to negative controls in protein samples taken at 11 DIV, 24 hours following the preconditioning. This finding suggests that CREB phosphorylation may be involved in 4-AP preconditioning, with the possibility that samples taken during or at the conclusion of the preconditioning period would gain further information towards answering this question. This would be consistent with the finding in cerebral cortical neurones that CREB phosphorylation occurred during neuronal stimulation but not after (Tauskela *et al.*, 2008).

CREB has been associated with neuroprotection and is activated by calcium currents via NMDA receptors or L-type calcium channels (Mabuchi *et al.*, 2001). Phosphorylation of CREB in the gerbil hippocampal CA1 region has been shown in response to ischaemic preconditioning, an effect suppressed by the use of CRE decoy oligonucleotide or an NMDA receptor antagonist. The CRE decoy oligonucleotide did not affect the damage produced by actual ischaemia, indicating that CREB is involved in ischaemic preconditioning, but not in ischaemia-related death (Hara *et al.*, 2003).

Raised levels of phosphorylated CREB were found in rat brains *in vivo* in the core of an ischaemic lesion but with higher levels in cells in the penumbra which subsequently survived. The penumbra-located increase was only seen in rats receiving previous ischaemic preconditioning (Nakajima *et al.*, 2002). Phosphorylation of CREB occurred in both hippocampal and cortical neurones in response to both ischaemia *in vivo* and glutamate *in vitro*, with these responses again blocked by co-application of MK-801, but not CNQX or nifedipine (Mabuchi *et al.*, 2001, Meller *et al.*, 2005).

Over-expression of bcl-2 has been shown to reduce lipid peroxidation in plasma and mitochondrial membranes, with associated increased levels of Cu,Zn-SOD, glutathione and glutathione peroxidase. These potentially have direct antioxidant actions which are complemented by increased nuclear translocation of glutathione, altering nuclear redox and thereby averting apoptosis (Bruce-

Keller *et al.*, 1998, Wei *et al.*, 2000). Such an increase in antioxidant expression may enable bcl-2 to protect against oxidative damage and to increase mitochondrial DNA repair (Deng *et al.*, 1999).

Bcl-2 over-expression also protected against the toxicity of 3-HK, an effect not due to reduced 3-HK-induced ROS generation. This implied that the protective mechanism acted downstream of ROS-induced effects, such as preventing loss of mitochondrial membrane potential and resultant release of cytochrome c or by up-regulation of calcium-ATPase on the endoplasmic reticulum (Wei *et al.*, 2000). It has been demonstrated that bcl-2 reduced release of calcium from the endoplasmic reticulum, which may be an integral component of the neuroprotective action of this protein against neurotoxic stimuli (Lam *et al.*, 1994).

In our study however, the expression of bcl-2 in CGNs was not affected by either 4-AP preconditioning or by toxic exposure to glutamate, with bcl-2 levels in all samples comparable to untreated controls, indicating that bcl-2 up-regulation does not have a critical role in this protection.

5.7.3 Preconditioning with bicuculline

Bicuculline methobromide failed to induce preconditioning against either glutamate or 3-NPA in this study and actually reduced the protection given by 4-AP. This was in direct contrast to the work of Papadia *et al.* (2005) using hippocampal neurones, but was consistent with Lange-Asschenfeldt and co-workers (2005) who showed that bicuculline induced a dose-related reduction in the protection mediated by OGD-induced preconditioning in rat hippocampal slices. Therefore, blockade of $GABA_A$ receptors in CGNs for prolonged periods appears detrimental to CGN survival in our system, although this is not likely to be due to an excitatory effect, given that no damage was induced by 4-AP, even at notably high concentrations. It is possible that $GABA_A$ receptor activation increases pro-survival signalling, independent of neuronal excitation. Another possibility is that $GABA_A$ receptor activity plays a pro-survival role via regulation of neuronal stimulation; certainly it has been demonstrated that GABA receptor activity increases the survival of CGNs in higher K^+ concentrations (Ikonomovic *et al.*, 1997), and further evidence supporting this explanation is that the co-application of MK-801 prevented cell death due to bicuculline in this study. It

may be this particular characteristic of CGNs which explains the difference between the detrimental effect seen in this study and the preconditioning effect seen in studies using hippocampal neurones.

Stimulation of synaptic NMDA receptors by bicuculline in rat hippocampal neurones caused CREB phosphorylation which was not inhibited by nifedipine, but was blocked by MK-801 or APV. This stimulation was associated with upregulation of BDNF and TrkB receptor phosphorylation (Hardingham *et al.*, 2002a). The function of CREB was controlled via calmodulin kinase activation by calcium signals dependent on a nuclear calcium pool (Hardingham *et al.*, 2001). Repeated neuronal stimulation by APs triggered by bicuculline caused rapid CREB phosphorylation, with the amplitude of resultant nuclear calcium transients varied according to the frequency of the APs (Hardingham *et al.*, 2001).

The use of bicuculline as a stimulus targeted specifically at synaptic NMDA receptor activity (minimising activation of extrasynaptic NMDA receptors) caused increased CREB phosphorylation. This was reversed by exogenous glutamate exposures, which acted on both extrasynaptic and synaptic receptors, and possibly stimulated AMPA and kainate receptors, thereby acting as an alternative source of the CREB 'shut-off' signal (Hardingham *et al.*, 2002b).

Stimulation of synaptic NMDA receptors by bicuculline in rat hippocampal neurones has been shown to cause significant increases in CREB phosphorylation, phosphatidylinositol 3-kinase (PI3K)-Akt pathway activation and resistance to apoptosis caused by trophin deprivation, staurosporine, C-2 ceramide, retinoic acid or okadaic acid (Papadia *et al.*, 2005).

5.7.4 4-AP preconditioning effective against non-apoptotic death

Protection against apoptosis in neonatal rat CGNs induced by withdrawal of a depolarising potassium concentration or serum from culture medium, was conferred by 4-AP, with an associated dose-related reduction in inward potassium current, reversed by washout of 4-AP (Hu *et al.*, 2006). Cytochrome c release and caspase-3 activation were also significantly reduced, with maximal protection provided by 5mM 4-AP, a concentration which did not lower the resting membrane potential, hence interference with potassium currents was presumed to be necessary for apoptosis to occur (Hu *et al.*, 2006).

The lack of a significant increase in caspase-3 activation due to glutamate application was consistent with previous studies by others in cortical neurones (Hou and MacManus, 2002). Caspase-3 activation was reduced by preconditioning with 2500μM 4-AP, both in CGNs subsequently exposed to glutamate and in those left untreated; although this difference did not reach significance. The type of glutamate signalling is thought to regulate the death pathway induced: with sustained slow calcium influx leading to apoptosis and rapid severe influx leading to necrosis (Berliocchi *et al.*, 2005). It is therefore proposed that glutamate treatment in our study caused a rapid influx of calcium leading to caspase-independent cell death. Both 4-AP preconditioning and CREB activation have been previously identified as being protective against apoptosis, which indicates that the mechanism of protection induced by 4-AP preconditioning may be effective at providing neuroprotection against both apoptotic and necrotic forms of cell death.

6 Discussion

Although the use of primary neuronal cultures provides a useful tool for studying the effect of treatments and conditions specifically on neurones, it should be noted that since the conditions in culture differ in several respects from those *in vivo*, the results achieved may differ as a result. One of the main differences (and one which was deliberately achieved) is the absence of glial and other non-neuronal cells from the culture environment. This will alter the effect that is achieved with toxins, as the toxicity (for example) QA may in part be mediated by its effect on glial cells (Guillemin *et al.*, 2005), and any neuroprotective effect mediated by glial cells against any of the toxic treatments will be similarly absent.

Beyond the absence of the glial cells in the direct effects of toxic stimuli, the absence of glia will also affect excitotoxic stimuli in more subtle ways, such as the lack of glia sheathing synapses between CGNs, which will reduce the clear distinction between endogenous glutamate activating synaptic and extrasynaptic NMDA receptors. Another effect of producing monolayer cultures is to disrupt the normal neuronal architecture of the cerebellum, which may potentially alter the responses of CGNs to stimuli and toxins by interrupting the normal interplay between CGNs, mossy fibre neurones and Purkinje cells, although this effect is likely to be less significant than the absence of glia from cultures.

Therefore, although the purity of neuronal cultures allows a great degree of clarity in determining the precise effect of various stimuli on neurones, further work to determine how these effects are manifested *in vivo* would be required to better determine their relevance to the development of pathologies or treatments. An alternative would be to use cultures of tissue slices, which would preserve the tissue architecture at least to an extent, and also preserve the presence and function of glial cells. This latter course would however still involve removing the tissue from its normal physiological environment and replacing that with culture medium. It has been suggested that the culture procedure itself causes cells to be exposed to excessive amounts of oxidative stress, due to increased ROS generation and reduced antioxidant defences (Halliwell, 2003).

A delicate balance exists in CGNs regarding the extent of excitatory activity and associated influx of calcium, with neuronal death being the consequence of these variables becoming either excessive or insufficient. The establishment of optimal culturing conditions concerning cell density and K^+ concentration showed that even a moderate shift in levels of excitation (in either direction) caused striking effects on neuronal viability.

The effect of these on calcium influx has been clearly established, with excessive increases or decreases in influx triggered by alterations in culturing conditions inducing cell death (Gallo *et al.*, 1987, Peng *et al.*, 1991, Morán *et al.*, 1999). This occurs through various mechanisms, with necrotic or apoptotic cell death due to excessive calcium influx, in the case of receptor over-stimulation, or apoptosis in the case of inadequate stimulation. It has also been shown that neurones subjected to mild stimulation undergo a homeostatic change, increasing their vulnerability to a sudden reduction in excitation (Moulder *et al.*, 2003). Conversely, a mild increase in intracellular calcium allows neuronal survival in the absence of nerve growth factor (Franklin and Johnson Jr., 1994).

The protective effect of higher K^+ concentrations on CGNs is believed to be due to calcium flux and resultant alteration to intracellular calcium levels. Blockade of calcium channels was effective in both preventing the protective effect of raised K^+ concentrations and in decreasing the toxic effect of K^+ withdrawal, while inhibitors of calmodulin also blocked the protection from higher K^+ levels (Gallo *et al.*, 1987, Daniels and Brown, 2002). Conversely, dihydropyridine calcium agonists protected when combined with 15mM KCl but caused higher levels of death during K^+ withdrawal (Gallo *et al.*, 1987).

These findings might seem somewhat contradictory, but the differences in the effects of blocking or amplifying calcium signalling can be explained. Uptake of radio-labelled calcium is more than two-fold greater in CGNs cultured in a lower (5.4mM) than in a higher (24.5mM) K^+ concentration (Peng *et al.*, 1991). This disparity in calcium current magnitude caused by different K^+ concentrations could lead the effect of blocking calcium currents to be similarly disparate. If calcium currents were sufficient to generate beneficial effects (as could occur in CGNs in depolarising K^+ concentrations), then blockade of these currents would

lead to inadequate stimulation and increase neuronal death. Certainly, it has been shown that hippocampal neurones maintained in depolarising K^+ concentrations are vulnerable to a reduction in stimulation and resultant reduced calcium influx (Moulder *et al.*, 2003). Conversely, such blockade of channels in the presence of excessive calcium currents (as may occur in CGNs in lower K^+ concentrations) could be protective. Considering the key role of excessive calcium in NMDA receptor-mediated excitotoxic damage, this explanation is highly plausible.

A related finding concerning CGNs cultured in 25mM KCl but transferred to serum-free medium containing 5mM KCl at 6 DIV is that this change caused a drop in intracellular calcium from ~300nM to ~50nM, leading to cell death via caspase-3 activation (Morán *et al.*, 1999). A similar study compared neonatal rat CGNs transferred to 5mM KCl with CGNs maintained in 30mM KCl. It was found that incubation of neonatal rat CGNs in 5mM KCl for 4 hours caused increased caspase-3 and calpain activity, significant cell death and neurite retraction compared with cultures in 30mM KCl, with caspase-3 activation and cell death blocked by the p38 blocker SB-203580 (Nath *et al.*, 2001). This is also consistent with the theory that higher K^+ induces a lower sensitivity of calcium channels to stimulation, which makes a drop in stimulation potentially lethal. Conversely, maintenance from plating in lower K^+ leads to hypersensitivity of calcium channels and a resultant predisposition to excessive calcium influx.

The failure of NMDA antagonists to induce effective protection against stroke in clinical trials (Davis *et al.*, 2000), despite the success of NMDA receptor blockade in animal models (Iijima *et al.*, 1992, Mies *et al.*, 1993) suggests that this equilibrium of receptor stimulation is finely balanced, and may imply significant differences between animal models and human subjects. There is however another explanation for this failure, namely the simple –but critically important- logistical factor that emergency clinical management of stroke very rarely begins immediately after the event. Therefore, by the time NMDA antagonists can be applied, the excitotoxic damage has occurred and NMDA blockade prevents sublethal (and potentially beneficial) stimulation (Ikonomidou and Turski, 2002).

Further discrepancies in NMDA receptor activation have been noted in studies of neuronal excitation. The responses to stimulation of synaptic (predominantly

located on dendritic spines) and extrasynaptic (mostly located on the soma) NMDA receptors varied, with exclusively neurotrophic signals triggered by stimulation of the former, whereas excitation of the latter caused exclusively pro-death signalling (Hardingham *et al.*, 2002b). It is unlikely that this was due to a property of the extrasynaptic NMDA receptors themselves, given that low concentrations of exogenous NMDA induced protection effectively, as exclusively synaptic receptor stimulation with bicuculline had done (Papadia *et al.*, 2005, Soriano *et al.*, 2006).

Further evidence casting doubt on this theory is that NMDA receptor subunits NR2A and NR2B are found predominantly in synaptic and extrasynaptic receptors respectively, but both OGD and NMDA preconditioning have been successful in cultures with very low levels of NR2A, suggesting involvement of NR2B subunits or NR1 in this preconditioning (Tauskela and Morley, 2004). However, it has been demonstrated that NR2B-containing receptors may have either pro-survival or neurotoxic properties during different stages of development of the same neuron (Martel *et al.*, 2008), indicating that the alternative pathways leading to protection or toxicity are not due to the subunit composition of receptors.

A potential explanation for the discrepancy is the difference in sensitivity to calcium influx exhibited by mitochondria in each of these locations, with dendritic mitochondria showing a greater capacity for calcium uptake than somal mitochondria (Young *et al.*, 2008). It is possible therefore that activation of both groups of NMDA receptors leads to similar fluxes in calcium, but that these translate into opposing signals depending on the differing abilities of mitochondria in various cellular locations to respond to them.

Removal of extracellular calcium protects against glutamate-induced excitotoxicity in cortical, hippocampal and cerebellar neurones *in vitro,* as does NMDA, AMPA or kainate receptor antagonism (Manev *et al.*, 1989, Choi and Rothman, 1990). By far the most important receptor for glutamate-mediated excitotoxicity in CGNs however, is the NMDA receptor, blockade of which is far more protective than kainate receptor blockade (Manev *et al.*, 1989). The degree of cell death due to excitotoxicity in rat CGNs is proportional to neuronal calcium uptake and the NMDA dose applied; the intracellular calcium concentration at which 50% of CGNs died was calculated as being approximately

17mM, a striking contrast to the ~300nM normally present (Eimerl and Schramm, 1994, Morán *et al.*, 1999).

Further, glutamate-induced CGN death can be reduced by NMDA receptor antagonists applied after a toxic glutamate insult or by removal of extracellular calcium up to 30 minutes after glutamate exposure. This indicates that glutamate-induced excitotoxicity continues to damage beyond the initial insult (Manev *et al.*, 1989, Choi and Rothman, 1990). Activation of PKC attenuated NMDA-mediated calcium increases, perhaps by feedback inhibition of the NMDA receptor itself by PKC (Snell *et al.*, 1994).

Calcium imaging showed NMDA receptor activation led to calcium influx and mitochondrial calcium accumulation, with subsequent partial mitochondrial depolarisation preventing calcium uptake into the mitochondrial matrix, ameliorating increases both in cytoplasmic free calcium and in cell death (Budd and Nicholls 1996). This protective action of mitochondrial depolarisation affected the immediate calcium influx following NMDA receptor activation and also the calcium efflux into the cytoplasm, known as delayed calcium deregulation (DCD). This occurred approximately 40 minutes after the initial insult and was triggered by NMDA receptor activation, but was not reversed by NMDA receptor inhibition or prevention of mitochondrial permeability transition (MPT) pore opening (Castilho *et al.*, 1998, Ward *et al.*, 2005).

Excitotoxicity due to glutamate caused increased mitochondrial superoxide production, correlated with higher cytoplasmic calcium levels. Also antioxidant treatment was effective in delaying DCD, indicating that ROS induce loss of mitochondrial calcium regulation (Castilho *et al.*, 1999). Although MPT pore opening causes leakage of calcium and ROS from the mitochondria, release of cytochrome c from the mitochondria due to excess calcium influx can occur independently of MPT pore opening in rat brain mitochondria, in contrast to rat liver mitochondria (Andreyev and Fiskum, 1999, Chalmers and Nicholls, 2003).

Nitric oxide is also active in this process, as stimulation of NMDA receptors resulted in calcium-dependent production of NO and superoxide (which can lead to formation of the potent oxidative agent peroxynitrite). Production of ROS by glutamate was abolished by MK-801, SOD, removal of extracellular calcium or application of the NO scavenger reduced haemoglobin (Gunasekar *et al.*, 1995).

A possible key stage in cytoplasmic calcium deregulation is the destruction of the plasma membrane calcium pump by calcium-activated calpains (Bano *et al.*, 2005). Certainly this pump can be cleaved by caspases in mouse CGNs due to glutamate-induced excitotoxicity, a finding reproduced in rat neurones by ischaemia, and could be blocked by NMDA antagonists (Schwab *et al.*, 2002). This provided a possible link between apoptosis and necrosis, as cleavage of plasma membrane calcium pumps caused an excess of intracellular calcium, which in turn caused subsequent necrotic cell death (an effect delayed in cells with a non-cleavable mutant form of calcium pump) despite the initial triggering of apoptotic cell death mechanisms (Schwab *et al.*, 2002).

It is also evident that alterations in neuronal metabolic activity, which naturally affect mitochondria, will impact on excitotoxic and oxidative insults. Although neither the toxicity of glutamate nor that of 3-NPA were potentiated by increasing the glucose concentration in the medium to 25mM, this glucose concentration rise did have a potentiating effect on the toxicities of treatment with tryptophan and several of its metabolites. This was largely due to the osmotic effect of the increased glucose concentration, but the degree of potentiation was not entirely explained by this, suggesting that an underlying oxidative stress effect increased vulnerability, but was insufficient to cause cell death itself. This is consistent with previous findings identifying an increased vulnerability to excitotoxic and oxidative damage due to ischaemia (Muranyi *et al.*, 2003), and that a higher glucose concentration (45mM) *in vitro* can induce a number of indications of increased oxidative stress (Vincent *et al.*, 2005).

The potential sub-lethal effects of increased glucose concentration raise questions of what changes are induced, both in indications of cell damage and of increased activation of antioxidant defences. A proteomic study of neuronal tissue exposed to a range of different concentrations of glucose would be one possible route by which further information could be gained.

The demonstration that three of the compounds on the kynurenine pathway of tryptophan metabolism (3-HK, 3-HAA and 5-HAA) were potently neurotoxic gave scope for further investigation of the mechanisms involved and associated cell death pathway activation. The toxicity of all three was unaffected by SOD, but significantly reduced by catalase, indicating that the production of superoxide is

not a critical step in the development of neurotoxicity (and therefore the production of peroxynitrite is unlikely to be implicated), but that either H_2O_2 or its product the free hydroxyl radical is the likely agent which induces damage.

Superoxide was produced by both 3-HK and 3-HAA in PBS alone. Superoxide generation by 3-HAA, although not by 3-HK, was also significantly increased by Cu^{2+}. Both 3-HK and 3-HAA were unable to generate H_2O_2 in PBS alone, but when Cu^{2+} was present, both compounds produced significant amounts of H_2O_2, with copper ions cycling between oxidised and reduced status for multiple cycles of H_2O_2 generation. This increase in H_2O_2 production was completely abolished by catalase at a concentration of 1000U/ml and reduction in molecular oxygen concentration also markedly inhibited H_2O_2 production (Goldstein *et al.*, 2000).

In another study of 3-HAA oxidation, auto-oxidation in aerobic reaction solution was reported and oxidation of 3-HAA was increased dramatically by addition of Cu,Zn-SOD to anaerobic solution or by re-admittance of air in anaerobic conditions. The most likely explanation for this was not the catalytic activity of SOD (as Mn-SOD was ineffective), but copper ions acting as redox reagents for the oxidation of 3-HAA (altering from Cu^{2+} to Cu^{+}), followed by re-oxidation of Cu^{+} by O_2- (Liochev and Fridovich, 2001).

This process can be summarised as follows:

3-HAA + O_2 $\rightleftharpoons$ Anthranilyl radical + O_2^-

$2O_2^-$ + $2H^+$ —*SOD*→ H_2O_2 + O_2

H_2O_2 + Fe^{2+} → $HO^\cdot$ + OH^- + Fe^{3+}

Fe^{3+} + 3-HAA → Fe^{2+} + Anthranilyl radical

Consequently, 3-HAA (in the presence of oxygen) will increase levels of superoxide and with Fe^{3+} (or Cu^{2+}) increase levels of Fe^{2+} (or Cu^{+}). Both of these changes act on the middle equations to increase H_2O_2 levels if SOD is present and thus act to increase levels of hydroxyl radical formed from H_2O_2. Additionally, the removal of superoxide tips the equilibrium of the top equation towards generation of further anthranilyl radical and superoxide.

Certainly this explanation is consistent with the finding in cell-free buffer that 3-HAA produced hydroxyl radical; this process was enhanced by SOD, a more alkaline pH or the presence of EDTA (ethylene diamine tetra-acetic acid), but was abolished by the presence of either desferrioxamine or catalase (Iwahasi *et al.*, 1988). The amount of hydroxyl radical produced in a Fenton reaction solution containing hydrogen peroxide and Fe^{3+} ions was increased by addition of 3-HAA (adding 3-HK caused a lesser increase in hydroxyl radicals than 3-HAA), and assay of Fe^{3+} ion reduction suggested that reduction of Fe^{3+} was caused by 3-HAA under these conditions (Iwahashi *et al.*, 1988). Furthermore, auto-oxidation of 3-HAA in sodium phosphate buffer can be increased by Cu,Zn-SOD, Mn-SOD or catalase, although not by inactivated Cu,Zn-SOD. As catalase did not inhibit this effect, the action of SOD on auto-oxidation was not reliant on formation of H_2O_2, suggesting that removal of superoxide played a significant part (Ishii *et al.*, 1990).

Generation of ROS was achieved more readily when o-, m- and p-aminophenol were added instead of 3-HAA (Iwahashi *et al.*, 1988). The presence of an aminophenol ring structure on the 5-HAA molecule suggests that this is the generator of ROS in both 3-HAA and 5-HAA, and consequently that 5-HAA constitutes a source of oxidative damage of comparable severity to the established neurotoxins 3-HK or 3-HAA. This also provides a possible explanation for the link between infarct volume and higher ratios of anthranilic acid to 3-HAA, as 5-HAA is a metabolic product of anthranilic acid: higher levels of anthranilic acid may be a risk marker for higher levels of the actual neurotoxin 5-HAA, rather than being the actual mediator of the damage.

When reviewing the chemical equations covering the reactions involved in the activity of 3-HAA (and presumably of 5-HAA also), it was apparent that SOD alone should not be protective, as the molecular oxygen produced by the dismuting of H_2O_2 can be converted to superoxide radical by 3-HAA, which simply allows further generation of ROS by the compound to continue. Conversely, the action of catalase interrupts this process, removing both the source of hydroxyl radical and molecular oxygen required for 3-HAA to generate superoxide.

As it is already known that 3-HK, 3-HAA and the aminophenol ring structure common to both 3-HAA and 5-HAA produce both superoxide and H_2O_2 (Goldstein

et al., 2000), it is clear that these unavoidable metabolic products constitute an ongoing source of oxidative stress during life. Furthermore, treatment with 3-HK and 5-HAA was also associated with increased p38 activation, directly implicating them in signalling for apoptosis, although there was no indication of increased caspase-3 activation.

Oxidative stress is a significant source of pathology in neurones, as evidenced by the effects of amyloid-ß in Alzheimer's disease or the mimicry of Parkinson's disease by the mitochondrial poison MPTP. This suggests that the ongoing generation of low-level oxidative damage due to the actions of kynurenine pathway compounds or excessive glucose could be an important cause of cumulative neuronal loss.

The potentially neurotoxic actions caused by physiological levels of kynurenine pathway compounds are could also continue throughout life, and while subtoxic in healthy individuals, have the ability to induce gradual neurotoxic damage in the setting of abnormally vulnerable neurones. The abnormally functioning mitochondria of Huntington's disease patients could cause neurones to be abnormally vulnerable, resulting in the generation of neuronal death by one or more of these compounds, with QA being a likely source.

Hitherto, 5-HAA has received sparse attention as a potential generator of neurotoxic damage, having been noted for little more than being a potential generator of ROS in cataract formation (Truscott and Elderfield, 1995). The findings in this study clearly show that this compound should be considered as a potential source of neurotoxic damage alongside the other, more extensively studied tryptophan metabolites. As a result of this finding, there would appear to be little potential for a possible therapeutic intervention by reducing kynurenine mono-oxygenase activity (and thus reducing the amount of 3-HK formed), as the resultant relative increase in anthranilic acid would in turn lead to an increase in 5-HAA. Although anthranilic acid has less toxic potential than 3-HK, the subsequent conversion to 5-HAA would eliminate even this limited benefit. As kynureninase is involved in conversion of both kynurenine to anthranilic acid and 3-HK to 3-HAA, increasing this enzyme's activity would not be beneficial, and blockade of its activity is not an available therapy, as this would prevent formation of nicotinamide.

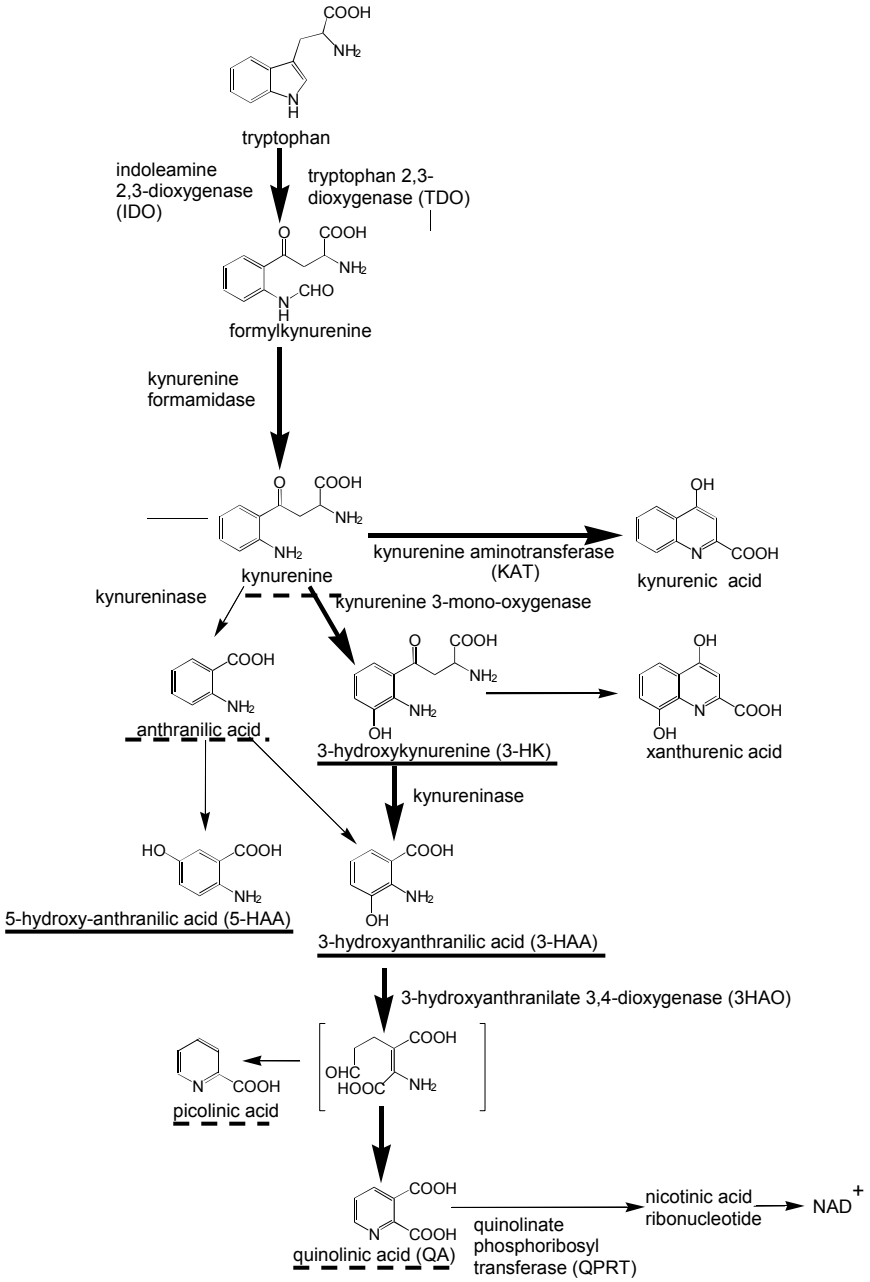

Figure 6.1 Adjusted diagram of kynurenine pathway, showing addition of findings of study: broken underlining denotes moderate neurotoxicity; solid underlining indicates a strong neurotoxic effect.

A potential intervention would be to increase the activity of 3-hydroxyanthranilic acid oxygenase, which metabolises 3-HAA, although this would increase levels of QA and picolinic acid. Therefore, the most inviting target for therapy in terms of manipulation of the pathway would be to increase the activity of the enzyme quinolinic acid phosphoribosyl transferase, which catalyses the first step of the conversion of QA to nicotinamide. This enzyme has been demonstrated to be present in the brain, having been identified in glial cells throughout the hippocampus (Köhler *et al.*, 1988), an area especially

vulnerable to QA's excitotoxic action. An alternative may lie in the action of the enzyme α-amino-ß-carboxymuconate-ε-semialdehyde decarboxylase, which acts on the precursor to QA (and picolinic acid) α-amino-ß-carboxymuconate-ε-semialdehyde, coverting it to a benign compound which may then be coverted to acetyl-CoA (Fukuoka *et al.*, 2002).

Although kynurenine pathway compounds may be involved in the pathology of neurodegenerative disorders, the excitotoxicity and oxidative stress induced by ischaemia is better modelled by subjecting CGNs to OGD. The development of an effective system for generating OGD allowed this insult to be applied. As an important part of the toxicity of OGD when applied to CGN cultures is the increase in glutamate release which it induces (Tauskela *et al.*, 2003), it is likely that a relatively minor alteration in response to OGD (in terms of altered endogenous glutamate release) could cause a notable disparity in the neurotoxic effect in CGNs.

In order to achieve a consistent neurotoxic insult, CGN cultures were subjected to OGD for 5 hours, a period which both successful preconditioning protocols were unable to protect against, suggesting that this insult was extremely severe. However, it should be noted that despite the successful use of NMDA preconditioning to protect CGNs by ourselves and other groups, we are unaware of any studies where this has been used to effectively protect CGNs against OGD.

That OGD of 5 hours duration was a severe insult was also demonstrated by the fact that blockade with MK-801 or kynurenic acid was ineffective in protecting against it, indicating that OGD was likely causing cell death by preventing ATP production, independent of receptor activation. The finding that protein synthesis blockade during and after OGD was not protective also indicates that OGD of this severity induced necrotic cell death, in a manner paralleling that seen in an infarct 'core' (Hou and MacManus, 2002).

A future route of investigation to further clarify the effects of OGD on CGN neurones could be to vary the duration of the OGD period, studying the extent of neurotoxicity (and degree of variation in this) at each time point, and identifying the efficacy of NMDA receptor blockade in protecting against this insult as the duration of OGD increases. Furthermore, the effects of OGD on calcium influx and mitochondrial calcium control, particularly how these alter as OGD duration

increases could provide valuable information both on the neurotoxic actions of OGD and also the mechanisms active in different regions of an infarct.

The use of a relatively high-intensity, but comparatively brief preconditioning stimulus with NMDA in this study was capable of providing protection against subsequent excitotoxicity and oxidative stress. It is possible that NMDA preconditioning involves calcium-induced cell death mechanisms, as calpain expression in rat cerebral cortical neurones was significantly reduced by NMDA preconditioning prior to either toxic NMDA or OGD exposure (Tauskela *et al.*, 2001). Additionally, preconditioning with NMDA caused a significant decrease in intracellular calcium signalling during otherwise lethal OGD treatments, although this did not occur with exposure to a lethal dose of NMDA (Tauskela *et al.*, 2001), suggesting the involvement of different mechanisms in each of these insults. Similar findings have been reported with reduced cytosolic calcium levels after two days in hippocampal slices preconditioned with NMDA and gerbil brain preconditioned by ischaemia (Ohta *et al.*, 1996, Shimazaki *et al.*, 1998).

The discrepancy in effect of NMDA preconditioning on intracellular calcium signals between cultures subjected to OGD and toxic NMDA (Tauskela *et al.*, 2003) suggests that changes to calcium signals were secondary to differences between stimulation with endogenous and exogenously-applied NMDA receptor agonists. This could be due either to OGD-induced endogenous glutamate release stimulating only synaptic NMDA receptors (excluding extrasynaptic NMDA receptors) or to stimulation of non-NMDA glutamate receptor subtypes by glutamate, with related effects on depolarisation and calcium influx. However, excitotoxicity induced by either exogenously applied glutamate or MPP^+-induced release of endogenous synaptic glutamate caused cleavage of plasma membrane calcium pumps (Schwab *et al.*, 2002). This suggests that differences in response may be due to factors other than the location of the NMDA receptors.

Variation between the two insults was also seen by Tauskela and co-workers (2003) in that inhibition of calmodulin-dependant protein kinase II with KN-62 caused a significant loss of protection by NMDA preconditioning against OGD, but not protection against toxic NMDA, although the KN-62 also significantly reduced the toxicity of exogenous NMDA in non-preconditioned neurones: an effect not seen against OGD (Tauskela *et al.*, 2003).

Calcium flux through the NMDA receptor activates CaMKII, found in glutamatergic synapses and involved in synthesis and release of neurotransmitters, which provides a potential mechanism by which NMDA preconditioning could reduce extracellular glutamate during OGD (Fink and Meyer, 2002).

Generation of oxidative stress was also induced by NMDA preconditioning, as co-application of antioxidants during preconditioning significantly reduced the degree of protection afforded against subsequent OGD (Tauskela *et al.*, 2003). Part of the protection involved was due to ROS generation in the mitochondria, as blockade of the mitochondrial anion channel with 4,4'-diisothiocyanostilbene-2,2'-disulfonic acid (DIDS) caused a significant reduction in protection against subsequent NMDA or OGD exposure (Tauskela *et al.*, 2003). However, this did not completely abolish protection due to NMDA preconditioning, indicating that it was not of critical importance, even if it was a component of protection.

Mitochondrial calcium levels increase when cytosolic calcium levels increase (e.g. NMDA receptor activation, plasma membrane depolarisation), or due to physiological calcium signalling. It is therefore possible that preconditioning brings calcium levels to a level just below the threshold at which cell death would be induced, although as this seems not to be a mitochondrial calcium level and could instead be a cytosolic one.

3-Nitropropionic acid as a toxic insult was also investigated alongside glutamate since the dual toxic properties of this compound (NMDA receptor activation and inhibition of succinate dehydrogenase) induce simultaneous excitotoxic and more directly oxidative insults to neurones. Both of these effects are further augmented by 3-NPA's reduction of ATP production.

As a result of this, preconditioning with NMDA against subsequent 3-NPA exposure was also tested, and effective protection was thus demonstrated against a range of neurotoxic mechanisms. Although this method of preconditioning was not associated with any reduction in neuronal viability, the degree of protection conferred varied in extent between experiments, apparently due to variations in sensitivity to excitatory stimulation from one set of neurones to the next. This finding is in keeping with other work using cerebral cortical neurones (Tauskela *et al.*, personal communication) and suggests that

there is a very narrow range of stimulation intensities which will successfully induce preconditioning via this method.

This is strengthened by clinical evidence in patients suffering cardiac ischaemia, where even ischaemic preconditioning stimuli sufficiently severe to cause pain may still be inadequate to induce protection against a subsequent infarction (Psychari *et al.*, 2004). It is possible that this treatment is actually essentially mildly damaging, but the protective response invoked reduces vulnerability for a brief period afterwards (perhaps being somewhat comparable to the increase in antioxidant defences that occurs in response to hyperglycaemia). Generation of ROS by NMDA preconditioning in neurones was show to be an essential component of protection, as this was significantly reduced by antioxidant treatment during preconditioning is further evidence in support of this (Tauskela *et al.*, 2003).

These issues raise serious questions over whether this method of preconditioning would be effective in providing a sound basis for the development of clinical treatments to prevent or ameliorate damage caused by excitotoxic or oxidative damage due to ischaemia or any other pathology. The evidently very narrow therapeutic window raises concerns that the treatment risks being not only ineffective, but potentially a source of excitotoxic damage itself.

As a result of these concerns, the successful induction of protection using a stimulus which showed no toxic potential, was consistently effective and provided a higher degree of protection against a range of insults was an important development of this study. Considering the correlation between increasing NMDA concentrations and toxicity-linked loss of mitochondrial membrane potential, and the strikingly different calcium level alterations seen with different doses (Soriano *et al.*, 2006), the use of an excitatory stimulus more distant to the threshold of excitotoxic damage warrants further experiments.

Exposure of CGNs to 50-2500μM 4-AP was an effective preconditioning stimulus that gave protection against excitotoxic treatments (glutamate and NMDA) and also against a combined excitotoxic and oxidative insult (3-NPA). Interestingly, and in contrast both to our previous findings with NMDA and to work using similar prolonged stimulations (Tauskela *et al.*, 2008), there was no dependence

on NMDA receptor activation, suggesting a notably different mechanism to our previous work. It was advantageous to identify such a difference, given the shortcomings of the previous paradigm that have already been considered.

Although NMDA receptor activation was not required for the development of this protection, neuronal electrical activity was a critical component, as blockade of sodium channels with TTX reduced or prevented protection. This suggests that the source of neuroprotection in this model of preconditioning may in fact be based on the actual depolarisation of neurones, irrespective of neurotransmitter or receptor activity. It is possible that this method of preconditioning with 4-AP causes a homeostatic change that leads to reduced vulnerability to over-excitation, in a manner comparable to that seen by Moulder *et al*. (2003).

The use of 4-AP to precondition the hippocampi of mice *in vivo* against kainate was shown to be dependent on NMDA receptor activation, although increased expression of c-Fos suggested that calcium influx via the NMDA receptor was most likely a key component of protection (Ogita *et al.*, 2005). That CREB phosphorylation may be involved in 4-AP preconditioning in our study suggests a similar mode of action exists in both models. Our finding that 4-AP preconditioning may act independently of NMDA receptor activation may therefore indicate that this method of protection can protect both glutamatergic and non-glutamatergic neurones equally effectively.

Further investigation of 4-AP preconditioning identified that the cell death induced by glutamate was independent of caspase-3 activation, suggesting that 4-AP preconditioning was effective against necrotic insults. The importance of the finding that this protection was active against non-apoptotic neuronal cell death is that a very similar method of protection has been previously demonstrated to be effective against apoptotic cell death (Papadia *et al.*, 2005). Therefore, this method of preconditioning could provide the basis for protection of neurones that is effective in both the core and penumbra of an infarct. An additional benefit would be giving protection to cells vulnerable to both mechanisms, i.e. those initially targeted for apoptosis, but which subsequently switch to necrotic cell death due to falling ATP.

The potential involvement of calcium influx (with resultant CREB activation) in 4-AP preconditioning was independent of NMDA receptors, so may have occurred

due to calcium influx via voltage-dependent calcium channels, an effect which has been shown to be neuroprotective (Mabuchi *et al.*, 2001). The neurotoxic effect of nifedipine treatment prevented the role of these channels in preconditioning from being established in this study. This was similar to the deleterious effect of NMDA receptors post-stroke, where even neurones with increased calcium influx suffer from the complete blockade of calcium channel currents and resultant disruption of calcium homeostasis.

There is significant scope for further investigation of how this method of preconditioning effects protection, such as whether the use of simultaneous blockade of AMPA and NMDA receptors would be effective in preventing protection. As influx of calcium due to AMPA receptor activation is an integral part of the activation of long-term potentiation, it is possible that this source of calcium influx is also critical to the development of this method of protection.

More generally, determining the role played by calcium in this paradigm would be of great value, both in terms of understanding the effects of prolonged 4-AP stimulation on calcium currents during preconditioning, and ascertaining the role they play in relation to CREB activation. Identifying the effect of temporary L-type calcium channels blockade on 4-AP-induced calcium currents during preconditioning would also provide useful information. Another aspect of this would be to discover what changes 4-AP preconditioning makes to the calcium influxes induced by subsequent glutamate or 3-NPA exposure, either to the initial influx of calcium from the extracellular environment or to the subsequent efflux of mitochondrial calcium. Alteration of mitochondrial regulation of calcium levels either during preconditioning or the toxic treatment gives a possible explanation for the protective mechanism of 4-AP preconditioning.

Given the prolonged period over which 4-AP preconditioning has been applied in this study, an obvious question is what duration of stimulation is necessary to induce protection, and whether the duration of preconditioning correlates with the longevity of protection. Additionally, investigation of the effects on protein synthesis could provide key information to further identifying the mechanism of protection. A limited investigation of potential candidate proteins gave mixed results: activation of CREB may be involved, although an up-regulation of bcl-2 was not implicated; likely alternative candidate proteins could include PKC and

ERK. An alternative course of investigation would be to perform proteomic studies of preconditioned tissue in order to identify potential mechanisms.

Although further work is required to gain better understanding of the mechanisms involved, the identification of 4-AP preconditioning as effective in providing protection against excitotoxic and oxidative neurotoxicity indicates that this may provide the basis for successful protective treatments.

7 Potential future avenues of study

There are a number of different areas which could be considered for further study based on this work:

- Proteomic study of products of hyperglycaemia in neuronal cultures
- Study of effect of OGD over range of durations on NMDA receptor activation and calcium influx in CGNs
- Calcium imaging of 48-hour preconditioning
- Exploration of onset and duration of 48-hour 4-AP protection
- Study of effect of 48-hour preconditioning on ERK and PKC expression
- Proteomic study of 48-hour preconditioning: effects on protein production

7.1 List of Publications

Smith AJ, Smith RA, Stone TW, (2007). Effects of preconditioning on viability of cultured cerebellar neurones (Abstract). British Neuroscience Association Abstracts 19, p141. (ISSN 1345-8301)

Smith AJ, Stone TW, Smith RA, (2007). Neurotoxicity of tryptophan metabolites. Biochemical Society Transactions 35: 1287-1289

Smith AJ, Stone TW, Smith RA (2008). Preconditioning with NMDA protects against toxicity of glutamate or 3-nitropropionic acid in cultured cerebellar granule neurones. Neuroscience Letters, in press, doi:10.1016/j.neulet.2008.05.066

References

Abe T, Takahashi S, Fukuuchi Y, (2002). Reduction of Alamar Blue, a novel redux indicator, is dependent on both the glycolytic and oxidative metabolism of glucose in rat cultured neurons. Neuroscience Letters 326: 179-182

Ahmadian G, Ju W, Liu L, Wyszynski M, Lee SH, Dunah AW, Taghibiglou C, Wang Y, Lu J, Wong TP, Sheng M, Wang YT, (2004). Tyrosine phosphorylation of GluR2 is required for insulin-stimulated AMPA receptor endocytosis and LTD. The EMBO Journal 23: 1040-1050

Ahmed SA, Gogal RM Jr, Walsh JE, (1994). A new rapid and simple non-radioactive assay to monitor and determine the proliferation of lymphocytes: an alternative to [^{3}H] thymidine incorporation assay. Journal of Immunological Methods 170: 211-224

Aketa S, Nakase H, Kamada Y, Hiramatsu K, Sakaki T, (2000). Chemical preconditioning with 3-nitropropionic acid in gerbil hippocampal slices: therapeutic window and the participation of adenosine receptor. Experimental Neurology 166: 385-391

Alexi T, Hughes PE, Faull RLM, Williams CE, (1998). 3-Nitropropionic acid's lethal triplet: cooperative pathways of neurodegeneration. NeuroReport 9: R57-R64

Altman J, Bayer SA, (1978). Prenatal development of the cerebellar system in the rat I: cytogenesis and histogenesis of the deep nuclei and the cortex of the cerebellum; Journal of Comparative Neurology 179: 23-48

Altman SA, Randers L, Rao G, (1993). Comparison of Trypan blue dye exclusion and fluorometric assays for mammalian cell viability determination. Biotechnology Progress 9: 671-674

Alvarez S, Blancas S, Morán J, (2006). Effect of NMDA antagonists on the death of cerebellar granule neurons at different ages. Neuroscience Letters 398: 241-245

Andiné P, Lehmann A, Ellrén K, Wennberg E, Kjellmer I, Nielsen T, Hagberg H, (1988). The excitatory amino acid antagonist kynurenic acid administered after hypoxia-ischemia in neonatal rats offers neuroprotection. Neuroscience Letters 90: 208-212

Andreyev A, Fiskum G, (1999). Calcium induced release of mitochondrial cytochrome c by different mechanisms selective for brain versus liver. Cell Death and Differentiation 6: 825-832

Ankarcrona M, Zhivotovsky B, Holmstrom T, Diana A, Eriksson JE, Orrenius S, Nicotera P, (1996). Laminin and ß–tubulin fragmentation precede chromatin degradation in glutamate-induced neuronal apoptosis. NeuroReport 7: 2659-2664

Annepu J, Ravindranath V, (2000). 1-Methyl-4-phenyl-1,2,3,6-tetrahydropyridine-induced complex I inhibition is reversed by disulfide reductant, dithiothreitol in mouse brain. Neuroscience Letters 289: 209-212

Arthur PG, Lim SCC, Meloni BP, Munns SE, Chan A, Knuckey NW, (2004). The protective effect of hypoxic preconditioning on cortical neuronal cultures is associated with increases in the activity of several antioxidant enzymes. Brain Research 1017: 146-154

Atabay C, Cagnoli CM, Kharlamov E, Ikonomovic MD, Manev H, (1996). Removal of serum from primary cultures of cerebellar granule neurons induces oxidative stress and DNA fragmentation: protection with antioxidants and glutamate receptor antagonists. Journal of Neuroscience Research 43: 465-475

Atlante A, Gagliardi S, Minervini GM, Ciotti MT, Marra E, Calissano P, (1997). Glutamate neurotoxicity in rat cerebellar granule cells: a major role for xanthine oxidase in oxygen radical formation. Journal of Neurochemistry 68: 2038-2045

Baines CP, Goto M, Downey JM, (1997). Oxygen radicals released during ischemic preconditioning contribute to cardioprotection in the rabbit myocardium. Journal of Molecular and Cellular Cardiology 29: 207-216

Balázs R, Jørgenson OS, Hack N, (1988). *N*-methyl-D-aspartate promotes the survival of cerebellar granule cells in culture. Neuroscience 27: 437-451

Bano D, Young KW, Guerin CJ, Lefeuvre R, Rothwell NJ, Naldini L, Rizzuto R, Carafoli E, Nicotera P, (2005). Cleavage of the plasma membrane Na^{+}/Ca^{2+} exchanger in excitotoxicity. Cell 120: 275-285

Behan WMH, McDonald M, Darlington LG, Stone TW, (1999). Oxidative stress as a mechanism for quinolinic acid-induced hippocampal damage: protection by melatonin and deprenyl. British Journal of Pharmacology 128: 1754-1760

Behan WMH, Stone TW, (2000). Role of kynurenines in the neurotoxic actions of kainic acid. British Journal of Pharmacology 129: 1764-1770

Behan WMH and Stone TW, (2002). Enhanced neuronal damage by co-administration of quinolinic acid and free radicals, and protection by adenosine A_{2a} receptor antagonists; British journal of Pharmacology 135: 1435-1442

Bejot Y, Benatru I, Rouaud O, Fromont A, Besancenot JP, Moreau T, Giroud M, (2007). Epidemiology of stroke in Europe: geographic and environmental differences. Journal of the Neurological Sciences 262: 85-88

Bellac CL, Coimbra RS, Christen S, Leib SL, (2006). Pneumococcal meningitis causes accumulation of neurotoxic kynurenine metabolites in brain regions prone to injury; Neurobiology of Diseases 24: 395-402

Ben-Ari Y, Gaiarsa JL, Tyzio R, Khazipov R, (2007). GABA: a pioneer transmitter that excites immature neurons and generates primitive oscillations. Physiological Reviews 87: 1215-1284

Ben-Ari Y, Khazipov R, Leinekugel X, Caillard O, Gaiarsa JL, (1997). GABAA, NMDA and AMPA receptors: a developmentally regulated ‘ménage à trois’. Trends in Neuroscience 20: 523-529

Berliocchi L, Bano D, Nicotera P, (2005). Ca^{2+} signals and death programmes in neurons. Philosophical Transactions of the Royal Society 360: 2255-2258

Besirli CG, Deckwerth TL, Crowden RJ, Freeman RS, Johnson Jr. EM, (2003). Cytosine arabinoside rapidly activates Bax-dependent apoptosis and a Bax-

independent death pathway in sympathetic neurons. Cell Death and Differentiation 10: 1045-1058

Blondeau N, Widmann C, Lazdunski M, Heurteaux C, (2001). Activation of nuclear factor-κB is a key event in brain tolerance. The Journal of Neuroscience 21: 4668-4677

Boeck CR, Ganzella M, Lottermann A, Vendite D, (2004). NMDA preconditioning protects against seizures and hippocampal neurotoxicity induced by quinolinic acid in mice. Epilepsia 45: 745-750

Boeck CR, Kroth EH, Bronzatto MJ, Vendite D, (2005). Adenosine receptors co-operate with NMDA preconditioning to protect cerebellar granular cells against glutamate neurotoxicity. Neuropharmacology 49: 17-24

Bolanos JP, Almeida A, Fernandez E, Medina JM, Land JM, Clark JB, Heales SJ, (1997). Potential mechanisms for nitric oxide-mediated impairments of brain mitochondrial energy metabolism. Biochemical Society Transactions 25: 944-949

Brambrink AM, Schneider A, Noga H, Astheimer A, Götz B, Körner I, Heimann A, Welschof M, Kempski O, (2000). Tolerance-inducing dose of 3-nitropropionic acid modulates bcl-2 and bax balance in the rat brain: a potential mechanism of chemical preconditioning. Journal of Cerebral Blood Flow and Metabolism 20: 1425-1436

Brandt J, Bylsma FW, Gross R, Stine OC, Ranen N, Ross CA, (1996). Trinucleotide repeat length and clinical progression in Huntington's disease. Neurology 46: 527-531

Bruce-Keller AJ, Begley JG, Fu W, Butterfield DA, Bredesen DE, Hutchins JB, Hensley K, Mattson MP, (1998). Bcl-2 protects isolated plasma and mitochondrial membranes against lipid peroxidation induced by hydrogen peroxide and amyloid ß–peptide. Journal of Neurochemistry 70: 31-39

Budd SL and Nicholls DG, (1996). Mitochondria, calcium regulation and acute glutamate excitotoxicity in cultured cerebellar granule cells. Journal of Neurochemistry 67: 2282-2291

Caballero-Benitez A, Alavez S, Uribe RM, Morán J, (2004). Regulation of glutamate-synthesising enzymes by NMDA and potassium in cerebellar granule cells. European Journal of Neuroscience 19: 2030-2038

Cannazza G, Baraldi M, Braghiroli D, Tait A, Parenti C, (2003). High-performance liquid chromatographic method for the quantification of anthranilic acid and 3-hydroxyanthranilic acid in rat brain dialysate. Journal of Pharmaceutical and Biomedical Analysis 32: 287-293

Castilho RF, Hansson O, Ward MW, Budd SL, Nicholls DG, (1998). Mitochondrial control of acute glutamate excitotoxicity in cultures cerebellar granule cells. The Journal of Neuroscience 18: 10277-10286

Castilho RF, Ward MW, Nicholls DG, (1999). Oxidative Stress, mitochondrial function, and acute glutamate excitotoxicity in cultured cerebellar granule cells. Journal of Neurochemistry 72: 1394-1401

Cerstiaens A, Huybrechts J, Kotanen S, Lebeau I, Meylaers K, De Loof A, Schoofs L, (2003). Neurotoxic and neurobehavioural effects of kynurenines in adult insects. Biochemical and Biophysical Research Communications 312: 1171-1177

Chalmers S, Nicholls DG, (2003). The relationship between free and total calcium concentrations in the matrix of liver and brain mitochondria. Journal of Biological Chemistry 278: 19062-19070

Chan FCT, Spriggs DL, Benton BJ, Keller SA, Capacio BR, (1997). 4-Aminopyridine reverses saxitoxin (STX)- and tetrodotoxin (TTX)-induced cardiorespiratory depression in chronically instrumented guinea pigs. Fundamental and Applied Toxicology 38: 75-88

Chebib M, (2004). $GABA_C$ receptor ion channels. Clinical and Experimental Pharmacology and Physiology 31: 800-804

Cheng Y, Deshmukh M, D'Costa A, Demaro JA, Gidday JM, Shah A, Sun Y, Jacquin MF, Johnson Jr. EM, Holtzman DM, (1998). Caspase inhibitor affords neuroprotection with delayed administration in a rat model of neonatal hypoxic-ischemic brain injury. Journal of Clinical Investigation 101: 1992-1999

Chiarugi A, Carpenedo R, Moroni F, (1996). Kynurenine disposition in blood and brain of mice: effects of selective inhibitors of kynurenine hydroxylase and of kynureninase. Journal of Neurochemistry 67: 692-698

Chinopolous C, Adam-Vizi, V, (2006). Calcium, mitochondria and oxidative stress in neuronal pathology. FEBS Journal 273: 433-450

Choi DW, Rothman SM, (1990). The role of glutamate toxicity in hypoxic-ischaemic neuronal death. Annual review of Neuroscience 13: 171-82

Chuang DM, Gao XM, Paul SM, (1992). *N*-methyl-D-aspartate exposure blocks glutamate toxicity in cultured cerebellar granule cells. Molecular Pharmacology 42: 210-216

Ciotti MT, Giannetti S, Mercanti D, Calissano P; A glutamate-sensitizing activity in conditioned media derived from rat cerebellar granule cells. European Journal of Neuroscience 8: 1591-1600; 1996

Clark CJ, Mackay GM, Smythe GA, Bustamante S, Stone TW, Phillips RS, (2005). Prolonged survival of a murine model of cerebral malaria by kynurenine pathway inhibition. Infection and Immunity 73: 5249-5251

Collinson N, Kuenzi FM, Jarolimek W, Maubach KA, Cothliff R, Sur C, Smith A, Otu FM, Howell O, Atack JR, McKernan RM, Seabrook GR, Dawson GR, Whiting PJ, Rosahl TW, (2002). Enhanced learning and memory and altered GABAergic synaptic transmission in mice lacking the α5 subunit of the $GABA_A$ receptor. The Journal of Neuroscience 22: 5572-5580

Courtney MJ, Lambert JJ, Nicholls DG, (1990). The interactions between plasma membrane depolarisation and glutamate receptor activation in the regulation of cytoplasmic free calcium in cultured cerebellar granule cells. The Journal of Neuroscience 10: 3876-3879

Courtney MJ, Coffey ET, (1999). The mechanism of Ara-C-induced apoptosis of differentiating cerebellar granule neurons. European Journal of Neuroscience 11: 1073-1084

Cumming R, Burgoyne RD, Lytton NA, (1984). Immunofluorescence distribution of α-tubulin, ß-tubulin and microtubule-associated protein 2 during in vitro maturation of cerebellar granule cell neurones. Neuroscience 12: 775-782

Cummings JL, Vinters HV, Cole GM, Khachaturian ZS, (1998). Alzheimer's disease: etiologies, pathophysiology, cognitive reserve, and treatment opportunities. Neurology 51: S2-17

Damschroder-Williams P, Irwin RP, Lin SZ, Paul SM, (1995). Characterisation of the excitoprotective actions of *N*-methyl-D-aspartate in cultured cerebellar granular neurons. Journal of Neurochemistry 65: 1069-1076

Daniels M, Brown DR, (2002). High extracellular potassium protects against the toxicity of cytosine arabinoside but is not required for the survival of cerebellar granule cells *in vitro*. Molecular and Cellular Neuroscience 19: 281-291

Dargent B, Arsac C, Tricaud N, Couraud F, (1996). Activation of voltage-dependant sodium channels in cultured cerebellar granular cells induces neurotoxicity that is not mediated by glutamate release. Neuroscience 73: 209-216

Darlington LG, Mackay GM, Forrest CM, Stoy N, George C, Stone TW, (2007). Altered kynurenine metabolism correlates with infarct volume in stroke. European Journal of Neuroscience 26: 2211-2221

Dave KR, Lange-Asschenfeldt C, Raval AP, Prado R, Busto R, Saul I, Pérez-Pinzón MA, (2005). Ischemic preconditioning ameliorates excitotoxicity by shifting glutamate/ γ-butyric acid release and biosynthesis. Journal of Neuroscience Research 82: 665-673

Davis SM, Lees KR, Albers GW, Diener HC, Markabi S, Karlsson G, Norris J, (2000). Selfotel in acute ischemic stroke. Stroke 31: 347-354

de Mendonça A, Sebastião AM, Ribeiro A, (2000). Adenosine: does it have a neuroprotective role after all? Brain Research Reviews 33: 258-274

Del Angel-Meza AR, Ramírez-Cortés L, Olvera-Cortés E, Pérez-Vega MI, González-Burgos I, (2001). A tryptophan-deficient corn-based diet induced plastic responses in cerebellar cortex cells of rat offspring. International Journal of Developmental Neuroscience 19: 447-453

Delgado-Esteban M, Almeida A, Bolanos JP, (2000). D-Glucose prevents oxidation and mitochondrial damage after glutamate receptor stimulation in rat cortical Primary Neurons. Journal of Neurochemistry 75: 1618-1624

Deng G, Su JH, Ivins KJ, Van Houten B, Cotman CW, (1999). Bcl-2 facilitates recovery from DNA damage after oxidative stress. Experimental Neurology 159: 309-318

Dessi F, Charriaut-Marlangue C, Khrestchatisky M, Ben-Ari Y, (1993). Glutamate-induced neuronal cell death is not a programmed cell death in cerebellar culture. Journal of Neurochemistry 60: 1953-1955

Diano S, Matthews RT, Patrylo P, Yang L, Beal MF, Barnstable CJ, Horvath TL, (2003). Uncoupling protein-2 prevents neuronal death including that occurring during seizures: a mechanism for preconditioning. Endocrinology 144: 5014-5021

Didier M, Heaulme M, Soubrie P, Bockaert J, Pin JP, (1990). Rapid, sensitive and simple method for quantification of both neurotoxic and neurotrophic effects of NMDA on cultured cerebellar granule cells. Journal of Neuroscience Research 27: 25-35

Dirnagl U, Iadecola C, Moskowitz A, (1999). Pathobiology of ischaemic stroke: an integrated view. Trends in Neuroscience 22: 391-397

Dong-Ruyl L, Sawada M, Nakano K, (1998). Tryptophan and its metabolite, kynurenine, stimulate expression of nerve growth factor in cultured mouse astroglial cells. Neuroscience Letters 244: 17-20

Dus L, Canu N, Zona C, Ciotti MT, Calissano P, (1997). NMDA receptor modulation by a conditioned medium derived from rat cerebellar granule cells. European Journal of Neuroscience 9: 2668-2676

Dykens JA, Sullivan SG, Stern A, (1987). Oxidative reactivity of the tryptophan metabolites 3-hydroxyanthranilate, quinolinate and picolinate. Biochemical Pharmacology 36: 211-217

Dykens JA, Sullivan SG, Stern A, (1989). Glucose metabolism and haemoglobin reactivity in human red blood cells exposed to the tryptophan metabolites 3-hydroxyanthranilate, quinolinate and picolinate. Biochemical Pharmacology 38: 1555-1562

Eimerl S, Schramm M, (1994). The quantity of calcium that appears to induce neuronal death. Journal of Neurochemistry 62: 1223-1226

Espey MG, Chernyshev ON, Reinhard JF, Namboodiri MAA, Colton CA, (1997). Activated human microgila produce the excitotoxin quinolinic acid. NeuroReport 8: 431-434

Fatokun AA, Stone TW, Smith RA, (2007). Cell death in rat cerebellar granule neurons induced by hydrogen peroxide in vitro: mechanisms and protection by adenosine receptor ligands. Brain Research 1132: 193-202

Fatokun AA, Stone TW, Smith RA, (2008a). Adenosine receptor ligands protect against a combination of apoptotic and necrotic cell death in cerebellar granule neurons. Experimental Brain Research 186: 151-160

Fatokun AA, Stone TW, Smith RA, (2008b). Responses of differentiated MC3T3-E1 osteoblast-like cells to reactive oxygen species. European Journal of Pharmacology 587: 35-41

Favaron M, Manev H, Alho H, Bertolino M, Ferret B, Guidotti A, Costa E, (1988). Gangliosides prevent glutamate and kainate neurotoxicity in primary neuronal cultures of neonatal rat cerebellum and cortex. Proceedings of the National Academy of Sciences, USA 85: 7351-7355

Feksa LR, Cornelio AR, Vargas CR, Wyse ATDS, Dutra-Filho CS, Wajner M, Wannmacher CMD, (2003). Alanine prevents the inhibition of pyruvate kinase activity caused by tryptophan in cerebral cortex of rats. Metabolic Brain Disease 18: 129-137

Ferrer I, Blanco R, Carmona M, (2001). Differential expression of active, phosphorylation-dependent MAP kinases, MAPK/ERK, SAPK/JNK and p38, and specific transcription factor substrates following quinolinic acid excitotoxicity in the rat. Molecular Brain Research 94: 48-58

Feustel PJ, Jin Y, Kimelberg HK, (2004). Volume-regulated anion channels are the predominant contributors to release of excitatory amino acids in the ischemic cortical penumbra. Stroke 35: 1164-1168

Fink CC, Meyer T, (2002). Molecular mechanisms of CaMKII activation in neuronal plasticity. Current Opinion in Neurobiology 12: 293-299

Fink K, Zhu J, Namura S, Shimizu-Sasamata M, Endres M, Ma J, Dalkara T, Yuan J, Moskowitz MA, (1998). Prolonged therapeutic window for ischemic brain damage caused by delayed caspase activation. Journal of Cerebral Blood Flow and Metabolism 18: 1071-1076

Fink SL, Ho DY, Sapolsky RM, (1996). Energy and glutamate dependency of 3-nitropropionic acid neurotoxicity in culture. Experimental Neurology 138: 298-304

Foster AC, Vezzani A, French ED, Schwarcz R, (1984). Kynurenic acid blocks neurotoxicity and seizures induced in rats by the related brain metabolite quinolinic acid. Neuroscience Letters 48: 273-278

Franklin JL, Johnson Jr. EM, (1994). Block of neuronal apoptosis by a sustained increase of steady-state free Ca2+ concentration. Philosophical Transactions of the Royal Society of London B 345: 251-256

Fukui S, Schwarcz R, Rapoport SI, Takada Y, Smith QR, (1991). Blood-brain barrier transport of kynurenines: implications for brain synthesis and metabolism. Journal of Neurochemistry 56: 2007-2017

Fukuoka SI, Ishiguro K, Yanagihara K, Tanabe A, Egashira Y, Sanada H, Shibata K, (2002). Identification and expression of a cDNA encoding human α-amino-ß-carboxymuconate-ε-semialdehyde decarboxylase (ACMSD). The Journal of Biological Chemistry 277: 35162-35167

Galli C, Meucci O, Scorziello A, Werge TM, Calissano P, Schettini G, (1995). Apoptosis in cerebellar granule cells is blocked by high KCl, forskolin and IGF-1 through distinct mechanisms of action: the involvement of intracellular calcium and RNA synthesis. The Journal of Neuroscience 15: 1172-1179

Gallo V, Kingsbury A, Balazs R, Jorgensen OS, (1987). The role of depolarisation in the survival and differentiation of cerebellar granule cells in culture. The Journal of Neuroscience 7: 2203-2213

Gavrieli Y, Sherman Y, Ben-Sasson SA, (1992). Identification of programmed cell death in situ via specific labelling of nuclear DNA fragmentation. The Journal of Cell Biology 119: 493-501

Goda H, Ooboshi H, Nakane H, Ibayashi S, Sadoshima S, Fujishima M, (1998). Modulation of ischemia-evoked release of excitatory and inhibitory amino acids by adenosine A_1 receptor agonist. European Journal of Pharmacology; 357: 149-155

Goforth PB, Ellis EF, Satin LS, (1999). Enhancement of AMPA-mediated current after traumatic injury in cortical neurons. The Journal of Neuroscience 19: 7367-7374

Goldstein LE, Leopold MC, Huang X, Atwood CS, Saunders AJ, Hartshorn M, Lim JT, Faget KY, Muffat JA, Scarpa RC, Chylack Jr. LT, Bowden EF, Tanzi RE, Bush AI, (2000). 3-Hydroxykynurenine and 3-hydroxyanthranilic acid generate hydrogen peroxide and promote α–crystallin cross-linking by metal ion reduction. Biochemistry 39: 7266-7275

Gorus FK, Hooghe-Peters EL, Pipeleers DG, (1984). Glucose metabolism in murine fetal cortical brain cells: lack of insulin effects. Journal of Cellular Physiology 121: 45-50

Grabb MC, Choi DW, (1999). Ischaemic tolerance in murine cortical cell culture: critical role for NMDA receptors. The Journal of Neuroscience 19: 1657-1662

Grabb MC, Lobner D, Turetsky DM, Choi DW, (2002). Preconditioned resistance to oxygen-glucose deprivation-induced cortical neuronal death: alterations in vesicular GABA and glutamate release. Neuroscience 115: 173-183

Grant S, (1998). Ara-C: cellular and molecular pharmacology. Advances in Cancer Research 72: 197-233

Greenwood SM, Mizielinska SM, Frenguelli BG, Harvey J, Connolly CN, (2007). Mitochondrial dysfunction and dendritic beading during neuronal toxicity. The Journal of Biological Chemistry 282:26235-26244

Grillo CA, Piroli GG, Rosell DR, Hoskin EK, McEwen BS, Reagan LP, (2003). Region specific increases in oxidative stress and superoxide dismutase in the hippocampus of diabetic rats subjected to stress. Neuroscience 121: 133-140

Guidetti P, Eastman CL, Schwarcz R, (1995). Metabolism of [5-^{3}H] kynurenine in the rat brain in vivo: evidence for the existence of a functional kynurenine pathway. Journal of Neurochemistry 65: 2621-2632

Guidetti P, Schwarcz R, (1999). 3-Hydroxykynurenine potentiates quinolinate but not NMDA toxicity in the rat striatum. European Journal of Neuroscience 11: 3857-3863

Guidetti P, Luthi-Carter RE, Augood SJ, Schwarcz R, (2004). Neostriatal and cortical quinolinate levels are increased in early grade Huntington's disease. Neurobiology of Disease 17: 455-461

Guillemin GJ, Kerr SJ, Smythe GA, Smith DG, Kapoor V, Armati PJ, Croitoru J, Brew BJ, (2001). Kynurenine pathway metabolism in human astrocytes: a paradox for neuronal protection. Journal of Neurochemistry 78: 842-853

Guillemin GJ, Wang L, Brew BJ, (2005). Quinolinic acid selectively induces apoptosis of human astrocytes: potential role in AIDS dementia complex. Journal of Neuroinflammation 2: 16-21

Gunasekar PG, Kanthasamy AG, Borowitz JL, Isom GE, (1995). NMDA receptor activation produces concurrent generation of nitric oxide and reactive oxygen species: implication for cell death. Journal of Neurochemistry 65: 2016-2021

Halestrap AP, Clarke SJ, Khaliulin I, (2007). The role of mitochondria in protection of the heart by preconditioning. Biochimica et Biophysica Acta 1767: 1007-1031

Halliwell B, (2003). Oxidative stress in cell culture: an under-appreciated problem? FEBS Letters 540: 3-6

Hamid R, Rotsheyn Y, Rabadi L, Parikh R, Bullock P, (2004). Comparison of Alamar blue and MTT assays for high through-put screening. Toxicology in Vitro 18: 703-710

Han Y, Zhang S, Wang X, Wu J, (2006). Inhibition of mitochondria responsible for the anti-apoptotic effects of melatonin during ischaemia-reperfusion. Journal of Zheijang University Science B 7: 142-147

Hara T, Hamada J, Yano S, Morioka M, Kai Y, Ushio Y, (2003). CREB is required for the acquisition of ischaemic tolerance in gerbil hippocampal CA1 region. Journal of Neurochemistry 86: 805-814

Hardingham GE, Cruzalegui FH, Chawla S, Bading H; Mechanisms controlling gene expression by nuclear calcium signals. Cell Calcium 23: 131-134; 1998

Hardingham GE, Arnold FJL, Bading H, (2001). Nuclear calcium signalling controls CREB-mediated gene expression triggered by synaptic activity. Nature Neuroscience 4: 261-267

Hardingham GE, Fukunaga Y, Bading H, (2002a). Extrasynaptic NMDARs oppose synaptic NMDARs by triggering CREB shut-off and cell death pathways. Nature Neuroscience 5: 405-414

Hardingham GE, Bading H, (2002b). Coupling of extrasynaptic NMDA receptors to a CREB shut-off pathway is developmentally regulated. Biochemica et Biophysica Acta 1600: 148-153

Hassel B, Bråthe A, (2000). Neuronal pyruvate carboxylation supports formation of transmitter glutamate. The Journal of Neuroscience 20: 1342-1347

Hayashi K, Kawai-Hirai R, Ishikawa K, Takata K, (2002). Reversal of neuronal polarity characterised by conversion of dendrites into axons in neonatal rat cortical neurons *in vitro*. Neuroscience 110: 7-17

Hazell AS, (2007). Excitotoxic mechanisms in stroke: an update of concepts and treatment strategies. Neurochemistry International 50: 941-953

Heidenreich KA, Gilmore PR, Garvey WT, (1989). Glucose transport in primary cultured neurons. Journal of Neuroscience Research 22: 397-407

Hervé C, Beyne P, Jamault H and Delacoux E, (1996). Determination of tryptophan and its kynurenine pathway metabolites in human serum by high-performance liquid chromatography with simultaneous ultraviolet and fluorometric detection. Journal of Chromatography B 675: 157-161

Heyes MP, Brew BJ, Martin A, Price RW, Salazar AM, Sidtis JJ, Yergey JA, Mouradian MM, Sadler AE, Keilp J, Rubinow D, Markey SP, (1991). Quinolinic acid in cerebrospinal fluid and serum in HIV-1 infection: relationship to clinical and neurological status. Annals of Neurology 29: 202-209

Horiguchi T, Kis B, Rajapakse N, Shimizu K, Busija DW, (2003). Opening of mitochondrial ATP-sensitive potassium channels is a trigger of 3-nitropropionic acid-induced tolerance to transient focal cerebral ischaemia in rats. Stroke 34: 1015-1020

Hou ST, MacManus JP, (2002). Molecular mechanisms of cerebral ischaemia-induced neuronal death. International Review of Cytology 221: 93-148

Hou ST, Jiang SX, Desbois A, Huang D, Kelly J, Tessier L, Karchewski L, Kappler J, (2006). Calpain-cleaved collapsin response mediator protein-3 induces neuronal death after glutamate toxicity and cerebral ischaemia. Journal of Neuroscience 26: 2241-2249

Hou ST, Jiang SX, Smith RA, (2008). Permissive and repulsive cues and signalling pathways of axonal growth and regeneration. International Review of Cell and Molecular Biology 267: 125-181

Hu CL, Liu Z, Zeng XM, Liu ZQ, Chen XH, Zhang ZH, Mei YA, (2006). 4-Aminopyridine, a K_V channel antagonist, prevents apoptosis of rat cerebellar granule neurons. Neuropharmacology 51: 737-746

Huang R, Hertz L, (1994). Effect of anoxia on glutamate formation from glutamine in cultured neurons: dependence on neuronal subtype. Brain Research 660: 129-137

Iadecola C, (1997). Bright and dark sides of nitric oxide in ischemic brain injury. Trends in Neuroscience 20: 132-139

Iijima T, Mies G, Hossmann KA, (1992). Repeated negative DC deflections in rat cerebral cortex following middle cerebral artery occlusion are abolished by MK-801: effect on volume of ischemic injury. Journal of Cerebral Blood Flow and Metabolism 12: 727-733

Ikonomidou C, Turski L, (2002). Why did NMDA receptor antagonists fail clinical trials for stroke and traumatic brain injury? The Lancet Neurology 1: 383-386

Ikonomovic S, Kharlamov E, Manev H, Ikonomovic MD, Grayson DR, (1997). GABA and NMDA in the prevention of apoptotic-like cell death in vitro. Neurochemistry International 31: 283-290

Inglefield JR, Mundy WR, Meacham CA, Shafer TJ, (2002). Identification of calcium-dependent and –independent signalling pathways involved in polychlorinated biphenyl-induced cyclic AMP-responsive element-binding protein phosphorylation in developing cortical neurons. Neuroscience 115: 559-573

Isaev NK, Stelmashook EV, Halle A, Harms C, Lautenschlager M, Weih M, Dirnagl U, Victorov IV, Zorov DB, (2000). Inhibition of Na^+, K^+-ATPase activity in cultured rat cerebellar granule cells prevents the onset of apoptosis induced by low potassium. Neuroscience Letters 283: 41-44

Ishii T, Iwahashi H, Sugata R, Kido R, Fridovich I, (1990). Superoxide dismutases enhance the rate of autoxidation of 3-hydroxyanthranilic acid. Archives of Biochemistry and Biophysics 276: 248-250

Ito H, Watanabe Y, Isshiki A and Uchino H, (1999). Neuroprotective properties of propofol and midazolam, but not pentobarbital, on neuronal damage induced by forebrain ischemia, based on the $GABA_A$ receptors. Acta Anaesthesiologica Scandinavica; 43: 153-162

Iwahashi H, Ishii T, Sugata R, Kido R, (1988). Superoxide dismutase enhances the formation of hydroxyl radicals in the reaction of 3-hydroxyanthranilic acid with molecular oxygen. Biochemistry Journal 251: 893-899

Izquierdo I, (1994). Pharmacological evidence for a role of long-term potentiation in memory. The FASEB Journal 8: 1139-1145

Jenner P, Olanow CW, (1998). Understanding cell death in Parkinson's disease. Annals of Neurology 44: S72-84

Jhamandas K Boegman RJ, Beninger RJ, Bialik M, (1990). Quinolinate-induced cortical cholinergic damage: modulation by tryptophan metabolites. Brain Research 529: 185-191

Jhamandas K Boegman RJ, Beninger RJ, Flesher S, (1998). Role of zinc in blockade of excitotoxic action of quinolinic acid by picolinic acid. Amino Acids 14: 257-261

Johns L, Sinclair AJ, Davies AJ, (2000). Hypoxia/hypoglycaemia-induced amino acid release is decreased *in vitro* by preconditioning. Biochemical and Biophysical Research Communication 276: 134-136

Jonas W, Lin Y, Tortella F, (2001). Neuroprotection from glutamate toxicity with ultra-low dose glutamate. Neruroreport 12: 335-339

Jones PA, Smith RA, Stone TW, (1998). Protection against kainite-induced excitotoxicity by adenosine A_{2A} receptor agonists and antagonists. Neuroscience 85: 229-237

Juhaszora M, Zorov DB, Kim SH, Pepe S, Fu Q, Fishbein KW, ZIman BD, Wang S, Ytrehus K, Antos CL, Olson EN, Sollott SJ, (2004). Glycogen synthase kinase-3 beta mediates convergence of protection signalling to inhibit the mitochondrial permeability transition pore. Journal of Clinical Investigation 113: 1535-1549

Kalda A, Eriste E, Vassiljev V, Zharkovsky A, (1998). Medium transitory oxygen-glucose deprivation induced both apoptosis and necrosis in cerebellar granule cells. Neuroscience Letters 240: 21-24

Kalda A, Kaasik A, Vassiljev V, Pokk P, Zharkovsky A, (2000). Neuroprotective action of group I metabotropic glutamate receptor antagonists against oxygen-glucose deprivation-induced neuronal death. Brain Research 853: 370-373

Kalisch BE, Jhamandas K, Boegman RG, Beninger RJ, (1994). Picolinic acid protects against quinolinic acid-induced depletion of NADPH diaphorase containing neurons in the rat striatum. Brain Research 668: 1-8

Kaltschmidt C, Kaltschmidt B, Bauerle PA, (1995). Stimulation of ionotropic glutamate receptors activates transcription factor NF-kappa B in primary neurons. Proceedings of the National Academy of Sciences USA 92: 9618-9622

Kam PCA, Ferch NI, (2000). Apoptosis: mechanisms and clinical implications. Anaesthesia 55: 1081-1093

Kass IS, Lipton P, (1999). Mechanisms involved in irreversible anoxic damage to the *in vitro* rat hippocampal slice. Journal of Physiology 332: 459-472

Kawasaki H, Morooka T, Shimohama S, Kimura J, Hirano T, Gotoh Y, Nishida E, (1997). Activation and involvement of p38 mitogen-activated protein kinase in glutamate-induced apoptosis in rat cerebellar granule cells. The Journal of Biological Chemistry 272: 18518-18521

Kharlamov E, Cagnoli CM, Atabay C, Ikonmović S, Grayson DR, Manev H, (1995). Opposite effect of protein synthesis Inhibitors on potassium deficiency-induced apoptotic cell death in immature and mature neuronal cultures. Journal of Neurochemistry 65: 1395-1398

Kitagawa K, Matsumoto M, Tagaya M, Hata R, Ueda H, Niinobe M, Handa N, Fukunaga R, Kimura K, Mikoshiba K, Kamada T, (1990). 'Ischemic tolerance' phenomenon found in the brain. Brain Research 528: 21-24

Köhler C, Eriksson LG, Flood PR, Hardie JA, Okuno E, Schwarcz R, (1988). Quinolinic acid metabolism in the rat brain. Immunohistochemical identification of 3-hydryanthranilic acid oxygeanse ans quinolinic acid phopshoribosyltransferase in the hippocampal region. The Journal of Neuroscience 8: 975-987

Lam M, Dubyak G, Chen L, Nuez G, Miesfield RL, Distelhorst CW, (1994). Evidence that blc-2 represses apoptosis by regulating endoplasmic reticulum-associated Ca^{2+} fluxes. Proceedings of the National Academy of Sciences USA 91: 6569-6573

Lange W, (1975). Cell number and cell density in the cerebellar cortex of man and some other animals. Cell Tissue Research 157: 115-124

Lange-Asschenfeldt C, Raval AP, Pérez-Pinzón MA, (2005). Ischemic tolerance induction in organotypic hippocampal slices: role for the $GABA_A$ receptor? Neuroscience Letters 384: 87-92

Lee HJ, Bach JH, Chae HS, Lee SH, Joo WS, Choi SH, Kim KY, Lee WB, Kim SS, (2004). Mitogen-activated protein kinase/extracellular signal-regulated kinase attenuates 3-hydroxykynurenin-induced neuronal cell death. Journal of Neurochemistry 88 (3): 647-656

Lee J, Bruce-Keller AJ, Kruman Y, Chan SL, Mattson MP, (1999). 2-Deoxy-D-glucoseproects hippocampal neurons against excitotoxic and oxidative injury: evidence for the involvement of stress proteins. Journal of Neuroscience Research. 57: 48-61

Lee JM, Grabb MC, Zipfel GJ, Choi DW, (2000). Brain tissue responses to ischemia. The Journal of Clinical Investigation 106: 723-731

Leino RL, Gerhart DZ, Van Bueren AM, McCall AL, Drewes LR, (1997). Ultrastructural localization of GLUT1 and GLUT3 glucose transporters in rat brain. Journal of Neuroscience Research. 49: 617-626

Leipnitz G, Schumacher C, Dalcin KB, Scussiato K, Solano A, Funchal C, Dutra-Filho CS, Wyse ATS, Wannmacher CMD, Latini A, Wajner M, (2007). In vitro evidence for an antioxidant role of 3-hydroxykynurenine and 3-hydroxyanthranilic acid in the brain. Neurochemistry International 50: 83-94

Leski ML, Valentine SL, Coyle JT, (1999). L-type voltage-gated calcium channels modulate kainic acid neurotoxicity in cerebellar granule cells. Brain Research 828: 27-40

Li PA, He QP, Ouyang YB, Liu CL, Hu BR, Siesjö BK, (2001). Early release of cytochrome C and activation of caspase-3 in hyperglycaemic rats subjected to transient forebrain ischemia. Brain Research 896: 69-76

Lin WW, Wang CW, Chuang DM, (1997). Effects of Depolarization and NMDA Antagonists on the Survival of Cerebellar Granule Cells: A Pivotal Role for Protein Kinase C Isoforms. Journal of Neurochemistry 68: 2577-2568

Liochev SI, Fridovich I, (2001). The oxidation of 3-hydroxyanthranilic acid by Cu,Zn superoxide dismutase: mechanism and possible consequences. Archives of Biochemistry and Biophysics 388: 281-284

Lipsky RH, Xu K, Zhu D, Kelly C, Terhakopian A, Novelli A, Marini AM, (2001). Nuclear factor κB is a critical determinant in N-methyl-D-aspartate receptor-mediated neuroprotection. Journal of Neurochemistry 78: 254-264

Liu D, Slevin JR, Lu C, Chan SL, Hansson M, Elmér E, Mattson MP, (2003). Involvement of mitochondrial K^+ release and cellular efflux in ischaemic and apoptotic neuronal death. Journal of Neurochemistry 86: 966-979

Liu Q, Wu J, (2006). Neuronal nicotinic acetylcholine receptors serve as sensitive targets that mediate ß-amyloid neurotoxicity. Acta Pharmacologica Sinica 27: 1277-1286

Liu SJ, Zukin RS, (2007). Ca^{2+}-permeable AMPA receptors in synaptic plasticity and neuronal death. TRENDS in Neuroscience 30: 126-134

Loo DT, Copani A, Pike CJ, Whittemore ER, Walencewicz AJ, Cotman CW, (1993). Apoptosis is induced by ß–amyloid in cultured central nervous system neurones. Proceedings of the National Academy of Sciences of the U.S.A. 90: 7951-7955

Lynch DR, Guttman RP, (2002). Excitotoxicity: perspectives based on *N*-methyl-D-aspartate receptor subtypes. Journal of Pharmacology and Experimental Therapeutics 300: 717-723

Mabuchi T, Kitagawa K, Kuwabara K, Takasawa K, Ohtsuki T, Xia Z, Storm D, Yanagihara T, Hori M, Matsumoto M, (2001). Phosphorylation of cAMP response element binding protein in hippocampal neurons as a protective response after exposure to glutamate *in vitro* and ischemia *in vivo*. The Journal of Neuroscience 21: 9204-9213

Maher F, Simpson IA, (1994). Modulation of expression of glucose transporters GLUT3 and GLUT1 by potassium and *N*-methyl-D-aspartate in cultured cerebellar granule neurons. Molecular and Cellular Neurosciences 5: 369-375

Maher F, Davies-Hill TM, Simpson A, (1996). Substrate specificity and kinetic parameters of GLUT3 in rat cerebellar granule neurons. Biochemical Journal 315: 827-831

Manev H, Favaron M, Guidotti A, Costa E, (1989). Delayed increase of Ca^{2+} influx elicited by glutamate: role in neuronal death. Molecular Pharmacology 36: 106-112

Marini AM, Paul SM, (1993). Induction of a neuroprotective state in cerebellar granular cells following activation of *N*-methyl-D-aspartate receptors. Annals of the New York Academy of Sciences 679: 253-259

Marini AM, Rabin SJ, Lipsky RH, Mocchetti I, (1998). Activity-dependent release of brain-derived neurotrophic factor underlies the neuroprotective effect of *N*-methyl-D-aspartate. The Journal of Biological Chemistry 273: 29394-29399

Mark RJ, Pang Z, Geddes JW, Uchida K, Mattson MP, (1997). Amyloid beta-peptide impairs glucose transport in hippocampal and cortical neurons: involvement of membrane lipid peroxidation. Journal of Neuroscience 17: 1046-1054

Martel MA, Wyllie DJ, Hardingham GE, (2008). In developing hippocampal neurons, NR2B-containing N-methyl-D-aspartate receptors (NMDARs) can mediate signalling to neuronal survival and synaptic potentiation, as well as neuronal death. Neuroscience (E-publication ahead of print)

Martin LJ, (2001). Neuronal cell death in nervous system development, disease and injury. International Journal of Molecular Medicine 7: 455-478

Martin RL, Lloyd HE, Cowan AI, (1994). The early events of oxygen and glucose deprivation: setting the scene for neuronal death? Trends in Neuroscience 17: 251-257

Mattiasson G, Shamloo M, Dido G, Mathi K, Tomasevic G, Yi S, Warden CH, Castilho RF, Melcher T, Gonzalez-Zulueta M, Nikolich K, Wieloch T, (2003). Uncoupling protein-2 prevents neuronal death and diminishes brain dysfunction after stroke and brain trauma. Nature Medicine 9: 1062-1068

Mattson MP, (1998). Modification of ion homeostasis by lipid peroxidation: roles in neuronal degeneration and adaptive plasticity. Trends in Neuroscience 21: 53-57

Mattson MP, (2000). Apoptosis in neurodegenerative disorders. Nature Reviews – Molecular Cell Biology 1: 120-129

Mattson MP; Metal-catalyzed disruption of membrane protein and lipid signalling in the pathogenesis of neurodegenerative disorders. Annals of the New York Academy of Sciences 1012: 37-50; 2004

Mazzio EA, Soliman KFA, (2003). Cytoprotection of pyruvic acid and reduced ß-nicotinamide adenine dinucleotide against hydrogen peroxide toxicity in neuroblastoma cells. Neurochemical Research 28: 733-741

Medana IM, Day NPJ, Salahifar-Sabet H, Stocker R, Smythe G, Bwanaisa L, Njobvu A, Kayira K, Tuner GDH, Taylor TE, Hunt NH, (2003). Metabolites of the kynurenine pathway of tryptophan metabolism in the cerebrospinal fluid of Malawian children with malaria; Journal of Infectious Diseases 188: 844-849

Mei YA, Wu MM, Huan CL, Sun JT, Zhou HQ, Zhang ZH, (2000). 4-Aminopyridine, a specific blocker of K^+ channels, inhibited inward Na^+ current in rat cerebellar granule cells. Brain Research 873: 46-53

Melani A, Pantoni L, Bordoni F, Gianfriddo M, Bianchi L, Vannucchi MG, Bertorelli R, Monopoli A, Pedata F, (2003). The selective A_{2A} receptor antagonist SCH58261 reduces striatal transmitter outflow, turning behaviour and ischaemic damage induced by permanent focal ischaemia in the rat. Brain Research 959: 243-250

Meller R, Minami M, Cameron JA, Impey S, Chen D, Lan JQ, Henshall DC, Simon RP, (2005). CREB-mediated bcl-2 protein expression after ischemia preconditioning. Journal of Cerebral Blood Flow and Metabolism 25: 234-246

Mies G Iijima T, Hossmann KA, (1993). Correlation between peri-infarct DC shifts and ischemic neuronal damage in rat. NeuroReport 4: 709-711

Minervini M, Atlante A, Gagliardi S, Ciotti MT, Marra E, Calissano P, (1997). Glutamate stimulates 2-deoxyglucose uptake in rat cerebellar granule cells. Brain Research 768: 57-62

Miranda AF, Boegman RK, Beninger RJ, Jhamandas K, (1997). Protection against quinolinic acid-mediated excitotoxicity in nigrostriatal dopaminergic neurons by endogenous kynurenic acid. Neuroscience 78: 967-975

Mishra OP, Delivoria-Papadopoulos M, (1999). Cellular mechanisms of hypoxic injury in the developing brain. Brain Research Bulletin 48: 233-238

Moncayo J, De Freitas GR, Bogousslavsky J, Altieri M, Van Melle G, (2000). Do transient ischaemic attacks have a neuroprotective effect? Neurology 54: 2089-2094

Monti B, Marri L, Contestibile A, (2002). NMDA receptor-dependent CREB activation in survival of cerebellar granule cells during *in vivo* and *in vitro* development. European Journal of Neuroscience 16: 1490-1498

Morán J, Patel AJ, (1989). Stimulation of the *N*-methyl-D-aspartate receptor promotes the biochemical differentiation of cerebellar granule neurons and not astrocytes. Brain Research 486: 15-25

Morán J, Itoh T, Reddy UR, Chen M, Alnemri ES, Pleasure D, (1999). Caspase-3 expression by cerebellar granule neurones is regulated by calcium and cyclic AMP. Journal of Neurochemistry 73: 568-577

Morita AU, Saito K, Takemura M, Maekawa N, Fujigaki S, Fujii H, Wada H, Takeuchi S, Noma A, Seishima M, (2001). 3-Hydroxyanthranilic acid, an L-tryptophan metabolite, induces apoptosis in monocyte-derived cells stimulated by interferon-gamma. Annals of Clinical Biochemistry 38: 242-251

Moulder KL, Cormier RJ, Shute AA, Zorumski CF, Mennerick S, (2003). Homeostatic effects of depolarisation on Ca^{2+} influx, synaptic signalling, and survival. The Journal of Neuroscience 23: 1831-1825

Muranyi M, Fujioka M, He QP, Han A, Yong G, Csiszar K, Li PA, (2003). Diabetes activates cell death pathway after transient focal cerebral ischaemia. Diabetes 52: 481-486

Murry CE, Jennings RB, Reimer KA, (1986). Preconditioning with ischemia: a delay of lethal cell injury in ischaemic myocardium. Circulation 74: 1124-1136

Nakajima T, Iwabuchi S, Miyazaki H, Okuma Y, Inanami O, Kuwabara M, Nomura Y, Kawahara K, (2002). Relationship between the activation of cyclic AMP responsive element binding protein and ischemic tolerance in the penumbral region of rat cerebral cortex. Neuroscience Letters 331: 13-16

Nakanishi S, Okazawa M, (2006). Membrane potential-regulated Ca^{2+} signalling in development and maturation of mammalian cerebellar granule cells. Journal of Physiology 575: 389-395

Nath R, McGinnis K, Dutta S, Shivers B, Wang KKW, (2001). Inhibition of p38 kinase mimics survival signal-linked protection against apoptosis in rat cerebellar granule neurons. Cellular and Molecular Biology Letters 6: 173-184

Novelli A, Reilly JA, Lysko PG, Henneberry RC, (1988). Glutamate becomes neurotoxic via the *N*-methyl-D-aspartate receptor when intracellular energy levels are reduced. Brain Research 451: 205-212

Ogita K, Okuda H, Watanebe M, Nagashima R, Sugiyama C, Yoneda Y, (2005). In vivo treatment with the K^+ channel blocked 4-aminopyridine protects against kainate-induced neuronal cell death through activation of NMDA receptors in murine hippocampus. Neuropharmacology 48: 810-821

Ohkuna S, Katsura M, Hibino Y, Hara A, Shirotani K, Ishikawa E, Kuriyama K, (1998). Mechanisms for facilitation of nitric oxide-evoked [^{3}H] GABA release by removal of hydroxyl radical. Journal of Neurochemistry 71: 1501-1510

Ohta S, Furuta S, Matsubara I, Kohno K, Kumon Y, Sakaki S, (1996). Calcium movement in ischemia-tolerant hippocampal CA1 neurons after transient forebrain ischemia in gerbils. Journal of Cerebral Blood Flow and Metabolism 16: 915-922

Okuda S, Nishiyama, Saito H, Katsuki H, (1996). Hydrogen peroxide-mediated neuronal cell death induced by an endogenous neurotoxin, 3-hydroxykynurenine. Proceedings of the National Academy of Sciences USA 93: 12553-12558

Okuda S, Nishiyama, Saito H, Katsuki H, (1998). 3-Hydroxykynurenine, an endogenous oxidative stress generator, causes neuronal cell death with apoptotic features and region selectivity. Journal of Neurochemistry 70: 299-307

Olney JW, de Gubareff T, (1978). Glutamate neurotoxicity and Huntington's chorea. Nature 271: 557-559

Olsen C, Rustad A, Fonnum F, Paulsen RE, Hassel B, (1999). 3-Nitropropionic acid: an astrocyte-sparing neurotoxin in vitro. Brain Research 850: 144-149

Ona VO, Li M, Vonsattel JP, Andrews LJ, Khan SQ, Chung WM, Frey AS, Li XJ, Stieg PE, Yuan J, Penney JB, Young AB, Cha J, Friedlander RM, (1999). Inhibition of caspase-1 slows disease progression in a mouse model of Huntington's disease. Nature 399: 263-267

O'Neill LAJ, Kaltschmidt C, (1997). NF-κB: a crucial transcription factor for glial and neuronal cell function. Trends in Neuroscience 20: 252-258

Orr DJ, Smith RA, (1988). Neuronal maintenance and neurite extension of adult mouse neurones in non-neuronal cell-reduced cultures is dependent on substratum coating. Journal of Cell Science 91: 555-561

Paoletti P, Neyton J, (2007). NMDA receptor subunits: function and pharmacology. Current Opinion in Pharmacology 7: 39-47

Papadia S, Stevenson P, Hardingham NR, Bading H, Hardingham GE, (2005). Nuclear Ca^{2+} and the cAMP response element-binding protein family mediate a late phase of activity-dependent neuroprotection. The Journal of Neuroscience 25: 4279-4287

Papadia S, Hardingham GE, (2007). The dichotomy of NMDA receptor signaling. The Neuroscientist 13: 572-579

Pellegrini-Giampietro DE, Peruginelli F, Meli E, Cozzi A, Albani-Torregrossa S, Pellicciari R, Moroni F, (1999). Protection with metabotropic glutamate 1 receptor antagonists in models of ischemic neuronal death: time course and mechanisms. Neuropharmacology 38: 1607-1619

Peng L, Juurlink BHJ, Hertz L, (1991). Differences in transmitter release, morphology, and ischaemia-induced cell injury between cerebellar granule cell cultures developing in the presence and absence of a depolarizing potassium concentration. Brain Research: Developmental Brain Research 63:1-12

Perkins MN, Stone TW, (1983). Pharmacology and regional variations of quinolinic acid-evoked excitations in the rat central nervous system. The Journal of Pharmacology and Experimental Therapeutics. 226: 551-557

Phillis JW, (1995). The effects of selective A_1 and A_{2a} adenosine receptor antagonists on cerebral ischaemic injury in the gerbil. Brain Research 705: 79-84

Picot L, Abdelmoula SM, Merieau A, Leroux P, Cazin L, Orange N, Feuilloley MGJ, (2001). Pseudomonas fluorescens as a potential pathogen: adherence to nerve cells. Microbes and Infection 3: 985-995

Pineiro P, Mulle C, (2006). Kainate receptors. Cell Tissue Research 326: 457-482

Pittinger GL, Liu D, Vinik AI, (1997). The apoptotic death of neuroblastoma cells caused by serum from patients with insulin-dependent diabetes and neuropathy may be Fas-mediated. Journal of Neuroimmunology 76: 153-160

Polgár E, Hughes DI, Arham AZ, Todd AJ, (2005). Loss of neurons from laminas I-III of the spinal dorsal horn is not required for development of tactile allodynia in the spared nerve injury model of neuropathic pain. The Journal of Neuroscience 25: 6658-6666

Pons S, Trejo JL, Martinez-Morales J, Marti E, (2001). Vitronectin regulates Sonic hedgehog activity during cerebellum development through CREB phosphorylation. Development 128: 1481-1492

Popoli P, Betto P, Reggio R, Ricciarello G, (1995). Adenosine A_{2A} receptor stimulation enhances striatal extracellular glutamate levels in rats. European Journal of Pharmacology; 287: 215-217

Psychari SN, Iliodromotis EK, Hamodraka E, Liakos G, Velissaridou A, Apostolou TS, Kremastinos DT, (2004). Preinfarction angina does not alter infarct size and in hospital outcome after acute myocardial infarction with ST elevation. International Journal of Cardiology 94: 187-191

Pugliese AM, Latini S, Corradetti R, Pedata F, (2003). Brief, repeated, oxygen-glucose deprivation episodes protect neurotransmission from a longer ischaemic episode in the *in vitro* hippocampus: role of adenosine receptors. British Journal of Pharmacology 140: 305-314

Rabbani M, Wright EJ and Little HJ, (1995). Tolerance to competitive NMDA antagonists, but no cross-tolerance with barbiturates. Pharmacology Biochemistry and Behaviour 50: 9-15

Ravati A, Ahlemeyer B, Becker A, Klumpp S, Kreiglstein J, (2001). Preconditioning-induced neuroprotection is mediated by reactive oxygen species and activation of the transcription factor nuclear factor-κB. Journal of Neurochemistry 78: 909-919

Renkawek K, Spatz M, Murray MR, Klatzo I, (1978). Uptake of radiolabeled glucose analogues by organotypic cerebellar cultures. Journal of Neurobiology 9: 111-119

Resink A, Villa M, Benke D, Möhler H, Balázs R, (1995). Regulation of the expression of NMDA receptor subunits in rat cerebellar granule cells: effect of chronic K^+-induced depolarization and NMDA exposure. Journal of Neurochemistry 64: 558-565

Ribble D, Goldstein NB, Norris DA, Shellman YG, (2005). A simple technique for quantifying apoptosis in 96-well plates. BMC Biotechnology 5:12-18

Ribo M, Grotta JC, (2006). Latest advances in intracerebral hemorrhage. Current Neurology and Neuroscience Reports 6: 17-22

Rintoul GL, Filiano AJ, Brocard JB, Kress GJ, Reynolds IJ, (2003). Glutamate decreases mitochondrial size and movement in primary forebrain neurones. Journal of Neuroscience 23: 7881-7888

Rios C, Santamaria A, (1991). Quinolinic acid is a potent lipid peroxidant in rat brain homogenates. Neurochemical Research 16: 1139-1143

Ristic H, Wiley JW, Hall KE, Sima AAF, (1996). Failure of nimodopine to prevent or correct the long-term nerve conduction defect and increased neuronal Ca^{2+}-currents in the diabetic BB/W-rat. Diabetes Research and Clinical Practice 32: 135-140

Rivera-Cervantes MC, Torres JS, Feria-Velasco A, Armendariz-Borunda J, Beas-Zarate C, (2004). NMDA and AMPA receptor expression and cortical neuronal death are associated with p38 in glutamate-induced excitotoxicity in vivo. Journal of Neuroscience Research 76: 678-687

Rizk NN, Rafols JA, Dunbar JC, (2006). Cerebral ischemia-induced apoptosis and necrosis in normal and diabetic rats: effects of insulin and C-peptide. Brain Research 1096: 204-212

Rodrigues CM, Solá S, Silva R, Brites D, (2000). Bilirubin and amyloid-beta peptide induce cytochrome c release through mitochondrial membrane permeabilization. Molecular Medicine 6: 936-946

Rohn TT, Head E, Nesse WH, Cotman CW, Cribbs DH, (2001). Activation of caspase-8 in the Alzheimer's disease brain. Neurobiology of Disease 8: 1006-1016

Rohn TT, Rissman RA, Davis MC, Kim YE, Cotman CW, Head E, (2002). Caspase-9 activation and caspase cleavage of tau in the Alzheimer's disease brain. Neurobiology of Disease 11: 341-354

Rotman B, Papermaster BW, (1966). Membrane properties of living mammalian cells as studied by enzymatic hydrolysis of fluorogenic esters. Proceedings of the National Academy of Sciences 55: 134-141

Roy M, Sapolsky R, (1999). Neuronal apoptosis in acute necrotic insults: why is this subject such a mess? Trends in Neuroscience 22: 419-422

Ruscher K Isaev N, Trendelenburg G, Weih M, Iurato L, Meisel A, Dirnagl U, (1998). Inhibition of hypoxia inducible factor 1 by oxygen glucose deprivation is attenuated by hypoxic preconditioning in rat cultured neurones. Neuroscience Letters 254: 117-120

Ryu H, Smith K, Camelo SI, Carreras I, Lee J, Iglesias AH, Dangond F, Cormier KA, Codcowicz ME, Brown Jr. RH, Ferrante RJ, (2005). Sodium phenylbutyrate prolongs survival and regulates expression of anti-apoptotic genes in transgenic amyotrophic lateral sclerosis mice. Journal of Neurochemistry 93: 1087-1098

Rzeski W, Kocki T, Dybel A, Wejksza K, Zdzisińska B, Kandefer-Szerszeń M, Turski WA, Okuno E, Albrecht J, (2005). Demonstration of kynurenine aminotransferases I and II and characterisation of kynurenic acid synthesis in cultured cerebral cortical neurons. Journal of Neuroscience Research 80: 677-682

Sanchez I, Xu CJ, Juo P, Kakizaka A, Blenis J, Yuan J, (1999). Caspase-8 is required for cell death induced by expanded polyglutamine repeats. Neuron 22: 623-633

Sapolsky RM, (2001). Cellular defenses against excitotoxic insults. Journal of Neurochemistry 76: 1601-1611

Saurin AT, Pennington DJ, Raat NJ, Latchman DS, Owen MJ, Marber MS, (2002). Targeted disruption of the protein kinase C epsilon gene abolishes the infarct size reduction that follows ischaemic preconditioning of isolated buffer-perfused mouse hearts. Cardiovascular Research 55: 672-680

Sawa A, Wiegand GW, Cooper J, Margolis RL, Sharp AH, Lawler Jr. JF, Greenamyre JT, Snyder SH, Ross CA, (1999). Increased length of Huntington disease lymphoblasts associated with repeat length-dependent mitochondrial depolarisation. Nature Medicine 5: 1194-1198

Schäfer M, Goodenough S, Moosmann B, Behl C, (2004). Inhibition of glycogen synthase kinase 3β is involved in the resistance to oxidative stress in neuronal HT22 cells. Brain Research 1005: 84-89

Schramm M, Eimerl S, Costa E, (1990). Serum and depolarizing agents cause acute neurotoxicity in cultured cerebellar granule cells: role of the glutamate receptor responsive to N-methyl-D-aspartate. Proceedings of the National Academy of Sciences of the USA 87: 1193-1197

Schurr A, Reid KH, Tseng MT, West C, Rigor BM, (1986). Adaptation of adult brain tissue to anoxia and hypoxia *in vitro*. Brain Research 374: 244-248

Schwab BL, Guerini D, Didszun C, Bano D, Ferrando-May E, Fava E, Tam J, Xu D, Xanthoudakis S, Nicholson DW, Carafoli E, Nicotera P, (2002). Cleavage of

plasma membrane calcium pumps by caspases: a link between apoptosis and necrosis. Cell Death and Differentiation 9: 818-831

Schwarcz R, Whetsell Jr. WO, Mangano RM, (1983). Quinolinic acid: an endogenous metabolite that produces axon-sparing lesions in rat brain. Science 219: 316-318

Scorziello A, Pellegrini C, Forte L, Tortiglione A, Gionelli A, Iossa S, Amaroso S, Tufano R, Di Renzo G, Annunziato L, (2001). Differential vulnerability of cortical and cerebellar neurons in primary culture to oxygen glucose deprivation followed by reoxygenation. Journal of Neuroscience Research 63: 20-26

Scorziello A, Pellegrini C, Sceondo A, Sirabella R, Formisano L, Sibaud L, Amaroso S, Canzoniero LMT, Annunziato L, Di Renzo G, (2004). Neuronal NOS activation during oxygen glucose deprivation triggers cerebellar granule cell death in the later reoxygenation phase. Journal of Neuroscience Research 76: 812-821

Sei Y, Fossom L, Goping G, Skolnick P, Basile AS, (1998). Quinolinic acid protects rat cerebellar granule cells from glutamate-induced apoptosis. Neuroscience Letters 241: 180-184

Shamloo M, Wieloch T, (1999). Changes in protein tyrosine phosphorylation in the rat brain after cerebral ischemia in a model of ischemic tolerance. Journal of Cerebral Blood Flow and Metabolism 19: 173-183

Shimazaki K, Ishida A, Kawai N, (1994). Increase in bcl-2 oncoprotein and the tolerance to ischemia-induced neuronal death in the gerbil hippocampus. Neuroscience Research 20: 95-99

Shimazaki K, Nakamura T, Nakamura K, Oguro K, Masuzawa T, Kudo Y, Kawai N, (1998). Reduced calcium elevation in hippocampal CA1 neurons of ischaemia-tolerant gerbils. NeuroReport 9: 1875-1878

Shimoni Y, Rahamimoff R, (1983). Stereospecific glucose transport across motor nerve terminal membrane: an electrophysiological study. American Journal of Physiology 245: C308-C315

Sima AAF, (2003). New insights into the metabolic and molecular basis for diabetic neuropathy. Cellular and Molecular Life Sciences 60: 2445-2464

Simonian NA, Getz RL, Leveque JC, Konrad C, Coyle JT, (1996). Kainate induces apoptosis in neurons. Neuroscience 74: 675-683

Sims NR, Zaidan E, (1995). Biochemical changes associated with selective neuronal death following short-term cerebral ischaemia. International Journal of Biochemistry and Cell Biology 27: 531-550

Sitzer M, Foerch C, Neumann-Haefelin T, Steinmetz H, Misselwitz B, Kugler C, Back T, (2004). Transient ischaemic attack preceding anterior circulation infarction is independently associated with favourable outcome. Journal of Neurology, Neurosurgery and Psychiatry 75: 659-660

Sloop GD, Roa JC, Delgado AG, Balart JT, Hines MO, Hill JM, (1999). Histological sectioning produces TUNEL reactivity. Archives of Pathology and Laboratory Medicine 123: 529-532

Smith RA, Jiang ZG, (1994). Neuronal modulation and plasticity in vitro. International Review of Cytology 153: 233-296

Smith RA, Walker T, Xie X, Hou ST, (2003). Involvement of the transcription factor E2F1/Rb in kainic acid-induced death of murine cerebellar granule cells. Molecular Brain Research 116: 70-79

Snell LD, Iorio KR, Tabakoff B, Hoffman PL, (1994). Protein kinase C activation attenuates *N*-methyl-D-aspartate-induced increases in intracellular calcium in cerebellar granule cells. Journal of Neurochemistry 62: 1783-1789

Soriano FX, Papadia S, Hofmann F, Hardingham NR, Hardingham GE, (2006). Preconditioning doses of NMDA promote neuroprotection by enhancing neuronal excitability. Journal of Neuroscience 26: 4509-4518

Soriano FX, Hardingham GE, (2007). Compartmentalised NMDA receptor signalling to survival and death. Journal of Physiology 584: 381-387

Stadelmann C, DEckwerth TL, Srinivasan A, Bancher C, Brück W, Jellinger K, Lassmann H, (1999). Activation of caspase-3 in single neurons and autophagic granules of granulovacuolar degeration in Alzheimer's disease. American Journal of Pathology 155: 1459-1466

Stone TW, (2000). Kynurenines in the CNS: from endogenous obscurity to therapeutic importance. Progress in Neurobiology 64: 185-218

Stone TW, Addae JI, (2002). The pharmacological manipulation of glutamate receptors and neuroprotection. European Journal of Pharmacology 447: 285-296

Stoy N, Mackay GM, Forrest CF, Christophides J, Egerton M, Stone TW, Darlington LG, (2005). Tryptophan metabolism and oxidative stress in patients with Huntington's disease. Journal of Neurochemistry 93: 611-623

Su JH, Anderson AJ, Cummings BJ, Cotman CW, (1994). Immunohistochemical evidence for apoptosis in Alzheimer's disease. 5: 2593-2533

Su TZ, Campbell GW, Oxender DL, (1997). Glutamine transport in cerebellar granule cells in culture. Brain Research 757: 69-78

Sullivan PG, Dube C, Dorenbos K, Steward O, Baram TZ, (2003). Mitochondrial uncoupling protein-2 protects the immature brain from excitotoxic neuronal death. Annals of Neurology 53: 711-717

Tang XQ, Chen J, Tang EH, Feng JQ, Chen PX, (2005a). Hydrogen peroxide preconditioning protects PC12 cells against apoptosis induced by oxidative stress. Sheng Li Xue Bao 57: 211-6

Tang XQ, Feng JQ, Chen J, Chen PX, Zhi JL, Cui Y, Guo RX, Yu HM, (2005b). Protection of oxidative preconditioning against apoptosis induced by H_2O_2 in PC12 cells: mechanisms via MMP, ROS, and bcl-2. Brain Research 1057: 57-64

Tang XQ, Zhi JL, Cui Y, Feng JQ, Chen PX, (2005c). Hydrogen peroxide preconditioning protects PC12 cells against apoptosis induced by dopamine. Life Sciences 78: 61-66

Tauskela JS, Comas T, Hewitt K, Monette R, Paris J, Hogan M, Morley P, (2001). Cross-tolerance to otherwise lethal *N*-methyl-D-aspartate and oxygen-glucose deprivation in preconditioned cortical cultures. Neuroscience 107: 571-584

Tauskela JS, Brunette E, Monette R, Comas T, Morley P, (2003). Preconditioning of cortical neurons by oxygen-glucose deprivation: tolerance induction through abbreviated neurotoxic signalling. American Journal of Cell Physiology 285: C899-C911

Tauskela JS, Gendron T, Morley P, (2004). Delayed cross-tolerance to cerebral ischemia. Cerebral ischemic tolerance. Chapter 4, 45-94, Nova Science Publishers

Tauskela JS, Morley P, (2004). On the role of Ca^{2+} in cerebral ischemic preconditioning. Cell Calcium 36: 313-322

Tauskela JS, Fang H, Hewitt M, Brunette E, Morley P, (2008). Activity-dependent preconditioning induces cross-tolerance of neurons to oxygen-glucose deprivation. Journal of Biological Chemistry (in press)

Taylor TN, Davis PH, Torner JC, Holmes J, Meyer JW, Jacobson MF, (1996). Lifetime cost of stroke in the United States. Stroke 27: 1459-1466

Tong L, Perez-Polo R, (1998). Brain-derived neurotrophic factor (BDNF) protects cultured rat cerebellar granule neurons against glucose deprivation-induced apoptosis. Journal of Neural Transmission 105: 905-914

Truscott RJ, Elderfield AJ, (1995). Relationship between serum tryptophan and tryptophan metabolite levels after tryptophan ingestion in normal subjects and age-related cataract patients. Clinical Science (London) 89: 591-599

Trushina E, McMurray CT, (2007). Oxidative stress and mitochondrial dysfunction in neurodegenerative diseases. Neuroscience 145: 1233-1246

Vacas J, Fernandez M, Ros M, Blanco P, (2003). Adenosine modulation of $[Ca^{2+}]_i$ in cerebellar granular cells: multiple adenosine receptors involved. Brain Research 992: 272-280

Valencia A, Morán J, (2001). Role of oxidative stress in the apoptotic cell death of cultured cerebellar granule neurons. Journal of Neuroscience Research 64: 284-297

Valencia A, Morán J, (2004). Reactive oxygen species induce different cell death mechanisms in cultured neurons. Free Radical Biology and Medicine 36: 1112-1125

Vila M, Przedborski S, (2003). Targeting programmed cell death in neurodegenerative diseases. Nature Reviews 4: 1-11

Vincent AM, McLean LL, Backus C, Feldman EL, (2005). Short-term hyperglycaemia produces oxidative damage and apoptosis in neurons. The FASEB Journal 19: 638-40

Wan Q, Xiong ZG, Man HY, Ackerley CA, Braunton J, Lu WY, Becker LE, MacDonald JF, Wang YT, (1997). Recruitment of functional GABA(A) receptors to postsynaptic domains by insulin. Nature 6643: 868-690

Wang J, Simonavicius N, Wu X, Swaminath G, Reagan J, Tian H, Ling L, (2006). Kynurenic acid as a ligand for orphan G protein-coupled receptor GPR35. Journal of Biological Chemistry 281: 22021-22028

Ward MW, Kushnareva Y, Greenwood S, Connolly CN, (2005). Cellular and subcellular calcium accumulation during glutamate-induced injury in cerebellar granule neurons. Journal of Neurochemistry 92: 1081-1090

Wartenberg HC, Urban BW, Duch DS, (1999). Distinct molecular sites of anaesthetic action: pentobarbital block of human brain sodium channels is alleviated by removal of fast inactivation. British Journal of Anaesthesia 82: 74-80

Watanebe M, Ohe Y, Katakai K, Kabeya K, Fukumura Y, Kobayashi I, Miyamato K, Ishikawa K, (1998). Glutamine is involved in the dependency of brain neuron survival on cell plating density in culture. NeuroReport 9: 2353-2357

Watanabe M, Hitomi M, van der Wee K, Rothenberg F, Fisher SA, Zucker R, Svoboda KKH, Goldsmith EC, Heiskanen KM, Nieminen AL, (2002). The pros and cons of apoptosis assays for use in the study of cells, tissues and organs. Microscopy and Microanalysis 8: 375-391

Waxman EA, Lynch DR, (2005). *N*-methyl-D-aspartate receptor subtype mediated bidirectional control of p38 mitogen-activated protein kinase. The Journal of Biological Chemistry 280: 29322-29333

Wegener S, Gottschalk B, Jovanovic V, Knab R, Fiebach JB, Schellinger PD, Kucinski T, Jungehülsing GJ, Brunecker P, Müller B, Banasik A, Amberger N, Wernecke KD, Siebler M, Röther J, Villringer A, Weih M, (2004). Transient ischaemic attacks before ischaemic stroke: preconditioning the human brain? A multicentre magnetic resonance imaging study. Stroke 35: 616-21

Wei H, Leeds P, Chen RW, Wei W, Leng Y, Bredesen DE, Chuang DM, (2000). Neuronal apoptosis Induced by pharmacological concentrations of 3-hydroxykynurenine: characterisation and protection by dantrolene and bcl-2 overexpression. Journal of Neurochemistry 75: 81-90

Weih M, Bergk A, Isaev NK, Ruscher K, Megow D, Riepe M, Meisel A, Victorov IV, Dirnagi U, (1999). Induction of ischemic tolerance in rat cortical neurons by 3-nitropropionic acid: chemical preconditioning. Neuroscience Letters 272: 207-210

Weisbrot-Lefkowitz M, Reuhl K, Perry B, Chan PH, Inouye M, Mirochnitchenko O, (1998). Overexpression of human glutathione peroxidase protects transgenic mice against focal cerebral ischemia/reperfusion damage. Molecular Brain Research 53: 333-338

Weller M, Paul SM, (1993). 3-Nitropropionic acid is an indirect excitotoxin to cultured cerebellar granule neurons. European Journal of Pharmacology 248: 223-228

White MJ, DiCaprio MJ, Greenberg DA, (1996). Assessment of neuronal viability with Alamar blue in cortical and granule cell cultures. Journal of Neuroscience Methods 70: 195-200

Whitesell RR, Ward M, McCall AL, Granner DK, May JM, (1995). Coupled glucose transport and metabolism in cultured neuronal cells: determination of the rate-limiting step. Journal of Cerebral Blood Flow and Metabolism 15: 814-826

Wick A, Wick W, Waltenburger J, Weller M, Dichgans J, Schulz JB, (2002). Neuroprotection by hypoxic preconditioning requires sequential activation of vascular endothelial growth factor receptor and Akt. The Journal of Neuroscience 22: 6401-6407

Widdowson PS, Gyte A, Upton R, Smith JCE, Pitts M, Moores R, Wyatt I, (1997). L-2-Chloropropionic acid-induced cerebellar granule cell necrosis is potentiated by L-type calcium channel antagonists. Archives of Toxicology 71: 751-755

Wiegand F, Liao W, Busch C, Castell S, Knapp F, Lindauer U, Megow D, Meisel A, Redetzky A, Ruscher K, Trendelenburg G, Victorov I, Riepe M, Diener HC, Dirnagl U, (1999). Respiratory chain inhibition induces tolerance to focal cerebral ischaemia. Journal of Cerebral Blood Flow and Metabolism 19: 1229-1237

Wu L, Ding A, Zhao T, Ma Z, Wang F, Fan M, (2004). Involvement of increased stability of mitochondrial membrane potential and overexpression of bcl-2 in enhanced anoxic tolerance induced by hypoxic preconditioning in cultured hypothalamic neurons. Brain Research 999: 149-154

Wood KA, Dipasquale B, Youle RJ, (1993). In situ labeling of granule cells for apoptosis-associated DNA fragmentation reveals different mechanisms of cell loss in developing cerebellum. Neuron 11: 621-632

Yang XM, Procter JB, Cui L, Krieg T, Downey JM, Cohen MV, (2004). Multiple, brief coronary occlusions during early reperfusion protect rabbit hearts by targeting cell signalling pathways. Journal of the American College of Cardiology 44: 1103-1110

Yao M, Nguyen TV, Pike CJ, (2005). Beta-amyloid-induced neuronal apoptosis involves c-Jun N-terminal kinase-dependent downregulation of Bcl-w. Journal of Neuroscience 25: 1149-1158

Young TH, Huang JH, Hung SH, Hsu JP, (2000). The role of cell density in the survival of cultured cerebellar granule neurons. Journal of Biomedical Materials Research 52: 748-753

Young KW, Bampton ETW, Pinòn L, Bano D, Nicotera P, (2008). Mitochondrial Ca^{2+} signalling in hippocampal neurones. Cell Calcium 43: 296-306

Zhan RZ, Fujihara H, Baba H, Yamakura T, Shimoji K, (2002). Ischemic preconditioning is capable of inducing mitochondrial tolerance in the rat brain. Anaesthesiology 97: 896-901

Zhang HX, Du GH, Zhang JT, (2003). Ischemic pre-conditioning preserves brain mitochondrial functions during the middle cerebral artery occlusion in rat. Neurological Research 25: 471-476

Zhao ZQ, Vinten-Johanson J, (2006). Postconditioning: reduction of reperfusion-induced injury. Cardiovascular Research 70: 200-211

Zoccorato F, Cavallini L, Alexandre A, (2001). Adenosine inhibits glutamate exocytosis largely without interfering with Ca^{2+} influx in rat cerebrocortical synaptosomes. Neuroscience Letters 309: 181-184

Bibliography

Banker G, Goslin K; Culturing Nerve Cells. 2nd edition; MIT press; Cambridge MA; 1998

Bowsher D; Introduction to the anatomy and physiology of the nervous system. 5th edition; Blackwell Scientific Publications; Oxford; 1988

Champe PC, Harvey RA; Lippincott's Illustrated Reviews: Biochemistry. 2nd edition; J.B. Lippincott; Philadelphia; 1994

Krstulovic AM, Brown PR; Reversed-phase high-performance liquid chromatography; theory, practice and biomedical applications. 1st edition; Wiley-Interscience; New York; 1982

Rang HP, Dale MM, Ritter JM; Pharmacology. 3rd edition; Churchill Livingstone; Edinburgh; 1995

Trenkner E; Cerebellar Cells in Culture: Chapter 12 of Banker G and Goslin K; Culturing Nerve Cells. 2nd edition; MIT Press; Cambridge MA; 1998